About the book

EXPLOSIVE PRODUCTION OF NEW MATERIALS: SCIENCE, TECHNOLOGY, BUSINESS, AND INNOVATIONS

Edited by

A.A. Deribas Institute of Structural Macrokinetics and Materials Science
Russian Academy of Sciences
Chernogolovka, Moscow, 142432 Russia

Yu.B. Scheck Institute of Structural Macrokinetics and Materials Science
Russian Academy of Sciences
Chernogolovka, Moscow, 142432 Russia

R.L. Mendes Assoc. Desenv. Aerodinâmica Industrial
University of Coimbra
Coimbra, 3030-289 Portugal

The book is a collection of revised, edited and formatted abstracts submitted to the XIII International Symposium on Explosive Production of New Materials: Science, Technology, Business and Innovations (EPNM-2016) held in Coimbra, Portugal, June 20-24, 2016. The contents of the book include recent world-wide accomplishments in basic and applied studies on application of explosives (explosion, shock and impact) to materials synthesis and processing. The book is addressed to practicing engineers, research workers, and graduate students active in the field.

NobelClad

explomet
HIGH-ENERGY TECHNIQUES WORKS
EXPLOSIVE CLADDING OF METALS

ЭНЕРГОМЕТАЛЛ

MISIS
National University of Science and Technology

Office of Naval Research Global Science & Technology

FCT
Fundação para a Ciência e a Tecnologia
MINISTÉRIO DA CIÊNCIA, TECNOLOGIA E ENSINO SUPERIOR

ORDEM DOS ENGENHEIROS
REGIÃO CENTRO

Explosive Production of New Materials

ISMAN

Russian Academy of Sciences

laeta laboratório associado

· U C ·

XIII INTERNATIONAL SYMPOSIUM ON EXPLOSIVE PRODUCTION OF NEW MATERIALS: SCIENCE, TECHNOLOGY, BUSINESS AND INNOVATIONS

Coimbra - 2016

XIII EPNM

Edited by

A. A. Deribas
Yu. B. Scheck
R. L. Mendes

Explosive Production of New Materials:

Science, Technology, Business, and Innovations

Edited by
A. A. Deribas
Yu. B. Scheck
R. L. Mendes

Andrei A. Deribas
Joint Institute for High Temperatures
Russian Academy of Sciences
Moscow, Russia

Yury B. Scheck
Institute of Structural Macrokinetics and Materials Science
Russian Academy of Sciences
Chernogolovka, Moscow, 142432 Russia

Ricardo L. Mendes
Association for the Development of Industrial Aerodynamics
University of Coimbra
Coimbra, 3030-289 Portugal

Explosive Production of New Materials: Science, Technology, Business, and Innovations [Edited by A.A. Deribas, Yu.B. Scheck and R. L. Mendes] — Coimbra: 2016.

ISBN 978-989-99080-6-2

This book is a collection of revised, edited, and formatted abstracts submitted to the XIII International Symposium on Explosive Production of New Materials: Science, Technology, Business, and Innovations (EPNM-2014) held in Coimbra, Portugal, June 20–24, 2016. The contents of the book include recent worldwide accomplishments in basic and applied research on application of explosives (explosion, shock, and impact) to materials synthesis and processing. The book is addressed to practicing engineers, research workers, and graduate students active in the field.

Printed in Portugal

aciv – Associação para o Desenvolvimento da Engenharia Civil

PREFACE

EPNM-2016 — the XIII edition of International Symposium on Explosive Production of New Materials — is organized by the Association for the Development of Industrial Aerodynamics (ADAI) and Institute of Structural Macrokinetics and Materials Science (ISMAN). Tradition begun on 2006, in Moscow, Russia and carried on with EPNM-2008 in Lisse, the Netherlands; EPNM-2010 in Bechichi, Montenegro; EPNM-2012 in Strasbourg, France; and EPNM-2014 in Cracow, Poland.

The present symposium is dedicated to the memory of Dr. Igor Plaksin. During last 40 years, he has contributed greatly to explosives science and detonation physics with great achievements. In the last 20 years he worked in ADAI/LEDAP University of Coimbra giving enormous personal contributions to the success of his research group.

The amount and diversity of abstracts submitted to XIII EPNM2016 held in Coimbra, Portugal prove the importance of the shock/detonation physics for material processing and the research efforts dedicated to the field.

In the classical area of explosive welding, new approaches to mathematical modelling of the process have been suggested based on modern numerical methods. New results and applications of explosive welding on the industrial scale were presented by such manufacturing companies as NobelClad (USA), EnergoMetall (Russia), Explomet (Poland), Bitrub (Russia), and Asahi KASEI Chemicals Corp. (Japan).

A significant number of works about application of SHS to materials processing and synthesis was registered.

Special attention was given not only to explosive characterization namely sensitivity and performance, but also to the characterization of detonation phenomena and shock wave process.

The success of past EPNM symposia made it a reference symposium and very popular in scientific community, greatly contributing to the science and technology of materials processing by explosion.

R. Mendes
M. Alymov

In memoriam

Doctor Igor Y. Plaksin

08/09/1954

08/05/2016

After completing in 1971 the High School course with the Golden Medal Award of the Ministry of Education, Igor Y. Plaksin joined the graduate program in physical engineering at Moscow Physical Engineering Institute - State Nuclear University MIFI, and then a special education program at MIFI's department integrated with Semenov's Institute of Chemical Physics, RAS. Igor earned his master degree in physical engineering, with specialization on Chemistry of Ultra-Fast Processes, including Physics of Combustion and Explosion from State Nuclear University MIFI and his Ph.D., in the same area, from All-Russian Scientific Research Institute on Experimental Physics – VNIIEF. He was appointed as VNIIEF Fellow from 1977 to 1995, initially as physicist-research engineer, then as physicist-research associate/technical staff member and later as senior research associate/scientific staff member at Shock Dynamics Department where he worked on, and led, a number of shock initiation, detonation performance and energy related programs. In 1980, 1986 and 1990, he received the VNIIEF's Fellow's

Prize for Advanced Research. His work at the VNIIEF spanned 18 years, up to 1995 when he accepted a position of Invited Research and Invited Professor at the Laboratory of Energetics and Detonics (LEDAP) of the University of Coimbra.

From 1995 to the present he worked at LEDAP & ADAI, where he was responsible for providing technical and programmatic guidance for the Portuguese MoD, Western European Armament Group and the European Defense Agency Programs in a number of areas of advanced PBXs, sensitivity to shock initiation and energy cumulating researches.

Igor was a brilliant and dedicated scientist who promoted research in the field of the physics of shock and detonation waves. With his geniality he developed an innovative space (micrometer scale) and temporal (nanosecond scale) resolved experimental technique for the characterization of almost all aspects of shock and detonation waves. The results he obtained with that technique allowed him to propose a new mechanism for detonation wave ignition, propagation and extinction phase and the introduction of a new parameter to characterize PBX's shock reactivity.

He is the author of more than 150 publications and co-author of a book published by Fraunhofer IRB Verlag in 2007. He served as a Scientific Advisor and Coordinator for seven PhD- and MS-students and Program Committee Member at European Working Group on Non-Lethal Weapons. From 2002 to 2011, Igor served as a Principal Technical Investigator at ten research projects hosted at NSWC-Indian Head, LANL and ONR and two European projects under the umbrella of EUROPA MOU (WEAG and EDA).

He will be remembered forever by his colleagues as an outstanding scientist, an exceptional human being and a great friend.

He deceased on 8th of May of 2016, in Suvorove, his hometown.

SYMPOSIUM SPONSORS

NobelClad
A DMC Company
5405 Spine Road, Boulder, CO
80301 USA
www.nobelclad.com
tel.: +1 800 821-2666

NobelClad, a DMC Company, is the world's leading provider of explosion-welded clad metal plates. Its Detaclad TM products are used in a variety of industries, including petrochemicals, refining, hydrometallurgy, aluminum smelting, and shipbuilding. Most recently known as DMC, the Boulder, Colorado, USA based company began business in 1965 as an explosion forming specialist, producing complex three-dimensional parts for aerospace equipment manufacturers. NobelClad became a publicly traded company in 1976 under the ticker symbol "BOOM" and shortly thereafter licensed technology from E. I. DuPont de Nemours and Company ("DuPont") to explosively bond, or clad, two or more dissimilar metal plates together. The explosion-bonded clad metal business remains NobelClad's core business today. The acquisitions of DuPont's Detaclad Division in 1996, Nobelclad Europe in 2001, and DynaEnergetics in 2007 have strengthened the Company's world-wide position in explosion cladding. In 2013, Dynamic Materials Corporation became DMC to serve as the parent company for its subsidiary businesses. The explosion welding entities (DMC Clad Metal U.S., Nobelclad France, DynaPlat Germany) now operate under the single global trade name of NobelClad.

EnergoMetall Co.
St. Petersburg, Russia
tel. +7 (812) 535-7243, 336-6465
fax +7 (812) 534-1919
e-mail: info@emet.ru
http://emet.ru

EnergoMetall Co., St. Petersburg, Russia. Production of two- and multilayer clad metals by explosive welding, their subsequent machining, and manufacturing industrial products.

Explomet Co.
ul. Oświęcimska 100H, Opole, 45-641 Poland
tel./fax: +48 (0) 77 45 62 511
e-mail: biuro@explomet.pl; explomet@op.onet.pl
http://www.explomet.pl

The company is located in an area of strong, wide co-operating companies. Explomet has the ability to perform explosive works on own cladding area and possesses own production technology of explosives.

The Company's structure, adapted to the scale and scope of production ensures efficient implementation of orders received from domestic and foreign customers. Production is under constant supervision of the quality control department. Produced cladding materials are subject to standard test and control procedures compatible with European regulations, AD-2000 Merkblatt W0-W8, ASME / ASTM rules or other designated by the customer. Each batch of manufactured products receives full documentation attesting the production process and quality. Dimensional assortment of offered cladding products is very wide. We are using practically all of material's grades, applied in this technology. For industrial purposes, thickness of the clad material is mostly more than 1 mm and not more than 25mm, in one shot. The maximal area of a single cladding element, depending on the thickness of the component materials can be more than 20m^2.

National University of Science and Technology MISiS
Leninskii pr. 4, Moscow, 119991 Russia
tel: +7 495 955-0032
fax: +7 499 236-2105
http://en.misis.ru/university/

National University of Science and Technology MISiS has a proud and distinguished history, having celebrated its 80th anniversary in June 2010. It originated as the Department of Metallurgy at the Moscow Academy of Mines established in 1918 and in the following decades it went through several transformations before achieving its current designation.

In the 20th century, the Moscow Academy of Mines and then the Moscow Steel Institute (founded in 1930) each played a prominent role in the industrialization of Soviet Russia. Today, the National University of Science and Technology MISiS is at the forefront in the development of Russia's innovative, knowledge-based economy, supporting the nation's ability to successfully compete with other advanced economies as well as to fully integrate into the international community.

Just as in the past, MISiS remains one of Russia's leading educational and research centers. It provides a first-class professional education for over 14 000 undergraduate and graduate students, and it offers extensive opportunities for specialized scientific research with the objective of transferring the university's ideas, innovations, and technologies to real-life application. MISiS aims at developing and nurturing pioneering processes in a variety of fields ranging from its historic expertise in metallurgy and materials science to relatively new directions in nanotechnology, biotechnology, information technologies and telecommunications, sustainable development, and energy-effective technologies. These technologies are essential for improving the quality of life not only in the Russian Federation but in all countries worldwide.

MISiS supports a multi- and cross-disciplinary approach to education. Our mission emphasizes providing fundamental instruction on an undergraduate and postgraduate level as well as creating an organic link between education and science.

MISiS is working to develop new mutually-beneficial relations with international industrial and educational partners, while continuing to nurture those already existing. Our institutional vision recognizes the seeming paradox that in the world of competition it is international cooperation that has the potential of creating an environment uniquely conducive to attainment of university's goals and continued evolution.

Fundação para a Ciência e a Tecnologia
Av. D. Carlos I, 126
1249-074 Lisboa
Portugal
Tel: + 351 213 924 300
Fax: + 351 213 956 519
http://www.fct.pt/

Fundação para a Ciência e a Tecnologia (FCT) is the national funding agency that supports science, technology and innovation, in all scientific domains, under responsibility of the Ministry for Science, Technology and Higher Education. FCT started its activity in August 1997, succeeding the *Junta Nacional de Investigação Científica e Tecnológica* (JNICT). Since March 2012 FCT has coordinated public policies for the Information and Knowledge Society in Portugal, after the integration of the Knowledge Society Agency-UMIC.

Ordem dos Engenheiros – Região Centro
Rua Antero de Quental, nº 107
3000-032 COIMBRA
Tel.: +351 239 855 190
Fax: +351 239 823 267
http://www.ordemengenheiros.pt/

The Engineers Order is a public Portuguese association which represents professionals who exercise the engineer profession.
Its statutory mission is to control access to the profession; defend, promote and disseminate of Engineering in society; stimulate efforts of its member scientifically, technically professionally and socially and to strive for compliance with the rules of professional ethics.

Office of Naval Research (ONR)
875 North Randolph Street, Suite 1224-C
Arlington, VA 22203-1771
Phone: 703-696-5031
Fax: 703-696-5940
http://www.onr.navy.mil/en.aspx

ONGR connects the international science and technology (S&T) community to the U.S. naval S&T community. The challenge is to help U.S. naval forces maintain technology superiority by both leveraging the accelerating global S&T output at a fundamental level and speeding the delivery of technology to our Navy and Marine Corps warfighters.

CONTENTS

RECENT ADVANCEMENTS OF ISMAN IN SHS AND IN EXPLOSION/COMBUSTION-ASSISTED MATERIALS PROCESSING

M. I. Alymov

Institute of Structural Macrokinetics and Materials Science, Russian Academy of Sciences, Chernogolovka, 142432 Russia

e-mail: director@ism.ac.ru

Basic research on explosive welding and shock-assisted densification and synthesis of new materials, such as carbon steels, stainless steels, and copper, aluminum, cobalt, and niobium alloys.

Structural transformations taking place during explosive welding and hot rolling of ХВГ–08кп–45ХСНМА stacks. The diffusion of carbon from low-carbon steel into a transition layer was found to improve the stack hardness. Suggested is a combined process (explosive welding + hot rolling) for fabrication of bimetal with enhanced mechanical strength and high-quality weld seam.

Structural steel 08кп was joined with pig iron ЧНМШ by explosive welding. The structure and properties of the joint were explored as a function of welding conditions. An amorphous ‘white phase’ close to low-alloyed pig iron was found to undergo phase transformation into the perlite–graphite structure whose composition is close to that of pre-eutectic pig iron.

Elaborated is a new process for fabrication of the brass/invar clad metal by combined use of explosive welding with cold/hot rolling. The process ensures good quality of the seam zone, no wavy structure, and the mechanical strength close to that of brass at a nominal ratio of plates’ thickness: between 1.2 : 1 and 1.3 : 1.

In order to protect the surface of flyer plate in the explosive welding of М1 + АД1 clad metal, the use of a damping layer was found to be effective. For the purpose, a 96 : 4 mixture of microporous ammonium nitrate with diesel oil was found to be optimal.

Explored was the influence of preliminary shock processing on the efficiency of SHS production of cermet composites in TiB_2–Al and TiC–Ni SHS reactions. For Ti + B and Ti + C mixtures, determined the conditions for steady initiation of SHS reactions in recovery ampoules. It has been demonstrated that the combined use of welding and shock compaction can be readily applied to synthesis of laminated cermets of required composition.

The Al_2O_3–AlN compacts were fabricated by the method of shock compaction. Process conditions for fabrication of high-temperature electric insulators by shock

compaction were optimized and respective practical recommendations have been formulated.

Developed is the process for SHS-fabrication of powders, such as aluminum nitride for heat-conducting dielectric ceramics and heat-conducting glues and compounds. SHS-produced aluminum nitride is also used in production of radioactive isotope C^{14}. The ceramic obtained by sintering SHS-produced aluminum nitride shows the thermal conductivity of up to 200 W/m K.

The process for SHS-fabrication of α-AlN powder in the presence of MgO as a sintering agent was developed and used for preparation of heat-resistant structural ceramics. Such ceramics fabricated by hot pressing showed the bending strength up to 900 MPa and microhardness up to 18 GPa.

Explored was the combustion of granulated Ti + 0.5C in a flow of nitrogen gas to yield titanium carbonitride $TiC_{0.5}N_{0.5}$ widely used in production of tungsten-free hard alloys and deposition of protective coatings. Due to the use of granules, the gas permeability of the sample could be kept sufficiently high over the entire process of wave propagation over the burning sample.

The methods of SHS metallurgy developed at ISMAN were applied to produce heat-resistant alloys based on niobium silicides with alloying agents (Hf, Ti, Al, etc.) and cast items made thereof. The alloys look promising for aerospace applications.

Theoretical backgrounds for the influence of pressure/shear strains on SHS reactions made a basis for designing new processes for energy-saving fabrication of refractory oxygen-free materials with desired properties.

New composites based on ZrB_2 and a CrB binder (residual porosity <1%) were fabricated by SHS under pressure. With increasing amount of binder, the mean size of ZrB_2 particles was found to decrease from 10 to 0.3 μm. The CrB binder suppressed the growth of ZrB_2 particles. In composites with ceramic binder, the average size of ZrB_2 grains is smaller than that in the absence of binder by a factor of в 5–7.

ONCE MORE ON THE ROLE OF SHOCKED GAS IN EXPLOSIVE WELDING

M. I. Alymov, I. S. Gordopolova, and A. A. Deribas

Institute of Structural Macrokinetics and Materials Science, Russian Academy of Sciences, Chernogolovka, Moscow, 142432 Russia

e-mail: gis@ism.ac.ru

As is known, explosive welding of some dissimilar metals (including titanium) gives poor results in the presence of air in the welding gap. For this reason, in some cases special measures should be taken in order to replace the atmospheric air in the gap by He or H_2 and thus to decrease the temperature/pressure in the detonation wave (cf. the table below taken from [1]).

V_c, m/s	Wave parameters	Air	He	H_2
1500	*V*, m/s	1800	2200	2500
	T, ºC	1850	300	200
	P, MPa	4.0	0.6	0.4
2500	*V*, m/s	3000	3300	3500
	T, ºC	4800	620	400
	P, MPa	10.0	1.25	0.8
3000	*V*, m/s	3600	3850	4000
	T, C	6800	860	520
	P, MPa	14.0	1.75	1.05
4000	*V*, m/s	4800	5050	5150
	T, C	11800	1450	850
	P, MPa	24.5	3.0	1.7
5000	*V*, m/s	6000	6150	6300
	T, C	18000	2150	1280
	P, MPa	38.0	4.5	2.6

This can be expected to hamper harmful overheating of clad plates and to avoid sharp temperature/pressure jumps in the gap [2]. High-quality joining between Ti and steel was achieved in the presence of He in the weld gap.

Local bulging and rupture of metal observed in explosive welding of Ti [3, 4] was explained by ignition and combustion of gas-saturated Ti particles ejected into the gap due to the jet-formation effect. An attempt to check the above assumption was made in

[5] by using the method of traps. However, in the experiments under Ar no trapped unburned Ti particles have been detected. This suggests that there is some other cause for overheating a Ti plate.

Previously [6], we have demonstrated that the duration of contact between shock-compressed gas and metal surface is too short for any kind of heat-exchange processes. Since the mass of gas in the gap is much smaller than the mass of metal plates, the contribution of shock-compressed gas to the overheating of Ti plate can be safely neglected. Moreover, explosive welding in vacuum was found [7] to give the same results as that in air. Nevertheless, vivid discussion on the decisive role of shocked gas in explosive welding is still continuing in the literature.

The problems encountered in explosive welding of titanium should be associated not the temperature and other parameters of shocked gas but with specific properties of Ti metal; such as the ability to adsorb and retain large amounts of gaseous hydrogen, oxygen, and nitrogen. This circumstance must be taken into account in practical implementation of explosive welding.

1. U. Richter, J.F. Roth, Grundlagen und Anwendung des Sprengsplattierens, *Naturwiss*., 1970, vol. 57, no. 10, pp. 487–493.
2. V.M. Kudinov, A.Ya. Koroteev, *Svarka vzryvom v metallurgii* (Explosive Welding in Metallurgy), Moscow: Metallurgiya, 1978.
3. A.A. Berdychenko, B.S. Zlobin, L.B. Pervukhin, A.A. Sterzer, Possible ignition of powders ejected into the gap in explosive welding, *Combust. Explos. Shock Waves*, 2003, vol. 39, no. 2, pp. 232–239.
4. A.A. Berdychenko, L.B. Pervukhin, Explosive welding of titanium on large areas, *Polzun. Al'man*., 2008, no.3, pp. 25–27.
5. A.A. Berdychenko, L.B. Pervukhin, O.L. Pervukhina, Defects of explosive welding of titanium with steel on large areas, *Polzun. Vestn*., 2009, no. 4, pp. 216–219.
6. M.I. Alymov, A.A. Deribas, I.S. Gordopolova, *Perspekt. Mater*., 2013, no. 12, pp. 51–55.
7. A.A. Deribas, *Fizika uprocheniya i svarki vzryvom* (Physics of Explosive Strengthening and Welding), Novosibirsk: Nauka, 1980.

SELF-INFLAMMATION OF Fe NANOPOWDERS IN AIR: INFLUENCE OF PASSIVATION

M. I. Alymov[1], N. M. Rubtsov[1], B. S. Seplyarskii[1], V. A. Zelenskii[1,2], and A. B. Ankudinov[2]

[1] Institute of Structural Macrokinetics and Materials Science, Russian Academy of Sciences, Chernogolovka, Moscow, 142432 Russia
[2] Baikov Institute of Metallurgy and Materials Science, Russian Academy of Sciences, Moscow, Russia

e-mail: sepl@ism.ac.ru

In this work, we explored the influence of passivation on the self-inflammation of Fe nanopowders in air. Experiments were carried out with Fe nanopowders prepared in a flow reactor schematically shown in Fig. 1. A weighed amount of iron oxide was placed in a quartz trough and kept at 400°C in hydrogen flow for 1 h, and then allowed to cool down to room temperature in an Ar flow. Passivation of thus prepared powder (for a period of up to 1 h) was carried out in the same reactor but in the Ar flow containing 3% oxygen.

The self-inflammation of Fe nanopowders in air was monitored with a high-speed camcorder (CasioExilim F1 PRO, 300–1200 frames per second). The results are collected in Fig. 2.

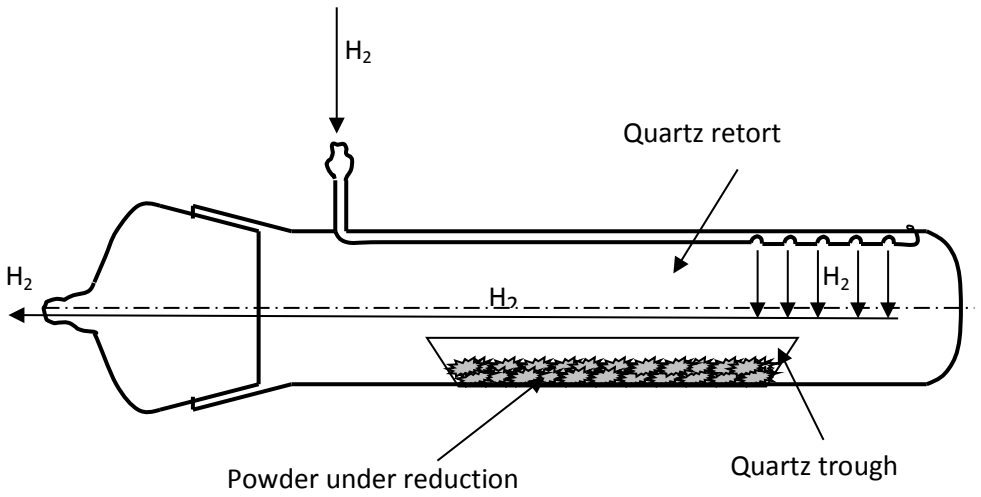

Fig. 1. Retort for preparation and passivation of Fe nanopowders.

Upon contact with atmospheric air, individual hot spots were found to appear on the powder surface, their number being smaller in case of passivated powder. Then these spots gave rise to propagation reaction waves. After passivation for $\tau > 5$ min, there was no self-inflammation (see Fig. 2).

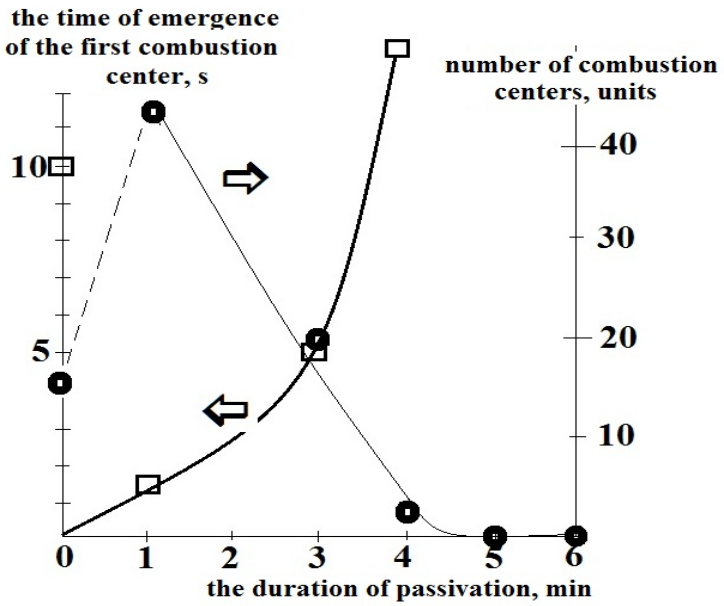

Fig. 2. Induction period for the appearance of first hot spots (rectangular data points) and amount of primary hot spots (spherical data points) as a function of passivation time τ: T_0 = 20C°, layer thickness 1 mm; the data points for τ = 0 were obtained at T_0 = 0ºC.

The powder extracted from under the near-surface layer also did not catch fire but could be readily ignited an external energy source. According to XRD results, the nanopowders passivated for $\tau > 6$ min in an Ar flow containing 3% air comprise pure iron.

This work was financially supported by the Russian Science Foundation (project no. 16-13-00013).

SHOCK COMPACTION OF TUNGSTEN/TEFLON POWDER MIXTURES

M. I. Alymov, S. G. Vadchenko, I. V. Saikov, and I. D. Kovalev

Institute of Structural Macrokinetics and Materials Science, Russian Academy of Sciences, Chernogolovka, Moscow, 142432 Russia

e-mail: revan.84@mail.ru

Three powder mixtures — tungsten/Teflon (mix **1**), tungsten/Teflon/Al (mix **2**), and tungsten/Teflon/(Ti + B) (mix **3**) — were subjected to shock compaction in the recovery fixtures with and without axial rod (Fig. 1). Type **I** fixtures were loaded with compressed pellets. The tubular gap in Type **II** fixtures was filled with bulk density powder mixtures. Ammonite 6ZhV was used as explosive.

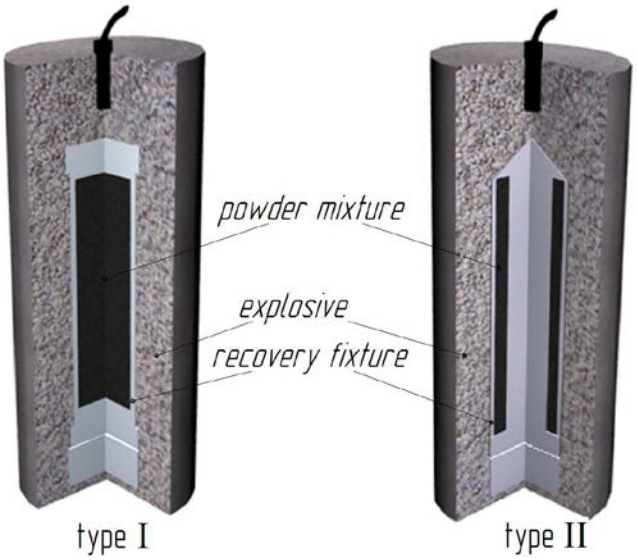

Fig. 1. Geometries of shock compaction.

In type **I** fixtures with mix **1** and type **II** fixtures with mix **2**, no formation of new phases was detected by XRD. Shock compaction of mix **2** in fixture **I** was found to yield WC, W_2C, and small admixture of AlF_3 at the fixture bottom (Fig. 2).

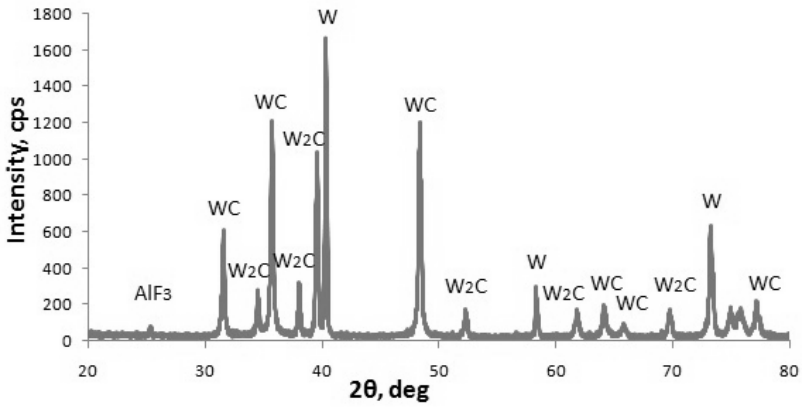

Fig. 2. Diffraction pattern of shocked mix **2** taken from the bottom of fixture **I**.

Shock compaction of mix **3** in both fixtures resulted in explosive destruction of the fixtures. The XRD data for the remnants showed the presence of W_2C and W_2B.

This work was financially supported by the Russian Foundation for Basic Research (project no. 16-03-00777a).

CHARACTERISTICS OF STEEL AND TITANIUM CYLINDERS AFTER EXPLOSIVE JOINING

S. Yu. Ananev, T. I. Borodina, G. E. Valiano, A. A. Deribas, and B. D. Yankovsky

Joint Institute for High Temperatures, Russian Academy of Sciences, ul. Izhorskaya 13 Bld. 2, Moscow, 125412 Russia

e-mail: yiy2004@mail.ru

The modern mechanical engineering widely uses elements from bimetal materials. The considerable part of such materials is received by explosive loading methods. The feature of explosion loading is the transience of the process at high energy density, which can lead to changes in properties of the materials used. The report describes the experiments on explosive joining of coaxial steel and titanium cylinders and the results of x-ray diffraction analysis.

The steel (stainless steel) and titanium cylinders explosive joining was carried out for obtaining the transition element with specified performance parameters, in particular, sealing. The implementation of the final element bases on cylindrical dovetail connection type. (Fig. 1a). For this purpose on the inner surface of the outer cylinder (1) formed two rectangular teeth by way of machine (2). On the outer surface of the inner cylinder (3) there are two rhomboid grooves (4). The implementation of dovetail joining scheme requires the opposite arrangement of the teeth (2) with shaped grooves (4). Equal volumes of opposing teeth and grooves performed the joint tightness. Disc-shaped explosive charge (5) disposed outside the cylinder (1) and initiated 16 points (Fig.1 b).

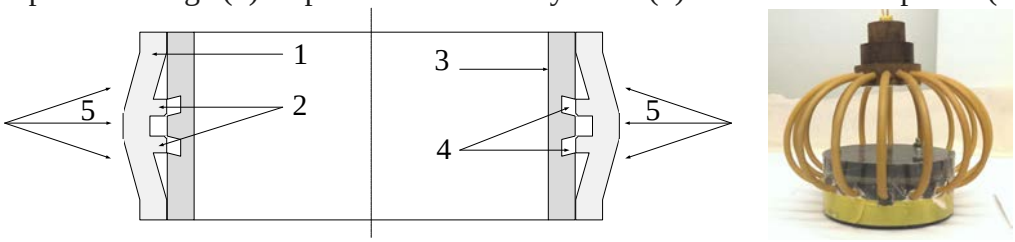

(a) (b)

Fig. 1 The cylinders joining according to the dovetail scheme (a) and a photograph of the assembly with 16-point initiation scheme.

As a result of cylinders explosive loading radially converging detonation wave causes the penetration of teeth into grooves. Due to the geometry features realized the mutual friction, plastic deformation and ring elements sealing. Pattern of joining has a complex picture of plastic deformation (Fig. 2a). General view of the sanded surface suggests that along with tight contact areas (Fig. 2b) a slit-like borders are observed (Fig. 2c). As a result in the teeth with grooves joining area material deformation, shifts, cracks, cuts, etc. can appears. A significant role is played by the precision longitudinal alignment of teeth and grooves, which affects the symmetry of the dovetail scheme. Also the differences in parameters of used steel: young's modulus, ductility, strength, etc. play an important role. At the macro level a 10% thinning while the elongation of cylinders occurs.

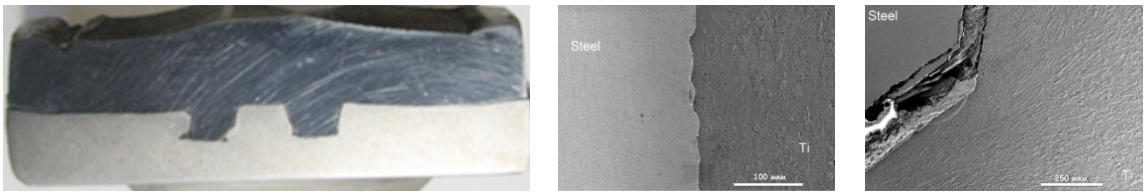

(a) (b) (c)

Fig. 2 A photo of steel and titanium cylinders joining under the dovetail scheme (a). The scheme distorted due to excessive plastic deformation caused by an axial cylinders displacement and difference of the metals parameters. There are electronic micrographs of dense zones (b) and slit-like contacts (c).

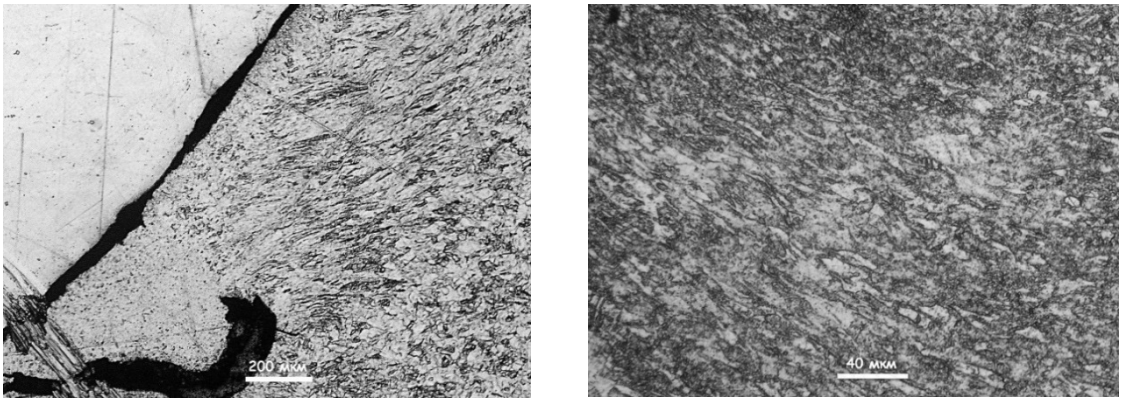

(a) (b)

Fig. 3 An optical micrographs of the titanium intense plastic shear area with longitudinal grains deformation (a) and region inside the cylinder body (b).

The optical surface analysis of etched samples surface showed a changes in titanium granular structure forms and in grains characteristic size within the deformation defects of a detail (Fig. 3). In the area of titanium intensive deformation the group of grains

elongated along the shear plastic, and the characteristic size decreased from 20 μm inside the detail body to ~2 μm in the areas bordering with steel. The grain structure of stainless steel samples has significantly smaller changes.

The metal microstructure also changes. The X-ray diffraction analysis showed that the explosive loading of titanium-steel cylinders pair leads to a transition of a stainless steel state from single-phase austenitic into two-phase ferritic-austenitic. The content of ferrite in the different areas of detail, characterized by different loading degree, varies from 56 to 100 percent vol. It is known that such transition is accompanied by increase in the volume of 4.57%. The austenite lattice parameter in all the investigated spots exceeds the reference steel lattice parameter to 20 nm. Explosive loading also leads to increasing the deformation of austenite crystal lattice. The lattice micro distortions grew up by a factor of 1.3–2.7 in comparison with an initial level.

The changes in titanium caused by compression of cylinders are less pronounced than in steel. There is a compression of titanium crystal lattice unit cell to 1.4% compared to the original.

SYNTHESIS OF Ti–Al-BASED INTERMETALLICS FROM OXIDE RAW MATERIALS BY CENTRIFUGAL SHS

D. E. Andreev, D. M. Ikornikov, V. I. Yukhvid, and V. N. Sanin

Institute of Structural Macrokinetics and Materials Science, Russian Academy of Sciences, Chernogolovka, Moscow, 142432 Russia

e-mail: ade@ism.ac.ru

This work was focused on preparation of Nb-doped Ti–Al material by centrifugal SHS [1]. TiO_2 + Nb_2O_5 +Al mixtures (mix **1**) were used as a metallothermic component, while CaO_2 + Al + Ca mixtures (mix **2**) were added as a booster. Green mixtures also contained some amount of functional additives.

Green mixtures became ignitable when the mix **2** content of green mixture (x) exceeded 10 wt %. Upon approaching to x = 100%, burning velocity U increased by a factor of ten and attained a value of 14 cm/s. Variation in the Al content of green mixtures (between 20 and 40 wt %) had little or no influence on combustion characteristics but affected chemical composition of alloys, the amount of nonmetal impurities, and decreased the amount of oxygen in a target ingot. Combustion parameters and composition/structure of target Ti–Al materials also strongly depended on a magnitude of centrifugal acceleration. The latter also strongly suppresses the material splashing during vigorous combustion. The presence of functional additives (in amounts below 3 wt %) and a reducing agent (Ca) in mix **2** was found to decrease the amount of nonmetal impurities in a target product. Further details will be discussed at presentation.

The obtained results make it possible to develop the technological combustion processes with accurate regulating metal phase composition for producing cast ceramics, alloys, and composite materials made thereof with unique structure and properties.

This work was financially supported by the Russian Governmental Program for younger researchers (grant MK-7885.2016.8).

1. V.I. Yukhvid, D.E. Andreev, V.N. Sanin, Zh.A. Sentyurina, Yu.S. Pogozhev, E.A. Levashov, Centrifugal SHS of cast Ti–Al–Nb–Cr alloys, *Int. J. Self-Propag. High-Temp. Synth*., 2015, vol. 24, no. 4, p. 177–181.

SHS OF FINE-GRAINED CERAMICS CONTAINING CARBIDES, NITRIDES, AND BORIDES

Z. G. Aslamazashvili, G. V. Zakharov, G. Sh. Oniashvili, G. F. Tavadze, and M. N. Chikhradze

Tavadze Institute of Metallurgy and Materials Science, 15 Al. Kazbegi Ave., Tbilisi, 0160 Georgia

e-mail: oniash@gtu.ge

As is known [1], the hard alloys and composites prepared by forced SHS compaction exhibit a combination of valued properties such as hardness, compression strength, wear resistance, dross resistance and chemical inertness at high temperatures. But in view of their brittleness, these materials have low impact resistance [2, 3]. The above drawback can be overcome by designing graded or fine-grained materials [4, 5, 6]. The method of SHS compaction can be expectedly used to prepare materials with a fine-grained (~1 μm) non-equilibrium structure.

This work aimed at synthesis of Ti-based fine-grained composites (armor plates) with high impact resistance by forced SHS compaction from inexpensive raw materials.

SHS reactions in the systems Ti–B–N–Cu (**I**) and Ti–B–N–C–Cu (**II**) ([Cu] = 0–10 wt %) were carried out in the following two geometries. In one cylindrical compacts 20 mm in diameter and 20–30 mm in height were ignited in atmospheric air. The direction of front propagation coincided with the pressure applied during pre-compaction. In the second, compacts in the form of square rods (70 × 70 mm and 20–30 mm long) were installed in a press mold under the pressure approximately equal to that, which was applied during preliminary sample forming. In this case the direction of front propagation was normal that of pre-compaction.

In experiments, we measured burning velocity U as a function of density ρ_0. Synthesized materials were characterized by SEM and secondary electron backscatter diffraction (EBSD).

It has been found that in second case the burning velocities were markedly higher than in the first case. With increasing ρ_0, the burning velocity was found to pass through a maximum. As is well known [7], that an initial increase in U is caused by improvement of contact between the reagents while subsequent decrease, by increasing heat sinks from the reaction zone. Note that in second case the maximum values of U are shifted toward lower ρ_0.

In several points the Kikuchi diffraction patterns (BKDP) were taken, and the crystallographic orientation of different microcrystals were determined. The Kikuchi

lines pair up to form bands from single crystalline specimens and are indicative of a perfect structure of the crystals under study.

The study of the microstructure of the material formed in system **I** shows that some areas correspond to nano-grained (120–130 nm) Ti–Ni ceramic while other areas, to a Ti–B ceramic. The same was observed for the material formed in system **II**. The material represents a matrix (90%–95%) of a nano-grained (90–100 nm) Ti–C–N ceramic doped with a Ti–B ceramic.

The processes taking place in the systems under study can be outlined as follows. Apparently, low-melting Cu and Ti undergo melting within the warm-up zone and this is followed by capillary melt spreading over B particles in system **I** and over B and C particles in system **II**.

In system **I**, the boron of BN reacts with Ti melt to produce active nitrogen gas which also reacts with Ti melt to yield titanium nitride and titanium boride. In system **II**, C particles and the boron of BN react with Ti melt to yield titanium nitride and titanium boride. The reaction of active nitrogen formed upon decomposition of BN with newly formed titanium carbide gives titanium carbonitrides. Upon cooling down, the above borides, nitrides, and carbonitrides of titanium turn fixed in the form of fine particles. The voids are filled with a binding alloy (0–5 wt %). The final product structure is formed within the crystallization zone.

Under optimized conditions, we managed to fabricate practically pore-free compacts with the following parameters: porosity 0.4–1.2%, hardness 91.5–92.5 and 92.3–93.3 HRA; density 4.3–4.4 and 4.5-4.7 g/cm^3, for systems **I** and **II** respectively. The materials were found to withstand impacts with an energy of 18 000–20 000 J (for materials with d = 6.8–6.5 g/cm^2).

1. Merzhanov, A.G. and Borovinskaya, I.P., SHS in the chemistry and chemical engineering of refractory compounds, *Zh. Vses. Khim. O-va im. Mendeleeva*, 1979, vol. 24, no. 3, pp. 223–227.
2. Borovinskaya, I.P., SHS ceramics: Synthesis, production processes, and application, *Nauka Proizv*., 2001, no. 10, pp. 11–18.
3. Batuev, G.S., *Issledovaniya udarnykh protsessov* (Investigations of Shock Phenomena), Moscow: Mashinostroenie, 1977.
4. Borovinskaya, I.P. and Pityulin, A.N., Fabrication of cermet FGMs with high impact resistance, *Proc. V Int. Symp. on FGM*, Kaysser, W.A., Ed., Dresden, 1998, pp. 134–139.
5. Aslamazashvili, Z., Zakharov, G., Oniashvili, G., and Iaklobidze, N., Preparation of graded materials by SHS, *Conf. on Prospective for Development and Practical Application of SHS in South Caucasus*, Book of Abstracts, Tbilisi, 2005, p. 34.

6. Tavadze, G.F.; Oniashvili G.Sh.,"Synthesis of Single Phase Intermetallics", *Int. Conf. on Modern Processes and Methods in Inorganic Materials Science*, Tbilisi, 2012, pp. 58–65.
7. Merzhanov, A.G. and Mukasyan, A.S., *Tverdoplamennoe gorenie* (Solid-Flame Combustion), Moscow: Torus Press, 2007.

SYNTHESIS AND FABRICATION OF Cu–W COMPOSITES COMBINING SHS AND HEC TECHNOLOGIES

S. V. Aydinyan[1,2], H. V. Kirakosyan[1], S. L. Kharatyan[1,2], A. Peikrishvili[3], G. Mamniashvili[4], B. Godibadze[3], E. Sh. Chagelishvili[3], D. R. Lesuer[5], and M. Gutierrez[6]

[1]Nalbandyan Institute of Chemical Physics, National Academy of Sciences, P. Sevak str. 5/2, Yerevan, 0014 Armenia
[2]Yerevan State University, A. Manukyan str. 1, Yerevan, 0025 Armenia
[3]Tsulukidze Institute of Mining and Technology, Tbilisi, Georgia
[4]Jazvakhishvili Tbilisi State University, Andronikashvili Institute of Physics
[5]Lawrence Livermore National Laboratory, Livermore, CA, USA
[6]Technalia Research Institute, San Sebastian, Spain

e-mail: sofiya.aydinyan25@gmail.com

W–Cu alloys have been growing industrial interest for superior thermal managing and as microwave materials due to the high thermal conductivity of copper and the low thermal expansion coefficient of tungsten [1]. W–Cu alloy parts are generally fabricated by Cu infiltration into W skeleton or liquid phase sintering of W–Cu powder mixtures [2]. However, because of the W–Cu system exhibits mutual insolubility, W–Cu powder compacts show very poor sinterability [3]. Physicomechanical properties of the composite largely depend on both microstructure and composition relating to fabrication methods and synthesis conditions.

In this work a new approach for the preparation of Cu-W composite materials was proposed, the essence of which is the joint reduction of tungsten and copper oxides by energy saving combustion synthesis or self-propagating high-temperature synthesis (SHS process) method [4] using Mg + C mixture as combined reducer. The latter will allow us to control the reaction temperature in a wide range, and perform the complete reduction of both oxides giving W–Cu composite powders in a controllable combustion mode. The combustion experiments in the CuO–WO_{3-x}Mg–yC quaternary system were performed based on the preliminary thermodynamic calculations made for that system, as well as considering the experimental results of binary and ternary systems. It has been shown that, at some certain amount of reducers and slow propagation of combustion wave, it becomes possible the joint and complete reduction of both oxides. According to XRD results, at optimal conditions combustion products contain only W, Cu, and MgO. After the acid treatment (10 wt HCl) of the product obtained at optimal conditions, it represents a desired W–Cu composite with submicron particle sizes. EDS analysis

certifies the homogeneity of the obtained W–Cu composite material with similar distribution of both metals.

W–Cu precursors developed by CS process were subjected to consolidation into cylindrical rods using hot explosive consolidation (HEC) technology and hot vacuum compaction (HVC) process. The consolidation temperature was changed up to 1000°C at the shock wave loading intensity under 10 GPa. The investigations showed that the fine W–Cu precursors obtained by combustion–coreduction process and their further explosive consolidation allows us to fabricate highly dense cylindrical billets near to theoretical density without cracks and uniform distribution of constituent phases. The consolidated samples are characterized by good integrity which depends on the distribution and size of the W and Cu particles. It was further established that the electrical properties (resistance and susceptibility) of the consolidated W–Cu composites depend on phase composition and density of the consolidated material.

It was demonstrated that combination of CS and HEC undoubtedly has advantages compared to other technologies and may be considered as an alternative way to fabricate novel Cu–W composites with enhanced properties.

Acknowledgment
The authors acknowledge the financial support of the International Science and Technology Center (ISTC Project # A-2123).

1. J.R. Davis, *Copper and Copper Alloys*, ASM International, 2001, p. 621.
2. A. Ghaderi Hamidi, H. Arabi, S. Rastegari, Tungsten–copper composite production by activated sintering and infiltration, *Int. J. Refr. Met. Hard Mater.*, 2011, vol. 29, pp. 538–541.
3. M. Amirjan, N. Parvin, K. Zangeneh-Madar, Mutual dependency of mechanical properties and contiguity in W–Cu composites, *Mater. Sci. Eng. A*, 2010, vol. 527, pp. 6922–6929.
4. A.G. Merzhanov, A.S. Mukasyan, *Tverdoplamennoe gorenie* (Solid Flame Combustion), Moscow: Torus Press, 2007.

COMPOSITE Cu–C COATINGS

T. Babul, M. Baranowski, and A. Olbrycht

Institute of Precision Mechanics, 3 Duchnicka St., Warsaw, 01-796 Poland

e-mail: michal.baranowski@imp.edu.pl

Carbon is the element that can exist in various allotropic forms with different properties. Graphite and diamond are the most known forms. For example, dark and non-transparent graphite is soft and well conducts electricity. In contrast, colorless mostly and transparent diamond is the hardest element that does not conduct electricity.

Recently graphene, a planar structure which consists of carbon atoms connected in hexagons, has become a very popular allotropic form. For a long time, it has been a theoretical material. The breakthrough came in 2004, when a group of researchers [1] obtained graphene with adhesive tape, repeatedly cleaving the layers from graphite. New material was subjected to numerous tests to determine its properties. The results were very promising, causing rapid increase in interest in graphene. The race in developing methods for graphene synthesis has started from that moment [1].

The properties of graphene make it a very promising material. Primarily due to the good thermal and electrical conductivity of graphene, it can be used, among others, in electronic equipment and heat exchangers. Graphene can also be combined with other materials. For example graphene in combination with other materials could cause or improve the thermal conductivity of such composites [1, 2].

Fig. 1. Powder of copper covered with graphene (Graphene $3D^{IMP}$).

Researches on the production of composites with graphene as a disperse phase are carried out at the Institute of Precision Mechanics. The Institute produces Graphene $3D^{IMP}$ composite material (Fig. 1), where graphene covers powders of copper. Graphene $3D^{IMP}$ can be produced in thermochemical processes, in which the Institute has many years of experience. The method for producing Graphene $3D^{IMP}$ is the compilation of several processes, including CarboTermoFluid® technology and the technology described in the patent application P.409141, 2014 [3, 4].

In the production of Graphene $3D^{IMP}$ fluidization processes are used. Thermochemical processes are carried out on the stand for fluidization produced by the Institute of Precision Mechanics. Gas flow provides fluidization in the working chamber, the process being assisted by vibrations. The process of nucleation and growth of carbon structures on the surface of the copper occurs through interaction of gases containing hydrocarbon which surrounds the particles of powder. A high temperature causes decomposition of hydrocarbons which are carbon source in the production of Graphene $3D^{IMP}$ [2].

The low cost of technological process opens up various possibilities for use of Graphene $3D^{IMP}$ in production of a new generation of advanced materials. Consolidation of the Graphene $3D^{IMP}$ powders affords to create a solid composite material consisting of a copper matrix and uniformly distributed graphene as the disperse phase. Copper powder covered with graphene may also be used for preparation of composite coatings. Coatings based on the Graphene $3D^{IMP}$ were prepared by Detonation Gas Spraying (DGS) method (Fig. 2).

Fig. 2. Composite Cu–C coating on Al substrate.

During DGS process pure copper is strongly oxidized. A large amount of oxides in the coating which appear between the Cu grains strongly reduces the uniformity of the coating and deteriorates joining with the substrate. The presence of the graphene on the surface of copper protects the powder particles from excessive oxidation. Obtained

composite coatings exhibited a compact structure with low porosity and improved adhesion compared to coatings sprayed with powder of pure copper.

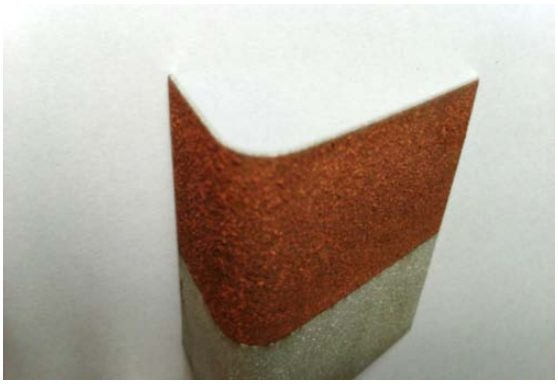

Fig. 3. Cu–C composite coating on the Al substrate after bending test.

A good solidity of the coating obtained from the Cu–graphene powder and the good joint with substrate were confirmed by bending test of coated Al plate. The sample was bended through an angle of 90 deg on a mandrel having a diameter of 10 mm. The study showed good adhesion and good formability (no cracks and scratches at the bend) of the sprayed coating (Fig. 3).

1. Novoselov K.S., Geim A.K., Morozov S.V., Jiang D., Zhang Y., Dubonos S. V., Grigorieva I.V., Firsov A.A., Electric field effect in atomically thin carbon films, *Science*, 2004, vol. 306, pp. 666–669.
2. Obuchowicz Z., Baranowski M., Babul T., Sobczak N., Kompozyty Cu–Grafen 3DIMP, *Inżynieria Powierzchni*, 2015, no. 2, pp. 10–14.
3. Babul T., Trzaska M., Jeleńkowski J., Wojciechowski A., Potencjał grafenu 3DIMP, *Logistyka*, 2015, no. 4, pp. 2282–2291.
4. Trzaska M., Babul T., Obuchowicz Z., Cieślak G., Production of graphene and nanocomposites of metal/graphene, *Abstr. Nano PL 2014 Conf. on Nanotechnology Adv. Mater. for Innovative Industry*, Kielce INNO TECH EXPO 2014, pp. 27–28.

METASTABLE STRUCTURES FORMED AT THE INTERFACE IN EXPLOSIVELY WELDED MATERIALS

I. A. Bataev[1], S. Tanaka[2], I. D. Kuchumova[1], O. E. Matts[1], D. V. Lazurenko[1], K. Hokamoto[2], and A. A. Bataev[1]

[1]Novosibirsk State Technical University, pr. K. Marksa 20, Novosibirsk, 630073 Russia
[2]Kumamoto University, 2-39-1 Kurokami, Chuo-ku, Kumamoto, 860-8555 Japan

e-mail: i.bataev@corp.nstu.ru

The properties of explosively welded (hereinafter exploclad) materials significantly depend on the structure of the interface. The material at the interface experiences significant plastic deformation taking place within a very short time period. Severe plastic deformation and heat phenomena provide the formation of vortex zones at the interface [1]. In this research, we explored the structure of the vortexes in Nb–stainless steel, Zr–Cu, Zr–Ni, Ti–Ni, Ti–Cu, and some other exploclad combinations.

Exploclad metals were characterized by TEM, SEM, and EDX. We show that several types of structures may appear in the vortexes depending on thermodynamic parameters and atomic size ratio of exploclad materials.

(a) When immiscible materials are joined (positive heat of mixing), the vortexes appear as extremely fine suspension of one component in the other. Typically, a low-melting component acts as a matrix, while the fine spherical precipitations of high-melting components are distributed in such a matrix. (b) When materials with nearly zero heat of mixing are welded, the solid solutions are formed at the vortexes. (c) When the heats of mixing of the welded materials are strongly negative, the intermetallic compounds are formed at the interfaces.

It should be noted, that the intermetallics formed at the interfaces may have crystalline, quasi-crystalline or amorphous arrangement of atoms [2–4]. This depends on several factors, such cooling rate, vortex composition, heat of mixing, etc. The crystalline and quasi-crystalline intermetallics produce negative effect on the weld brittleness, while amorphous intermetallics improve the ductility. By controlling of the welding parameters and choosing suitable interlayers, one may control the structure of the vortexes and properties of the weld seams. The effect of heat treatment on structural transformations in the vortexes [5] will be discussed at presentation.

1. Bataev, I.A. et al., Formation and structure of vortex zones arising upon explosion welding of carbon steels, *Phys. Met. Metallogr*, 2012. vol. 113, no 3, pp. 233–240.

2. Bataev, I.A. et al., Explosively welded multilayer Ni–Al composites, *Mater*. *Design*, 2015. **88**: p. 1082-1087.
3. Bataev, I.A. et al., Metallic glass formation at the interface of explosively welded Nb and stainless steel, *Met. Mater. Int*., 2015, vol. 21, no. 4, pp. 713–718.
4. Malyutina, I.N. et al., Structure and Microhardness of Cu-Ta Joints Produced by Explosive Welding, *Sci. World J*., 2013.
5. Bataev, I.A. et al., Nucleation and growth of titanium aluminide in an explosion-welded laminate composite, *Phys. Met. Metallogr,* 2012, vol. 113, no. 10, pp. 947–956.

FABRICATION OF HEAT-RESISTANT CERAMIC CRUCIBLES FOR MELTING ALLOYED STEELS AND NON-FERROUS METALS BY ALUMINOTHERMIC SHS

V. M. Batrashov, Ch. G. Pak, and D. O. Gus'kov

Penza State University, ul. Krasnaya 40, Penza, 440026 Russia

e-mail: shift150887@mail.ru

Existing methods for fabrication of ceramic crucibles for melting alloyed steels and non-ferrous metals involve the stages of drying and calcining at temperatures up to 1600°C), in contrast to SHS technology [1] using the energy released in exothermic reactions. As is known, SHS-produced ceramics take advantage of their low production cost, good mechanical strength (above 40 MPa), heat resistance (up to 2000°C), good resistance to cyclic thermal loading (above 50 thermal cycles), and high slag-resistance [2, 3].

In experiments, we used green powder composites containing Al powder, aluminosilicate oxidizers (SiO_2, Al_2O_3, Cr_2O_3, Fe_2O_3, etc.), fillers, and silica gel binders. The resultant items exhibited good mechanical strength (due to high-temperature sintering), high magnetic permeability (constituents without intrinsic magnetic field), good slag-resistance (due to proper composition), good resistance to cyclic loading (50 thermal cycles), and a heat resistance of up to 2000°C. Other details will be reported at presentation.

1. A. G. Merzhanov, A. S. Mukasyan, *Tverdoplamennoe gorenie*, Moscow: Torus Press, 2007.
2. Ch.G. Pak, S.V. Skiba, P.I. Serov, Protective ceramic coatings for refractory materials by the method of self-propagating high-temperature synthesis, in *Abstr. X Int. Symp. on SHS*, Tsakhkadzor (Armenia), 2009, pp. 328–329.
3. Ch.G. Pak, S.V. Skiba, P.I. Serov, Protective ceramic coatings for refractory materials by SHS method, in *Proc. All-Russia Conf. on Construction Materials Science*, Chelyabinsk, 2010, pp. 79–81.

ABNORMAL MASS TRANSFER IN CONDITIONS OF SHOCK LOADING

A. F. Belikova, S. N. Buravova, and E. V. Petrov

Institute of Structural Macrokinetics and Materials Science, Russian Academy of Sciences, Chernogolovka, Moscow, 142432 Russia

e-mail: svburavova@yandex.ru

Studies on the mobility of atoms (by radioactive isotopes) in conditions of shock loading demonstrated the occurrence of enhanced mass transfer in metals [1]. Under such conditions, the atomic diffusivity in solids turned greater than that in liquids and compared with the coefficients in the solid state by 6–7 orders of magnitude. Abnormal was also the behavior of mobility: it grew with decreasing temperature; a densely packed *fcc* crystal lattice better penetration of radioactive isotopes compared to a loose *bcc* one. A correlation between the durations of atomic migration and shock wave action has been a subject of vivid discussion for over past decades.

Our analysis of the literature cited in [1] has revealed that the samples subjected to high-speed straining often exhibit the adiabatic shear bands that are the precursors of material failure. According to our previous results [2], loading with a planar shock wave does not result in the localization of strains. It follows that the deep penetration (mass transfer) of radioactive isotopes into solids can be associated with their failure.

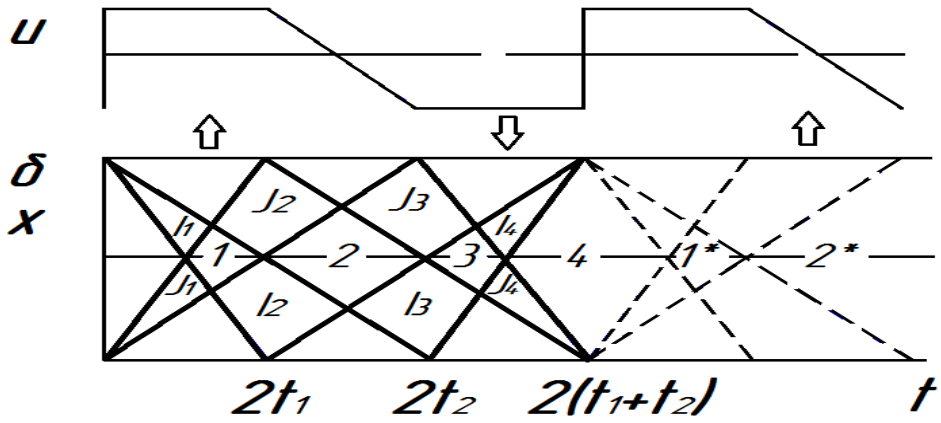

In terms of spall model for strain localization, the bands of adiabatic shear are formed upon the rarefaction waves interference, and without material failure [2]. In essence, the localization bands represent the unaccomplished spall cracks. As is seen in

the *x–t* diagram (see below), a characteristic feature of high-speed stretching within the bands *of localized deformation* (but not within spall cracks!) is the reverberation (circulation) of the load and rarefaction waves, that is *accompanied by periodic compression/tension cycles of material loading*.

Reverberation increases the duration of loading more than one order, compared with the time of the load pulse. Due to the above reverberations, the duration of vibrations in the zone of interference exceeds that of shock loading by 2–3 orders of magnitude, which provides conditions for abnormally fast mass transfer of embedded atoms.

Our results can be expected to shed new light on the mechanism of high-speed mass transfer at negative pressures developed in conditions of shock loading.

1. D.S. Gertsriken, A.I. Ignatenko, V.F. Mazanko, O.A. Mironov, V.M. Falchenko, G.K. Kharchenko, Determination of the mass transfer duration and temperature of the pulse deformable metal, *Phys. Met. Mater.*, 2005, vol. 99, no. 2, pp. 75–81.
2. A.F. Belikova, S.N. Buravova, E.V Petrov. Strain localization under dynamic loading, *Tech. Phys.*, 2013, vol. 58, no. 8, pp. 1152–1158.

$NiAl/Cr_2O_3$ COMPOSITE BY THERMAL EXPLOSION

O. D. Boyarchenko, A. E. Sytschev, L. M. Umarov, A. S. Shchukin, I. D. Kovalev, and M. A. Sichinava

Institute of Structural Macrokinetics and Materials Science, Russian Academy of Sciences, Chernogolovka, Moscow, 142432 Russia

e-mail: olgaboyarchenko@gmail.com

Along with Ni, Al and their alloys [1], fine powders of SiO_2, Al_2O_3, Cr_2O_3 find their application in aerospace industry [2].

In this work, we attempted to synthesize $NiAl/Cr_2O_3$ composite by combustion synthesis [3] in a mode of thermal explosion (TE) by the following overall reaction scheme:

$$Ni + Al \rightarrow NiAl$$
$$Cr_2O_3 + 2Al \rightarrow 2Cr + Al_2O_3$$
$$xNi + 3Al + Cr_2O_3 \rightarrow NiAl + Al_2O_3 + 2Cr + (x - 1)Ni$$

Cylindrical $Ni–Al–Cr_2O_3$ compacts (d = 12 mm) were placed in a reactor and heated under 1 atm of Ar until initiation of TE.

Combustion products were characterized by optical microscopy, SEM, XRD, and mechanical testing. Some results are presented in Figs. 1–3. Bright areas correspond to NiAl, Cr or solid solution NiAl[Cr], a dark-gray network to Al_2O_3, and dark areas to pores.

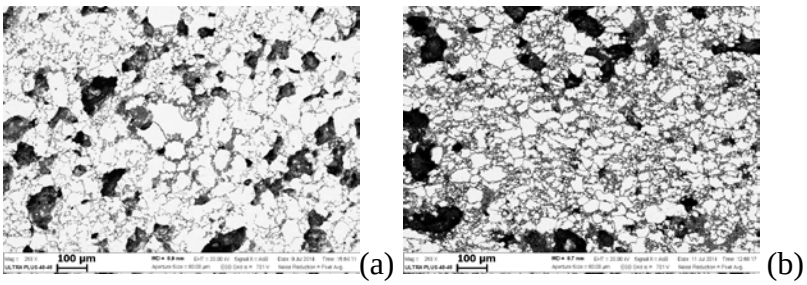

(a) (b)

Fig. 1. Microstructure of the composites derived from green compacts containing 10 (a) and 30 wt % Cr_2O_3 (b).

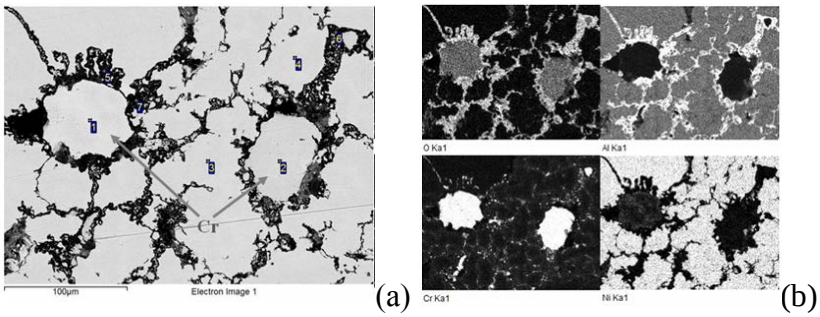

(a) (b)

Fig. 2. (a) SEM image and (b) elemental maps of O, Al, Cr. and Ni for the composite derived from Ni + Al + 10 wt % Cr_2O_3 compact.

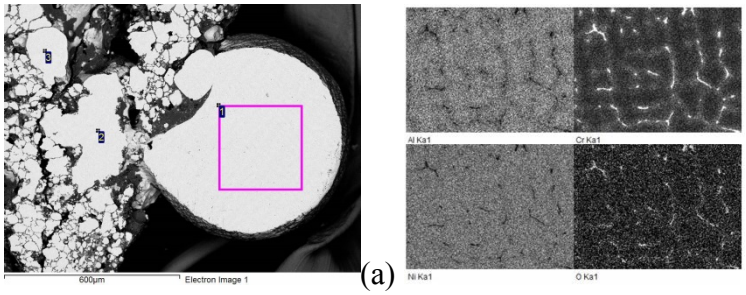

(a) (b)

Fig. 3. (a) Microstructure and (b) elemental maps of spherical Cr_2O_3 globules formed in the composite derived from green compacts containing 20 wt % Cr_2O_3.

The synthesized materials represent a class of NiAl-matrix composites containing the inclusions of Cr, NiAl[Cr] soild solution, and Al_2O_3. Our technique can be applied to fabrication of NiAl[Cr] solid solutions dispersion-strengthened with Cr_2O_3 globules.

1. *Aerospace Materials Handbook*, Zhang, S. and Zhao, D., Eds., Taylor & Francis, LLC, 2013, pp. 415–461.
2. C.L. Yeh, J.Z. Lin, Combustion synthesis of Cr–Al and Cr–Si intermetallics with Al_2O_3 additions from Cr_2O_3–Al and Cr_2O_3–Al–Si reaction systems, *Intermetallics*, 2013, vol. 33, pp. 126–133.
3. *Combustion Synthesis: Novel Routes to Novel Materials*, Lackner, M., Ed., Bentham Science, 2010.

DETONATION SYNTHESIS OF NANOPARTICLES: A FLOW-REACTOR MODEL

V. B. Bozhevolnov[1], Yu. V. Bozhevolnov[2], A. M. Yafyasov[1], and M. C. Archipov[1]

[1] St. Petersburg State University, ul. Ulyanovskaya 3, St. Petersburg, 198504 Russia
[2] Moscow State University, Moscow, 119991 Russia

e-mail: vladislav.bogevolnov@gmail.com

The emergence of carbon polytypes are traditionally associated with nucleation of the sp^3 phase in the high-pressure zone and the temperatures reached in the area of the detonation front in explosives with an excess of carbon [1]. The duration of exposure determines the mean size of resulting particles [2], and a set of medium parameters defines their size distribution. Relaxation processes in the detonation synthesis is traditionally viewed as destructive [2–5]. In this paper, we propose to consider [6, 7] the process of nano-particles formation from the standpoint of the theory for evolution of non-equilibrium systems.

An example of a constructive process of relaxation in the vicinity of the phase transition point is spinodal decomposition [8]. In this case the relaxation of carbon's non-equilibrium state at every point of the space leads to appearance of substantially different stable phases.

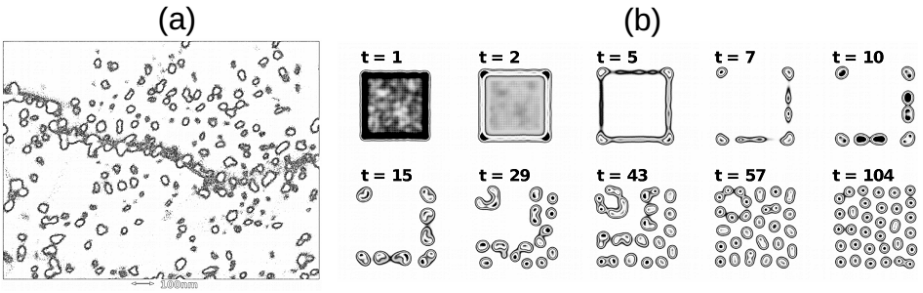

Fig. 1. (a) Typical image of the carbon generated by detonation of explosive and (b) the time evolution of the structures; the Grey–Scott model with parameters G = 0.02 and k = 0.06 (source: http://stemblab.github.io/gray-scott/).

Figure 1a shows the image obtained by edge determination of contours in a the SEM images taken in secondary electrons. White spots correspond to the aggregates of the sp^3 phase which was then extracted by chemical oxidation [3]. It is notable that the size distribution of the sp^3-carbon is discrete (see Fig. 1). Furthermore, the mean

separation between nearby spots remains unchanged despite chaotic distribution of the spots.

To qualitatively model the situation, we considered the autocatalytic mechanism of patterning at constant pressure and temperature. In this case, the role of the reactor is played by the area of chemical transformation in the detonation wave. Accordingly, the velocity of the inflow and outflow of reagents into and out of the reactor is assumed to the velocity of detonation front propagation. We considered the following reaction scheme:

$$A + 2B \rightarrow 3B \quad (1)$$
$$B \rightarrow C \quad (2)$$

where A, B and C (inert product) are the reagents described by the Gray–Scott equations [9]:

$$\frac{\partial u}{\partial t} = r_u \Delta u - uv^2 + G(1-u),$$
$$\frac{\partial v}{\partial t} = r_v \Delta v + uv^2 - (G+k)v,$$

where u and v stand for concentrations of reagents A and B, respectively, r_u and r_v are the respective speeds of diffusion, k is the rate of reaction (2), and G is the inflow and outflow rate for reagents A, B and C (inert agent).

Solutions to these equations describe the structure of the aggregates of varied geometry [10–12], both motionless and mobile with respect to the reactor. An example of the tine evolution of these structures ($0 < t < 104$) is shown in Fig. 1b. Narrow size distribution of the spatial structures can be explained by the fact that the particle size is defined by some balance between its surface energy and internal energy. In contrast to the nucleation model, the duration of loading leads to an increase in the number (not size) of the sp^3 phase.

Thereby a comparison of the qualitative results of the quantitative modeling of the process of the non-equilibrium environment self-organization with the structure of the detonative carbon soot has shown that

It follows that in order to explain the granulometric characteristics of self-organized carbon polytypes it is necessary to use evolution models in conditions far from thermodynamic equilibrium. The Grey-Scott model has shown a good qualitative match with experiment at constant pressure and temperature. Our model can be readily used to describe the processes of detonation-driven transformation of explosives.

1. V.V. Danilenko, On the history of the discovery of nanodiamond synthesis, *Solid State Phys.*, 2004, vol. 46, no. 4, pp. 595–599.

2. V.V. Danilenko, Nanodiamonds: Problems and prospects, *J. Superhard Mater*., 2010, vol. 5, pp. 301–310.
3. V.Y. Dolmatov. *Detonation Nanodiamonds*, St. Petersburg: NPO Professional, SPb), 2010 (in Russian).
4. P.A. Vityaz, V.I. Zhornik, A.F. Ilyushchenko, et al., *Detonation Nanodiamonds*, Minsk: Belarusian Navuka, 2013 (in Russian).
5. L.F. Vereschagin, E.N. Yakovlev, L.M. Buchnev, B.K. Dymov. Terms of diamond thermodynamic equilibrium with various carbon materials, *Vys. Temp*., 1977,vol. 15, no. 2, pp. 316–321.
6. Y.V. Bozhevolnov, V.B. Bozhevolnov, A.M. Yafyasov, Formation of carbon structures with nanometer scale with characteristic relaxation chemically activated plasma, in *Proc. VII Int. Conf. on Amorphous and Microcrystalline Semiconductors*, St. Petersburg, 2010, pp. 162–163.
7. Y.V. Bozhevolnov, V.B. Bozhevolnov, A.M. Yafyasov, Structurization of nanocarbon upon relaxation of chemically activated plasma, in *Proc. XI Int. Symp. on Explosive Production of New Materials,* edited by A.A. Deribas and Yu.B. Scheck, 2012, pp. 23–25.
8. V.P. Skripov, A.V Skripov, Spinodal decomposition (phase transition involving unstable states), *Sov. Phys. Usp*., 1979, Vol. 22, pp. 193–231.
9. P. Gray, S. K Scott, Autocatalytic reactions in the isothermal, continuous stirred tank reactor: Oscillations and instabilities in the system $A + 2B \rightarrow 3B$, $B \rightarrow C$, *Chem. Eng. Sci*., 1984, vol. 39, no. 6, pp.1087–1097.
10. J. Pearson, Complex patterns in a simple system, *Science*, 1993, vol. 261, pp. 89–192 (available at arXiv.org: patt-sol/9304003).
11. K.J. Lee, W.D. McCormick, Q. Ouyang, H.L. Swinney, Pattern formation by interacting chemical fronts, *Science*, 1993, vol. 261, pp. 192–194.
12. R. Munafo, Stable localized moving patterns in the 2D Gray–Scott model, 2014 (arXiv: abs/1501.01990).

LE CHATELIER PRINCIPLE AND SPALL DAMAGEABILITY

S. N. Buravova and N.I. Mukhina

Institute of Structural Macrokinetics and Materials Science, Russian Academy of Sciences, Chernogolovka, 142432 Russia

e-mail: svburavova@yandex.ru

EDS analysis on the carbon of steel surface in the vicinity of a spall crack afforded to discern the presence of a carbon-lean metal layer 30–40 μm thick and a thin carbon-rich layer adjacent to the fracture zone. The spall crack is formed in the interference zone of the end unloading waves. The presence of the carbon-lean layer shows that carbon migrates from the surrounding area to the damage area. Oxygen dissolved in the starting material also migrates to the region of damaged material generated during high-speed deformation (Fig. 1a). The migration hardening microparticles leads to their location on the shore of the spall fracture (Fig. 2b). The impact of tensile stress leads to change in equilibrium, pressure, temperature, and phase composition. According to the Le Chatelier principle, the system tends to cure the defect arising in the destruction process.

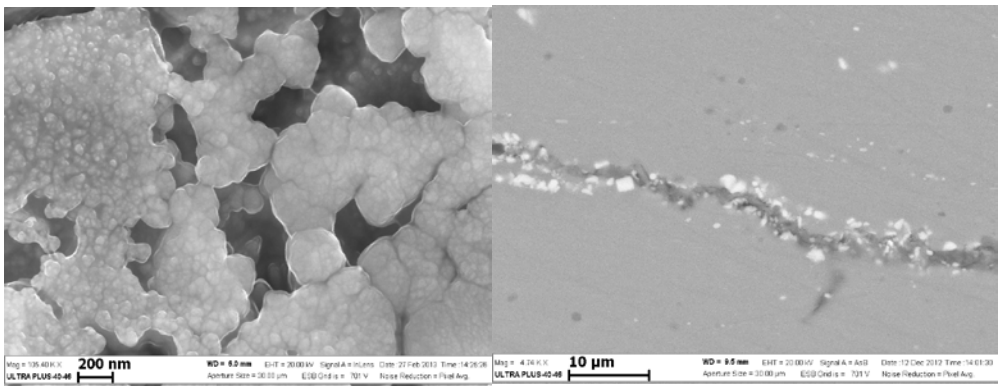

Fig. 1. (a) The nuclei of copper oxide formed on spall crack fragments and (b) the segregation of hardening elements in the aluminum alloy.

In the vicinity of the spall damage area, perlite decomposes and the flux of carbon atoms migrates toward the destruction zone. This is accompanied by mass transport of dissolved oxygen and alloying particles.

SPHEROIDIZATION OF PERLITE IN THE BANDS OF LOCALIZED DEFORMATION

S. N. Buravova, E. V. Petrov, and A. S. Shchukin

Institute of Structural Macrokinetics and Materials Science, Russian Academy of Sciences, Chernogolovka, Moscow, 142432 Russia

e-mail: svburavova@yandex.ru

Figure 1a shows the overall view of the band of localized deformation formed upon shock loading of a steel target. The constituent elements are characterized in the figure caption. The developed crater-like failures (3 in Fig. 1a) are formed on the concentrators (defects) present in starting material. Micro pores (4 in Fig. 1) in strongly deformed material can be regarded as the fracture nuclei arising in the course of rapid straining.

(a) (b)

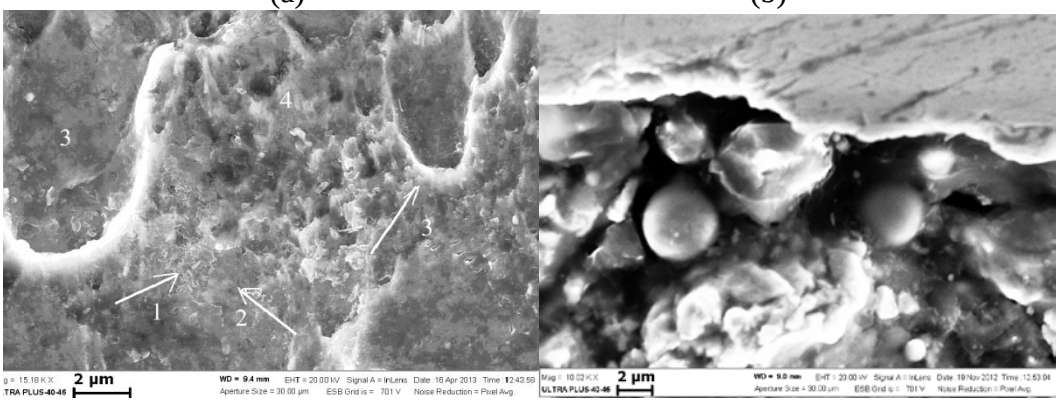

Fig. 1. (a) Band of localized deformation: 1, crashed cementite platelets; 2, fine ferrite particulates (<200 nm); 3, failure craters formed at material defects; 4, micro pores; and (b) spheroidal perlite particles formed within the bands of localized deformation.

An increase in the amplitude of incident shock waves, the microstructure of the spall zone changes and the size of perlite globules attains a value of 2–3 μm (Fig. 1b).

Note that, at normal conditions, the spheroidization of perlite requires by 5–7 orders of magnitude longer times than in conditions of dynamic loading or at high temperatures. So high rate of the process in the bands of localized deformation (i.e. only slightly above the room temperature) deserves further investigation.

EXPLOSIVE WELDING OF PIPES

O. A. Burtseva, A. O. Drennov, and O. B. Drennov

All-Russian Scientific Research Institute of Experimental Physics—Russian Federal Nuclear Center, pr. Mira 37, Sarov, 607188 Russia

e-mail: o.a.burtseva@gmail.com

Using various technological schemes, explosive welding can be employed for production of bimetal and multilayer pipes, clad cylindrical blanks, etc. [1]. When cladding pipes, choice of inert filler is of great importance. The basic requirements for the inert filler are the following. Simplicity of bringing filler into pipe channel should be provided, removal of it from the channel after dynamic loading should not be unnecessarily difficult. The most important requirement is that reliable resistance against radial converging deformations should be provided, i. e. the internal diameter of pipes should be actually unchanged after pulse effect.

Presently, as a filler capable to restrain radial deformations, monolithic steel cylinders of certain design facilitating removal of them from pipe cavity after dynamic loading are used [2]. However, use of steel fillers is limited by sizes of welded pipes. So, weight of such filler is $M \geq 100$ kg at pipe diameter of ≈ 0.5 m.

We suggest to perform explosive welding of pipes according to the following scheme, see Fig. 1.

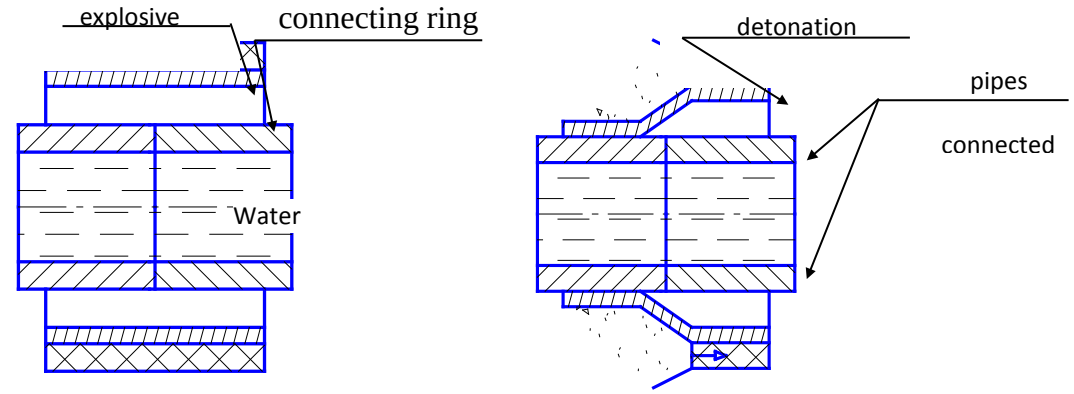

Fig. 1. Scheme of explosive welding of pipes with use of water as filler.

Ends of two pipes are connected. “Ring” is mounted above the joint place. HE charge is placed on the external surface of the ring. The basic problem is here elimination of strains and reduction of pipe diameter in the area of dynamic effect.

The following method is suggested for elimination of strains. Volume of pipes in the area adjacent to the zone of explosive welding is totally filled with water. (The principle of liquid non-compressibility at quasistatic loading will be used.) Area for filling should be chosen to be sufficient in pipe length for providing immobility of water mass for time before completion of welded joint formation and removal of pulse loading. After impact of the ring against surfaces of pipes, shock waves are propagating in filling water. The shock waves are collided near the pipe axis and are reflected. The process is repeated, when reflected waves reach the internal surfaces of pipes. 3–5 circulations of shock waves occur before complete attenuation of dynamic pulse and smoothing of increased pressure.

For time of circulation of shock waves, the perturbations, which are moving in water in the axial direction with sound velocity, should not reach the free boundary of the water volume. In this case, its mass will be kept quiet, non-deformed.

The model experiments were performed using the simplified scheme. We used segments of steel pipes having internal diameters of 114 mm, wall thickness of 6.5 mm. Thickness of the welded layer made of steel was 3 mm; thickness of HE layer (a mixture of ammonite 6ZhV with ammonium nitrate in the 50/50 ratio) was 25 mm.

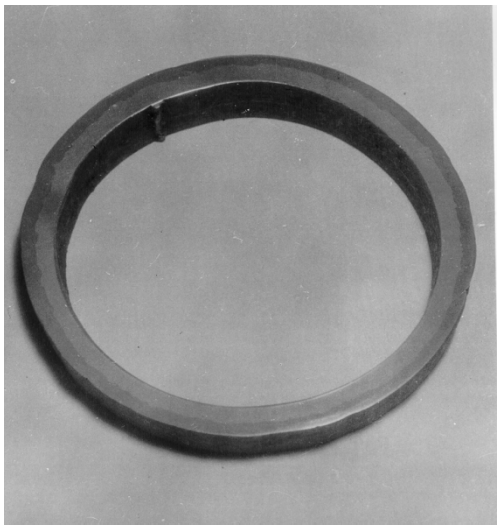

Fig. 2. Cross-section of two pipes connected by explosive welding. Deformation of the pipes (reduction of the internal diameter) was less than 2%.

Three experiments were performed. In these experiments we got reliable welded connection of the ring and pipe in the regime of 2.0 km/s $\leq v_c \leq$ 2.3 km/s; $20 \leq \gamma \leq 26°$.

After the experiments, the experimental assemblies were cut (in the zone of explosive welding). Figure 2 presents a photo of the bimetal steel ring produced by explosive welding.

1. Krupin A.V., Solov'ev V.Ya., Sheftel'N.I., et al., *Deformation of Metals by Explosion*, Moscow: Metallurgiya, 1975 (in Russian).
2. Kudinov V.M., Koroteev A.Ya. *Explosive Welding in Metallurgy*, Moscow: Metallurgiya, 1978 (in Russian).

FORMATION OF METAL-OXIDE NANOPARTICLES FROM CONDENSED DETONATION PRODUCTS: MODELLING AND EXPERIMENT

J. Campos, R. Mendes, J. Quaresma, and J. Pimenta

ADAI–Association for the Development of Mechanical Engineering, LEDAP–Laboratory of Energetics and Detonics, Department of Mechanical Engineering, University of Coimbra, Rua Luis Reis Santos, Coimbra, 3030-788 Portugal

e-mail: andrade.campos@dem.uc.pt

The method for predicting ceramic detonation products, from the reaction between metal and nitrated explosives, was presented in several symposia. Recently this study has progressed in order to accurately predict ceramic condensed products of detonation, not only of metal/oxidants reactants but also from metal nitrate precursors, generally hydrated ones. Modelling method starts using a thermochemical computer code, named THOR, assuming the thermodynamic equilibria for all the possible compounds, including condensed and intermediary species. These calculations require a large database (THOR DB), including Gordon and McBride (G&McB) polynomial coefficients, for gas and condensed transient and final products of detonation. The influence of an appropriated equation of state, for solid products, was discussed and optimized in previous works. The choice of an accurate model to be used in high pressure, high temperature simulations is essential to ensure better prediction of energetic substances performances and constitutes a major difficulty. This study starts with empirical equations used to describe graphite and diamond properties, based in relations between pressure and specific volume. Recently, these numerical predictions was optimized and discussed evaluating the formation and final concentration of metal oxides, in condensed species of the final products of detonation. The most known metal oxide, from detonation products formation, is alumina. A similar approach, using Cowan–Fickett optimized constants, were also applied to zirconia, titania, and magnesia. Using Cowan–Fickett modelling, considering Slatter–Dugdale–MacDonald and Vadchenko–Zubarev formulations, has led to a final presented and discussed calculation of Grüneisen parameters, to be used in THOR code.

Once achieved the prediction of condensed species in products of detonation, a new complementary problem must be solved: the interactions between the detonation products phenomena and particulate formation, coexisting with the evaluation of hydrodynamics of shock effects in order to predict final particle size distribution.

Experiments were performed using ammonium nitrate emulsion explosive and pure metal reactants, or metal-nitrated precursors. Ignition and reactants selection were

defined to reduce contaminants in the final products. Detonation measuring techniques, using optical fibers and sensors, allows us to optimize models and detonation products compositions. The collected metal oxide particles, cleaned sometimes with an aqueous solution of nitric acid and its particle size distribution was evaluated. The formation of metal oxide particles was assumed for the post detonation zone. It starts from an initial cluster of nanocrystals. This cluster was synthesized, at the end of the detonation products expansion, mainly as a function of detonation temperature. The detonation temperature is one of the more relevant parameter, it can be related to metal oxide melting temperature, conditioning the final synthesized particles from initial cluster of nanocrystals.

EFFECT OF ALUMINIUM TEMPERING ON THE QUALITY OF EXPLOSIVE WELDING

G. Carvalho[1], R. M. Leal[1,2], I. Galvão[1,3], R. Mendes[4], J. B. Ribeiro[4], and A. Loureiro[1]

[1]CEMUC, Department of Mechanical Engineering, University of Coimbra, Rua Luis Reis Santos, 3030-788 Coimbra, Portugal
[2]ESAD.CR, Polytechnic Institute of Leiria, Rua Isidoro Inácio Alves de Carvalho, 2500-321 Caldas da Rainha, Portugal
[3]ISEL, Department of Mechanical Engineering, Polytechnic Institute of Lisbon, Rua Conselheiro Emídio Navarro, 1959-007 Lisbon, Portugal
[4]ADAI–Association for the Development of Mechanical Engineering, LEDAP–Laboratory of Energetics and Detonics, Department of Mechanical Engineering, University of Coimbra, Rua Luis Reis Santos, 3030-788 Coimbra, Portugal

e-mail: altino.loureiro@dem.uc.pt

Explosive welding is a solid-state joining technology of current interest for several industrial sectors. This process, which consists of a detonation of an explosive on the surface of a flying plate promoting its projection against the base plate at a very high velocity (Fig. 1), enables the welding of various similar and dissimilar metals, most of them impossible to be joined by conventional fusion welding [1–3]. Owing to its ability to distribute the high energy density through explosion, this process also takes advantage of enabling joining with substantially higher surface areas than other technologies [1].

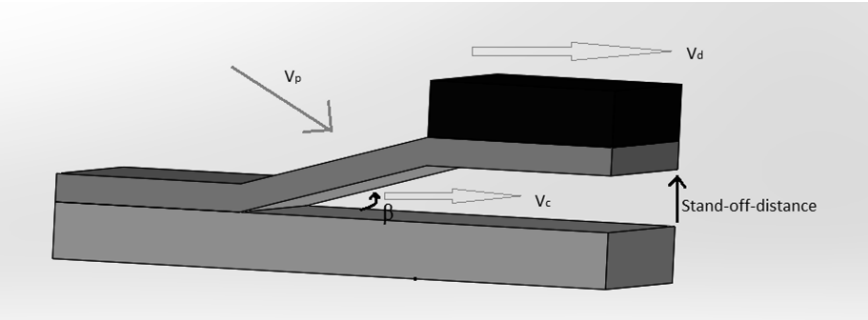

Fig. 1. Schematic of explosive welding.

The aim of this research is to study the influence of the material tempering on the final properties of partially overlapping welds ща 3-mm AA6082-O and AA6082-T6 plates. The plates (120 × 95 mm0 were assembled in parallel with a partial overlapping

of 40 mm. According to the base materials used to produce the welds, two different weld series were produced. Similar welding conditions were used to produce both weld series. Specifically, the explosive used in the welding tests was an ammonium nitrate-based explosive emulsion sensitized with hollow glass microspheres. The sensitizer was composed of particles with an average diameter of about 40 μm. The density of the explosive was 760 kg/m^3 and the detonation velocity was of about 3.4 km/s.

Analysis of the weld surface enabled to observe that all the joints displayed a homogenous appearance throughout the weld length. In turn, the morphological characterisation of the internal structure of the welds showed the formation of well-defined waves at the interface. Micrographs illustrating the morphology of the waves are displayed in Fig. 2. Formation of micro-fusion areas in the vicinity of the waves was observed for both weld series (weld EW1 in Fig. 2a and weld EW2 in Fig. 2b).

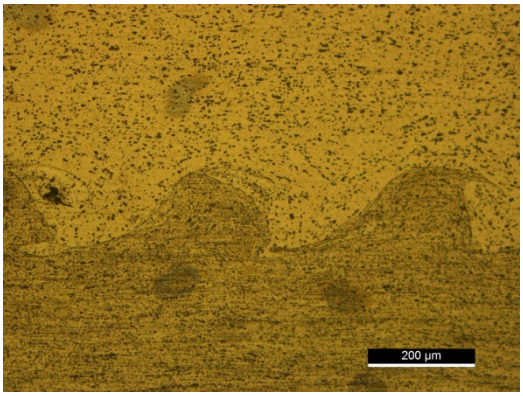

Fig. 2a. Wave morphology of weld EW1.

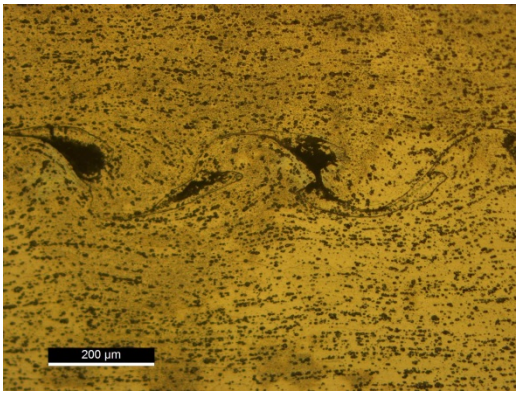

Fig. 2b. Wave morphology of weld EW2.

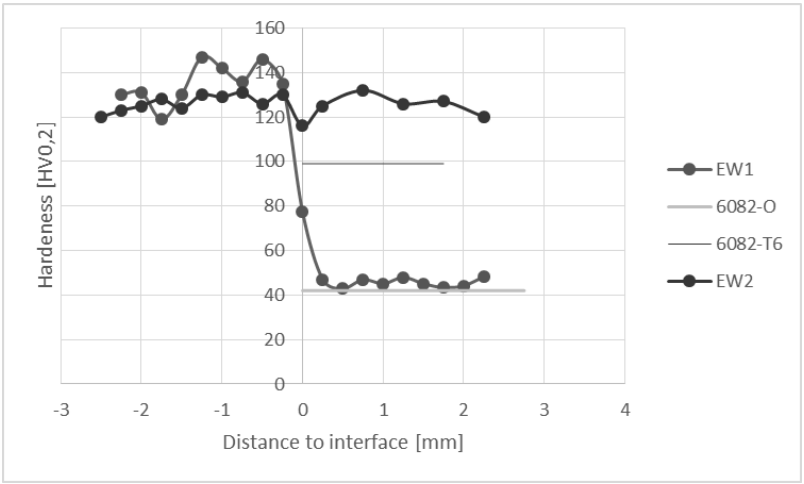

Fig. 3. In-depth hardness profiles.

Hardness values measured along the thickness of the welds are displayed in Fig. 3. The average hardness of the base materials, AA6082-O and AA6082-T6, are also represented in the figure. As follows from Fig. 3, the different weld series exhibit distinct hardness profiles. In fact, an increase in hardness relative to the base material was registered for the weld series EW2. It can also be observed that the hardness variation is roughly the same in the base plate and the flyer. On the other hand, substantial differences were observed between the hardness of the flyer and the base plate in welds EW1. The hardness registered in the flyer was thrice of that registered in the base plate.

1. F. Findik, Recent developments in explosive welding, *Mater. Design*, 2011, vol. 32, pp. 1081–1093.
2. V.I. Lysak, S.V. Kuzmin, Lower boundary in metal explosive welding: Evolution of ideas, *J. Mater Process. Technol*., 2012, vol. 212, pp. 150–156.
3. R. Mendes, J.B. Ribeiro, A. Loureiro, Effect of explosive characteristics on the explosive welding of stainless steel to carbon steel in cylindrical configuration, *Mater. Design*, 2013, vol. 51, pp. 182–192.

EXPLOSIVE WELDING OF ALUMINUM AND COPPER: EFFECT OF BASE PLATE MATERIAL

G. Carvalho[1], R. M. Leal[1,3], I. Galvão[1,4], R. Mendes[2], J. B. Ribeiro[2], and A. Loureiro[1]

[1]CEMUC, Department of Mechanical Engineering, University of Coimbra, Rua Luis Reis Santos, 3030-788 Coimbra, Portugal
[2]ADAI – Association for the Development of Mechanical Engineering, LEDAP – Laboratory of Energetics and Detonics, Department of Mechanical Engineering, University of Coimbra, Rua Luis Reis Santos, 3030-788 Coimbra, Portugal
[3]ESAD.CR, Polytechnic Institute of Leiria, Rua Isidoro Inácio Alves de Carvalho, 2500-321 Caldas da Rainha, Portugal
[4]ISEL, Department of Mechanical Engineering, Polytechnic Institute of Lisbon, Rua Conselheiro Emídio Navarro, 1959-007 Lisbon, Portugal

e-mail: altino.loureiro@dem.uc.pt

The fusion welding of copper and aluminum alloys is very difficult due to the difference in melting temperatures of the two materials and their chemical affinity. The explosive welding overcomes these problems as shown by several authors [1, 2]. The literature shows however that the interface morphology of these welds is very different from that observed in explosion welds between different materials but of the same family, that is for example between stainless steel and carbon steel [3]. In the latter case there is the appearance of more or less regular waves at the interface of the two materials, instead of bonds between Cu and Al, where the formation of pockets of melted material, not properly waves is observed [4].

The purpose of this investigation is to make a comparative analysis of welds on which the flyer is of the same material, copper, but the base plate is either aluminum (dissimilar welding) or copper (similar materials).

The flyer was 1 mm thick in both cases and the base plate was 3 mm thick. In both cases we used an emulsion explosive (EEx) sensitized with hollow glass microspheres (HGMS) in a ratio of about 15% and an explosive ratio—the ratio between the mass of explosive (C) and the mass of the flyer (M)—of 2.1, in a parallel configuration, with the plates partially overlapping, and a stand-off distance of 1.35 mm. The detonation velocity (Vd), impact velocity (V_c) as well as the angle of impact (β) between the flyer and base plate are indicated in Table 1.

Figure 1 illustrates the morphology of the weld Cu–Cu interface. Figure 1a shows the presence of regular waves with amplitudes on the order of 66 μm and wavelength

about 120 μm. The size of the waves at the end of the weld tends to increase due to the effect of inertia. Figure 1b is a detail of one of these waves where the melting of metal occurred. These areas have solidification morphology and are marked with arrows in the image. In the center of some of these zones the presence of cavities resulting from shrinkage during solidification was noted.

Table 1. Detonation velocities, impact velocities as well as β angles of the welds.

Pair	Explosive ratio C/M	V_d = V_c [m/s]	V_p [m/s]	β [deg]
Cu–Cu	2,1	3430	851	14.3
Cu–Al	2,1	3551	758	12.3

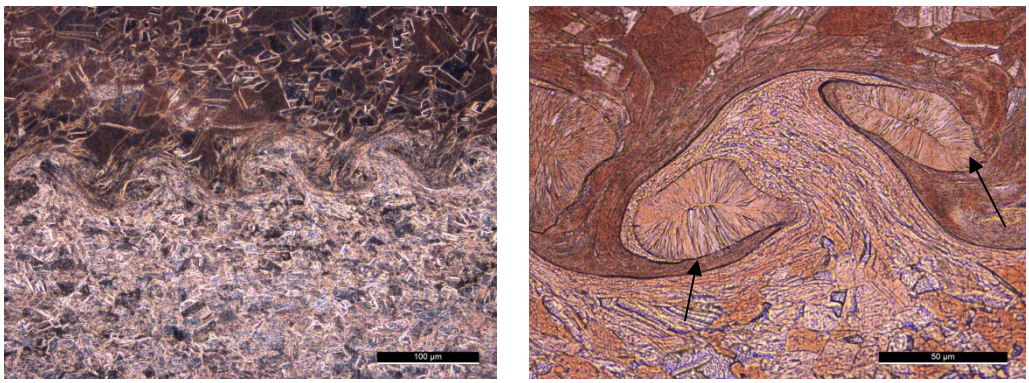

(a) (b)

Fig. 1. Morphology of the Cu–Cu weld: (a) ×50 and (b) ×200.

The weld Cu–Al exhibits a completely different morphology (Fig. 2). The upper part of the images corresponds to copper while the lower one, to aluminum. There is a lack of waves at the interface, however it exhibits the presence of intermittent melted areas, indicated an arrow in Fig. 2a.

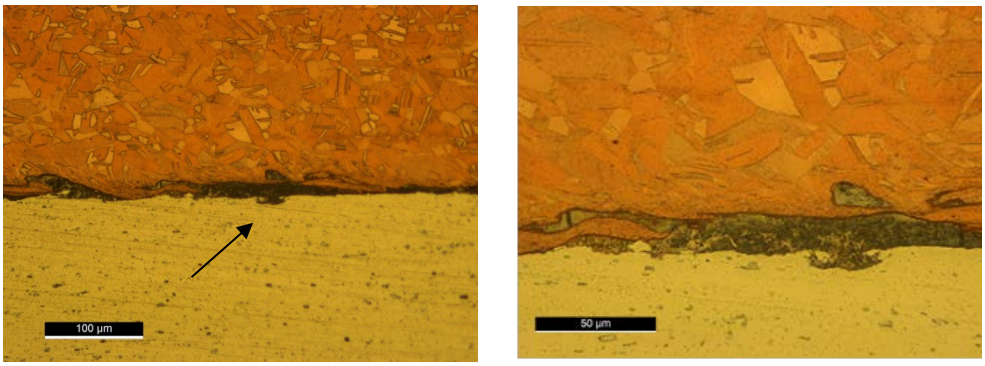

(a) (b)

Fig. 2. Morphology of the Cu–Al weld: (a) ×50 and (b) ×200.

Figure 2b shows, at higher magnification, one of these areas. Note the presence of a phase clearly distinct from Al and Cu. Note also the presence of that phase in the interior of the flying Cu plate. Analysis of SEM/EDS data has shown that the intermediate layer consists of several phases. Figure 3a shows one of such zones.

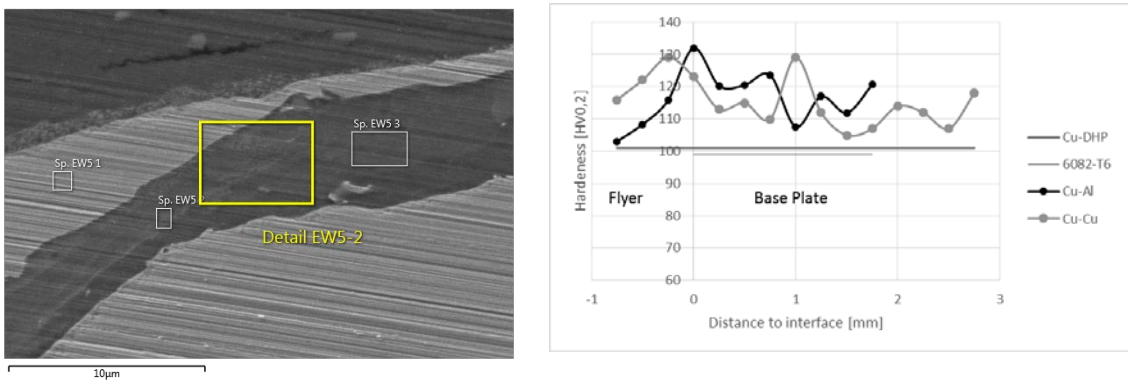

a) b)

Fig. 3. (a) SEM/EDS analysis of the weld interface and (b) in-depth variation of hardness.

The lower phase in Fig. 3a is Al and the dark phase at the top is Cu. The composition in the intermediate phase is not uniform. In EW52 point it was determined by an atomic composition of 68.94% Al and 30.63% Cu, which suggests that it is the $CuAl_2$ intermetallic while in EW53 point was measured 89.57% Al, and 10.43% Cu, suggesting the $Al/CuAl_2$ eutectic. Figure 3b shows the in-depth variation of hardness and the hardness of base materials. There has been a general increase in hardness either in the flying plate or on the base plate and the greater increase is observed at the welding interface. This increase is due to plastic deformation induced by the impact. The average

hardness measured on the melted zones containing intermetallic phases is higher than that given deformation, specifically about 366 H_V. As the two welds were made with approximately the same power, the morphological differences in the interface of welds also depend on difference in physical properties of the materials welded.

1. F. Findik, Recent developments in explosive welding, *Mater. Design*, 2011, vol. 32, pp. 1081–1093.
2. B. Gulenc, Investigation of interface properties and weldability of aluminum and copper plates by explosive welding method, *Mater. Design*, 2008, vol. 29, pp. 275–278.
3. R. Mendes, J.B. Ribeiro, A. Loureiro, Effect of explosive characteristics on the explosive welding of stainless steel to carbon steel in cylindrical configuration, *Mater. Design*, 2013), vol. 51, pp. 182–192.
4. M.M. Hoseini Athar, B. Tolaminejad, Weldability window and the effect of interface morphology on the properties of Al/Cu/Al laminated composites fabricated by explosive welding, *Mater. Design*, 2015, vol. 86, pp. 516–525.

HIGHLY DURABLE HIGH-MODULUS Al–Cu COMPOSITES BY EXPLOSIVE WELDING AND SUBSEQUENT HEAT TREATMENT

D. L. Chernyshev and N.A. Baidarova

Production Association START, pr. Mira 1, Zarechny, Penza region, 442965 Russia

e-mail: dim310374@yandex.ru

Current trend in modern mechanical engineering is the replacement of some structural materials by reinforced composites [1], such as aluminum–copper composites combining high ductility, low specific weight, and susceptibility to reinforcement with intermetallics (CuAl, $CuAl_2$, Cu_3Al_2, Cu_9Al_4, and Cu_3Al). The above-mentioned composites were fabricated in two ways:
Process A: Explosive welding of Al (AMg2 brand) in the form of semi-finished products (sheet, pipe) with copper layers (M1 brand) in the form of strips and perforated elements followed by rolling, stamping, machining and reinforcement by heat treatment (resulting in formation of inner intermetallic layers).
Process B: Gas-dynamic spraying of Al powder (55% Al, 30% Al_2O_3, 5% Zn) on a pre-fabricated copper (M1 brand) followed by subsequent heat treatment to obtain the desired intermetallic layer.

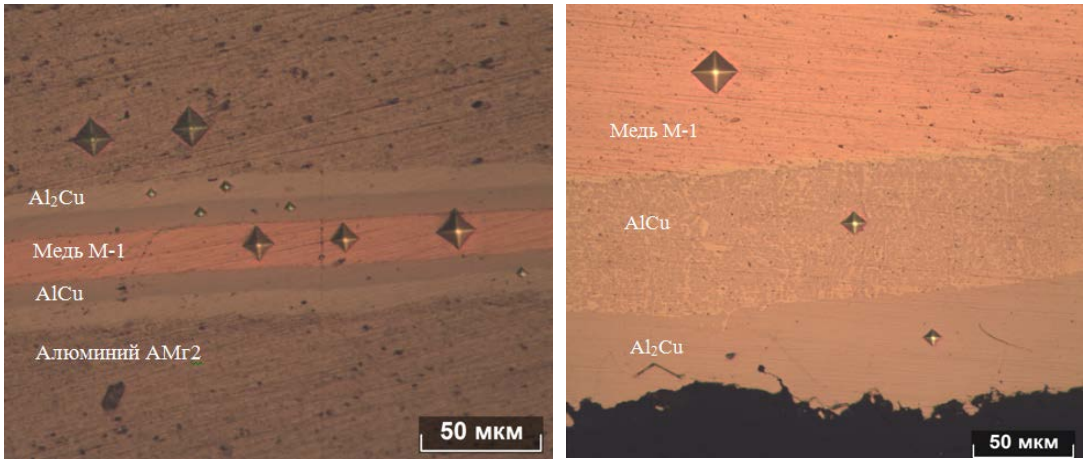

Fig. 1. Intermetallic layers formed in (a) samples *A* and (b) samples *B*.

Metallographic and XRD analyses of explosively clad samples showed the presence of distinct boundary between Al and Cu in both samples *A* and *B*.

Thermal treatment was carried out in two modes: (*i*) holding at 490°C for 1–8 h and (*ii*) heating with pulsed electric current to 470–510° C for 10–150 s. The results are presented in Fig. 1.

After heat treatment, the composite hardness grew by 50–130% while the elastic modulus, by 10–30%.

1. A.V. Khorin, I.S. Los', D.B. Kryukov, Copper-aluminum composites obtained by explosion welding, *Proc. Volgogr. Tech. Univ.: Explosion Welding and Properties of Welded Joints*, 2010, vol. 4, no. 5 (65), pp. 88–92.
2. A.V. Khorin, I.S. Los', M.S. Guskov, Properties of reinforced copper–aluminum composites obtained by explosion welding, in *Proc. Int. Conf. on New Materials and Technologies*, Moscow, 2008, p. 182.

STRUCTURAL INHOMOGENEITY OF WELD SEAM IN BRASS/STEEL CLAD METAL FABRICATED BY EXPLOSIVE WELDING

I. V. Denisov, O. L. Pervukhina, and I. V. Saikov

Institute of Structural Macrokinetics and Materials Science, Russian Academy of Sciences, Chernogolovka, Moscow, 142432 Russia

e-mail: ingener.denisov@yandex.ru

As is known, brass is a material that shows good weldability with steel (for brass sheets below 8 mm in their thickness). According to [1], good joining (within the weldability window) of brass sheet (L63 brand, 10–14 mm thick) to steel surface was achieved over a length (L) of up to 1 m.

An increase in the impact velocity (V_c) gave rise to an increase in L. This was accompanied by the formation of thin gray deposit on the brass surface and of thin yellow one on the steel surface. The weld seam did not show the presence of wavy structure. The formation of a foamed layer on the brass surface was associated with the action of shock-compressed gas, as well as the absence of the wavy structure. Further details will be discussed at presentation.

Based on these results, we formulated the recommendations as for proper choice of conditions for explosive welding of brass to steel. Our recommendations were then implemented to fabricate a batch of 100 (14 + 86) × 1100 × 2300 mm tube walls with 100-% continuity and a brass strength.

This work was financially supported by the Russian Foundation for Basic Research (project no. 14-08-00845A).

1. Yu.A. Konon, L.B. Pervukhin, A.D. Chudnovskii, *Svarka vzryvom* (Explosive Welding), Moscow: Mashinostroenie, 1987.

MECHANOACTIVATION AND DETONATION OF AMMONIUM PERCHLORATE/NANO-Al MIXTURES

A. Yu. Dolgoborodov[1–3], V. G. Kirilenko[1], A. A. Shevchenko[3], and M. A. Brazhnikov[1]

[1]Semenov Institute of Chemical Physics, Russian Academy of Sciences, ul. Kosygina 4, Moscow, Russia
[2]Joint Institute for High Temperature, Russian Academy of Sciences, ul. Izhorskaya 13 Bd. 2, Moscow, Russia
[3]National Research Nuclear University, Kashirskoye sh. 31, Moscow, Russia

e-mail: aldol@ihed.ras.ru

Mechanochemical activation of oxidizer–metal mixtures is one of new ways to production of energetic materials with increased rates of energy release in the processes of combustion and detonation. The conditions of treatment of components in a ball mill are selected so as to provide maximum grinding, mixing, and activation of the components, but prevent the reaction. The materials produced are called mechanically activated energetic composites (MAECs). MAECs are significantly superior over conventional mixtures in the rate of energy release, making it possible to obtain burning velocities previously infeasible for oxidizer–fuel mixtures with micro-sized components.

Aluminized compositions based on ammonium perchlorate (AP) in accordance with the classification of explosives belong to Group II. The dependence of the detonation velocity on the density, $D(\rho)$, of such explosives is of increasing character up to a certain density, and then it falls with transition to detonation failure, i.e. the $D(\rho)$ function has a maximum. Previous results [1] have shown that the preliminary mechanical activation makes it possible to extend the range of detonability of the mixtures of microsized powders of Al with AP to the region of higher density and smaller diameters with a more than 15% increase in D. In this paper, we consider the production of MAECs based on AP and nano-sized Al. We hoped that the use of nanosized Al would lead to further increases in D.

As initial materials for mixes, we used the powders of chemically pure AP with average particle size 20–50 μm and Alex (Aluminum Electroexploded) with a particle size of 150–200 nm (see Fig. 1a). Mixing and activation of the components was carried out in a planetary mill Activator-2sl with steel drums and balls. Weight load of a mixture was 10 g, the mass of balls 300 g. Hexane was added into the mixture to reduce frictional heating, and the treatment was carried out under water cooling of drums. The treatment was followed by mixture drying. The weight ratio of the components in most

cases was Alex/AP = 20/80, and the activation time t_a = 10 min. Selected conditions were based on the data [1], in this case there was the highest *D* value. The additive of 3% fluoropolymer-42 (F-42) was introduced to compositions for reducing the mechanical sensitivity and ensuring compressibility. Also for comparison, experiments were conducted with a short time of activation (t_a = 1 min). The treatment was followed by drying. The starting substances and the obtained MAEC were analyzed by X-ray diffraction, electron microscopy, and elemental microanalysis. An example of mechanically activated mixtures is given in Fig. 1b. Image analysis shows that the activation decreases the size of AP to comminuted particles of irregular shape with a size of about several microns. Alex is distributed both on the surface of AP particles and in-between. F-42 particles were deformed into fibers distributed between the powder particles.

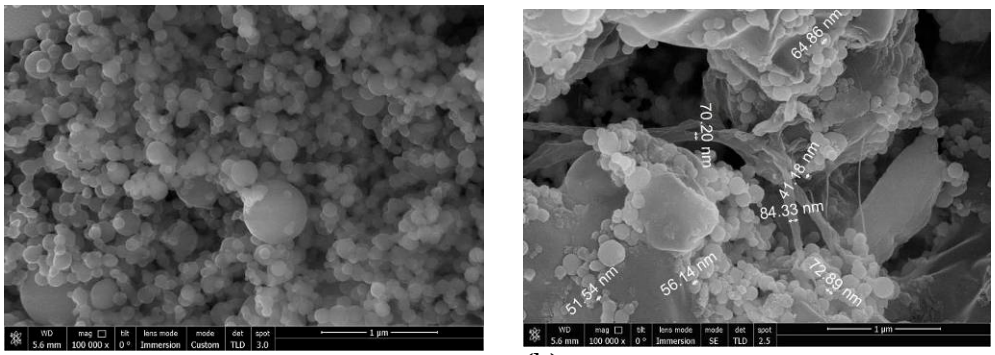

(a) (b)

Fig. 1. SEM images of Alex and MAEC Alex/AP 20/80 + 3% F-42, t_a = 10 min.

Charges for experiments were produced by cold pressing to relative density Δ = ρ/ρ_{max} = 0.5–0.95. Charge diameters (*d*) ranged from 10 to 50 mm. The length of the charges *L* was 5–6*d*.

The charges were initiated by detonator through RDX thin pellets and buster charge of the same density as the charges tested. The time of detonation wave travelling along the base equal to *d* was measured with the help of contact foil gages, in so doing there were measured *D* values, averaged over the base of measurement.

The dependencies *D*(Δ), *D*(L) and *D*(1/*d*) were obtained (see Figs. 2, 3). The *D*(Δ) dependence for non-activated mixture of Al(PP-2)/AP 20/80 with microsized particles has a maximum of *D* = 4.3 km/s at Δ ~ 0.70. Mechanoactivation of Al(PP-2)/AP (t_a = 10 min) allowed one to shift the *D* value up to a maximum of 4.8 km/s at Δ ~ 0.75. The *D*(Δ) dependence for nano-scale Alex/AP at short activation time (t_a = 1 min) has a maximum of *D* = 5.3 km/s at Δ ~ 0.83, and the additional activation (t_a = 10 min) resulted in a peak of *D* = 6.12 km/s at Δ ~ 0.91. Comparison of the data noted as 3 and 4 in Fig. 2 (Alex/AP, t_a = 1 min and t_a = 10 min) separately allows one to clarify the effects of both replacement of microsized Al by nano-sized one and mechanoactivation.

So, assuming the mixture treated in the mill within 1 min to be non-activated one, the increase in *D* would be mainly due to the introduction of nanosized Al, while 10-min treatment resulted in a high degree of activation leads to additional increase in *D*.

Most of the experiments in this work were carried out for charges with $\Delta = 0.75$. This is due to the fact that the maximum *D* for the mixture with microsized Al is achieved at $\Delta = 0.75$ [1], see Fig. 2. Initially, for the composition with Alex we expected to see a similar linear $D(1/d)$ but at a higher *D* level. However, from the data obtained it follows that the size of Al particles strongly affects the critical diameter and *D(d)*, and the formulations with the same chemical composition behave differently. The dependence $D(1/d)$ for Alex/AP is non-linear. At d = 20–40 mm, *D* is almost constant with increasing charge diameter, which indicates the staging process of energy release behind the front of detonation wave.

In general, our results show that the use of nanoscale components in conjunction with mechanochemical activation allows us to regulate the detonation ability of explosive oxidizer–fuel mixtures.

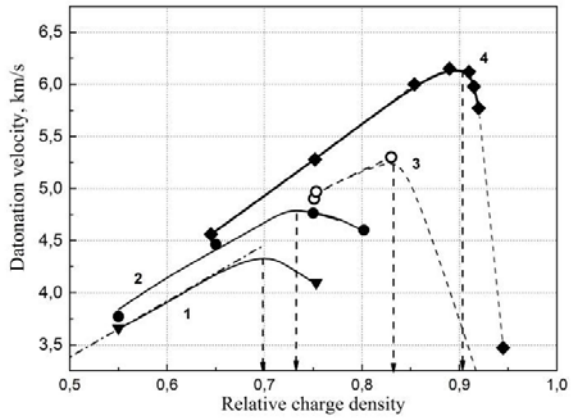

Fig. 2. $D(\Delta)$ at d = 25 mm:
(1) non-activated mixture Al(PP-2)/AP;
(2) Al(PP-2)/AP, t_a = 10 min [1];
(3) Alex/AP, t_a = 1 min;
(4) Alex/AP, t_a = 10 min.

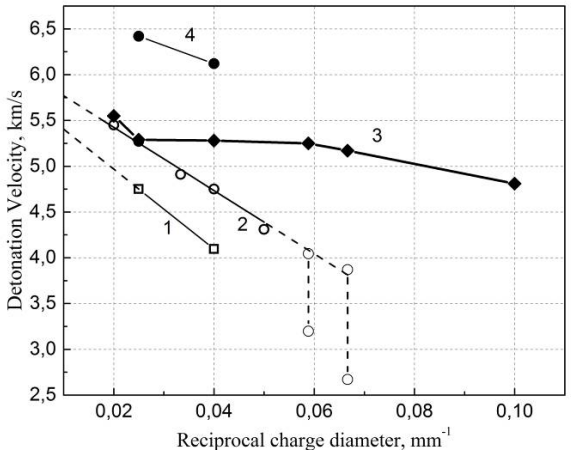

Fig. 3. $D(1/d)$:
(1) Al(PP-2)/AP, $\Delta = 0.75$, t_a = 1 min;
(2) Al(PP-2)/AP, $\Delta = 0.75$, t_a = 10 min;
(3) Alex/AP, Δ=0.75, t_a = 10 min;
(4) Alex/AP, $\Delta = 0.9$, t_a = 10 min.

This work was supported by the Russian Foundation for Basic Research (project no. 16-29-01030).

1. A.Yu. Dolgoborodov, V.G. Kirilenko, M.A. Brazhnikov, et al., Detonation-like processes in solid fuel–oxidizer mechanoactivated composites, in *Proc. 15th Int. Detonation Symp.*, 2014, pp. 1437–1443.

THERMAL ANALYSIS OF DETONATION NANODIAMONDS

V. P. Efremov[1], E. I. Zakatilova[1,2], I. V. Maklashova[2], A. A. Deribas[2], and N. V. Shevchenko[3]

[1]Joint Institute for High Temperatures, Russian Academy of Sciences, Moscow, Russia
[2]National Research Nuclear University MEPHI, Moscow, Russia
[3]CJSC Petrovsky Research Center FUGAS, Moscow, Russia

e-mail: ei.zakatilova@mail.ru

Detonation nanodiamond is new perspective meteriat. Utilisation ammunitions with high explosives and the obtaining nanodiamond as result detonation synthesis have given new motivation for search areas their application. Nanodiamonds have next attractive properties: high density (3,51 g/ sm^3), ultra high thermal conductivity and high dielectric properties. Use as fillers of nanodiamonds will allow to regulate heat conductivity, density, a thermal capacity and dielectric properties.

In this work nanodiamond powder have been researched by method synchronous thermal analysis. Experiments have been conducted at atmospheric pressure of argon. Nanodiamond powder were heated in the closed crucible (Al_2O_3) in a temperature range of 30 – 1500 ° C. After heat treatment, the samples have been researched by x-ray diffraction and electron microscopy. As a result of this work it have been found that detonation nanodiamond have started transition into graphite at a temperature of 800.

ULTRUFAST PROPAGATION OF DESTRUCTION WAVE IN SILICA FIBERS

V. P. Efremov, A. I. Frolov, and V. E. Fortov

Joint Institute for High Temperatures of the Russian Academy of Sciences, Moscow, Russia

e-mail: dr.efremov@gmail.com

A burning mode of optical fiber destruction was observed by R. Kashyap in 1987. A detonation mode was disclosed by our team in 2006. The present work aimed at investigating the effect of laser-driven destruction of optical fibers in more detail.

There are two modes of propagated damages caused by laser radiation in silica-based optical fibers. In a detonation-like mode, the plasma front is two orders of magnitude greater than for a fiber fuse effect (combustion mode). This mode is new object of laser destruction of silica-based optical fibers. Optical fiber and enough long laser pulse allow us obtain laser damage propagated more than hundred fiber core diameters during pulse. The optical fibers application provides the same advantages. It affords supply the same form of energy deposition in the every cross section of optical fiber. Tested regime demonstrates nearly constant velocities during 200 ns in the range of laser beam intensities 2.0–4.5 GW/cm^2. Plasma propagation produced irreversible damages in the optical fiber. Saved fragments were investigated by a scanning electron microscopy. Melted and crushability zones have been visualized and measured. Dynamic recordings of destruction process were compared with photos of the saved fragments. It has been received that destruction of a core and cover of quartz optical fibers has multilevel character from the micron size to nano-level destructions.

This work was financially supported by the Russian Academy of Sciences.

HIGH-SRENGTH AND HIGH-DAMPING CLAD METAL BY EXPLOSIVE WELDING

N. L. Fedotova[1], I. B. Chudakov[1], I. A. Korms[1], S. Yu. Makushev[1], L. B. Pervukhin[1], I. V. Saikov[2], and A. Yu. Malakhov[2]

[1]TsNIICherMet, Moscow, Russia
[2]Institute of Structural Macrokinetics and Materials Science, Russian Academy of Sciences, Chernogolovka, Moscow, 142432 Russia

e-mail: revan.84@mail.ru

Some materials used in aerospace engineering (30ХГСА, 40ХСН2МА, Н18К3МТ steels) exhibit low damping ability, which can lead to resonant wrecking of plane wings, propeller blades, and to noise in cabin. A promissory solution to the problems seems to be the design of damping alloys and composites based on 30ХГСА steel (σ_b above 1000 MPa).

Explosive welding was carried out by standard scheme using ammonite 6ZhV as an explosive. The sheet of quenched 30ХГСА steel was used as a flyer plate while the sheet of 60Г40Д alloy, as a base plate (thickness ratio 1 : 2). The flyer velocity was about 1016 m/s (developed pressure at collision around 20.7 GPa). After annealing at 400°C for 1 h, the transition layer in the clad metal was found to contain the nanocrystalline structure with a grain size of 1–2 nm.

After annealing at 400°C for 1–2 h, the specific damping ability of the clad metal was larger than that of 60Г40Д alloy, which is indicative of some changes in the tetragonal lattice and twin structure of the alloy caused by shock loading and subsequent thermal treatment.

MATHEMATICAL MODELING OF RAYLEIGH–TAYLOR INSTABILITY AT THE INTERFACE OF TWO COLLIDING METAL PLATES

S. V. Fortova, V. V. Shepelev, A. P. Pronina, and P. S. Utkin

Institute for Computer Aided Design, Russian Academy of Sciences, ul. Brestskaya 19/18, Moscow, 123056 Russia

e-mail: sfortova@mail.ru

The problem of explosive hardening and explosive welding is of current interest for production of high-strength bimetallic compounds and items [1]. Explosive welding is a process of metallic compound production as a result of high-speed impact due to the energy of detonation products of condensed explosives. The process is followed by the complex dynamic effects which are the subject numerous experimental and numerical studies [2]. The processes taking place at the interface of colliding plates were investigated experimentally [2]. This work is devoted to numerical simulation of high-speed impact of two metal plates in conditions qualitatively similar to those in [2] using 3D Euler equations and different equations of state.

We will consider the interaction of the lead plate (density $\rho \approx 11\ 300$ kg/m^3, thickness $h = 0.002$ m) with the steel plate ($\rho \approx 7\ 900$ kg/m^3) of the same thickness. The lead plate is thrown in the vertical direction with at velocity $w = 500$ m/s. As the initial disturbance, we set the point disturbance 500 m/s of the velocity on the lead plate surface. The initial pressure is equal to $P = 10^{12}$ Pa, acceleration is equal to $g = 10^7$ m/s^2 and directed to metal with the lower density. The computational area is the cube with the edge length 0.004 m. We set slip conditions on the upper (upper surface of the lead plate) and lower (lower surface of the metal plate) boundaries and periodic conditions of the side faces.

Mathematical model is based on 3D non-stationary two-component Euler equations supplemented by equations of state (EOS). We use three different EOS namely: (*i*) ideal gas with specific heat ratio $\gamma = 5/3$, (*ii*) barotropic gas EOS, and (*iii*) wide-range EOS for real metals [3].

Numerical algorithm is based on the physical processes and spatial directions splitting techniques. The set of equations is written in the characteristics form. We solve three 1D systems along each coordinate directions independently using Roe numerical flux function. Time integration is performed using explicit Euler scheme. Spatial approximation order of the scheme is increased up to second with the use of hybrid schemes approach. In this approach, the switching between the central and upwind

differences is realized for each characteristics based on the sign of characteristics. The detailed description of the numerical algorithm could be found elsewhere [4].

For numerical simulations of the problems which are described by the hyperbolic system of equations the authors developed computer code TurboProblemSolver (TPS) [5]. TPS has modular structure and consists of the independent blocks responsible for different parts of the numerical method. TPS provides to the user the possibility to change numerical scheme, initial and boundary conditions and mass forces. The code is written in C++ and is parallelized using Message Passing Interface (MPI) package using domain decomposition approach.

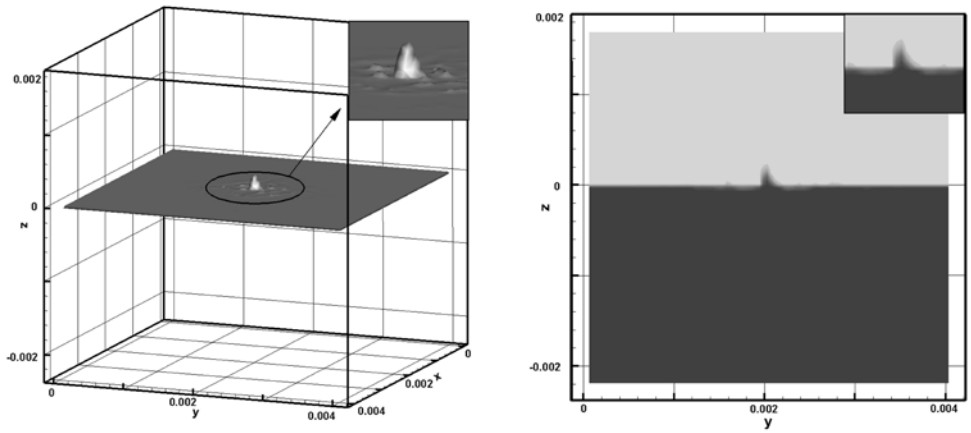

Fig. 1. Density isosurface and cross section; the splash in the direction of lead plate; and calculation with the use of ideal gas EOS.

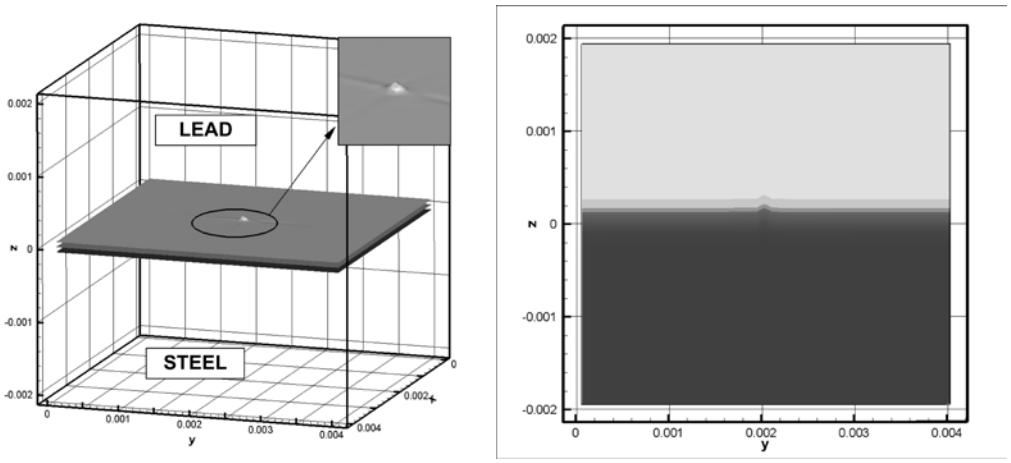

Fig. 2. Density isosurface and cross section; the splash in the direction of lead plate; and calculation with the use of barotropic EOS.

The presented results concern the ideal gas EOS and barotropic EOS. For the ideal gas EOS with the point disturbance in the center of one of the plates we obtained the splash in the direction to the lead plate. The shape of the splash is similar to that observed in [2]. Fig. 1 shows the density isosurface in 5 μs after the impact. The domain $z > 0$ corresponds to the lead plate and $z < 0$ to the steel plate.

For the barotropic EOS, we also get the splash in the direction to the lead plate. The splash has a crateriform shape. Figure 2 shows the density isosurface in 5 μs after the impact. The results obtained using two different EOS are in qualitative agreement.

The main features of the process under study can be outlined as follows:

– The instability development on the interface of the metal plates is characterized by splashes from the metal plate to the lead one.

– The increase of the lead plate thickness with the velocity of throwing fixed leads to the disturbance wavelength growth on the interface.

– Comparison of the throwing of the lead plate to the metal and copper ($\rho \approx 8\ 900$ kg/m^3) shows that the splashes on the copper plate have a smaller wavelength and larger amplitude.

1. A.A. Deribas, *Physics of Hardening and Explosive Welding*, Novosibirsk: Nauka, 1972 (in Russian).
2. I.V. Yakovlev, Instability of the interface between colliding metal surfaces, *Fiz. Gorenia Vzryva*, 1973, vol. 9, no. 3, pp. 447–452.
3. A.V. Bushman, I.V. Lomonosov, V.E. Fortov, The models of wide-range equations of state under the high energy densities, *Preprint JIHT*, 1989, vol. 6-287.
4. S.V. Fortova, Eddy cascade of instabilities and transition to turbulence, *Comp. Math. Math. Phys.*, 2014, vol. 54, no. 3, pp. 553–560.
5. S.V. Fortova, L.M. Kraginkskii, A.V. Chikitkin, E.I. Oparina, Software package for solving hyperbolic-type equations, *Math. Modeling. Comp. Simul.*, 2013, vol. 25, no. 5, pp. 607–616.

EXPLOSIVE WELDING FOLLOWED BY ANNEALING: MICROSTRUCTURE OF Al/Ti/Al AND Al/Mg/Al CLADS

D. M. Fronczek[1], R. Chulist[1], L. Litynska-Dobrzynska[1], Z. Szulc[2], N. Schell[3], P. Zieba[1], J. Wojewoda-Budka[1]

[1]Institute of Metallurgy and Materials Science, Polish Academy of Sciences, Reymonta Str. 25, Cracow, 30-059 Poland
[2]High Energy Technologies Works EXPLOMET, Oswiecimska Str. 100H, Opole, 45-641 Poland
[3]Institute of Materials Research, Helmholtz-Zentrum Geesthacht, Max-Planck Str. 1, Geesthacht, D-21502 Germany

e-mail: d.fronczek@imim.pl

In explosive welding (EXW), the joint is achieved by impelling the flyer plate towards the base plate using a significant energy from explosion. The large sections of various plates can be joined in a single operation using this solid-state process. A very important advantage of this technique is that the jet strips away any surface contamination such as oxides and impurities, therefore, no special pre-treatment before the shot is needed [1].

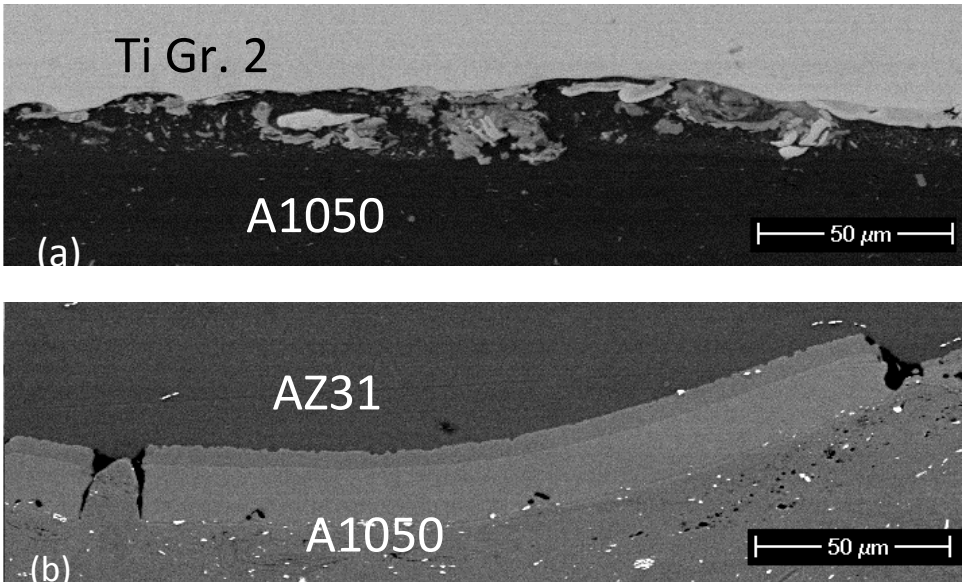

Fig. 1. SEM images of the Al/Ti/Al (a) and Al/Mg/Al (b) joints formed upon explosive welding.

Multilayered materials manufactured by explosive welding find application in production of electrical wires and industrial machinery e.g. aluminum–copper systems [2, 3], aerospace industry e.g. titanium and aluminum clads [1] or medical applications e.g. titanium, aluminum oxide and nickel chromium ($Ti/Al_2O_3/NiCr$) composites [4]. Moreover, the EXW followed by annealing enables to manufacture composite laminates in a large-scale and relatively low-cost way. Metallic–intermetallic composites are materials composed of the alternately arranged metallic and intermetallic layers. As they combine ductile metals and hard intermetallic phases, they are characterized by unique mechanical properties [1].

Microstructure and phase composition of two types of three-layer clads were intensively studied: Al/Ti/Al and Al/Mg/Al. Figures 1a, b present the upper layer of a joint in the Al/Ti/Al and Al/Mg/Al clads in the state just after EXW, respectively. The electron backscatter diffraction technique in the scanning electron microscope (SEM) was used to investigate the microstructural changes (grain size, shape and orientation) caused by the high impact during explosion with respect to position of the interfaces.

These results were supplemented by the in-depth information on the interfaces microstructure and phase composition with application of various techniques such as energy dispersive X-ray spectroscopy in SEM, synchrotron radiation as well as transmission electron Microscopy. As a next step, the evolution of microstructure of both joined materials and their interface upon annealing at various temperature and time intervals was studied. In each experiment the growth kinetics of the phases present at the interface was determined.

We are grateful to High Energy Technologies Works EXPLOMET for providing the samples of explosion-clad composites.

1. I.A. Bataev, A.A. Bataev, V.I. Mali, D.V. Pavlyukova, Structural and mechanical properties of metallic–intermetallic laminate composites produced by explosive welding and annealing, *Mater. Design*, 2012, vol. 35, pp. 225–234.
2. M. Honarpisheh, M. Asemabadi, M. Sedighi, Investigation of annealing treatment on the interfacial properties of explosive-welded Al/Cu/Al multilayer, *Mater. Design*, 2012, vol. 37, pp. 22–127.
3. M.M. Hoseini Athar, B. Tolaminejad, Weldability window and the effect of interface morphology on the properties of Al/Cu/Al laminated composites fabricated by explosive welding, *Mater. Design*, 2015, vol. 86, pp. 516–525.
4. B. Wang, F. Xie, B. Wang, X. Luo, Microstructure and properties of the $Ti/Al_2O_3/NiCr$ composites fabricated by explosive compaction/cladding, *Mater. Sci. Eng. C*, 2015, vol. 50, pp. 324–331.

INFLUENCE OF HYDROGEN ON EXPLOSION-WELDED CORROSION RESISTANT CLAD MATERIALS FOR GEOTHERMAL PLANTS

M. Gloc[1], Ł.Ciupiński[1], and G. Kwiatkowski[2]

[1] Warsaw University of Technology, University Research Centre Functional Materials, Warsaw, Poland
[2] ZTW Explomet Co. A.Gałka, Z.Szulc; Opole, Poland

e-mail: michalgloc@wp.pl

Depleting resources of fossil fuels and global warming effect lead to development of renewable energy sources. Geothermal energy has been used for heating and electricity production in several countries. In simple worlds it is the power derived from the Earth internal heat. The use of geothermal energy is being constantly developed and is gaining more importance in the global energy mix. Widespread use of geothermal energy as well as exploration of deeper geothermal sources bring about new challenges in the area of corrosion and use of materials that directly influence the effectiveness, quality of service, reliability and economy of the power plants.

Hydrogen, dissolved CO_2, H_2S, NH_3, and chloride ions lead to corrosion of metallic materials and their progressive degradation that in conjunction with applied stresses results in component failures. Fatigue tests conducted on different types of steels exploited in Icelandic geothermal systems have shown that the decrease in strength parameters and reduced materials life span can be attributed to stress corrosion cracking and hydrogen embrittlement [1, 2].

Hydrogen embrittlement of metals is one of the most serious problems in the wide variety of industry installations where hydrogen is involved. It is well known that the mechanism of hydrogen degradation is complex. It has a detrimental effect on a number of structural steels. This negative effect of hydrogen on metals is termed as hydrogen embrittlement. Stainless steels undergo embrittlement by hydrogen in the aqueous media and in the hydrogen atmosphere. Hydrogen deteriorates microstructure and reduces mechanical properties of stainless and low alloy steels. In the case of corrosion resistant steels after hydrogen charging numerous microcracks and blisters are observed. In the case of the clad materials, hydrogen may induce underclad cracking [3–5].

When considering suitable materials for geothermal environments often the idea of cladded materials is introduced both for pipelines and vessels. Clads offer a cost effective solution even for the most demanding applications. They are widely used in harsh corrosive environments such as those prevailing in chemical processes, offshore oil production, oil refining or electric power generation industries. Recently, clads

obtained by explosive welding are gaining more and more attention as materials for highly demanding application. The transition zone (melted zone), occurring in the explosive welded joint, is expected to constitute a diffusion barrier for hydrogen, provided the parameters of joining are appropriately selected.

The ion-etched microstructure of transition zone in Inconel-cladded carbon steel is given in Figure 1.

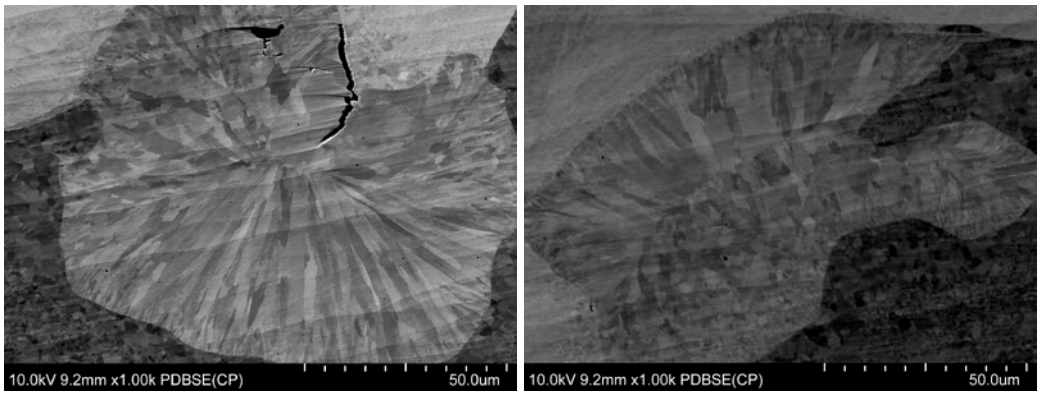

Fig. 1. The ion etched microstructure of melted zones in the Inconel C-276/P355NH carbon steel joint after heat treatment.

The present work studies the influence of hydrogen on the microstructure and mechanical properties of cladded materials obtained by explosive welding. The hydrogen influence on bonded materials and melted zones created at the interface between the base steel P355NH and flyer Inconel C-276 and Super Duplex SAF 2507 steel is described. Materials are investigated in as-cladded condition and after post-processing heat treatment. The microstructure was studied using SEM/TEM and mechanical properties were assessed in the shear tests according to ASTM SA-264.

1. T. Kaya, P. Hoşhan, Corrosion and material selection for geothermal systems, in *Proc. World Geothermal Congr*., Antalya (Turkey), April 24–29, 2005.
2. S.N. Karlsdóttir, Corrosion, scaling and material selection in geothermal power production, *Compreh. Renew. Energ*., 2012, vol. 7, pp. 241–259.
3. M. Szwed, K. Lublińska, G. Wojas, M. Gloc, K.J. Kurzydłowski, Ultrasonic testing of clad plates for evaluation of hydrogen degradation, Proc. VI Eur. Stainless Steel Conf., Finland, 2008, p. 63.
4. P. Lacombe, J. Chêne, Hydrogen trapping and hydrogen embrittlement, in Hydrogen Embrittlement and Stress Corrosion Cracking, Metals Park, Ohio: ASM, 1955, p. 44073.

5. A. Oudriss, J. Creus, J. Bouhattate, E. Conforto, C. Berziou, C. Savall, X. Feaugas, Grain size and grain-boundary effects on diffusion and trapping of hydrogen in pure nickel, *Acta Mater*., 2012, vol. 60, pp. 6814–6828.

EXPLOCLAD MULTILAYER MATERIALS WITH ENHANCED SERVICE LIFE FOR REPOSITORY OF LIQUID RADIOACTIVE WASTES

V. A. Grachev[1], A. E. Rosen[2], G. V. Kozlov[3], S. G. Usatyi[3], A. A. Rosen[2], and D. A. Verevkin[3]

[1] ROSATOM State Corporation, ul. Bolshaya Ordynka 24, Moscow, 119017 Russia
[2] ROMET Ltd., ul. Druzhba 6, Penza, 440067 Russia
[3] Penza State University, ul. Krasnaya 40, 440026 Penza, Russia

e-mail: vagrachev@gmail.com; aerozen@bk.ru; aarozen@bk.ru

The problem of reliable repositories for liquid radioactive wastes (LRW) is of current importance worldwide. To date, about 1.5 billion m^3 of LRW are kept in metallic storage reservoirs each with a capacity of 3000–10 000 m^3. Despite their low radioactivity (below $3.7 \cdot 10^6$ Bq/l), LRW contain corrosion-active compounds (halogens and reactive anions) which can be withstood only by high-alloyed austenite-class stainless steels. At a layer thickness of 25 mm, their service life does not exceed 30 years. In many countries, a task objective has been declared to increase the above indicator up to 80–100 years. A 3-fold increase in the wall thickness elevates not only production cost but also creates a number of technological complications concerning the shaping of thick sheets and their welding.

An increase in the amount of alloying agents (such as Ni and Cr) in steels has also been practically exhausted. A growth in the electrochemical potential of steels inevitably activates the pitting corrosion that results in formation through pores in exceedingly small volumes. In most cases, the diameter of pitting does not exceed 200 μm, while the propagation rate varies between 4 and 7 mm a year.

In other words, novel technical solutions are needed as it posted in the document *Energy Technology Perspectives: Scenarios and Strategies to 2050* distributed by Organization of Economic Cooperation and Development (OECD) [1].

In this context, a promissory solution to the problem seems to be the use of multilayer materials with a protective (oblational) sublayer placed beneath the outer one made of steel [2–4]. In materials with "protector pitting prevention", the composition and number of layers (at least three in case of one inner protector and five at two inner protectors), are selected so that the relation between the electrochemical potentials favored the pitting corrosion in uneven layers and the overall (contact) corrosion in the even ones. As is known, the above multilayer sheets (up to 200 m^2 in surface area) can be readily fabricated by explosive welding.

We carried out the purpose-oriented R&D research on elaboration of welding geometry and experimental procedures for testing the mechanical strength and corrosion resistance of multilayer thin sheets of fabricated composite materials.

A theoretical model was developed by combining the geometrical method of fractal dimensionality with dynamic analysis of interface boundaries in terms of the physics of fast processes. This model was used to analyze structural defects and properties of interlayer surfaces upon variation in the conditions of explosive welding. The results may turn helpful in designing multilayer structures with controllable characteristics.

The service parameters of our materials with protector pitting prevention are close to those of tantalum and platinum, while the production cost is on a level of conventional chromonickel stainless steels.

1. *Energy Technology Perspectives: Scenarios and Strategies to 2050*, ISBN 92–64–10982–X.
2. Multilayer material with enhanced corrosion resistance (variants) and methods for preparing same (variants), Euro-Asian Patent 016878, 2012.
3. Multilayer material with enhanced corrosion resistance and methods for its fabrication, Ukr. Patent 10188, 2012.
4. Multilayer material with enhanced corrosion resistance (variants) and methods for preparing same, Korean Patent 10-1300674, 2013.

A NEW METHOD TO MAKE UNIDIRECTIONAL POROUS STRUCTURE BY EXPLOSIVE WELDING TECHNIQUE

K. Hokamoto

Institute of Pulsed Power Science, Kumamoto University, 2-39-1 Kurokami, Chuo-ku, Kumamoto, 860-8555 Japan

e-mail: hokamoto@mech.kumamoto-u.ac.jp

Recently, various porous materials have been developed and the lotus-type porous metals are being investigated actively [1]. Normally, such lotus-type porous metals are fabricated using one-directional solidification process with gas [1], so the pore structures are not uniform in the sample and there is no control of the pore size and porosity.

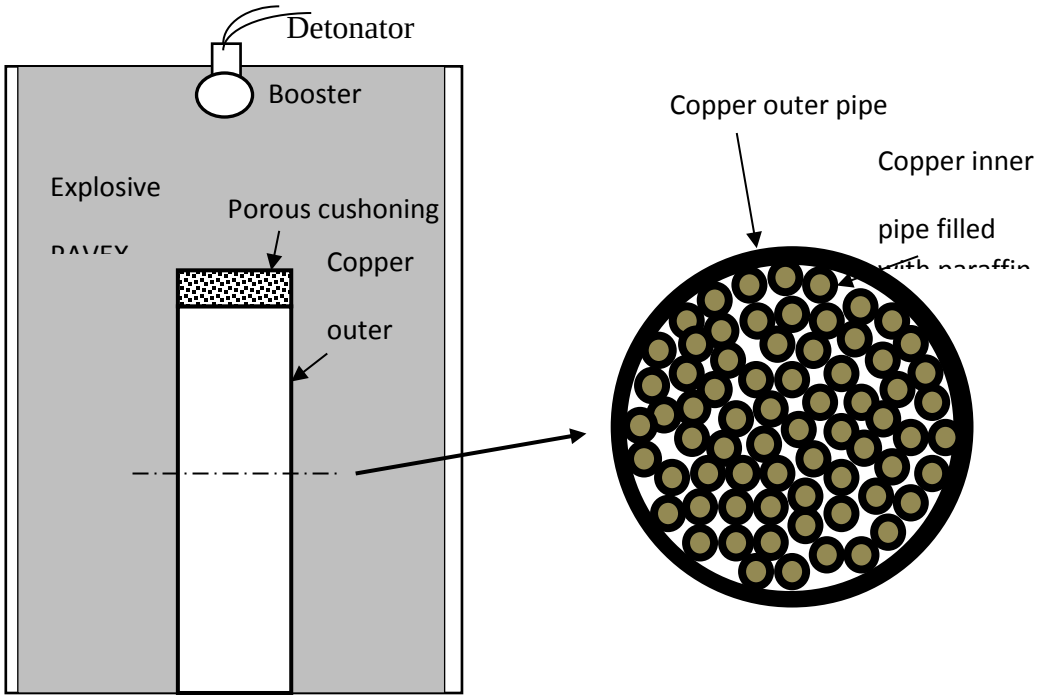

Fig. 1. Cylindrical assembly used for making unidirectional porous structure.

A new method to produce such uniform size pored structure is proposed by the author employing explosive welding technique [2, 3]. The experimental fixture is shown

in Fig. 1. An outer copper pipe (30, 27 mm, outer and inner diameter) inserted more than 60 small copper pipes (3mm outer diameter filled with paraffin) was explosively compacted by PAVEX explosive (ammonium nitrate based, produced by Kayaku Japan Co., Ltd., detonation velocity 2–2.5 km/s, density about 530 kg/m^3, layer thickness 26.5 mm). The recovered samples were boiled in hot water to remove the paraffin inserted. The compacted and welded samples were consolidated without pores between the small copper pipes. The cross-sectional microstructure showed collapsed metal jets and wavy interface in some areas as the evidence that the bonding was achieved based on the explosive welding mechanism. By changing the thickness of the small copper pipes, it is also confirmed that the change of the porosity possible.

The estimated collision velocity, the mechanical properties, and other findings are to be demonstrated at the time of presentation.

Similar method using metalworking technology has been proposed [4], but the rod length should be limited by the elongation toward the direction of deformation expected to cause instability (necking) of the thin wall.

1. H. Nakajima, *Porous Metals with Directional Pores*, Springer, 2014; DOI: 10.1007/978-4-431-54017-5
2. K. Hokamoto, M. Vesenjak, Z. Ren, Fabrication of cylindrical unidirectional porous metal with explosive compaction, *Mater. Lett.*, 2014, vol. 137, pp. 323–327.
3. M. Vesenjak, K. Hokamoto, M. Sakamoto, T. Nishi, L. Krstulović-Oparad, Z. Ren, Mechanical and microstructural analysis of unidirectional porous (UniPore) copper, *Mater. Design*, 2016, vol. 90, pp. 867–880.
4. H. Koh, H. Utsunomiya, J. Miyamoto, T. Sakai, Fabrication of porous copper by cold extrusion and leaching, *J. Jpn. Inst. Metals*, 2007, vol. 71, no. 9, pp. 708–711 (in Japanese).

DEPOSITION OF MULTILAYER CERAMIC COATINGS ONTO Ti SUBSTRATE BY SHS METHOD

O. K. Kamynina, S. G. Vadchenko, A. S. Shchukin, and I. D. Kovalev

Institute of Structural Macrokinetics and Materials Science, Russian Academy of Sciences, Chernogolovka, Moscow, 142432 Russia

e-mail: kuz@ism.ac.ru

Current trend in modern industry is the design of novel hard multifunctional coatings and composites for the needs of mechanical engineering, aerospace industry, and cutting machinery [1, 2]. For deposition of multilayer intermetallic coatings rather promising seems to the SHS technology [3, 4], including SHS joining [5–6].

In this communication we report on deposition of multilayer ceramic coatings onto a Ti substrate by SHS method. Sandwich-type combinations used in experiments are shown in Fig. 1. The experiments were carried out with no applied pressure during combustion. Products were characterized by SEM, EDS, and XRD.

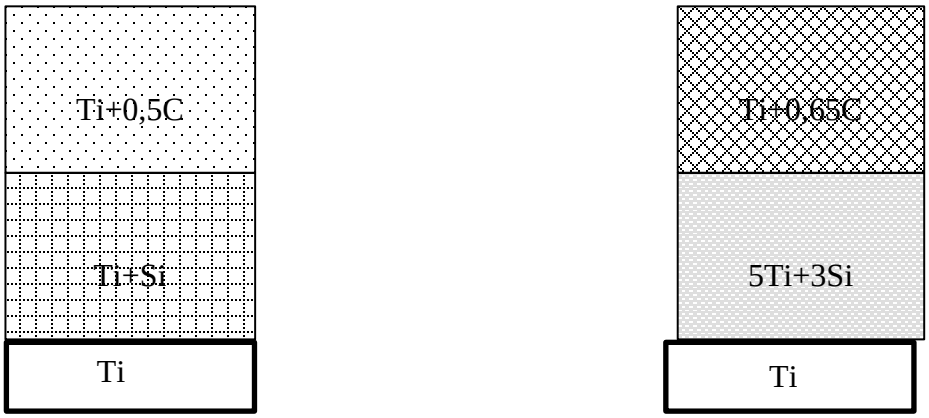

Fig. 1. Sandwich-type combinations used in experiments (ignition from the top).

The deposited coatings were characterized by modern physicochemical methods and the process conditions had been optimized. The details will be discussed at presentation.

This work was financially supported by the Russian Foundation for Basic Research (project no. 15-08-04595-a).

1. P.H. Mayrhofer, C.Mitterer, L. Hultman, H. Clemens, Microstructural design of hard coatings, Prog. Materi. Sci., 2006, vol. 51, no. 8, pp. 1032–1114.
2. G. Erkens, New approaches to plasma enhanced sputtering of advanced hard coatings, *Surf. Coat. Technol*., 2007, vol. 201, pp. 4806–4812.
3. A.E. Sytschev, S.G. Vadchenko, O.K. Kamynina, N.V. Sachkova, Simultaneous synthesis and joining of a Ni–Al-based layer to a Mo Foil by SHS, *Int. J. Self-Propag. High-Temp. Synth*., 2009, vol. 18, no. 3, pp. 213–216.
4. A.E. Sytschev, S.G. Vadchenko, O.D. Boyarchenko, D. Vrel, N.V. Sachkova, SHS joining of intermetallics with metallic substrates, *Int. J. Self-Propag. High-Temp. Synth*., 2011, vol. 20, no. 3, pp. 185–190.
5. S.G. Vadchenko, O.D. Boyarchenko, A.E. Sytschev, N.V. Sachkova, SHS joining in the Ti–Si–C system: Structure of transition layer, *Int. J. Self-Propag. High-Temp Synth*., 2013, vol. 22, no. 1, pp. 46–51.
6. O.K. Kamynina, S.G. Vadchenko, A.S. Shchukin, I.D. Kovalev, A.E. Sytschev, SHS joining in the Ti–C–Si System, *Int. J. Self-Propag. High-Temp. Synth*., 2016, vol. 25, no. 1, pp. 62–65.

SHS-LIKE REACTIONS IN COMMERCIAL MASONRY MORTARS

R. D. Kapustin

Institute of Structural Macrokinetics and Materials Science, Russian Academy of Sciences, 142432, Chernogolovka, Moscow, 142432 Russia

e-mail: kapustin-roman@mail.ru

SHS-like reactions in commercial masonry mortars—such as KR-1, M-1, and VBF—yielding refractory and heat-insulating aluminosilicate composites have been studied experimentally. The kinetics of thermal reactions yielding refractory mullite structures and corundum in thin coatings and masonry mortars was determined by various physicochemical methods. The strength, density, and scaling effects were determined as a function processing conditions (slip viscosity, humidity of dry mixture, etc.). Reactions in porous VBF materials were found to be strongly affected by heat sink through thin walls between the cells.

This work was financially supported by the Russian Foundation for Basic Research (project no. 14-08-00866/14).

RESIDUAL STRESS DISTRIBUTION IN THREE-LAYER PLATE OBTAINED BY EXPLOSIVE WELDING

A. Karolczuk[1], Z. Szulc[2], K. Kluger[1], M. Najwer[2], and G. Kwiatkowski[1]

[1]Opole University of Technology, Faculty of Mechanical Engineering, Mikołajczyka 5, Opole, 45-271 Poland
[2]ZTW EXPLOMET sp.j. Gałka, Szulc, Oświecimska 100, Opole, 46-020 Poland

e-mail: a.karolczuk@po.opole.pl

Unique physical properties of multilayer materials are very attractive for application in the field of geothermal energy. Structural elements in geothermal plants are subjected to the action of highly corrosive media, erosion, high temperature and pressure. Multilayer materials can be specially designed in order to work under such conditions. One of the technologies that are used to produce multilayer metallic materials is explosive welding. The technology is preferable in case of jointing large sheets made of materials with different physical properties which causes difficulties in joining by using other methods. However, during the explosive welding some part of the stresses generated during collision can be locked inside the plate due to rapid cooling process and strain hardening. Those residual stresses can accelerate the process of material degradation. The main aim of the paper is to present the residual stress distribution along three layers of a plate fabricated by explosive welding.

Explosive welding was used to join three plates made of carbon steel (CS), titanium Grade 1 (Ti1) and titanium Grade 12 (Ti12), respectively. The joining process was performed in two stages. At the first stage, a 3-mm layer of Ti1 was cladded onto a 70-mm CS plate. At the second stage, a Ti12 plate 9 mm thick was cladded on the previously obtained bimetallic plate. The welded plate was not subjected to any heat treatment. In order to investigate the residual stress distribution, three samples were cut off from the three-layer plate. Each sample contained three layers with a total thickness of 70 + 3 + 9 mm. Then several thin sheets were cut off from the samples using water jet to reduce heat generation. The thin sheets were taken starting from the outer surface of Ti12. Due to relaxation of residual stresses, the thin sheets are deformed. The deformation of each sheet was measured and recalculated using simplified model into residual stresses. The applied method has in principle similarity to the slitting method described in [1]. Due to deformation measurement of several thin sheets the residual stress distribution could be evaluated. Two samples were cut off along parallel direction to detonation wave and one along perpendicular direction. One of the samples that were

cut off along parallel direction was subjected to heat treatment in order to investigate its influence on the residual stress distribution.

For comparison, the hole drilling method [2, 3] was used in residual stress measurement in four points on the outer surface of Ti12. This method was applied on a welded plate without any additional preparation. The drilled depth of holes equal to 2 mm allows determining averaged (over 2 mm in depth) values of residual stresses in Ti12.

[1] *Practical Residual Stress Measurement Methods*, Schajer G.S., Ed., Chichester (UK): Wiley, 2013.
[2] ASTM E837-13a. Standard Test Method for Determining Residual Stresses by the Hole-Drilling Strain-Gage Method, West Conshohocken, PA: ASTM Int., 2013; DOI: 10.1520/E0837
[3] Karolczuk A, Kowalski M, Kluger K, Żok F., Identification of residual stress phenomena based on the hole drilling method in explosively welded steel–titanium composite, Arch. Metall. Mater., 2014, vol. 59; DOI: 10.2478/amm-2014-0195

FORMATION OF INTERMETALLIC INTERLAYERS IN EXPLOCLAD Al–Cu COMPOSITES: CALCULATED KINETIC PARAMETERS

A. V. Khorin, A. V. Pryshchak, D. L. Chernyshev, and A. P. Pen'shin

Penza State University, ul. Krasnaya 40, Penza, 440026 Russia

e-mail: metal@pnzgu.ru

The kinetic parameters were calculated on the basis of SEM and XRD results for the samples of the Al–Cu composites explosively welded in optimal conditions (no incomplete fusion and no intermetallic interlayers). Rolled copper wire (M0 brand) was used as an armoring fiber while Al alloy (AMg5 brand), as a matrix.

Thermal treatment of the Al–Cu composites was found to result in the formation of two stable intermetallic phases: $CuAl_2$ from the aluminum side and CuAl from the copper side [1, 2]. The latent period for the formation of intermetallics was determined experimentally. In calculations, we determined nucleation energy E_n, activation energy E_a, pre-exponential factor t_0, and diffusion coefficients D_0 for each phase. The set of equations involved the Arrhenius equation, expressions for first and second Fick laws, with account of the incubation period for nucleation of intermetallic phases [3].

The kinetic parameters derived from two values of time and temperatures are collected below.

Phase	Nucleation energy E_n, J/mol	Pre-exponential factor t_0	E_a, J/mol	D_0, μm^2/s	
				400°C	450°C
CuAl	47 721	0.321	150 289	$3.6\cdot10^{-19}$	$5.1\cdot10^{-18}$
$CuAl_2$	41 130	0.319	96 294	$9.4\cdot10^{-16}$	$5.1\cdot10^{-15}$

Our results may turn useful for predicting the growth of intermetallic phases in design of heterogeneous composite materials with desired properties.

1. A.V. Khorin, I.S. Los', D.B. Kryukov, Cu–Al composites by explosive welding, *Izv. Volgograd. Tekh. Univ., Ser. Svarka Vzryvom S-va Svarn. Soedin*., 2010, no. 5 (65), issue 4, pp. 88–92.
2. I.S. Los', A.V. Khorin, E.G. Troshkina, Intermetallic composite by explosive welding, in *Explosive Production of New Materials: Science, Technology, Business, and Innovations*, A.A. Deribas, Yu.B. Scheck, Eds., Moscow: Torus Press, 2012, pp. 67.

3. L.N. Larikov, V.R. Ryabov, V.V. Fal'chenko, *Diffusion in Solids during Welding*, Moscow: Mashinostroenie, 1975 (in Russian).

PROTECTIVE Al–2Mg–*n*C COATINGS BY COLD GAS-DYNAMIC SPUTTERING: DEPOSITION AND CHARACTERIZATION

D. S. Khrenov[1,2], A. V. Sobol'kov[1], A. I. Elkin[1], A. V. Aborkin[1], A. E. Sytschev[2]

[1] Vladimir State University, Vladimir, Russia
[2] Institute of Structural Macrokinetics and Materials Science, Russian Academy of Sciences, Chernogolovka, Moscow, 142432 Russia

e-mail: vertin.dmitry@yandex.ru

In this communication, we report on deposition of protective Al–2Mg–*n*C coatings onto Steel 0.8 by cold gas-dynamic sputtering (DIMET-420 stand). Nanopowders of Al–2Mg–1C and Al–2Mg–5C composites used as starting materials were prepared as described elsewhere [1–3]. Deposited coatings were characterized by SEM/EDS (Zeiss Ultra plus 55) and elemental mapping. The micrographs of deposited coatings along with relevant EDS data are presented in Fig. 1.

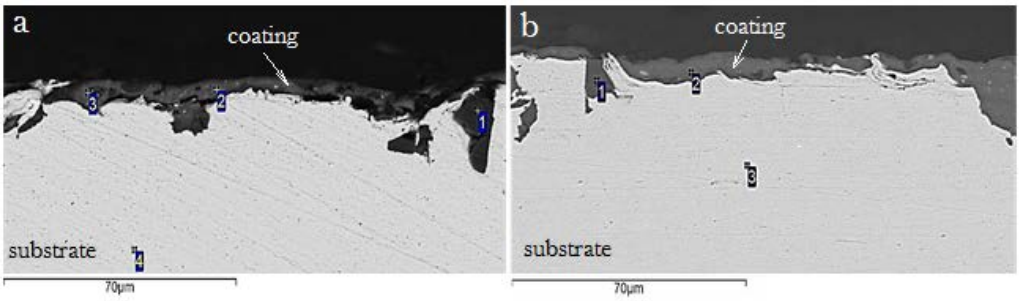

(a)

Spot	C	O	Mg	Al	Mn	Fe
1	5.8	51.6	-	41.9	-	0.55
2	11.5	4.7	1.36	78.5	0.98	2.56
3	13.7	8.6	1.43	70.98	0.8	1.90
4	4.19	-	-	1.19	-	94.6

(b)

Spot	C	O	Mg	Al	Mn	Fe
1	16.4	40	-	42.4	-	0.92
2	12.6	8.2	1.4	74.8	0.64	1.88
3	2.30	-	-	1.48	-	96.2

Fig. 1. The Al–2Mg–*n*C coatings deposited in regime 3 (a) and regime 5 (b).

The coatings exhibit no lengthy pores and cracks. The coatings are seen to be uniform and follow the relief of substrate surface.

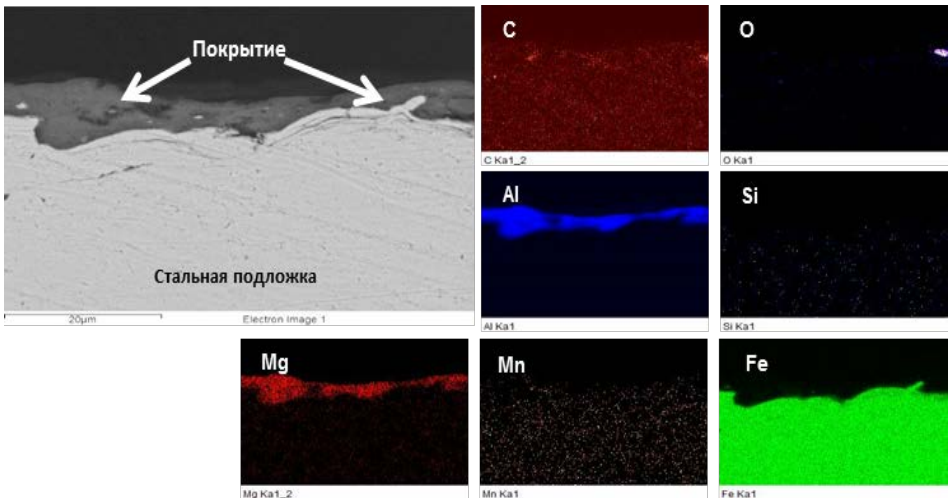

Fig. 2. Elemental maps of the coating under investigation.

1. D.S. Khrenov, A.V. Sobol'kov, A.E. Sytschev, Mechoactivation of AMg-2–graphite powder mixtures, in *Abstr. XIII All-Russia School-Seminar on Structural Macrokinetics*, Moscow: OOO Print, 2015, pp. 73–75.
2. A.V. Aborkin, I.A. Evdokimov, Mechanoactivation of Al + 2Mg + *n*C mixtures, in *Proc. VI Int. Conf. on Deformation of Materials and Nanomaterials*, Moscow: Izd. IMET, 2015, pp. 427–428.
3. A.V. Aborkin, A.I. Zalesnov, D.M. Babin, A.V. Starikov, Characterization of Al–2Mg–*n*C composite, in *Proc. IV Int. Conf. on Basic Research and Innovations in Mechanical Engineering*, Moscow: SPEKTR, 2015, pp. 15–17.

MAX PHASE Ti_2AlN BY SINTERING IN VACUUM

A. A. Kondakov, I. A. Studenikin, A. V. Linde, N. A. Kondakova, and V. V. Grachev

Institute of Structural Macrokinetics and Material Science, Russian Academy of Sciences, Chernogolovka, Moscow, 142432 Russia

e-mail: kondakov@ism.ac.ru

This work aimed at the preparation of single-phase Ti_2AlN by vacuum sintering of various powder mixtures and optimization of the process with respect to better yield of the MAX phase.

In our experiments, we used the following powder mixtures: 2Ti + AlN (mix **1**), TiAl + TiN (mix **2**), and Ti + Al + TiN (mix **3**). These were intermixed in a ball mill for 30 min (mill/ball ratio 2 : 1) and placed into silica tubes (15 mm inner diameter) in amount of 15 g (bulk density 73–77 %). Experiments with 500-g samples were performed in a rectangular Mo crucible. Sintering was carried out in a vacuum furnace (SNVE-16/16) at T = 1100, 1200, 1300, 1400, and 1500°C (5.8×10^{-6} mm Hg) for 60 min. Sintering products were characterized by XRD (DRON-3M) and SEM/EDS (Zeiss Ultra Plus, Carl Zeiss equipped with an INCA Energy 350 XT accessory, Oxford Instruments).

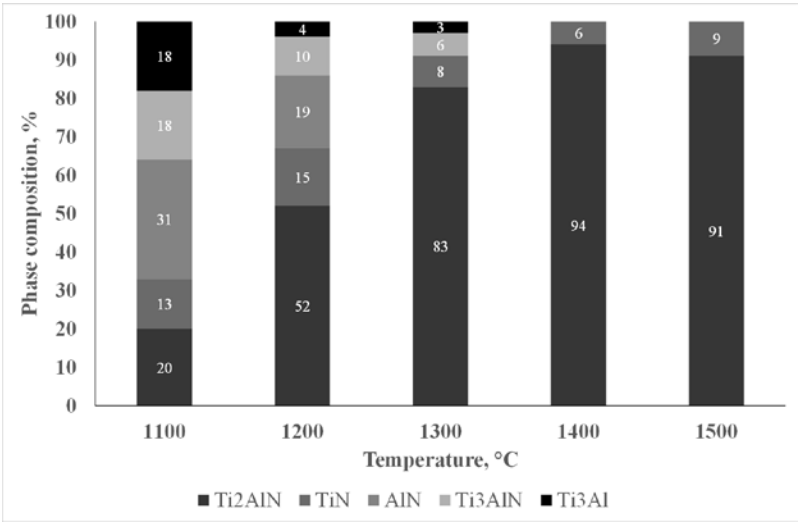

Fig. 1. Phase composition of products obtained by sintering mix **1** at indicated temperatures.

Phase compositions of the products obtained by sintering mix **1** at different *T* are schematically presented in Fig. 1. With increasing *T*, the Ti_2AlN content of product is seen to grow from 20 to 52%. The product formed at 1400°C contained фаз 94% Ti_2AlN and 6% TiN. But in the product formed at 1500°C the amount of Ti_2AlN decreases down to 91%. This implies that a maximum amount of MAX phase Ti_2AlN (94%) can be obtained at *T* = 1400°C, which agrees with literature data [1–3]. For this reason, the sintering of mixes **2** and **3** was carried out at this temperature.

The sintering of mix **2** at 1400°C yielded a multiphase product (cf. Fig. 2a) containing 94% Ti_2AlN, 4% TiN, and 25 Ti_3Al. A monophase product (100% Ti_2AlN) was obtained by sintering mix **3** at 1400°C. The diffraction pattern in Fig. 2b convincingly demonstrates that an increase in the charge weight (from 15 to 500 g) did not result in formation of byproducts, which opens up a feasibility for scaling the process under consideration.

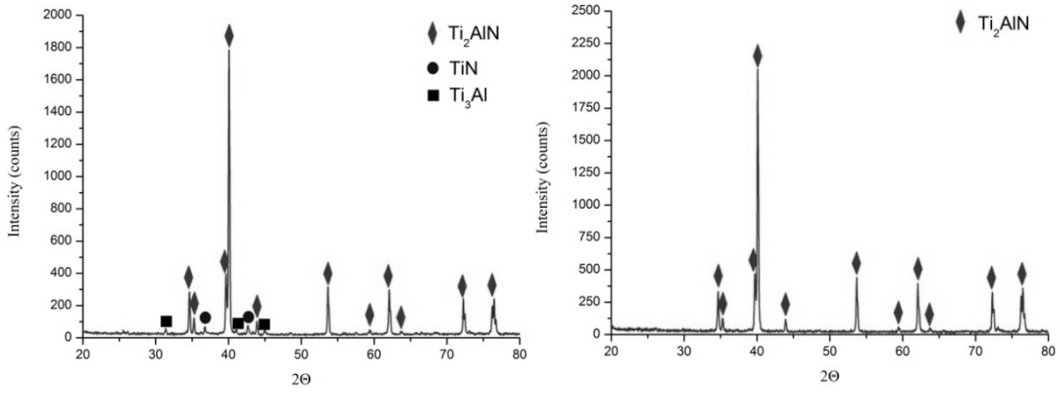

(a) (b)

Fig. 2. Diffraction patterns of products derived from (a) 15 g of mix **2** and (b) 500 g of mix **3**.

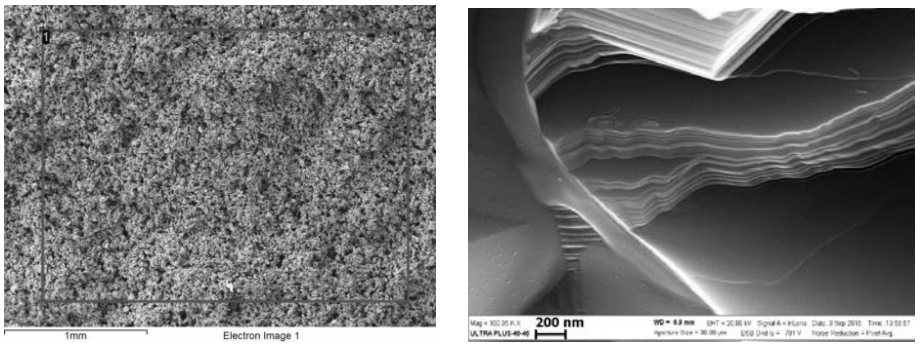

(a) (b)

Fig. 3. Fracture surface of the product derived from 500 g of mix **3**.

The EDS results for the area indicated in Fig. 3a gave the following elemental composition: N 23.56 at. %, Al 25.68 at. %, and Ti 50.76 at. %, which well agrees with that of Ti_2AlN. As is seen in Fig. 3b, the material exhibits a nano-laminate structure typical of MAX compounds.

This work was financially supported by the Russian Foundation for Basic Research (project no. 14-08-00714).

1. Barsoum M., Ali M., El-Raghy T., Processing and characterization of Ti_2AlC, Ti_2AlN, and $Ti_2AlC_{0.5}N_{0.5}$, *Metall. Mater. Trans. A*, 2000, vol. 31, no. 7, pp. 1857–1865.
2. Lin Z., Zhuo M., Li M., Wang J., Zhou Y. Synthesis and microstructure of layered ternary Ti_2AlN ceramic, *Scr. Mater*., 2007, vol. 56, no. 12, pp. 1115–1118.
3. Liu Y., Shi Z., Wang J., Qiao G., Jin Z., Shen Z. Reactive consolidation of layered ternary Ti_2AlN ceramics by spark plasma sintering of a Ti/AlN powder mixture, *J. Eur. Ceram. Soc*., 2011, vol. 31, no. 5, pp. 863–868.

SHS IN Zr–Al–C SYSTEM: A TIME-RESOLVED XRD STUDY

D. Yu. Kovalev, M. A. Luginina, and S.G. Vadchenko

Institute of Structural Macrokinetics and Materials Science, Russian Academy of Sciences, Chernogolovka, Moscow, 142432 Russia

e-mail: kovalev@ism.ac.ru

Self-propagating high-temperature synthesis (SHS) in the Zr–Al–C system was explored by Time-Resolved X-Ray Diffraction (TRXRD) method. The reaction kinetics was found to depend on heating rate. The reaction could be initiated in a mode of either high-temperature (Fig. 1) or low-temperature combustion (Fig. 2). The $ZrAl_2$ phase crystallizes in 3–4 s behind the combustion front. As the result, the products contain ZrC and zirconium intermetallics. The formation of ternary compounds was not observed (Fig. 1).

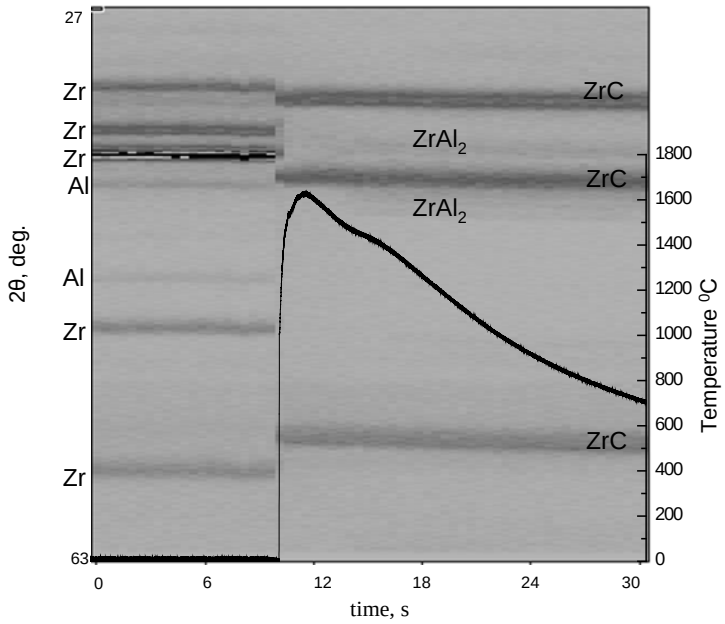

Fig. 1. Time-resolved diffraction patterns of high-temperature combustion.

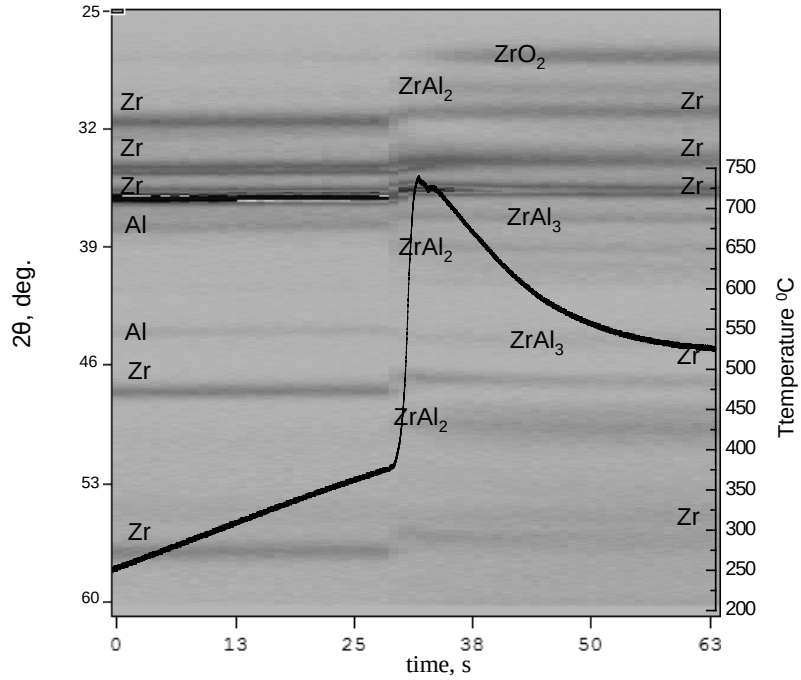

Fig. 2. Time-resolved diffraction patterns of low-temperature combustion.

The low-temperature combustion yielded solid solution Zr[Al], $ZrAlC_x$, $ZrAl_3$, $ZrAl_2$, and Zr_2Al_3 (Fig.2) due to interaction between the Al melt and the Zr particles when the reaction proceed in a mode of thermal explosion (volume reaction) in conditions of strong heat sink.

SYNTHESIS OF MgB_2 IN A MODE OF THERMAL EXPLOSION: A TIME-RESOLVED XRD STUDY

D. Yu. Kovalev[1], A. Yu. Potanin[2], E. A. Levashov[2], and N. F. Shkodich[1]

[1]Institute of Structural Macrokinetics and Materials Science, Russian Academy of Sciences, Chernogolovka, Moscow, 142432 Russia
[2]National University of Science and Technology MISiS, Leninskii pr. 4, Moscow, 119049 Russia

e-mail: kovalev@ism.ac.ru

The dynamics of phase transformations during combustion synthesis of magnesium diboride in a mode of thermal explosion (TE) was studied by time-resolved X-ray diffraction. Typical results are presented below.

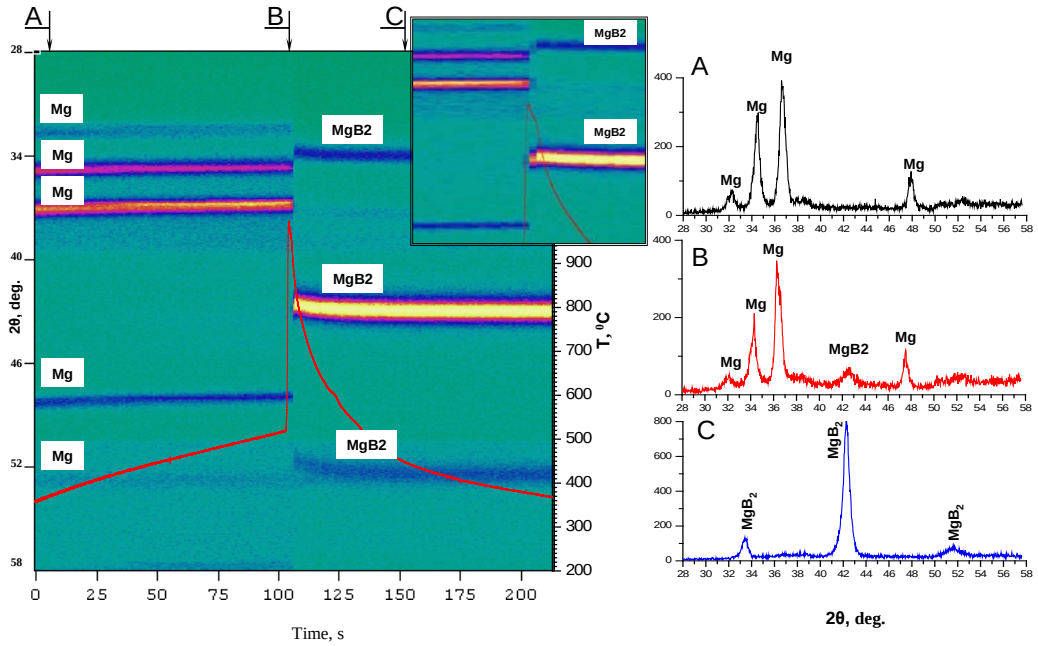

The MgB_2 phase was found to emerge without formation of intermediate compounds. The effect of heating rate on the formation mechanism of MgB_2 was established. The presence of oxygen impurities has a significant impact on the kinetics and formation mechanism of MgB_2. If the heating rate exceeds 150 deg/min, the oxide coating is not formed around the magnesium particles, which results in the solid-phase reaction $Mg + 2B = MgB_2$ by the mechanism of reactive diffusion. Moreover, the self-

ignition temperature was lower than the melting point for magnesium. Mechanical activation of green mixtures leads to variation in the kinetics of MgB_2 formation, significantly increases the period of simultaneous existence of Mg and MgB_2, and reduces the reaction temperature.

TEMPERATURE DEPENDENCE OF Ti_2AlN THERMAL EXPANSION AS DETERMINED FROM HIGH-TEMPERATURE XRD DATA

D. Yu. Kovalev and M. A. Luginina

Institute of Structural Macrokinetics and Materials Science, Russian Academy of Sciences, Chernogolovka, Moscow, 142432 Russia

e-mail: kovalev@ism.ac.ru

MAX phase Ti_2AlN belongs to the class of refractory materials with a layered structure and unique combination of metal and ceramic properties [1]. The knowledge of thermal expansion coefficient (TEC) of such compounds is essential for many applications. Earlier, the thermal expansion of Ti_2AlN was studied by high-temperature neutron diffraction [2] and no temperature dependence was found. In this work, we studied the temperature dependence and anisotropy of TEC for Ti_2AlN in the range 30–1000°C by high-temperature XRD.

The Ti_2AlN powder synthesized by reactive sintering [3] contained below 1 wt % TiN as an impurity. The cell parameters of thus obtained Ti_2AlN were a = 0.298(8) nm and c = 1.362(1) nm (in accordance with PDF card 00-55-0434).

The temperature dependence of TEC for Ti_2AlN was carried out by using an ARL X'TRA diffractometer (Cu-K_α radiation) and an NTK2000 camera. The registration of Diffraction spectra was recorded within the angular interval 2θ = 32–55° by the $\theta-\theta$ scheme. Ti_2AlN powder was applied on the surface of a tungsten heater in its central part. The thickness of the layer was about 100 μm. Heating was at some set heating rate (100 deg/min) and isothermal dwell time. Experiments were carried out in vacuum (2×10^{-5} mbar). Registration of XRD patterns started after reaching of the temperature of isothermal dwell time: 100, 300, 500, 700, 900, and 1000°C. The lattice parameters of Ti_2AlN at the temperature of isothermal annealing were determined by the position of the Bragg reflexes 100, 101, 104, 106.

The CTE of Ti_2AlN (α) was calculated from the temperature dependence of lattice parameters a and c (Fig. 1) by using the Einstein approximation:

$$a(T) = a_0 + a_0\alpha\Theta f_E(\Theta/T)$$

where a_0 is the lattice parameter at 0 K, Θ is the Debye–Einstein temperature, and $f_E(\Theta/T) = 1/[\exp(\Theta/T) - 1]$ is the Einstein function.

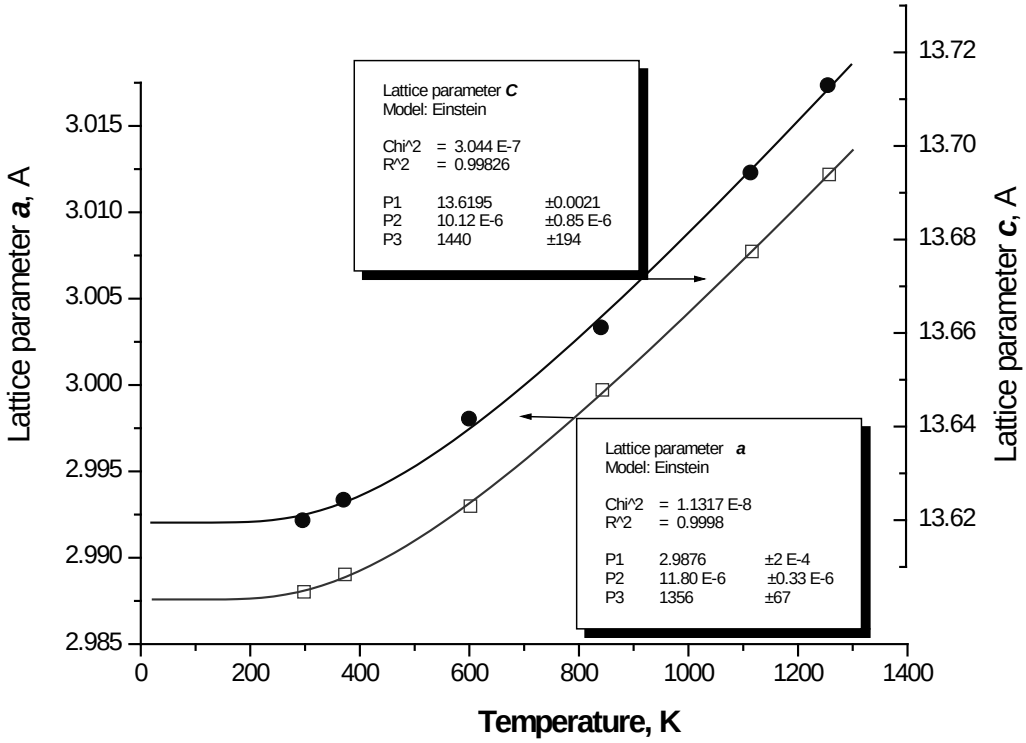

Fig. 1. Lattice parameters *a* and *c* as a function of temperature *T*.

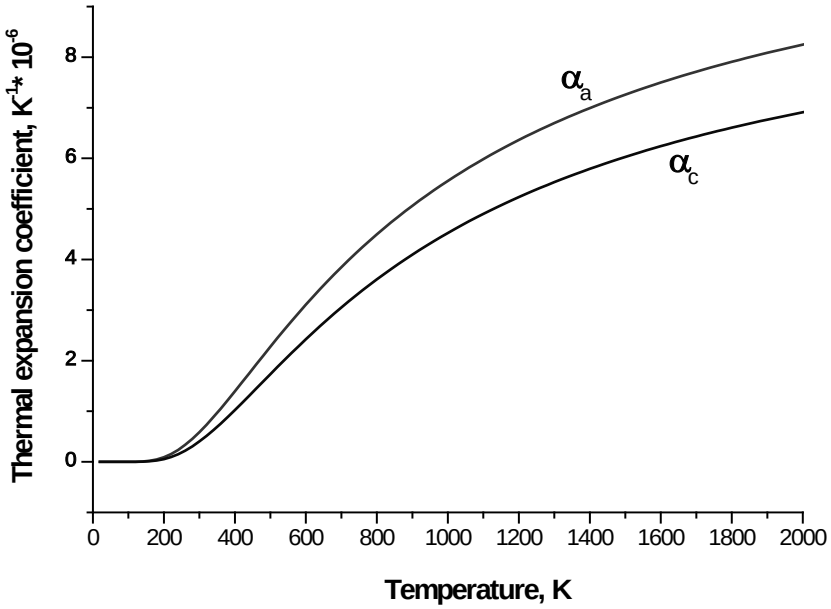

Fig. 2. Temperature dependence of α_a and α_c.

The obtained TECs values for Ti_2AlN—α_a = (11.80 ± 0.33) $\times\cdot 10^{-6}$ K^{-1} and α_c = (10.12 ± 0.86)$\cdot\times$ 10^{-6} K^{-1}—occupy an intermediate position between those of metals and ceramics. The temperature dependences of α_a and α_c are plotted in Fig. 2. It is worth noting that Ti_2AlN exhibits the anisotropy of TEC: the values of α_a are higher than α_c, and both tend to level-off at high temperatures.

1. M.W. Barsoum, The $M_{n+1}AX_n$ phases: A new class of solids, thermodynamically stable nanolaminates, *Prog. Solid State Chem.*, 2000, vol. 28, nos. 1–4, pp. 201−281.
2. N. J. Lane, S.C. Vogel, M. W. Barsoum, Temperature-dependent crystal structures of Ti_2AlN and Cr_2GeC as determined from high temperature neutron diffraction, *J. Am. Ceram. Soc*., 2011, vol. 94, no. 10, pp. 3473–3479.
3. M. A. Luginina, D. Yu. Kovalev, A. E. Sytschev, Preparation of Ti_2AlN by reactive sintering, *Int. J. Self-Propag. High-Temp. Synth*., 2016, vol. 25, no. 1, pp. 35–38.

EXPLOCLAD Ti–Al–Ti COMPOSITE WITH IMPROVED STRENGTH PARAMETERS

D. B. Kryukov, M. S. Gus'kov, and D. S. Gus'kov

Penza State University, ul. Krasnaya 40, Penza, 440026 Russia

e-mail: AspirantSLPiM@yandex.ru

In this communication, we report on fabrication of exploclad three-layer Ti–Al–Ti composites. The upper and lower layers were Ti-alloy plates (VT1-0 brand) while the intermediate one was an Al plate (AMg5M brand). In order to strengthen the resultant clad material, the Al plate had oppositely oriented conical perforations made in a staggered order over the entire plate.

Developed was a computer model that was used to estimate the strength of thus prepared clad metal composite under the assumption of complete transformation of aluminum into intermetallic. These calculations gave a value of 695 MPa.

After explosive welding and rolling, the samples were annealed at 550–630°C for a period of 0.15–235 h. Thermal treatment was used to ensure the growth of the intermetallic layer whose thickness attained a value of up to 100 μm. The formation of the $TiAl_3$ layer was confirmed by XRD analysis. The results of mechanical testing have shown that the mechanical properties of our composite are superior (by 38%) over those of the VT1-0 alloy.

PROSPECTS FOR USING EXPLOCLAD MATERIALS IN GEOTHERMAL APPLICATIONS

G. Kwiatkowski[1], Z. Szulc[1], M. Najwer[1], and M. Gloc[2]

[1]Zakład Technologii Wysokoenergetycznych EXPLOMET Gałka, Szulc Sp.J.
[2]Politechnika Warszawska, Wydział Inżynierii Materiałowej

e-mail: grzegorz.kwiatkowski@explomet.pl

The process of explosive cladding significantly affects the hardness of joined materials. As a result of collision of the flayer plate to the base material, both materials, base and clad, are significantly deformed in the bond zone. This causes an increase of the hardness in the bond zone and in areas close to bond, and for the clad material practically over the entire cross section. [1–3]. For full or partial elimination of the effect of strengthening for selected grades of bonded materials appropriate heat treatments are being used.

In relation to many of cladding materials, in addition to the required chemical corrosion resistance, it is also important to ensure the hydrogen corrosion resistance, information on this topic can be found in [4–6]. It is the industrial requirement that materials must have an adequate, impassable level of hardness. For each group of materials, these levels are defined by NACE regulations [7]. Such requirements are put also to many materials and components used in the construction of geothermal equipment and installations. Currently intensive work is carried out aiming at the development of geothermal energy. Among other things, these works aim at increasing a depth of steam collection, as well as at search for new or significantly improved materials, including clad ones, that would withstand hash conditions of their operation.

The present study describes the impact of explosive cladding and heat treatment on the hardness of the joined materials, where the base material is carbon steel P355NH and clad materials are chromium–nickel austenitic stainless steels (254 SMO, 316L, superduplex SAF 2507) and nickel alloys (Alloy 625 and Hastelloy C-276).

Above mentioned materials have been selected for testing as potentially applicable in the construction of geothermal installations. Elements of these installations are subjected to the action of aggressive corrosive environment and, in addition, to the overgrowth of some minerals on power junctions in superheated steam. Moreover the hydrogen corrosion has crucial meaning to the viability of some certain elements of geothermal installations.

At the core of the design and selection of materials with elevated hydrogen corrosion resistance, the explosively cladded materials must be subjected to hardness

testing. In accordance with the requirements of NACE, hardness testing is carried out on the material's surfaces. Considering specifics of the explosive cladding technology such testing should be performed perpendicularly to the cross-section area. This will afford the indication of depth from the surface to which the requirements of NACE are addressed. Tests were performed separately for the base material that was the same for each sample, and separately for each of used clad materials.

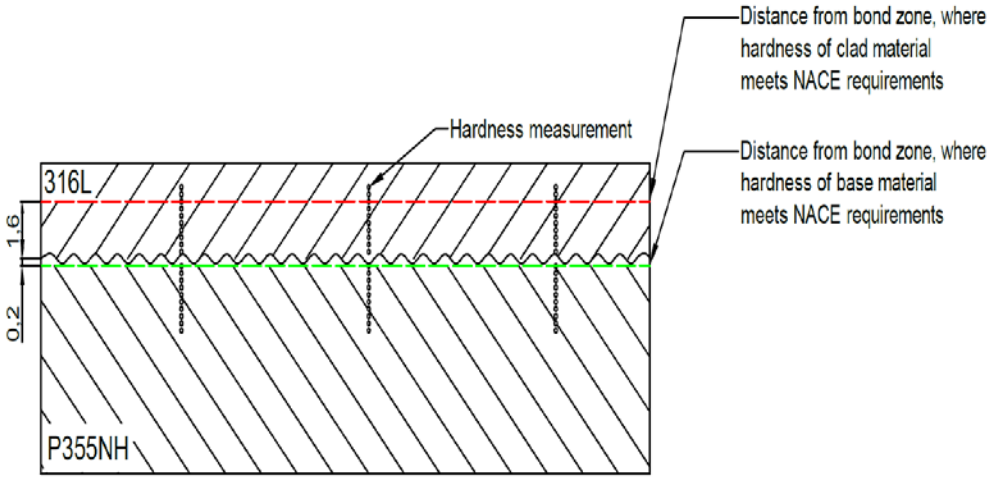

In this study, hardness measurements were performed on a cross section of the bond zone in the base material and in the clad material as well as on their surfaces. This made possible to determine the distance from the bond at which materials start to meet the requirements of NACE. Closer to the surface, the hardness decreased (see Fig. 1). In other words, for each of the materials it was determined up to which depth from the surface the NACE requirements to hardness are met.

Such a preliminary but necessary verification of materials was done on order to send a specific group of these materials for further tests and examinations. For all samples made of cladding materials, standard tests on mechanical and technological properties were performed.

1. J. Banker, Advances in explosion welding, in *The Handbook of Advanced Welding*, London: Woodhead Publishing, 2004.
2. B. Crossland, *Explosive Welding of Metals and Its Application*, Oxford: Clarendon Press, 1982.
3. W. Walczak, *Zgrzewanie wybuchowe metali*, Warszawa: Wyd. Naukowo-Techniczne, 1989.

4. K. Lublińska, A. Szummer, M. Gloc, K. Szpila, K.J. Kurzydłowski, Effect of hydrogen on degradation of explosion welded clad steel, *Acta Metall. Slovaca*, 2007, vol. 13, pp. 508–511.
5. M. Szwed, M. Gloc, M. Wielgat, L. Sarniak, K. Lublinska, A. Zagorski, K.J. Kurzydlowski, Evaluation of hydrogen degradation of steel plates by in situ ultrasonic testing with 2D phased array matrix probe, in *Proc. Asian Thermal Spray Conf*., 2012, pp. 98–101.
6. M. Szwed, K. Lublińska, M. Gloc, W. Manaj, K.J. Kurzydłowski, Steel clad plates hydrogen degradation evaluation using ultrasonic defectoscopy, *Adv. Manuf. Sci. Technol*., 2009, vol. 33, no. 4.
7. NACE Standard MR0103-2003, Materials Resistant to Sulfide Stress Cracking in Corrosive Petroleum Refining Environments.

EXPLOSIVE WELDING OF MULTILAYER TITANIUM/LOW-ALLOY STEEL COMPOSITES USING TANTALUM–COPPER AND NIOBIUM–COPPER INSERTS

D. V. Lazurenko[1], V. I. Mali[2], I. A. Bataev[1], Yu. N. Malyutina[1], B. N. Kyzylova[1], M. A. Esikov[2], and R. I. Kuz'min[1]

[1]Novosibirsk State Technical University, pr. K. Marksa 20, Novosibirsk, 630073 Russia
[2]Lavrent'ev Institute of Hydrodynamics (LIH), Siberian Branch, Russian Academy of Sciences, pr. Lavrent'eva 15, Novosibirsk, 630092 Russia

e-mail: pavlyukova_87@mail.ru

As is known, joining titanium alloys with steel is a difficult task. Interaction of these materials leads to formation of brittle intermetallic structures, such as TiFe and $TiFe_2$ [1]. The use of explosive welding allows to minimize the formation of brittle phases but interaction between dissimilar elements cannot be fully prevented [2, 3]. The formation of intermetallics can be suppressed by inserting interlayers [4, 5]. The inserts should not react with titanium and iron or possess good miscibility. The Ta–Cu and Nb–Cu inserts were selected for our experiments on explosive welding of low-alloy steel and high-strength multilayered titanium to reach enhanced impact toughness of the entire composite [6].

Explosive welding of two composites was carried out at LIH. Both materials were obtained in similar regimes. The main components of both composites were: 45HNM low-alloy steel plate and alternatively stacked dissimilar plates of α+β-Ti alloys with different β-stabilization coefficients (Table 1). Steel, VT14, and VT23 plates were 2.5, 0.6, and 1.5 mm thick, respectively. Interlayers consisted of copper with a thickness of 0.3 mm or 0.2-mm niobium in the former and latter cases, respectively.

Table 1. Chemical composition of steel and titanium plates, wt %.

	C	Si	Mn	Ni	Cr	Mo	S	P	Fe	V	Al	Zr	Ti
45HNM	0.47	0.34	0.44	1.06	1.57	0.51	0.01	0.01	bal.	-	-	-	-
VT14	0.01	0.15	-	-	-	3.4	-	-	0.3	1.4	4.8	0.3	bal.
VT23	0.04	0.03	-	-	0.53	1.2	-	-	0.6	3.4	4.02	0.3	bal.

As a result, two 8-layer materials were fabricated. The wavy interfaces formed between dissimilar materials are shown in Fig. 1. The lowest values of wave parameters

(amplitude and wavelength) were observed for the Cu–Nb(Ta) and Nb(Ta)–VT23 interfaces.

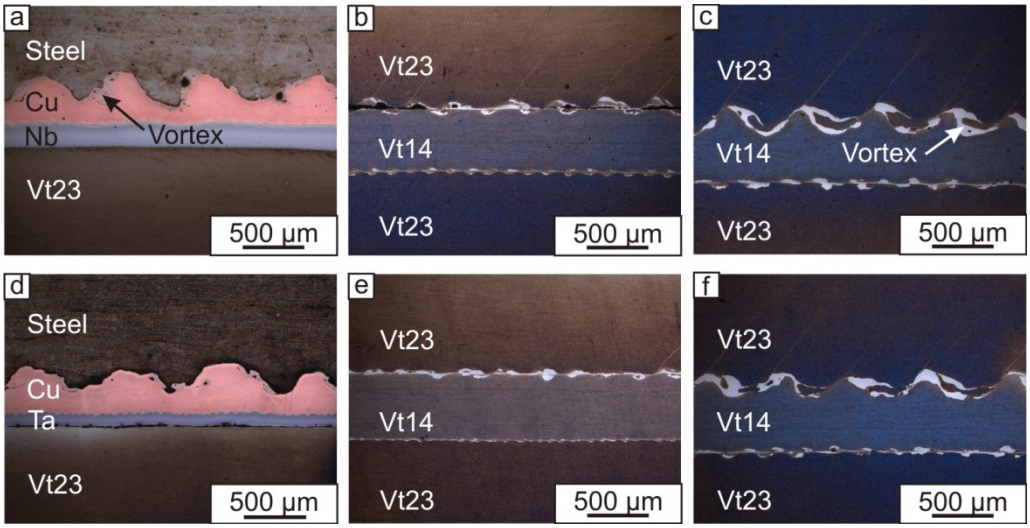

Fig. 1. Interfaces 1-3 (a), 4-5 (b), and 6-7 (c) in the composite with a Cu–Nb insert; and interfaces 1-3 (d), 4-5 (b), and 6-7 (d) in the composite with a Cu–Ta insert.

Among particularities observed at the interfaces of dissimilar materials, the formation of vortexes should be emphasized (Fig. 1). Due to the different character of interaction in different pairs—e.g. complete miscibility between Nb(Ta) and Ti or immiscibility between Cu and Fe(Ta, Nb)—structure and phase composition of these regions varied significantly from solid solutions to mechanical mixtures. But the formation of brittle intermetallics was prevented.

Strength of the composites was estimated by tensile testing. The Ta insert was found to provide a higher ultimate tensile strength of the composite (1060 MPa) in comparison with Nb (980 MPa). Impact toughness in both cases was minimum 2-fold higher than that of bulk titanium alloys and steel due to the positive influence of interfaces.

Thus, explosive welding of low-alloy steel with multilayer high-strength titanium provides high quality of joining and good mechanical properties. The preferable candidate for the insert can be recommended as a Ta–Cu pair.

1. H.O. Baker, *Alloy Phase Diagrams: ASM Handbook (Book 3)*, ASM International, 1992.
2. P. Liu, J. P. Jiang, H. G. Guo, B. L. Sun, Three wave interfaces of titanium/steel laminates manufactured by explosive welding, *Adv. Mater. Res.*, 2013, vols. 641–642, no. 5, pp. 570–573.

3. S.A.A. Akbari Mousavi, P. Farhadi Sartangi, Experimental investigation of explosive welding of cp-titanium/AISI 304 stainless steel, *Mater. Design*, 2009, vol. 30, no. 3, pp.459–468.
4. K. Ferjutz, J. R. Davis, *Welding, brazing, and soldering*: ASM Handbook : ASM International, 1993.
5. P. Manikandana, K. Hokamoto, M. Fujita, K. Raghukandan, R. Tomoshige, Control of energetic conditions by employing interlayer of different thickness for explosive welding of titanium/304 stainless steel, *J. Mater. Process. Technol.* 2008, vol. 195, pp. 232–240.
6. J. Wadsworth, D.R. Lesuer, Ancient and modern laminated composites: From the Great Pyramid of Gizeh to Y2K, *Mater. Charact.*, 2000, vol. 45, nos. 4–5, pp. 289–313.

COMBUSTION SYNTHESIS OF HIGH-ENTROPY ALLOYS AND THERMOELECTRIC MATERIALS

J. T. Li, Z. C. Yang, and G. G. Liu

Technical Institute of Physics and Chemistry, Chinese Academy of Sciences, Beijing, 100190 China

e-mail: lijiangtao@mail.ipc.ac.cn

High-entropy alloys consist of multiple elements with different crystal structures but can crystallize as a single phase. Recently, we developed a new technique to prepare high-entropy alloys (HEA), which is called high-gravity combustion synthesis. In the new technique, high-entropy alloys are produced by rapid solidification of hot melts from highly-exothermic aluminothermic reactions. High-gravity combustion synthesis may provide a fast and efficient way to produce high-entropy alloys with low energy consumption. Here, the CrMnFeCoNi alloy was successfully prepared by combustion synthesis under high gravity, and had exhibited a single *fcc* lattice and dendritic grain morphology. After remelting, the CrMnFeCoNi alloy retained the *fcc* structure, but the grain morphology became equiaxial. The CrMnFeCoNi alloy exhibits brittle fracture at room temperature but shows ductile behavior at 77 K, with much-improved strength and strain (Fig. 1).

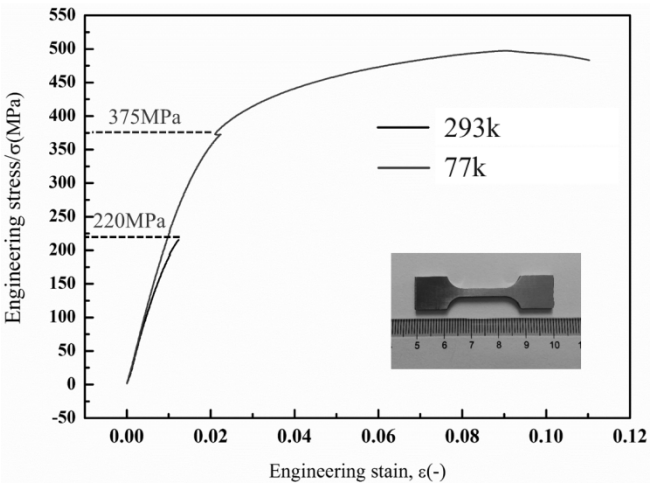

Fig. 1. Tensile test curve of high-entropy alloy CrMnFeCoNi prepared by combustion synthesis under high gravity.

Thermoelectric materials are attractive for solar thermal energy conversion and waste heat recovery. The existing methods for fabricating thermoelectric materials involve multi-step processes with considerable time and energy consumption. Here we report a fast and one-step way to prepare thermoelectric materials by gas-pressure or high-gravity assisted combustion synthesis.

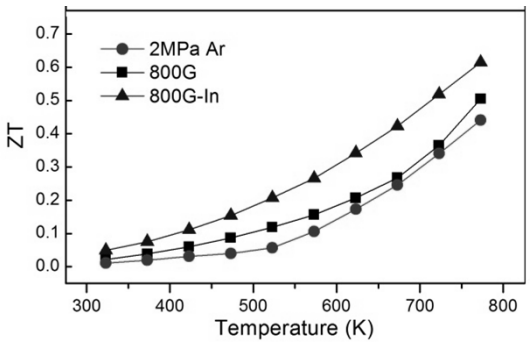

Fig. 2. Thermoelectric properties (ZT values) of Cu_2SnSe_3 samples prepared by combustion synthesis.

Dense Cu_2SnSe_3 samples with a porosity of below 2% were prepared from self-sustained combustion reaction of elemental powders. The electrical conductivity of the Cu_2SnSe_3 samples was greatly enhanced and the thermal conductivity was reduced by partial substitution of Sn with In. The ZT values of the un-doped and doped Cu_2SnSe_3 samples reached 0.51 and 0.62 at 773 K, respectively, which is comparable to the best results reported for Cu_2SnSe_3 produced by other methods. Combustion synthesis offers an efficient way to prepare thermoelectric materials with reduced time and energy consumption, which may open up new possibilities for synthesis of thermoelectric materials.

MECHANICAL TESTING OF EXPLOCLAD CORROSION-RESISRANT LIGHT-GAGE MULTILAYER SHEETS

I. S. Los', A. E. Rozen, M. S. Gus'kov, A. A. Rozen, and D. A. Verevkin

Penza State University, ul. Krasnaya 40, Penza, 440026 Russia

e-mail: silverelk@rambler.ru; aerozen@bk.ru

A new class of multilayer corrosion-resistant materials [1, 2] is designed for operating in aggressive media. These light-gage composites have three or more layers with a thickness of 2–3 mm each. For use in hazardous applications these materials have to be tested and licensed. In this work, we elaborated a procedure for testing each individual interlayer boundary for shear strength.

According to [3], simultaneous explosive welding of thin (below 3 mm) plates cannot provide full-strength joining of individual layers, because the impact velocity changes with increasing mass of flyer plates. In addition, standard procedures for measuring the join strength in multilayer metallic materials have not been developed so far.

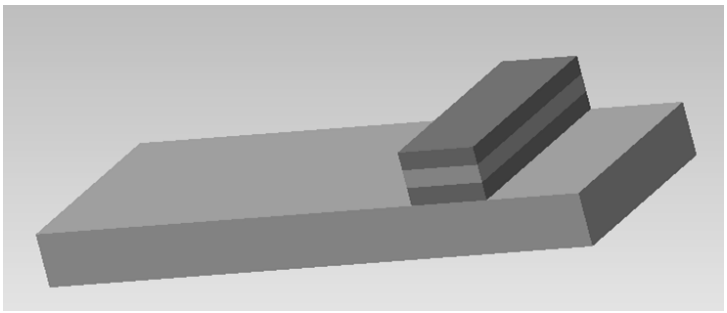

Fig. 1. Multilayer sample **1** for shear tests.

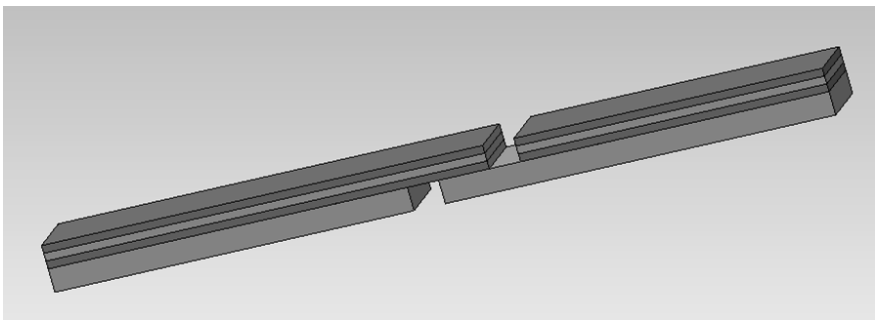

Fig. 2. Multilayer planar sample **2**.

The schematic of multilayer sample **1** (2 + 2 + 2 + 10 mm thick) for shear tests is shown in Fig. 1. Samples **2** had a geometry depicted in Fig. 2. On going from top, the materials were as follows: (1) 12Cr18Ni10Ti steel (analog of AISI 321), (2) St 3 (analog of A570), (3) 12Cr18Ni10Ti, and (4) St 3. The rate of loading was 10 mm/min.

No thermal treatment was done before testing. The shear failure of samples **1** was accompanied by cracking and happened on carbon steel (because stainless steel underwent some strengthening under the action of shock loading). The shear strength varied between 330 and 420 MPa. Samples 2 failed in the fourth layer under a tensile load of 290–326 MPa. Samples **1** were also tested after thermal treatment. The shear strength was found to exceed 147 MPa.

This work was supported by the Russian Ministry for Education and Science (project no. 490).

1. A.E. Rozen, I.S. Los', Yu.P. Perelygin, L.B. Pervukhin, Yu.A. Gordopolov, G.V. Kirii, P.I. Abramov, S.G. Usatyi, D.B. Kryukov, O.L. Pervukhina, I.V. Denisov, *Multilayer material with enhanced corrosion resistance and methods for preparing same*, Eurasian Patent 016878, 2012.
2. I.S. Los', Yu. P. Perelygin, A.E. Rozen, S.Yu. Kireev, *Multilayer light-gage corrosion resistance materials*, Penza: Izd. PSU, 2015.
3. V.I. Lysak, S.V. Kuz'min, *Explosive Welding*, Moscow: Mashinostroenie 1, 2005.

EXPLOSIVE COMPACTION OF POWDERS

A. R. Luchenok, L. V. Sudnik, G. V. Smirnov, N. V. Kirshina, and V. S. Tkachuk

Institute of Powder Metallurgy, Minsk, Belarus

e-mail: alar@tut.by

Commercial powders of Ti, $CrSi_2$-based resistive alloys (RA1 and RA2), and $MoSi_2$ were subjected to explosive compaction by using a standard planar scheme with a linear detonation front [1] and ammonite layer 20–60 mm thick as high explosive (HE). Some characteristics of compacted materials are given below.

Material	m.p.,°C	H_μ, GPa	ρ, g/cm^3
Ti	1671	1.6	4.5
Alloy 1 (RA1)	1400	6.8	4.7
Alloy 2 (RA2)	1250	7.4	5.0
$MoSi_2$	2020	12	6.31

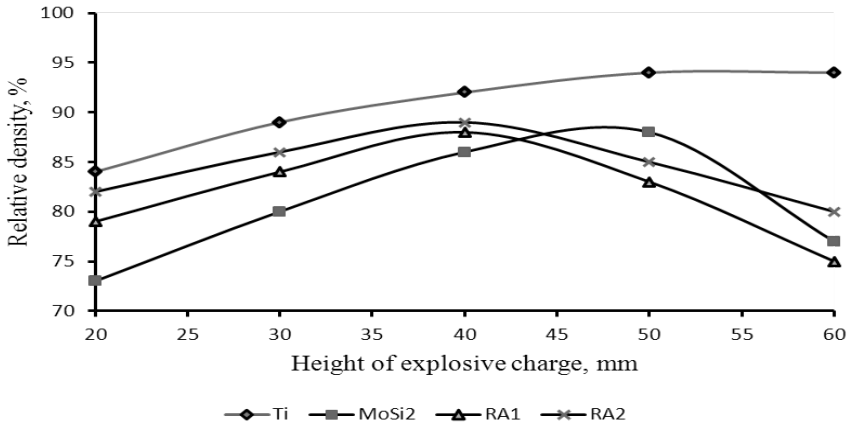

Fig. 1. Relative density ρ of the compacts vs. height *H* of charge layer.

The dependence of the relative density of the compacts as a function of height *H* of HE charge is given in Fig 1. For $H > 40$ mm, a decrease in ρ was accompanied by the emergence of longitudinal and slip cracks or equipment failure. The density of $MoSi_2$

compacts (material with highest m.p. and H_μ) attains its maximum value of 90% at $H \approx$ 50 mm.

For plastic Ti, no decrease in ρ with increasing H was observed. But at H = 60 mm, partial oxidation of titanium is observed, which should be kept in mind in practical implementations. At constant H, the density of compacts is inversely proportional to the m.p. and hardness of compacted material.

At our pilot-scale shop, we fabricated a batch of large-sized targets for vacuum sputtering up to 445 × 125 × 8 mm in their dimensions (Fig. 2). These items have been successfully tested at chip-producing plants in Belarus, Russia, and Poland.

It should be noted that the items obtained by explosive compaction take advantage of their better durability. In some cases, this technique affords to exclude the stage of sintering.

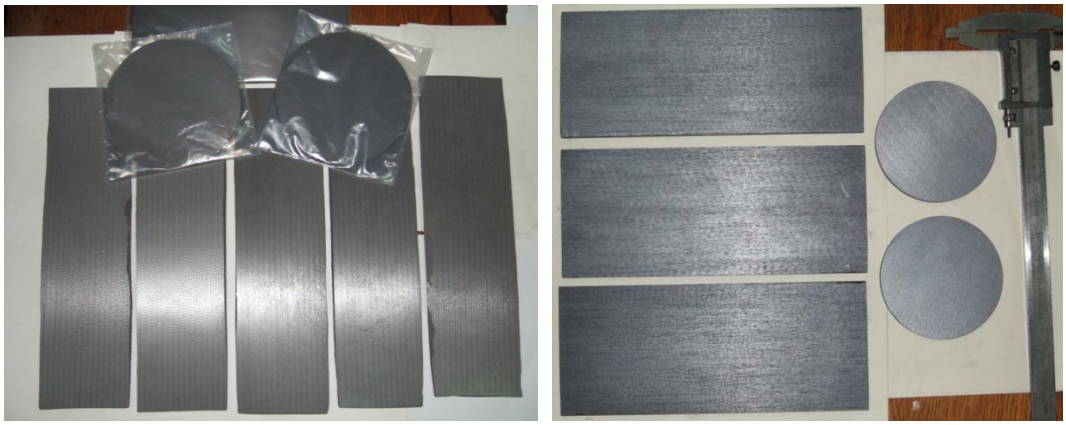

Fig. 2. Targets for vacuum sputtering obtained by explosive compaction.

The formation of strong contacts at the dynamic mode of compaction is achieved because the energy dissipation happens mainly in the point of contact between powder particles and, as a result, leads to the development of large shear deformations. The shock wave not only condenses powder but also causes interpartial shift which provides possibility of interparticle welding, just as in explosive welding of metals.

1. A.V. Krupin, V.Yu. Solov'ev, M.R. Krestev, *Processing of Metals by Explosion: A Textbook*, Moscow: Metallurgy, 1983 (in Russian).

THERMAL STABILITY OF MAX PHASE Ti_2AlN IN VACUUM

M. A. Luginina and D. Yu. Kovalev

Institute of Structural Macrokinetics and Materials Science, Russian Academy of Sciences, Chernogolovka, Moscow, 142432 Russia

e-mail: luginina@ism.ac.ru

Ti_2AlN compound is a representative of the $M_{n+1}AX_n$ phases. These materials exhibit a unique combination of properties such as low density, high strength and Young modulus, low thermal expansion, and high resistance to oxidation and thermal shock [1]. Ti_2AlN can be synthesized either from the elements or from TiN and/or AlN. It is known that heating of multi-component compounds leads to their thermal decomposition. In this study we explored the thermal stability of Ti_2AlN in vacuum in the temperature range 1150–1850 K.

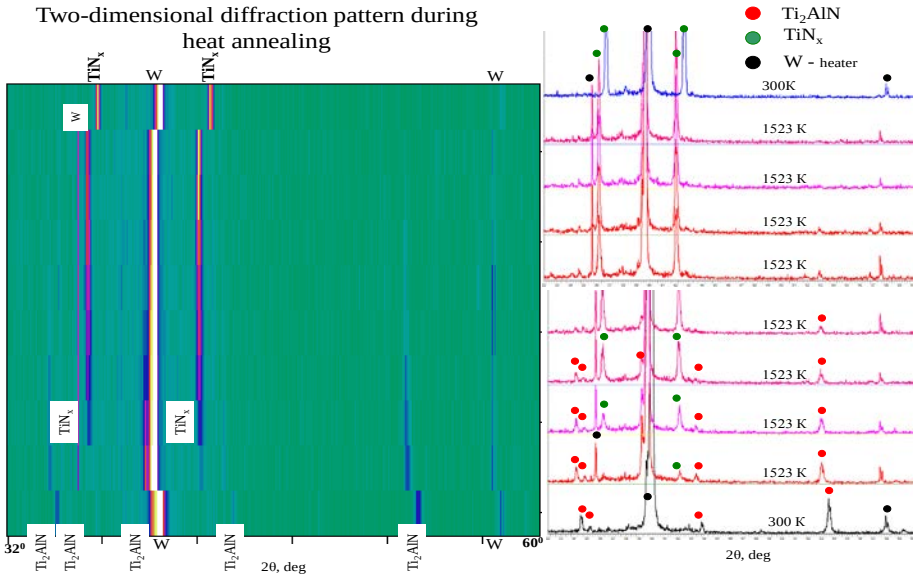

Fig.1 XRD patterns of Ti_2AlN during its annealing in vacuum, T = 1523 K.

Ti_2AlN powder was synthesized by reactive sintering [2]. The study of the thermal stability of Ti_2AlN phase was carried out on ARL X'TRA diffractometer (Cu-K_α) using high-temperature camera NTK2000 at temperatures up to 1850 K. The registration of diffraction patterns was carried out in the angular interval 2θ =32¯55° by θ−θ scheme. Ti_2AlN powder was applied on the surface of a tungsten heater in its central part. The

thickness of the layer was about 100 μm. Heating was carried out at some set heating rate and isothermal dwell time. The study was performed in vacuum (2×10^{-5} mbar). The heating rate was 100 deg/min. Registration of XRD patterns started after reaching of the temperature of isothermal dwell time (Fig. 1).

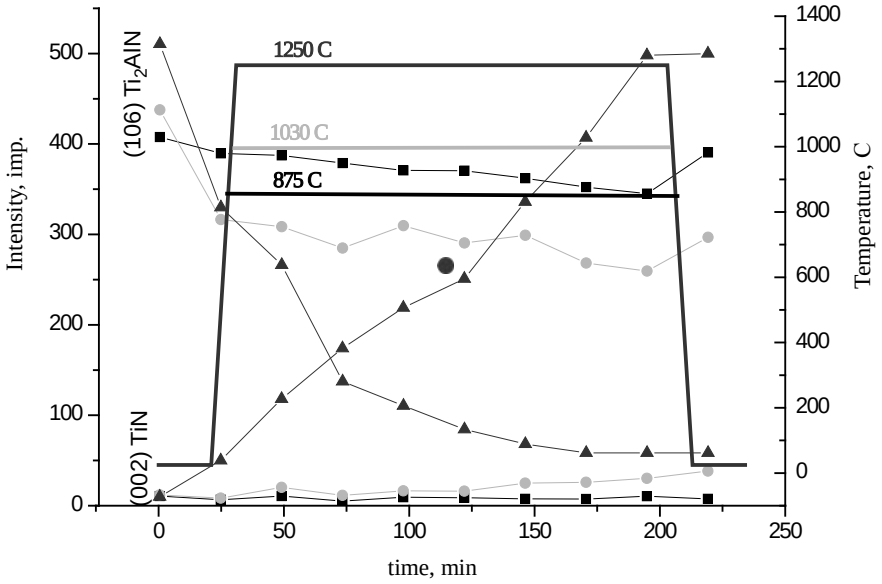

Fig. 2. Changes in the intensity of reflexes (106) Ti_2AlN and (200) TiN during annealing.

Thermal stability of Ti_2AlN in the vacuum was characterized by changes in the intensity of reflexes (106) for Ti_2AlN and (200) for TiN in the process of isothermal annealing (Fig. 2). The obtained kinetic dependences show that the Ti_2AlN phase is stable in vacuum at temperatures up to 1173 K. For $T > 1273$ K, we observed notable decomposition of Ti_2AlN and formation of TiN. Complete decomposition Ti_2AlN happens after 2 h of holding at $T > 1523$ K.

1. M.W. Barsoum, The $M_{n+1}AX_n$ phases: A new class of solids: Thermodynamically stable nanolaminates, *Prog. Solid State Chem.*, 2000, vol. 28, nos. 1–4, pp. 201−281.
2. M.A. Luginina, D.Yu. Kovalev, A.E. Sytschev, Preparation of Ti_2AlN by reactive sintering, *Int. J. Self-Propag. High-Temp. Synth.*, 2016, vol. 25, no. 1, pp. 35–38.

NOVEL MAX PHASE IN Zr–Ti–Al–C SYSTEM: SYNTHESIS AND STRUCTURE

M. A. Luginina, D. Yu. Kovalev, S. G. Vadchenko, S. V. Konovalikhin, and A. E. Sytschev

Institute of Structural Macrokinetics and Materials Science, Russian Academy of Sciences, Chernogolovka, Moscow, 142432 Russia

e-mail: kovalev@ism.ac.ru

In this communication, we report on combustion synthesis of MAX phase $(Zr_{0.5}Ti_{0.5})_3AlC_2$ from Zr–Ti–Al–C powder mixtures. Combustion product consisted of two phases: double carbide $Zr_{1-x}Ti_xC$ and MAX phase 312, $(Zr_{0.5}Ti_{0.5})_3AlC_2$ (Fig. 1). XRD results suggest that the content of $Zr_{1-x}Ti_xC$ is 28 wt % while that of $(Zr_{0.5}Ti_{0.5})_3AlC_2$, 72 wt %. In double carbide $Zr_{1-x}Ti_xC$, x was found to have a value of 0.75 ± 0.02.

Rietveld refinement of the atomic structure of a multiphase sample was carried out on the basis of our powder diffraction data. The phase $(Zr_{0.5}Ti_{0.5})_3AlC_2$ was attributed to a hexagonal crystal lattice with space group $P6_3/mmc$. This is a solid solution in which the Ti atoms and Zr atoms are located non-orderly in the metal–carbon layers, equally occupying positions 2A and 4E. The cell parameters of $Zr_{0.5}Ti_{0.5})_3AlC_2$ are presented in Table 1.

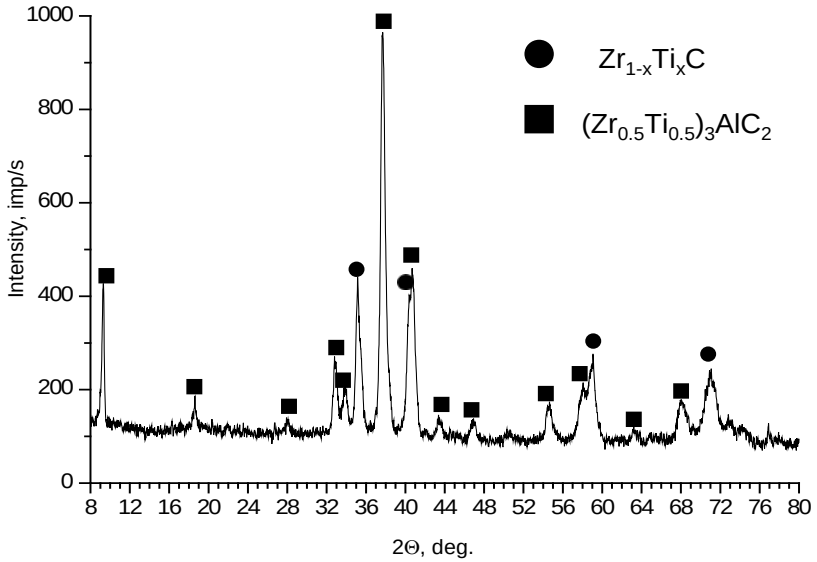

Fig.1. XRD pattern of combustion product.

Table 1. Crystal data of MAX phases.

	Ti_3AlC_2*	Zr_3AlC_2	$(Zr_{0.5}Ti_{0.5})_3AlC_2$**
Refs.	[1]	[2]	This work
a, Å	3.075(1)	3.3331(1)	3.174(2)
c, Å	18.578(1)	19.951(1)	19.080(9)
V, Å³	152.2(1)	191.94(4)	166.5(2)
Space group	*P*6$_3$/*mmc*	*P*6$_3$/*mmc*	*P*6$_3$/*mmc*
d, g/cm³	5.62	5.62	5.18
Zr^1–C, Å	2.137	2.377	2.503
Zr^2–C, Å	2.137	2.263	1.996 (2.062)
Zr^1–Zr^1, Å	3.075	3.330	3.174
Zr^2–Zr^2, Å	3.075	3.330	3.174 (3.174)
Zr^2–Zr^1, Å	2.968	3.225	3.098 (3.224)
Zr^2–Al, Å	2.879	3.076	2.919 (2.808)

* For Ti_3AlC_2 bond lengths correspond to Ti–X distance.
** For $(Zr_{0.5}Ti_{0.5})_3AlC_2$, Ti^2–X distance is given in parentheses.

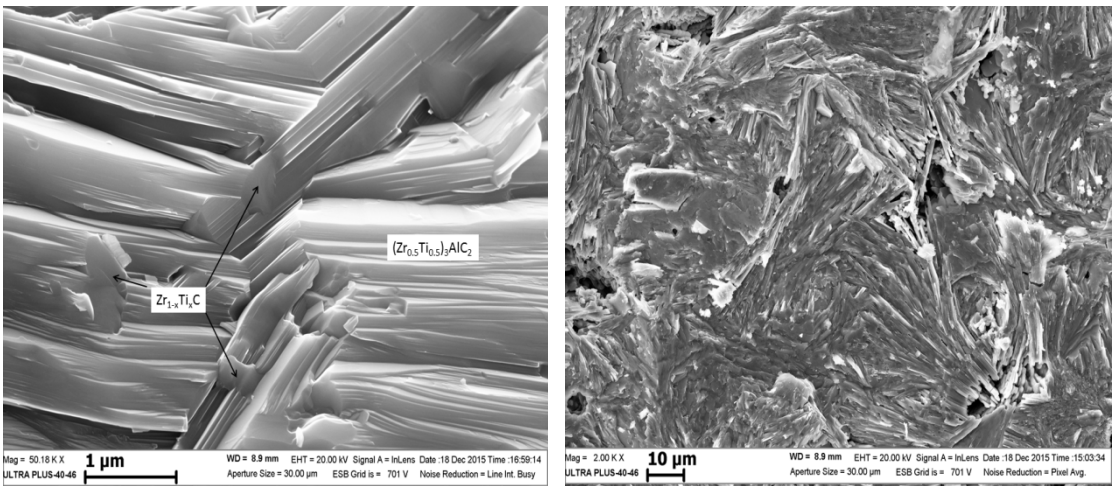

Fig. 2. SEM image of the product in system Ti–Zr–Al–C.

The microstructure of the fracture surface revealed the presence of two phases, one of which has a distinct laminated structure and belongs to the family of MAX phases, the second exhibits rounded grains typical of cubic carbides (Fig. 2).

This work was financially supported by the Russian Foundation for Basic Research (project no. 15-08-02331A).

EXPLOSIVE WELDING OF LONG-LENGTH PIPES AND RODS

A. Yu. Malakhov[1], I. V. Saikov[1], L. B. Pervukhin[2], and P.A. Nikolaenko [1]

[1] Institute of Structural Macrokinetics and Materials Science, Russian Academy of Sciences, Chernogolovka, Moscow, 142432 Russia
[2] Bardin Research Institute for Ferrous Metallurgy, Moscow, 105005 Russia

e-mail: sir.malahov2009@yandex.ru

The technology of explosive welding (EW) [1, 2] is widely used in fabrication of clad metals for use in oil industry, chemical engineering, shipbuilding, etc. [3]. The EW of pipes and cylinders exhibits its own specificity caused by curvature. [4].

In this context, we carried out experiments on the EW of pipes: outer layer steel 37G2F(108 × 12), inner (clad) layer steel 08Kh18N10T(80 × 2). In the rod, the core was copper (16 mm in diameter (M1 brand) and the shell was a Ti pipe 22 mm in diameter VT1-0 brand). Resultant clad items are shown in Fig. 1.

Fig. 1. Clad items: (a) 37G2F/08kh18H10T pipe and (b) M1/VT1-0 rod.

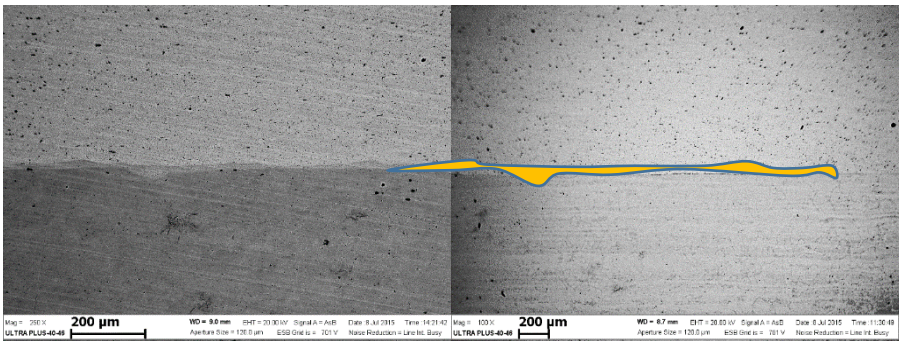

(a) (b)

Fig. 2. Weld seam in the 37G2F(below)/08Kh18N10T pipe: L = 100 (a) and (b) 900 mm.

Preliminary thermodynamic calculations predict that the number of fused areas must grow with increasing length L. For $L > 10\ d$, one can expect for formation of the interlayer comprising of the eutectic and solid solutions. These expectations were confirmed experimentally (see Fig. 2). In order to suppress the formation of the above interlayers we suggest that the EW should be carried out in an inert heat-conducting atmosphere (helium).

1. V.V. Selivanov, I.F. Kobylkin, S.A. Novikov, *Explosive Technologies: A Handbook*, Moscow: Izd. Bauman Tech. Univ., 2008 (in Russian).
2. J. Pearson, *Explosive Welding, Forming, and Compaction*, Appl. Sci. Publ., 1983.
3. A.A. Berdychenko, G.A. Volferz, L.B. Pervukhin, Cladding long-size Ti sheets with copper, *Polzun. Vestn*., 2012, no. 1, pp. 41–45.
4. V.P. Melikhov, Explosive welding of excentrically set cylinders, in *Explosive Welding and Cutting*, V.M. Kudinov, Ed., Kiev: Izd. Paton Inst., 1979, pp. 25–28 (in Russian).

Ti–Cu CONDUCTIVE CYLINDERS BY EXPLOSIVE WELDING

A. Yu. Malakhov[1], I. V. Saikov[1], L. B. Pervukhin[2], and P. A. Nikolaenko[1]

[1] Institute of Structural Macrokinetics and Materials Science, Russian Academy of Sciences, Chernogolovka, Moscow, 142432 Russia
[2] Bardin Research Institute for Ferrous Metallurgy, Moscow, 105005 Russia

e-mail: sir.malahov2009@yandex.ru

This work aimed at explosive welding of Ti–Cu conductive cylinders for use in electrolytic production of nickel [1]. For explosively welded bimetallic cylinders shown in Fig. 1 we explored the effect of weld integrity on the electroconductivity (voltage drop ΔV at U = 5 V and I = 500 A)) at different areas of the item. The results of measurements at the conical holes shown in Fig. 1 are presented in Table 1.

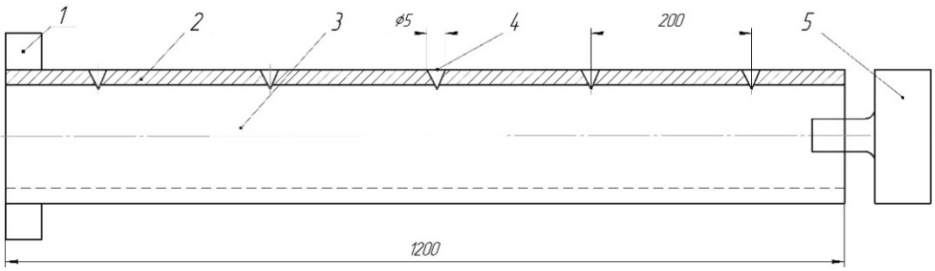

Fig. 1. Schematic of ΔV measurements: *1* movable electrode, *2* Ti pipe, *3* Cu coating, *4* conical holes, and *5* motionless electrode.

Table 1. Pressure drop ΔV (mV) over the Cu and Ti layers of the clad metal.

100% continuity		50% continuity	
Cu	Ti	Cu	Ti
13.4	13.5	12.8	13.2
25.2	25.3	21.4	21.5
36.9	36.9	32.5	32.4
48.7	48.9	42.9	42.9
58.7	58.8	53.2	53.3

The voltage drop is defined largely by the resistance of copper. The minimal percentage of contact area must not be less than 20%.

1. A.A. Berdychenko, G.A. Wolfhertz, L.B. Pervukhin, Cladding large-size Ti sheets with copper, *Polzun. Vestn.*, 2012, no. 1, pp. 41–45.

PROPERTIES OF Ti–Cr18Ni10 CLAD METALL UNDER DYNAMIC LOADING

E. Mazancová[1], K. Saksl[2], D. Ostroushko[1], M. Ďurišin[2], D. Balga[2], J. Szabo[2], and P. Kučera[1]

[1]VŠB-Technical University of Ostrava, Faculty of Materials Engineering, Tř. 17 listopadu 15, Ostrava, 708 33 Czech Republic
[2]Institut of Material Research, Slovak Academy of Science, Watsonova 47, Košice, 040 01 Slovak Republic

e-mail: eva.mazancova@vsb.cz

Weld of Ti-clad (6 mm in thickness) Cr/Ni (110 mm thick plate) was studied. After welding, the annealing at 600°C/1.5 h/air (HT 1) was carried out. For Charpy V tests (ČSN EN ISO 148-1) samples 10 × 10 × 55 mm (notch tip finished in Ti, 2 mm above weld) were manufactured. One set was after one annealing (1h) and the second set after double annealing (HT 2) at 600°C/1.5 h/air. After 2HT, the Ti phase showed a fine balanced microstructure, relaxed internal stresses and the presence of intermetallic phase Fe_2Ti [1–3]. Charpy tests were carried out in range from –120°C (Cr/Ni–Ti bimetal), resp. –75°C (C/Mn–Ti bimetal) to +20°C.

In the second step, the SSC in tensile and bent-beam test for Ti-clad Cr/Ni after 2HT were carried out. With respect to thicknesses of both welded materials and to the SSC testing bar dimensions according the NACE Standard TM0177-2005, samples for the SSC tensile test were manufactured with thread, which was glued up with quick-setting silicon adhesive so that bimetal weld would be exposed to corrosive medium (Fig. 1): standard solution A, $pH_{s/f}$ = 3.5/3.8. Bars were tested from 150 to 35 MPa, under the yield stress similar to that used in [4]. After removal of exposed samples from corrosive solution, those were looked over. Samples were 64 mm in length and exposed body was 3 mm in diameter. Six mm of Ti-clad Cr/Ni was lengthened by Ti of the same grade so that regular testing bar according NACE Standard TM0177-2005 could be manufactured. Samples (Fig. 1b) were subjected to three-point bending under loading ranging between 160 and 35 MPa (solution A, $pH_{s/f}$ = 2.7/2.9) and after this possible failures were investigated using a stereoscope and deflections (all in accord with the above mentioned standard).

Results of Charpy V tests (CNV) of bimetal Ti-clad Cr/Ni after HT 1and HT 2, in comparison with the similarly treated bimetal Ti-clad C/Mn steel, show (Fig. 1c) the positive effect of used HT. For HT 1, transition temperature is on a level of –60°C (310 J/cm^2) and difference of notch toughness values between low and upper shelf (from –120°C to +20°C) corresponds to 96.4 J/cm^2. Transition temperature after HT 1 was

shifted approx. by 20°C at the level of –40°C (241 J/cm^2). In this case both shelfs shows a difference of 46 J/cm^2. Bimetal with basic C/Mn steel demonstrates shifting of transition temperature to more positive values to –38°C (140 J/cm^2) and to –5°C (129 J/cm^2) after HT 1. The curves are more typically erect with differences (174 J/cm^2) of both shelfs. Fracture surfaces predominantly show trans-crystalline ductile failure with shallow dimples and at the lowest temperatures trans-crystalline cleavage failure dominates, with numerous finer ductile ridges responsible for generally high toughness levels. In fractured Charpy V samples, cracks were propagated both in bonding line and often in area of vortexes, where recently Fe_2Ti phase was detected [3].

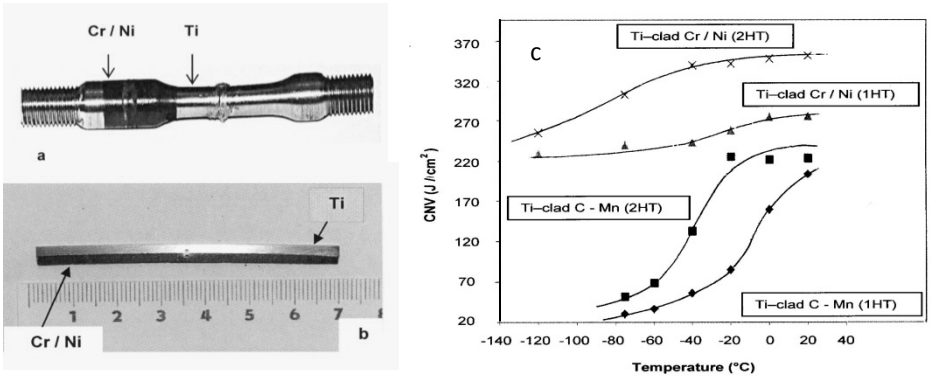

Fig. 1. Shape of used SSC bars after 720- h exposure (dark part represents Cr/Ni steel, the light one Ti): (a) sample after tensile test – dimensions are part of text, (b) sample after bent-beam test, and (c) summarized results of CNV vs temperature for two bimetal types at two different HT.

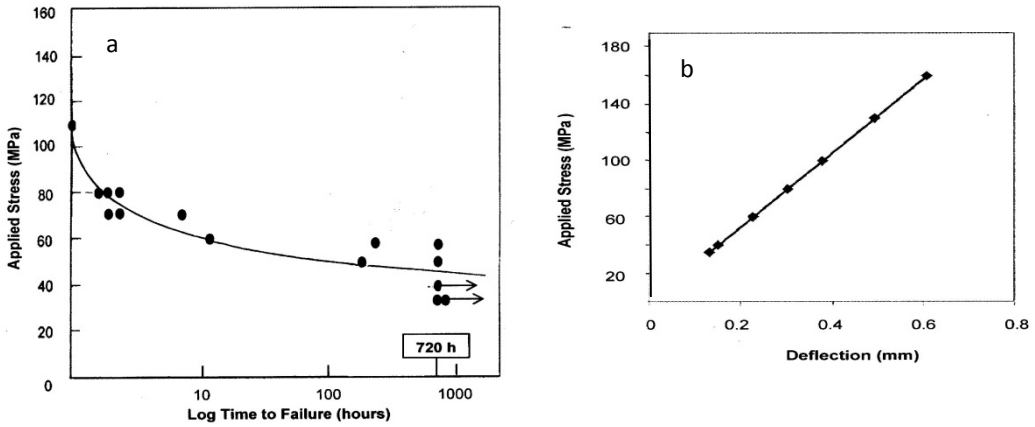

Fig. 2. Results of SSC testing (a) in tensile and (b) in three point-bent tests.

Figures 2a, b show the results of SSC tensile and bending tests. One sample loaded at 150 MPa and one at 50 MPa were raptured after loading in screw join (are not part of plotting). None failure was revealed at 40/35 MPa (tensile bars tested up to 820 h). It could be stated loading of bimetal weld of Ti-clad Cr/Ni equals 12–13 % of yield stress and under presented conditions represents reliable threshold level of H_2-susceptibility. In case of the same bimetal weld after 2HT, however under fatigue test (tension-pressure, at 20 Hz, charging in H_2SO_4/8 h [4]), loading of 40 MPa corresponded to lifetime threshold, as well. In case of SSC bent-test, deflection was in range from 0.133 mm (at 35 MPa) to 0.609 mm (at 160 MPa), see Fig. 2b. None failures or defects were observed in microstructure of the samples exposed for 720 h and deflections showed a linear increase at higher loading.

This work was supported by the Ministry of EYS, Czech Republic (project no. L01203). K. Saksl., M. Ďurišin, D. Balga, and J. Szabó are grateful to the Scientific Grant Agency of the Ministry of ESRS of the Slovak Republic and the Slovak Academy of Sciences (VEGA project no. 2/0021/16) and to the M-ERA.NET project ExploGuard for financial support. We are also grateful to EXPLOMET-Opole for important cooperation.

1. S.Yu. Mironov, G.A. Salishezev, Influence of grain size and microstructure homogeneity on deformation uniformity of commercially pure titanium, *Fiz. Met. Metalloved.*, 2001, vol. 92, pp. 81-88.
2. K. Saksl, D. Ostroushko, E. Mazancová, Z. Szulc, O. Milkovič, M. Ďurišin, D. Balga, J. Ďurišin, Structure of bimetals investigated by synchrotron radiation, in *Proc. 24th Int. Conf. on Metallurgy and Materials*, Ostrava, 2015, pp. 459–464.
3. K. Saksl, D. Ostroushko, E. Mazancová, Z. Szulc, O. Milkovič, M. Ďurišin, D. Balga, J. Ďurišin, U. Rűtt, O. Guttowski, Local structure of explosive welded titanium–stainless steel bimetal, *Int. J. Mater. Res.*, 2015, vol. 106, no. 6, pp. 621–627.
4. E. Mazancová, D. Ostroushko, K. Saksl, A. Nieslony, Joint hydrogen susceptibility of 304 SS welded with titanium, *Arch. Metall. Mater.*, 2014, vol. 59, no. 4, pp. 1605–1610.

EFFECT OF DETONATION CHARACTERISTICS ON THE PROPERTIES OF THE EXPLOSIVE WELDING INTERFACE

R. Mendes[1], I. Plaksin[1], J. B. Ribeiro[1], A. Loureiro[2] and J. Campos[1]

[1]ADAI/LEDAP – Department of Mechanical Engineering, University of Coimbra, R. Luis Reis Santos, 3030-788 Coimbra, Portugal
[2]CEMUC - Department of Mechanical Engineering, University of Coimbra, R. Luis Reis Santos, 3030-788 Coimbra, Portugal

e-mail: ricardo.mendes@dem.uc.pt

Explosive welding is understood as solid-state joining technology with increased interest for several industrial sectors. The working principle is based on the expansion of detonation products which can accelerates a flyer plate at very high velocity V_p against the base plate, as illustrated in Fig. 1. For plane and parallel configuration the collision point velocity V_c is equal to the detonation velocity V_d. This process is generally used to joining similar and dissimilar metals in plane or cylindrical geometry, most of them impossible to be joined through the conventional fusion welding techniques [1- 3].

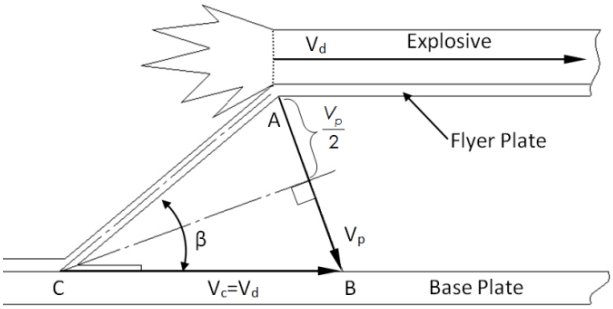

Fig 1. Schematic representation of the explosive welding process

The aim of this study is to investigate experimentally the effect of the explosive composition and the effect of explosive/flyer mass ratio on the joint interface characteristics of both metals.
ANFO, ANFO+20% emulsion matrix (EM) and emulsion matrix sensitized with hollow glass microballoons (HGMB) or with expanded polystyrene was the explosives used to perform the explosive welding tests.
Used compositions are covering several forms how the energetic material is present in the explosive composition. Emulsion explosive mixed with HGMB represents a quasi-

continuous energetic medium; Emulsion explosive mixed with coarse EPS (d=1,5mm) signifies energetic medium with coarse spherical discontinuities and ANFO represents an energetic medium localized on the ANFO particles (d=1-1,5mm). Detonation process of the referred compositions comprises some differences that were manifested on the interface [1, 4] and on the metal surface in contact with the explosive composition (vd. Fig. 2 and Fig. 3).

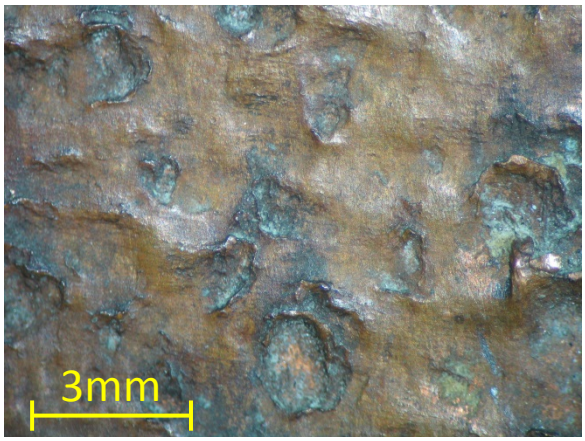

Fig. 2. Copper surface in contact with detonation products of ANFO+20%EM.

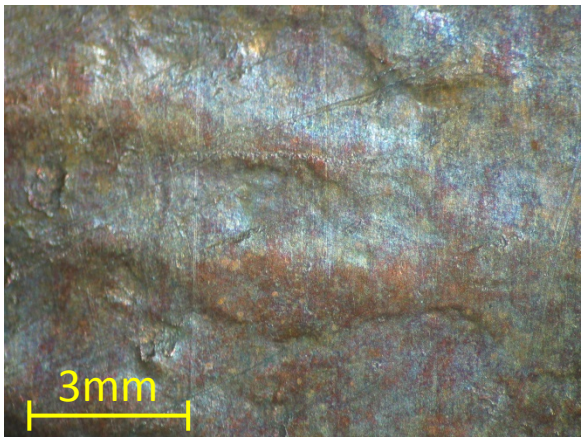

Fig 3. Copper surface in contact with detonation products of ANFO.

Recently conducted experiments reveal three main sources of the mesoscopic scale instabilities and perturbations occurring in PBX detonation flow: (1) Eruption of overdriven micro-jets (ejecta) from coarse HE-particles when subjected to strong shock or detonation, (2) Ejecta-driven detonation cells in detonation front, and (3) Galloping detonation regime caused by radiation-induced precursors [5].
Experimental results are showing that the joint interface was transformed from linear to wavy appearance by increasing explosive/flyer mass ratio. Moreover, with increasing explosive ratio, the wavelength and amplitude of waviness increased.
For the special case of welding Al-Cu, formation of intermetallic compounds at the welding interface was observed, nevertheless the welding resistance showed to be superior than of the materials, in this case copper.
Despite the influence of the collision angle and impact velocity on the Cu/Al, Al/Al, Cu/Cu the explosive composition plays also an important role. Explosive composition has a considerable role on the metal surface “quality” which is in contact with detonation products. Despite the Kelvin-Helmoltz instabilities, that is nowadays accepted as one of the most presumed mechanism of the wave formation, the wave amplitude and wavelength is also a function of the flyer plate instabilities that, in turn, are a consequence of the energy release localization, or the micro-jets formed during the spheres collapsing under detonation wave propagation process.

1. R. Mendes, J.B. Ribeiro, A. Loureiro, (2013), Effect of explosive characteristics on the explosive welding of stainless steel to carbon steel in cylindrical configuration, Materials and Design, 51 (2013) 182-192.
2. F. Findik, Recent Developments in Explosive Welding, Materials and Design 32 (2011) 1081–1093.
3. B. Gulenc, Investigation of interface properties and weldability of aluminum and copper plates by explosive welding method, Materials and Design 29 (2008) 275–278.
4. Plaksin, I., Campos, J, Ribeiro, J., Mendes, R., Direito, J., Braga, D., Pruemmer, R., "Novelties in physics of explosives welding and powder compaction", J. Phys. IV, 110 (2003) 797-802.
5. Igor Plaksin, Jose Campos, Ricardo Mendes et.al, "Kinetic Localizations in the DRZ Structure and the Effect upon the PBX-driven Inertial Confinement", in "Theory and Practice of Energetic Materials (Vol. VIII)", Science Press (LI Shengcai, WANG Yajun, CAO Fengxia, ZHAO Shanshan, and ZHOU Shuqiong, eds.), ISBN 978-7-03-025394-1, Beijing, P. R. CHINA (2009), pp. 683-692

OBSERVATION OF METAL JET GENERATED BY INCLINED COLLISION USING A POWDER GUN

A. Mori[1], S. Tanaka[2], and K. Hokamoto[3]

[1]Sojo University, 4-22-1 Ikeda, Nishi-ku, Kumamoto, 860-0082 Japan
[2]Kumamoto University, 2-39-1 Kurokami, Chuo-ku, Kumamoto, 860-8555 Japan
[3]Institute of Pulsed Power Science, Kumamoto University, 2-39-1 Kurokami, Chuo-ku, Kumamoto, 860-8555 Japan

e-mail: makihisa@mec.sojo-u.ac.jp

It is known that the metal jet is generated from the collision point of metals and is one of the important parameters to achieve the good welding conditions in explosive welding. The formation of the metal jet was investigated by Bergmann et al. [1] and Onzawa et al. [2]. Also some of authors also observed the metal jet and the collision of the metal jets using an image converter camera [3]. Optical observation of the metal jet is difficult, because the specimen and explosive have to be set away from the observation setup to prevent its damage. In the present work, the collision of a metal disc projected by using the powder gun to an inclined metal was investigated using a high-speed video camera and numerical simulation.

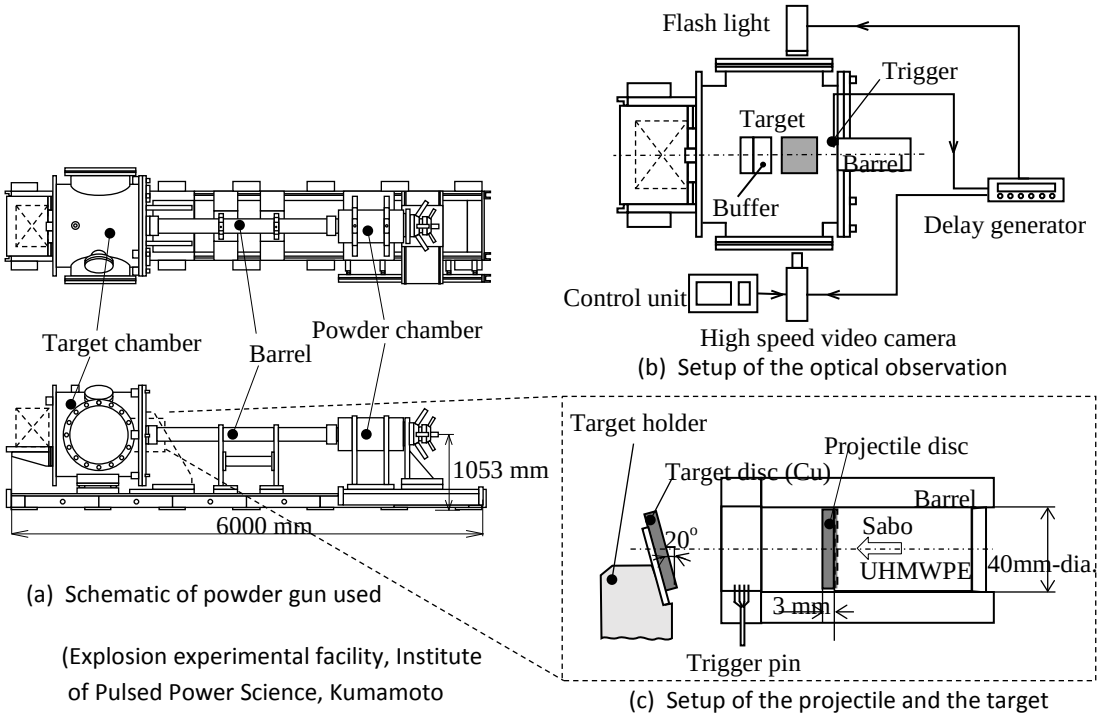

Fig. 1. Experimental setup for optical observation using a powder gun.

Figure 1 shows the schematic of the experimental setup. The projectile metal disc was fixed to the tip of sabot made of Ultra High Molecular Weight Polyethylene (UHMWPE) and accelerated by a powder gun. Projectile accelerated to about 600 m/s collided the target metal disc set at an inclination angle of 20°. A 3-mm copper disc (diameter 38 mm) was used as the target and copper disc (3 mm thick) and magnesium alloy disc (AZ31, 15.5 mm thick) were used as projectile discs. High-speed video camera (HPV-1, Shimadzu Inc.) was arranged in the opposite side of a flash light.

And in order to understand the phenomena of collision and generation of metal jet, numerical analysis was performed by using ANSYS AUTODYN commercial software. Projectile and target disc were modeled by SPH (Smoothed Particle Hydrodynamics) solver in 2D planar symmetry. Materials were analyzed by applying the Mie–Grüneisen form of the Hugoniot equation of state and the Johnson–Cook strength equation.

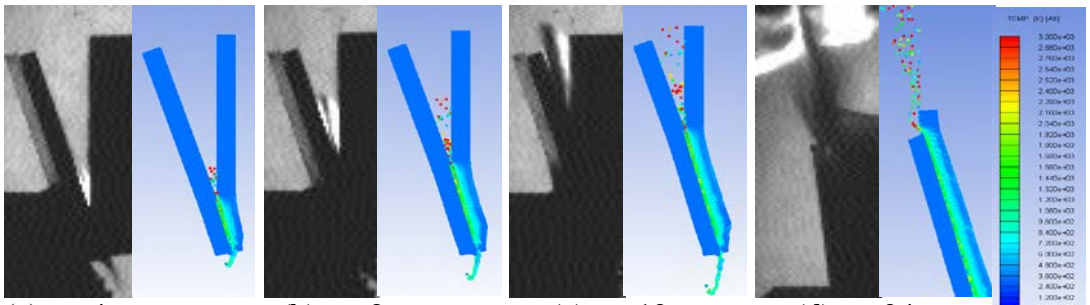

(a) t = 4 μs (b) t = 8 μs (c) t = 12 μs (d) t = 24 μs

Fig. 2. Comparison of the experimental and the numerical results for Mg/Cu: left: photograph and right: temperature contour (0–3000 K) of numerical results.

As follows from Fig. 2, phenomena of the metal jet were simulated by this numerical method and were agreed well with the experimental ones. Especially, in the case of Cu/Cu combination, wavy formation formed with the progressing of the welding could be confirmed continually in the numerical analysis. Shapes of wavy interface in numerical results also agree well with comparing the interface of specimen recovered.

1. O.R. Bergmann, G.R. Cowan, A.H. Holtzman, Experimental evidence of jet formation during explosion cladding, *Trans. Metall. Soc. AIME*, 1966, vol. 236, no. 5, pp. 646–653.
2. T. Onzawa, Y. Ishii, Fundamental studies on explosive welding: Observations of metal jet and wavy pattern, *Trans. Jpn. Weld. Soc.*, 1975, vol. 6, no. 2, pp. 98–104.
3. A. Kira, D. Takaenoki, H. Hamashima, R. Tomoshige, M. Fujita, K. Hokamoto, S. Itoh, Optical observation of extremely high impulsive pressure generator using collision of high velocity metal jets, *Mater. Sci. Forum*, 2004, vols. 465–466, pp. 265–270.

STRENGTH PROPERTIES OF Al2519/Ti6Al4V BIMETALL FABRICATED BY EXPLOSIVE WELDING

M. Najwer and G. Kwiatkowski

High-Energy Techniques Works EXPLOMET, Opole, 45-641 Poland

e-mail: michal.najwer@explomet.pl

Explosive welding is a method for joining materials with a different physical and chemical properties (such as density, melting point, chemical activity) for which other welding methods are inapplicable. An example of such joint is bimetal aluminum alloy 2519/titanium alloy Ti6Al4V. The process of joining brings about adverse stresses and strengthening, which negatively affects the material properties and makes difficult its further processing. This work determines the effect of influence of selected heat treatments on the mechanical properties of the tested bimetal.

Bimetal Al2519/Ti6Al4V was tested in two variants of thickness: 5 + 5 mm and 10 + 10 mm. Such bimetals can find their application in aerospace engineering. Bend tests were performed in a testing machine shown in Fig. 1a to simulate the process of forming.

(a) (b)

Fig. 1. Overall view of (a) test bench and (b) bent specimen.

Performed researches included tensile, bend, ram tests and hardness measurements. Analyzed was the influence of heat treatment on the strength parameters of joint which are defined a tolerable bend radius causing no material destruction. The evaluated parameters of the produced material and may be used as guideline for further process of modification of developed technology.

A RAPID, LOW-TEMPERATURE, SAFE PROCESS FOR DRYING WATER-WET NITRAMINES WITH REUSABLE SOLVENTS

S. Nandagopal, A. Kotbagi, S. Singh, A. Kumar, and M. Gupta

High Energy Materials Research Laboratory, SRP Division, Pune, 411021 India

e-mail: nandagopal.s@hemrl.drdo.in

Solid propellants are most widely used for powering missiles and rockets for military and space applications. Modern propellants contain high-energy additive like RDX/HMX to improve specific impulse, thereby the range of rockets and missiles. In India, RDX/HMX which belongs to nitramine class is shipped wetted with 25% water in cotton bags as per UN regulation for transportation of hazardous goods. Adjustment and control of moisture levels in nitramines through drying is a critical process in the manufacture of composite solid propellants.

As a unit operation, drying of energetic materials is one of the most common and important step. The effectiveness of drying processes can have a large impact on product quality and process efficiency. For example, the presence of surface moisture in more than acceptable limits may have deleterious effect on the propellant mechanical properties. Moreover, in propellant with diisocyanate curing system, the presence of moisture effectively decompose curing agent with the liberation of carbon dioxide, thereby leads to propellant grain with lot of voids. In the case of nitrate ester based propellants, the presence of moisture on fillers catalyze the decomposition of nitrate esters, thereby decreasing the shelflife and energy of the propellant as well as poses safety threats.

Water-wet nitramines must be dried to a water content that does not exceed 0.08% before it can be used in the production of solid propellants. Present method involves the draining of water from wet material, spreading of material in tray followed by drying of material in a water jacketed oven at 65°C. A disadvantage of this drying method is that it does not produce a uniform product. The outer layer dries faster than the inner parts and this results in a dry HMX that is lumpy and uneven in its moisture content and physical makeup. Before being used in the propellant the hard chunks in the dry material must be manually broken into small pieces, the fine hard agglomerates cause quite a bit of difficulty during production of the propellant. Another disadvantage is that the drying

operation is too time consuming in that it takes anywhere from three to five days to dry the wet nitramines. A further disadvantage is that this process requires too much manual handling of the friction sensitive nitramines and thus exposes personnel to the hazards of an explosion. Still another disadvantage is that drying large amounts of nitramines at elevated temperatures creates a potential safety hazard. Moreover, water used for wetting of nitramines may contain water soluble impurities, which on evaporation leave the impurities on the surface of nitramines, which may be detrimental to the propellant and affects storage life.

In the present study, an attempt was made to develop a safe, rapid process for drying water-wet nitramines with surface moisture content less than 0.08 % suitable for propellant formulation. The developed method offers the advantage of drying at ambient temperature (30°C) compared to conventional drying method at 65°C at the same duration. Moreover, the solvents can be reused several times without any additional purification step. A simple analytical tool based on refractive index and specific gravity measurements also described to determine the suitability of the solvent for reuse, making the whole process cost effective and economically viable. An attempt was also made to reduce the duration of drying to 8 h by conventional heating at 50°C after solvent washing and to 4 h by vacuum drying at 50°C. The process was demonstrated on a 1-kg level of water-wet nitramine but can be easily scaled up to any quantity. Thus, we developed a very safe, less time consuming and less energy required for drying water-wet nitramines using reusable solvents suitable for propellant formulation.

Drying process	Duration	Moisture	Volatile matter
Conventional drying at 65°C	3–5 days	0.08 %	0.20
Solvent washing, drying at 30°C	3 days	0.08%	0.05
Solvent washing, drying at 50°C	<8 h	0.08%	0.02
Solvent washing, vacuum rying at 50°C	<4 h s	0.08%	0.02

IMPACT VELOCITY OF CLADDING METAL AS MEASURED BY PHOTONIC DOPPLER VELOCIMETRY (PDV)

P. Nesvadba[1], J. Kucera[2], M. Kunzel[1], and J. Pachman[2]

[1]OZM Research s.r.o., Bliznovice 32, Hrochuv Tynec, 538 62 Czech Republic
[2]University of Pardubice, Faculty of Chemical Technology, Doubravice 41, Pardubice, 53210 Czech Republic

e-mail: nesvadba@ozm.cz

Explosive welding is a process of reliable joining of two different metals often difficult to join by other techniques. The results of the process depend on number of parameters out of which the most important one is the velocity of the cladding metal at the time of impact on the cladded one. This contribution focuses on development of methodology for determination of impact velocity during the welding process. The use of Photonic Doppler Velocimetry (PDV) was tested for this purpose with different types of probes under different probe angles. Well tested combination, in which copper plate is accelerated and welded to the steel base plate, was chosen for conducted experiments.

The experiments were done in parallel geometry with a stand-off distance of 4 mm. Copper plate was accelerated by detonation of explosive prepared from 25% PETN/ 75% $NaHCO_3$ mixture initiated by detonating cord. The density of this explosive was 1.105 g/cm^3. The schematic of the measurements is shown in Fig. 1.

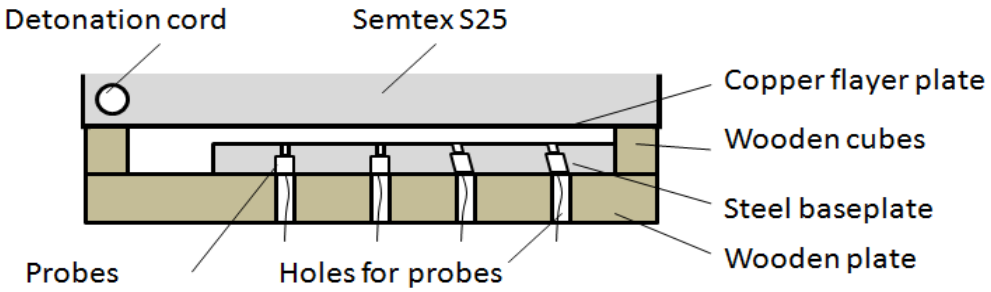

Fig. 1. Measurement of impact velocity in the process of explosive welding.

The measurement of impact velocity by the PDV technique is based on the reflection of Doppler shifted light from the moving surface back to the probe. The frequency of shifted light is mixed with original laser beam yielding a new beat frequency. The velocity of the plate is then obtained from the measured beat frequency by

deconvolution using Fourier or wavelet transform. The schematic of Photonic Doppler Velocimeter is shown in Figure 2.

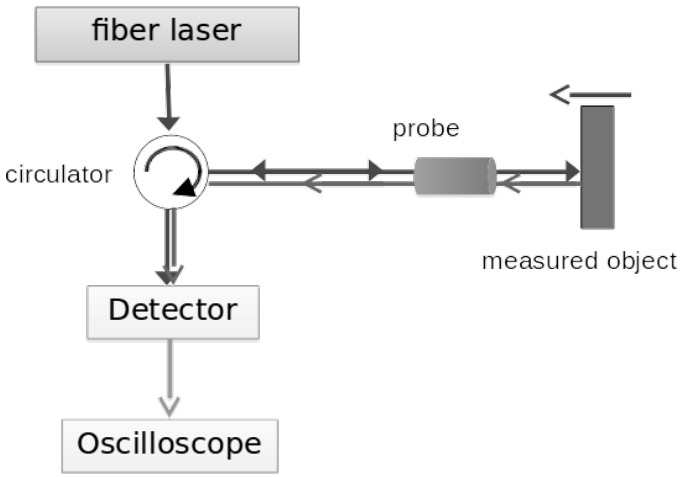

Fig. 2. Schematic of Photonic Doppler Velocimeter (PDV).

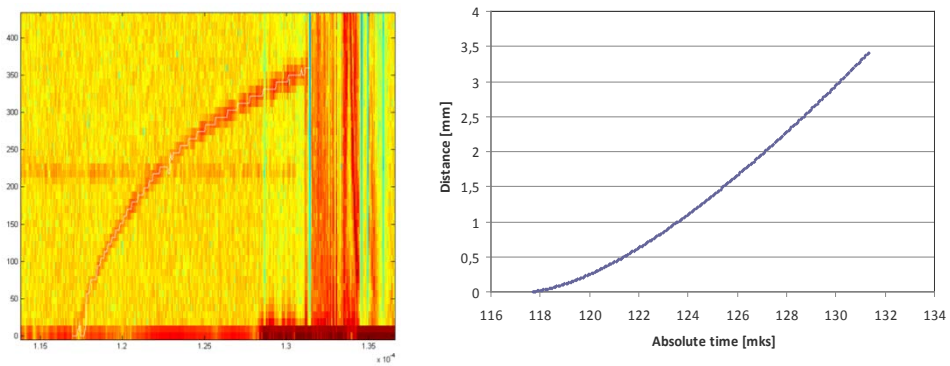

Fig. 3. Results of impact velocity measurement: velocity [m/s] vs. time [$1x10^{-4}$s] (left), distance [mm] vs. time [mks] (right) for measurement with probe angle 80°.

A signal from the probe is transformed from optical to electrical and recorded by a high bandwidth oscilloscope. An example of such signal after Fourier transform is shown as spectrogram in Fig. 3 on the left. The signal ends before the plate hits the collimating probe. The distance traveled by the plate is shown in Fig. 3 on the right, which is an integral of the velocity curve. The copper plate fly-off distance corresponding to the end of the velocity signal determined by PDV was 3.4 mm, which is probably due to the loss of reflectivity of the cladding plate due to the jet formation.

TITANIUM/STEEL EXPLOSIVE WELDING: INFLUENCE OF VANADIUM INTERLAYER

I. N. Nursainov[1], A. Yu. Malakhov[2], I. V. Saikov[2], O. L. Pervukhina[2], and V. S. Chelnokov[1]

[1] National University of Science and Technology MISiS, Moscow, Russia
[2] Institute of Structural Macrokinetics and Materials Science, Russian Academy of Sciences, Chernogolovka, Russia

e-mail: revan.84@mail.ru

The clad metal titanium/vanadium/stainless steel was prepared by explosive welding and the weld seam was characterized (after heat treatment at 500–800°) by SEM/EDS (Zeiss ULTRA plus equipped with an INCA 350 accessory Oxford Instruments). The V interlayer was used in order to suppress the formation of intermetallics. The presence of intermetallics was detected only after thermal treatment at 800°C for 1 h. The tensile strength of the joint was 545 MPa.

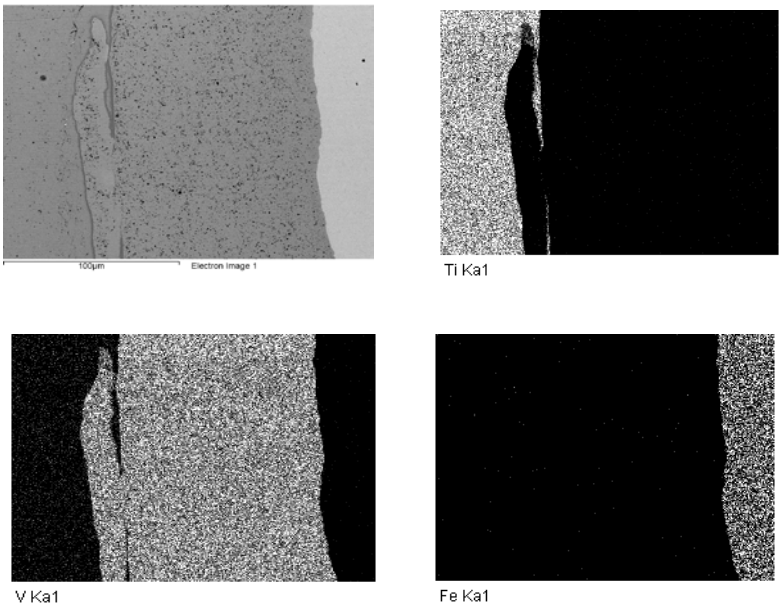

Fig. 1. Elemental map of the weld seam zone.

The use of V interlayer can be readily recommended for practical implementation.

MICROSTRUCTURE, PHASE COMPOSITION, AND MECHANICAL PROPERTIES OF Ti–Cr18Ni10 CLAD METALL

D. Ostroushko[1], E. Mazancová[1], K. Saksl[2], M. Ďurišin[2], D. Balga[2], and J. Szabo[2]

[1]VŠB-Technical University of Ostrava, Faculty of Materials Engineering, Tř. 17 listopadu 15, Ostrava, 708 33 Czech Republic
[2]Institut of Material Research, Slovak Academy of Science, Watsonova 47, Košice, 040 01 Slovak Republic

e-mail: dimitrij.o@vsb.cz

The studied material is Cr18Ni10 stainless steel (110-mm thick plate) and pure titanium (6 mm thick) welded by explosion. This bimetal finds application in heavy chemical industry. In this work, we studied the microstructure, phase composition, and mechanical properties of this bimetal. After welding, the plates were first annealed at 600°C/1.5 h/air (HT 1) and then at 600°C/1.5 h/air (HT 2). After 2HT, the Ti plate showed fine balanced microstructure, relaxed internal stresses and the presence of intermetallic phase Fe_2Ti [1–3].

Both materials (after HT 1 and HT 2) were characterized by optical microscopy (Olympus X70), microhardness and fatigue tests, and SEM/EDA analysis (SEM JEOL JSM-6490 LV equipped with EDA accessory OXFORD INCA Energy 350). The SEM/ EDA data showed the presence of local melted zones on the base of Ti–Cr–Fe–Ni, eventually with Mn and/or with Al and Si inclusions in close proximity with the 340 SS–Ti interface (Fig. 1, positions 1–6). According to the analysis, 4 (5) phases were detected in the melted zones. The C3–C4 zones contained Ti (about 70 at. %), Fe (approximately 20 at. %), Cr (about 4.5 at. %), and Ni (bal.). The phase marked as 2 showed the presence of Ti (about 79 at. %), Fe (approximately 15 at. %), Cr (4 at. %), Mn (under 1 at. %) and Ni (bal.). Phases 1 and 3 were on a complex oxides basis of the Fe–Ti–Cr type with Fe content in the range of 15–50 at. %, Ti 8–11 at. %, while the Cr content was 2–21 at. %. The Mn content was 0–1 at. %, Al with Si did not go over 6.5 at. %, and Ni was the rest. Similar zones were revealed in [4].

The bonding interface was found to be wavy in its nature and with some defects such as fused zones. Inhomogeneities in a form of molten zones begin to appear under the curls of waves. The reason is the kinetic energy dissipation at the collision process resulting in formation of melting zones at the interface. The formation of wavy structure is associated with material heating caused by high-pressure shock, severe plastic deformation, and the adiabatic heating of compressed gases in the gap.

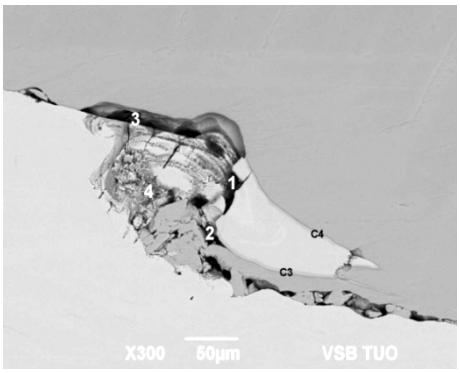

Fig. 1. Part of the joint line with EDS results.

	1	2	3	4	C3	C4
O	43.72	5.59	50.79	11.64		
Al			6.47	1.36		
Si			2.67	0.36		
Ti	8.07	73.7	10.69	10.89	69.40	70.84
Cr	13.20	3.69	2.28	21.08	4.70	4.51
Mn		0.58		1.32		
Fe	32.43	14.72	25.45	49.80	22.15	20.50
Ni	2.58	1.73	1.10	3.55	3.75	4.15

X-ray diffraction measurements were carried out by using the synchrotron P07 [5] at PETRA III (positron storage ring operating at energy 6 GeV with beam current 100 mA) [17]. During the experiment, monochromatic synchrotron radiation of energy 80.09keV (λ = 0.01548 nm) was used. The beam of photons was focused by compound refractive lenses down to a spot size of 2.2 × 34µm. The specimen was scanned shot-by-shot along a straight path of total length 0.4 mm with a step of 1µm. During each step, the sample was illuminated by highly intensive hard X-rays for 0.5 s. The resulting 2D XRD patterns were recorded using a Perkin Elmer 1621 detector [18]. The intensity was integrated to 2 Theta space by using the Fit2D software [19]. Phase analysis from the interfacial region proved the existence of the hexagonal close packed Fe_2Ti intermetallic phase together with main matrix components *fcc*-Fe (austenite) and *bcc*-Fe (ferrite), see Fig. 2. In the insert, black line corresponds to the HI 1 sample while the red one, to the HT 2 sample. Comparison of the above curves indicates the occurrence of intermetallic reduction.

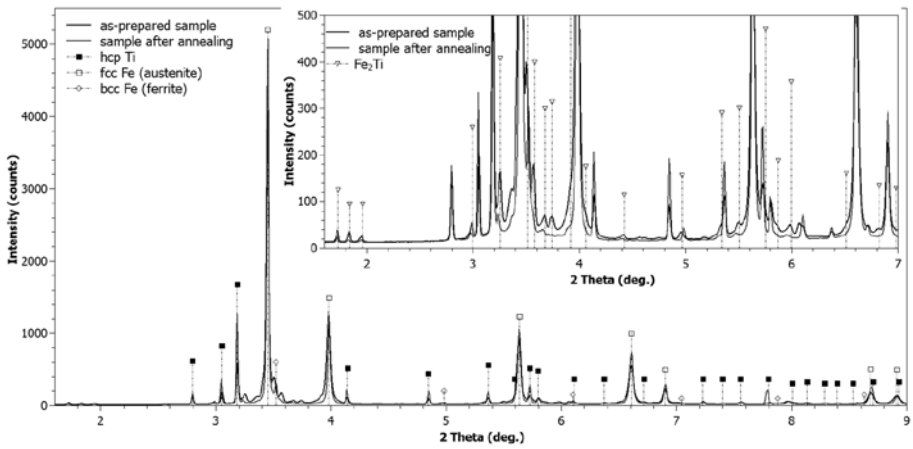

Fig.2. XRD pattern from the interface area of HT 1 and HT 2 samples Ti-Cr/Ni SS.

Volume percentage of Fe_2Ti in the sample HT 1 sample is about 17.5% while that of the HT 2 sample, 5.25 vol. %).

The fatigue response was tested by use of the MTS machine in a tensile mode. The results proved that the HT 2 procedure is effective for dissolving unwanted intermetallic compound and to improve the material service life.

This work was supported by the Ministry of EYS, Czech Republic (project no. L01203). K. Saksl., M. Ďurišin, D. Balga, and J. Szabó are grateful to the Scientific Grant Agency of the Ministry of ESRS of the Slovak Republic and the Slovak Academy of Sciences (VEGA project no. 2/0021/16) and to the M-ERA.NET project ExploGuard for financial support. We are also grateful to EXPLOMET-Opole for important cooperation.

1. S.Ju. Mironov, G.A. Salishezev, Influence of grain size and micro-structure homogeneity on deformation uniformity of commercially pure titanium, *Fiz. Met. Metalloved.*, 2001, vol. 92, pp. 81–88.
2. K. Saksl, D. Ostroushko, E. Mazancová, Z. Szulc, O. Milkovič, M. Ďurišin, D. Balga, J. Ďurišin, Structure of bimetals investigated by synchrotron radiation, in *Proc. 24th Int. Conf. on Metallurgy and Materials*, Ostrava, 2015, pp. 459–464.
3. K. Saksl, D. Ostroushko, E. Mazancová, Z. Szulc, O. Milkovič, M. Ďurišin, D. Balga, J. Ďurišin, U. Rűtt, O. Guttowski, Local structure of explosively welded titanium–stainless steel bimetal, *Int. J. Mater. Res.*, 2015, vol. 106, no. 6, pp. 621–627.
4. N.V. Rao, D.S. Sarma, S. Nagarjuna, G.M. Reddy, Influence of hot rolling and heat treatment on structure and properties of the HSLA steel explosively clad with austenitic stainless steel, *Mater. Sci. Technol.*, 2009, vol. 25, no. 11, pp. 1987–1396.

5. N. Schell, A. King, F. Beckmann, H.U. Ruhnau, R. Kirchhof, R. Kiehn, M. Mueller, A. Schreyer, in *Proc. Int. Conf. on Synchrotron Radiation Instrumentation*, Melbourne, 2009, vol. 10, pp. 391–394.
6. PETRA III Technical Design Report, DESY 2004-035.
7. L.B.S. Kinnera, Ch.J. Benmorea, J.B. Parise, *Nucl. Instrum. Meth. Phys. Res. A*, 2012, vol. 662**,** pp. 61–70.
8. A. P. Hammersley, S. O. Svensson, M. Hanfland, A. N. Fitch, D. Hausermann, *High Press. Res.*, 1996, vol. 14**,** pp. 235–248.

CERMET COATINGS BY ALUMINOTHERMIC SHS

Ch. G. Pak, V. M. Batrashov, and G. A. Koshkin

Penza State University, ul. Krasnaya 40, 440026 Penza, Russia

e-mail: gl.koshkin@yandex.ru

The main unit in industrial electrolyzers is a gas catcher that undergoes rapid corrosion and destruction under the action of aggressive media [1, 2]. The problem can be resolved by deposition of ceramic coatings onto their surface. In order to provide good adhesion between strongly dissimilar materials (steel and ceramic), a transition cermet layer is inserted in between.

In this work, we attempted to deposit a two-layer coating onto a steel substrate by aluminothermic SHS in a mode of thermal explosion. Green mixture for layer **1** containing Fe_2O_3, Al, frit, and silica gel as a binder was applied onto the surface of carbon steel and dried at 100°C for 3h. Green mix **2** also contained Fe_2O_3, Al, and silica gel as a binder, but alumina and silica were abundant in green composition. Green mix 2 was dried at 100°C 6 h.

Dried samples were then kept at 900°C for 60 min until initiation of aluminothermic reaction and temperature rise to 1550°C. This led to the sintering of ceramic materials in layer **2** and good joining between upper layer **1** and steel substrate.

1. M.Ya. Mintsis, G.A. Sirazutdinov, G.V. Galevskii, Soderberg electrolyzers and their modernization, *Tsvet. Met*., 2010, no. 12, pp. 49–52.
2. A.I. Begunov, A.A. Begunov, Modernization of Soderberg electrolyzers, *Tsvet. Met*., 2011, no. 7, pp. 45–49.

INDUSTRIAL EXPERIENCE ON EXPLOSIVE WELDING OF STEEL–Al ALLOY TRANSITION ELEMENTS FOR AEROSPACE APPLCATIONS

S. N. Pakhomov

State Design Bureau YUZHNOYE, ul. Krivorozhskaya 3, Dnepropetrovsk, 49008 Ukraine

e-mail: info@yuzhnoye.com

It is known that explosive welding of stainless steel and Al alloys is effective only in the presence of a sub-layer of commercial-grade aluminum in between the sheets [1, 2]. But in this case high strength of joining is achieved only within a narrow range technological parameters, such as detonation velocity, explosive/sheet mass ratio, and weld gap.

In this communication, we report on the explosion welding of batches of 400 × 450 mm sandwiches comprising (*i*) stainless steel (12X18H10T brand) as a base plate 5 or 20 mm thick, (*ii*) aluminum (A5 brand) plate as a sublayer 2 mm thick, and (*iii*) aluminum alloy (AMg6M brand) as a clad plate 5 or 20 mm thick. These workpieces were welded in a layer-by-layer mode. The mixtures of ammonite with ammonium nitrate were used as explosives. Detonation velocities were measured with an accuracy of up to 0.01 μs.

In our experiments, we measured detonation velocity D as a function of trotyl content, granulometric composition, charge density, explosive layer thickness, weld gap and analyzed the influence of the above parameters on the quality of welding [3]. The optimal strength of joints was achieved at D = 1500–1800 m/s for the steel–A5 pair and at D = 2100–2300 m/s for the A5–AMg6M pair. The strength of joining depends on the evenness of granulometric/chemical composition in all areas of the explosive. Additional compaction of the explosive made it possible to exclude the formation of faulty fusion in case of 2-mm A5 sheets and 5 or 20-mm steel sheets. Tentatively, the unwelded spots were provoked by local gas jets arising in small cavities of the explosive during its detonation.

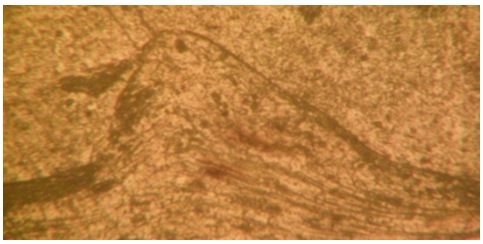

Fig. 1. Overall view of 12X18H10T–A5 joint.

The strength of joining was determined in pull/bending tests of samples with a width of 2–2.5 mm cut along the direction of detonation wave propagation. The strength of joining was defined by the yield strength of the Al sublayer and quality of the 12X18H10T–A5 joint.

The AMg6M–A5 joints exhibited (Fig. 1) a well pronounced wavy structure with a wavelength-to-amplitude ratio of approximately two; there were also small inclusions of an intermediate phase (see Fig. 1).

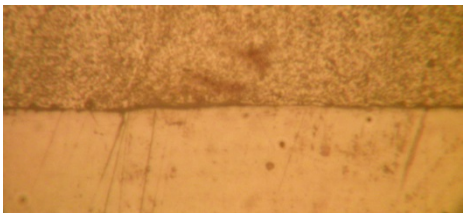

Fig. 2. AMg6M–A5 joint.

Leak tests (by aquarium method) after final mechanical treatment showed that leak-tight joining of layers was achieved all over the entire perimeter. The quality of joining was also tested ultrasonically (UD4-76 instrument).

Metallographic investigation showed that, at optimal conditions, the 12X18H10T–A5 interface was a smooth line (classical type of joining) with a discontinuous intermetallic interlayer 5–10 μm thick (Fig. 2).

The results were used in designing launch vehicles Dnepr and Cycloine-4 as well as in the program of international cooperation with the Liquid Propulsion Systems Centre, Indian Space Research Organization.

1. Kudinov V.M., Koroteev A.Ya., *Explosive welding in metallurgy*, Moscow: Metallurgiya, 1978 (in Russian).
2. Deribas A.A., Strengthening physics and explosive welding, Novosibirsk: Nauka, 1980 (in Russian).
3. Mostipan S.Ye., Pakhomov S.N., Reznichenko V.I., Influence of ammonite and ammonia nitrate properties on speed of detonation at explosive welding of bimetals, *Bull. Dnepropetr. Univ: Aerospace Hardware*, 2009, vol. 2, no. 13, pp. 55–60.

SHOCK-ASSISTED SHS AND CONSOLIDATION OF Ta–Al AND Nb–Al COMPOSITES

A. Peikrishvili[1,2], L. Kecskes[3], B. Godibadze[2], E. Chagelishvili[2], and G. Tavadze[1]

[1] Tavadze Institute of Metallurgy and Materials Science, Tbilisi, 0186 Georgia
[2] Tsulukidze Institute of Mining, Tbilisi, 0186 Georgia
[3] Weapons and Materials Research Directorate US Army Research Laboratory, Maryland, USA

e-mail: apeikrishvili@yahoo.com

The main purpose of presented work is to combine hot explosive consolidation technology (HEC) with Self propagated High Temperature Syntheses process (SHS) to obtain Ta–Al and Nab–Al based cylindrical billets with low porosity and improved physicomechanical properties.

Explosive consolidation of powders at room temperatures was used to obtain billets with increased density without cracks and activated surfaces of consolidated particles. Then these billets were subjected to consolidation in hot conditions above and under of combustion temperatures. The intensity of loading was under 10 GPa. The heating temperature was up to 950°C. The time of heating billets before loading was below 30 min.

The investigation showed that the initiation of the process and the complete SHS reaction in Ta–Al powder composites got started from 940°C. In order to fabricate billets near to theoretical density with perfect structure and correct geometry it is necessary to load billets before 940°C. The consolidation of billets above 940°C leads to cracking in whole volume of HEC billets. The addition of B_4C and HEC of Ta–Al–B_4C composites lead to the dissolution of the B_4C phase behind of shock wave front and formation of the TaB, $AlCTa_2$, and $TaAl_3$ phases behind of shock wave front. The reducing of HEC temperature and consolidation of Ta(Nb)–Al precursors near to 600°C provides only partial reaction between the phases and formation of aluminates on the surrounding surfaces of Ta(Nb) particles in whole volume of HEC billets. The type of obtained intermetalic compounds depends on the percentage of separate phases in starting composition.

The above mentioned and other features of structure–property relationship of consolidated Ta–Al and Nb–Al based composites depending on loading condition and set up of HEC device will be presented and discussed.

EXPERIMENTAL EVIDENCE FOR FORMATION OF SHOCK PLASMA DURING EXPLOSIVE WELDING

L. B. Pervukhin[1], O. L. Pervukhina[2], I. V. Denisov[2], and T. A. Shishkin[2]

[1]Bardin Research Institute for Ferrous Metallurgy, Moscow, 105005 Russia
[2]Institute of Structural Macrokinetics and Materials Science, Russian Academy of Sciences, Chernogolovka, Moscow, 142432 Russia

e-mail: opervukhina@mail.ru

Previously [1–4] we tentatively postulated the formation of shock plasma in the stand-off gap during explosive welding. In this communication, we will present some new experimental evidences in favor of the above hypothesis.

Theoretical calculations for the effect of shock-compressed gas show that, in typical conditions of explosive welding, the temperature ahead of the contact point can hardly exceed 600°C. But with account of the shock plasma formed under the action of hypersonic flow over the metal surfaces, one can expect for the appearance of a fused layer (cf. Fig. 1, curve 2). This well agrees with experiment (Fig. 1, curve1).

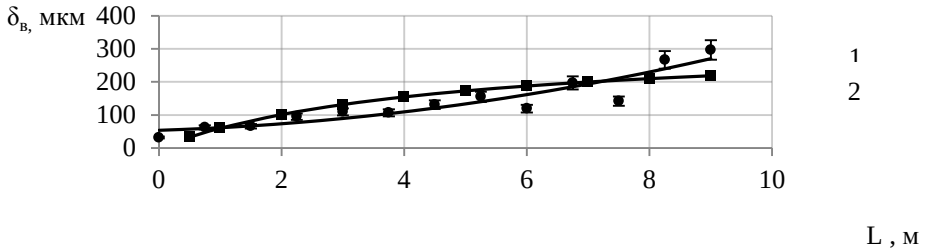

Fig. 1. Depth of fused layer vs. sheet length *L*: (1) experiment and (2) calculation.

The measured amplitudes of the wavy structure in weld seam were found to vary between 0.4 and 1.2 mm (Fig. 2). For $L > 7$ m, the wavy structure is lost and the seam turns fused.

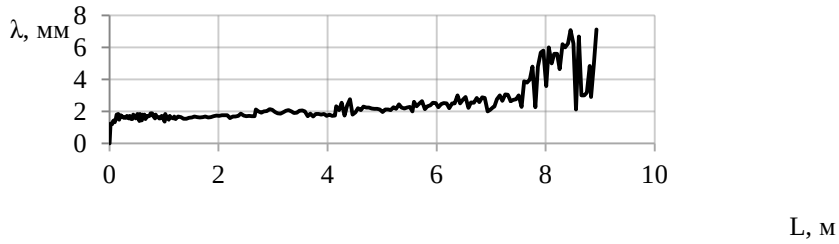

Fig. 2. Amplitude of wavy structure λ vs. sheet length *L*.

In the zone of incomplete fusion, we noticed the presence of crystalline precipitates up to 0.8 mm thick on the surface of flyer sheet (Fig. 3). These crystals were identified (by EDS analysis) as pure iron form upon reduction of oxides.

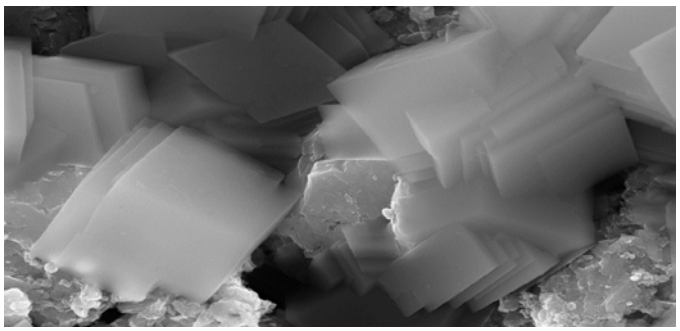

Fig. 3. Crystallites of pure iron formed in the zone of incomplete fusion.

In our opinion, the character of wavy structure (Fig. 2) and distribution of the crystallites shown in Fig. 3 over the length of large-sized sheet represent additional evidences for formation of the shock plasma that raises the metal surface temperature up to 3000 K and leads to formation of a fused layer (cf. Fig. 1).

This work was financially supported by the Russian Foundation for Basic Research (project no. 14-08-00845_a).

1. S.Yu. Bondarenko, O.L. Pervukhina., D.V. Rikhter, L. B. Pervukhin, Determination of the parameters of shock-compressed gas in the welding gap ahead of the contact point in explosion cladding, *Paton Welding J.*, 2009, no. 11, pp. 39–41.
2. L.B. Pervukhin, O.L. Pervukhina, S.Yu. Bondarenko, Cleaning and activation of welded surfaces during explosion welding, *Paton Welding J.*, 2010, no. 7, pp. 41–43.
3. O.L. Pervukhina, L.B. Pervukhin, S.Yu. Bondarenko, D.V. Rikhter, On the nature of processes taking place in technological gap during explosion welding, in

*Explosive Production of New Materials: Science, Technology, Business, and Innovations***,** A.A. Deribas, Yu.B. Scheck, Eds., Moscow: Torus Press, 2010, p. 55.

4. L.B. Pervukhin, O.L. Pervukhina, S.Yu. Bondarenko, S.Yu. Agaurov, On interaction between shock compressed gas and metallic surfaces in weld gap, in *Explosive Production of New Materials: Science, Technology, Business, and Innovations***,** A.A. Deribas, Yu.B. Scheck, Eds., Cracow: Nokturn, 2014, pp. 154–155.

TENSILE STRENGTH OF WELD SEAM IN EXPLOCLAD STEEL/Ti SHEETS

O. L. Pervukhina[1], I. A. Schastlivaya[2], A. M. Fedorov[2], L. B. Pervukhin[3], and P.A. Nikolaenko[1]

[1]Institute of Structural Macrokinetics and Materials Science, Russian Academy of Sciences, Chernogolovka, Moscow, 142432 Russia
[2]Central Research Institute of Structural Materials PROMETEI, ul. Shpalernaya 49, St. Petersburg, 191015 Russia
[3]Bardin Central Research Institute for Ferrous Metallurgy, Moscow, 105005 Russia

e-mail: opervukhina@mail.ru

For explosively clad steel/Ti bimetal sheets 31(26 + 5) × 3300 × 3700 mm, we explored the seam structure all over the sheet length (*L*). The quality of joint was determined by ultrasonic testing over the entire sheet surface.

The results presented in Fig. 1 were obtained with metallographic specimens cut out from the transversal section of the clad sheet. The depth of a fused zone (see Fig. 2) was determined as described in detail elsewhere [1].

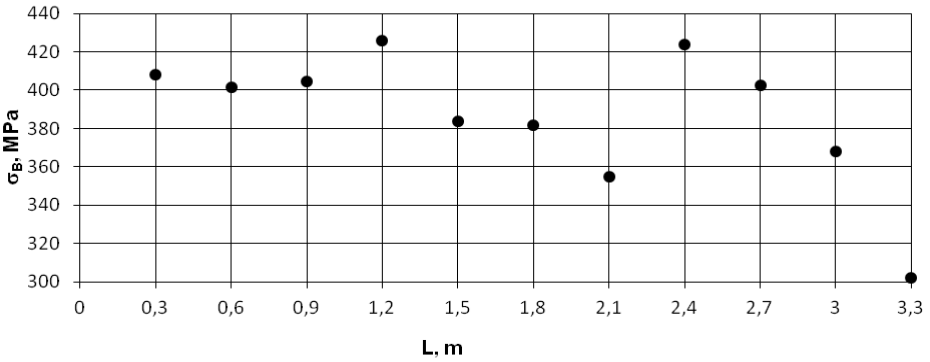

Fig. 1. Distribution of the tensile strength of weld seam over sheet length *L*.

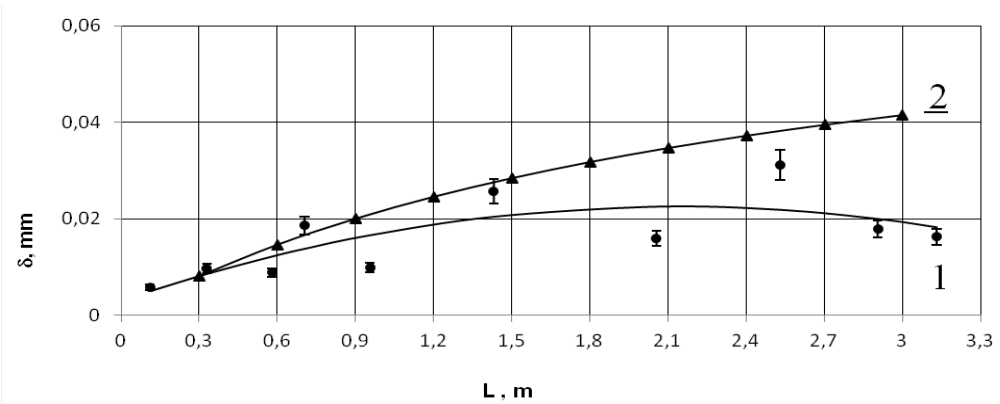

Fig. 2. Depth of a fused zone δ vs. sheet length *L*: (1) measured and (2) calculated.

Our results can be summarized as follows.

(1) Explosive welding of 3.3 × 3.7 m steel/Ti sheets provides the tensile strength of above 300 MPa all over the entire sheet surface, at good results of ultrasonic defectoscopy.

(2) The amount of fused inclusions is independent of *L*, slightly varies within narrow limits, and is close to a value theoretically predicted in [1].

(3) The areas of incomplete fusion in the form of cast inclusions and intermetallics can be associated with formation of ply blisters within the stand-off gap.

1. S.Yu. Bondarenko, O.L. Pervukhina, D.V. Rikhter, et al., Determination of the parameters of shock-compressed gas in the welding gap ahead of the contact point in explosion cladding, *Paton Welding J*., 2009, vol. 11, pp. 39–41.

SECURITY COMPLEX FOR FAST DEPLOYMENT OF EXPLOSIVE WORKS

V. A. Pervuninskikh and A. V. Pryshchak

Research and Design Institute of Radioelectronic Engineering, pr. Mira 1, Zarechny, Penza region, 442965 Russia

e-mail: office@nikiret.ru

As is known, explosive works require strict security measures to provide reliable control over unauthorized access to the territory. The problem may be solved by the security complex consisting of a rapidly deployable means for rapid detecting a person or a vehicle, an autonomous system of video surveillance and recording, data radio-transmission system, and a portable control panel. The complex includes security detection equipment based on different physical principles. This equipment provide intruder detection on all types of terrain, including uneven, overgrown with tall grass, bushes or forests. The following physical principles are used in the detection equipment: seismic, radio-ray, radio-wave, infrared, and break-wire. The use of a particular type of detection equipment is determined by the type of terrain for explosion works. On flat areas with little vegetation, radio-ray, infrared, and seismic detection equipment is applied. In areas overgrown with tall grass, bushes and forests equipment based on radio-wave detection and break-wire principles are used.

(a) radio-ray (b) radio-wave (c) infrared (d) seismic

Fig. 1. Detecting equipment of the security complex.

Composition of each detection equipment includes a stand-alone power source and a radio modem. Mobile video surveillance and registration system provide additional reliability and identification of the intruder in the controlled area. Video cameras, video monitoring, and registration systems are automatically activated when detection equipment starts operation. Transmission of information to a portable remote control is

provided by self-organized radio systems operating in the unlicensed radio frequency. The radio-system automatically selects the complex messaging routes and reliable messages delivery type on any type of terrain by using the detection equipment as message re-transmitters and the anti-interference algorithms of radio-system. When an explosion site is located further than 10 km from the central control panel, radio repeaters are used. A tablet computer is used as a central console, which displays a map or plan of the explosion area and installed equipment. GPS is used for geo-positioning of the ground detection equipment to geographic coordinates. Overall length of the controlled territories is up to 5 km. Total number of detection equipment is up to 200 pcs. Control areas are placed at the distance of 10 to 100 m. Figure 1 shows detecting equipment items of the security complex: (a) radio-ray, (b) radio-wave, (c) infrared, and (d) seismic. Figure 2 shows a video camera of the surveillance and recording system.

Fig. 2. Camera of the surveillance and recording system.

The continuous autonomous operating life of the security complex is minimum one month. Security complex operating temperature range: between $+50^{o}$ and –40°C.

IMPACT OF BOMBARDMENT WITH HIGH-SPEED TUNGSTEN PARTICLES ON STRUCTURE AND PROPERTIES OF STRUCTURAL STEEL

E. V. Petrov, V. S. Trofimov, and P. A. Nikolaenko

Institute of Structural Macrokinetics and Materials Science, Russian Academy of Sciences, Chernogolovka, Moscow, 142432 Russia

e-mail: petrow-ewgeni@mail.ru

The bombardment of metal surface with a flux of accelerated particles results in the formation of craters and a coating on the surface of bombarded material. The particles 8–100 μm in size accelerated velocities of 1000–3000 m/s are known to penetrate into target material to a depth exceeding their size by two orders of magnitude and thus to affect its structure. Although physical reasons for the phenomenon still remain obscure, nevertheless it seems reasonable to search after practical implementations of the phenomenon, such as bombardment-assisted strengthening of metallic surfaces.

Steel targets (20 mm in diameter and 30 mm long) were bombarded by a flux of W particles (mean size 10–16 μm) accelerated by explosion of a bulk density RDX charge. Two kinds of experiments were carried out: (**I**) bombardment with accelerated W particles followed by treatment with a shock wave bearing no W particles and (**II**) double bombardment with shock-accelerated W particles.

As is seen in Fig. 1, the shock-assisted bombardment with high-speed W particles leads to formation of a W coating with a thickness varying between 10 and 30 μm. Upon subsequent treatment with a shock wave bearing no W particles, the coating underwent either thickening or complete removal.

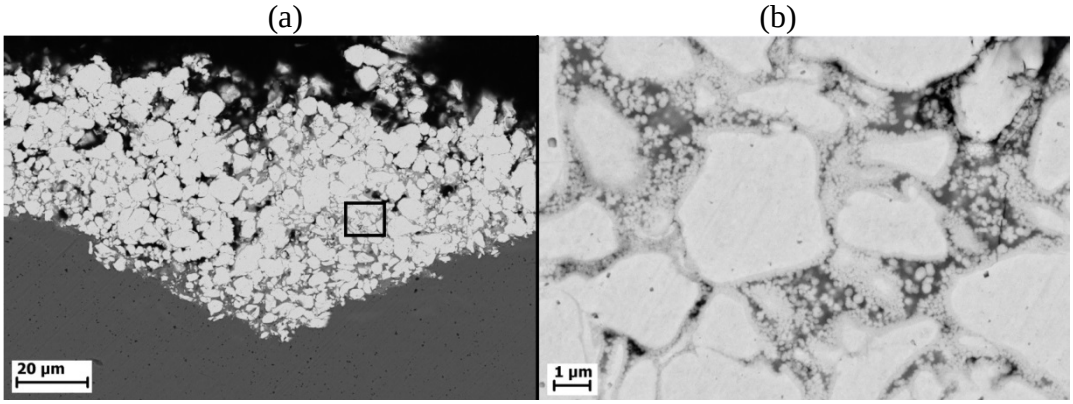

Fig. 1. SEM image of (a) the W particles shock-embedded into a steel target (experiment **I**) and (b) small intermetallic globules surrounding the embedded W particles formed in experiment **II**.

The formation of intermetallic globules with a mean size of about 200 nm (Fig. 1b) is indicative of the occurrence of the W–Fe reactive diffusion yielding the seeds of the intermetallic phase.

The bombardment was found to improve the microhardness whose maximum gain of 45 % and 39 % was reached at depths of 2 and 4 mm in experiments **II**.

This work was financially supported by the Russian Foundation for Basic Research (project no. 15-08-00571a).

MULTI-CHANNEL OPTICAL ANALYSIS AS AN ADVANCED METHOD IN DETONATION, POWDER COMPACTION, AND EXPLOSIVE WELDING

I. Plaksin

ADAI/LEDAP – Association for Development of Industrial Aerodynamics and Lab of Energetic and Detonics, University of Coimbra, Rua Luis Reis Santos, Polo-2, Coimbra, 3030-788 Portugal

e-mail: igor.plaksin@dem.uc.pt

Multi-Channel Optical Analyzer MCOA-UC [1] was developed in the University of Coimbra in 1996 with the goal to provide spatially resolved real-time measurements of shock fields in inert and reactive materials. Basic element of MCOA is an array of 64-96 optical PG-S250-64 PMMA fibers (S-grade, 250 μm in diameter, produced in TORAY®), which play a role of collectors and transducers of shock-induced radiation to a streak camera. Application of the Electronic Streak Camera (ESC) Thomson TSN 506 N provides recording the shock-induced radiation without any intermediate optical devices and elements. Fig. 1 shows the schematic of the MCOA-UC metrology and characteristics of optical probes, respectively. Optical array is connected at one end to the tested sample through the optical stacked monitor (SM) and by the second one to the optical slit of the ESC. Optical array is split in several parts which are integrated in the Multi-Fiber Optical Probes (MFOPs) of matrix type having a linear or circular configuration. The strip of 3–5m-total length terminated at the focal plane of the ESC, which recorded their output. The ESC Thomson TSN 506 N provides 0.2 ns-max temporal resolution of radiation pulses in the spectral range 380 nm < λ < 850 nm.

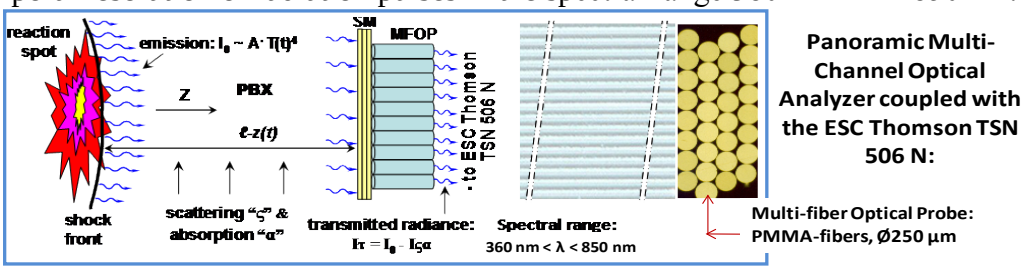

Fig. 1. Metrology MCOA-UC for meso-scale and micro-scale panoramic observation of the reaction spots origination and growth.

Three refined test-configurations were applied for characterization of shock and detonation flow in a mesoscopic scale range that is currently most appropriate for basic research of energetic materials (EMs): (1) Detonation Reaction Zone (DRZ)

Performance Test instrumented with the MCOA-UC for spatially resolved simultaneous measurements of reaction localizations in detonation front, local speed of detonation front, and 3D shock field at the interface with optical monitor; (2) Dynamic Performance Test of Powder Compaction, and (3) Dynamic Performance Test of Explosive Welding. Figure 2 shows two setup configurations applied for spatially resolved measurements of the DRZ structure of detonation wave on example of PBX material (HMX 82 wt. % /18 GAP) with density ρ_0 = 1.745 g/cm^3 (0.974 TMD).

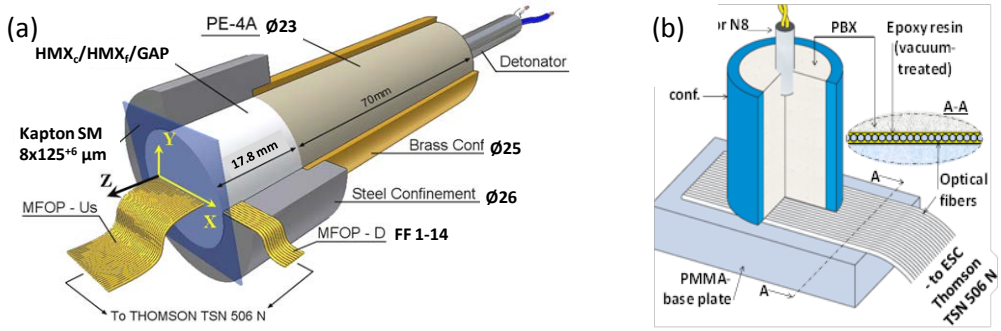

Fig. 2. Two **e**xperimental setups applied for spatially resolved measurements of the DRZ-structure: (a) simultaneous registration of detonation front propagation and the DRZ-induced shock field in the Kapton stacked monitor; (b) schematic of the mesoscale probing of the surface structure of DRZ through the side surface of optical fibers, "side-survey MFOP".

A laminated stack of eight Kapton films, each 125 µm thick, is placed in contact with the output face of the acceptor pellet. The stack of films was prepared with a 10 µm thick gap at each interface between layers. These gaps were filled with a noble gas so that they would produce a flash as the shock output from the acceptor pellet was transmitted through the film stack. The flashes were monitored with individual optical fibers in contact with the Kapton stack, so that spatial resolution of shock wave trajectory as well as time resolution could be obtained. Figure 3 illustrates typical streak camera records obtained in DRZ Performance Tests of PBX and Emulsion Explosive, which were conducted on schematics Fig. 2 (a) and (b) respectively. Fig 4 illustrates galloping regime of detonation front motion in PBX and the stress field obtained from measurements of shock front speed at its run through the Kapton layers, which was recorded by each of fifty optical fibers of the MFOP-Us probe. Topography of P-localizations is indicative of the cellular structure of the DRZ. The DRZ consist of detonation cells of 0.5–1.5 mm cross-section size having the lifetime from 20 to 70 ns. Galloping detonation and the cellular structure are recorded also in emulsion explosives at wide variation of porosity [2]. Instabilities and fluctuations revealed in detonation flow of condensed EMs have a negative impact on a performance of powder compaction and explosive welding [2]. Fig. 5 illustrates results of Dynamic Performance Test of explosive compaction of tungsten powder [2]. The MFOP-probe was installed in axial

plane of container filled with W-powder. Dynamic localizations in the surface of the conical convergent shock front were spatially resolved through the side surface of optical fibers at crossing three linear grooves. Significance of this test implies in opportunity to obtain not only the mean shape of shock front but also its fluctuations. Application of the MCOA-UC in Explosive Welding Test will be presented in full paper. Up to date, the MCOA-UC is a unique and the most advanced metrology providing the meso-scale probing of the 3D DRZ structure of detonations at best compromise between high temporal and spatial resolution (200 ps and 50–250 μm), large amount of independent registration channels, and design simplicity. It's not limited on pressure amplitude of the shocked flow or detonation flow as opposed to multipoint VISAR or line ORVIS.

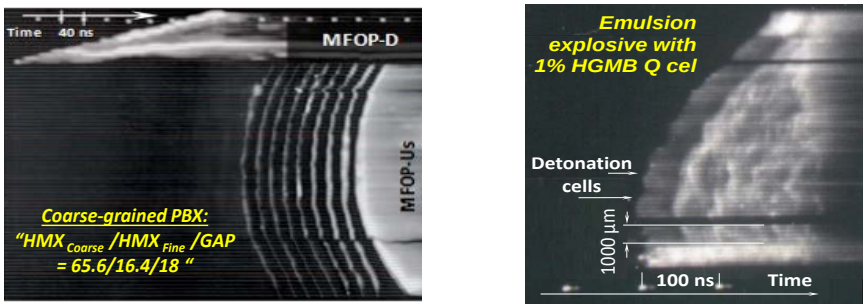

Fig. 3. Streak camera records obtained in experiments of schematics Fig. 2 (a) and (b) respectively.

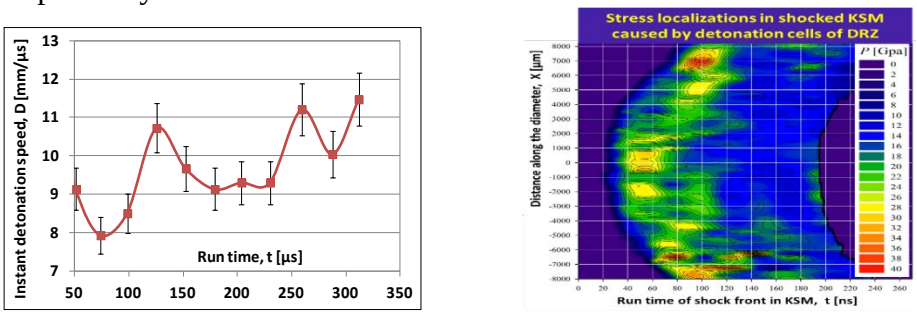

Fig. 4. The time history of detonation speed variation (left) and spatially resolved topography of the DRZ (right) are demonstrating the oscillating regime of front motion and cellular structure PBX of PBX detonation.

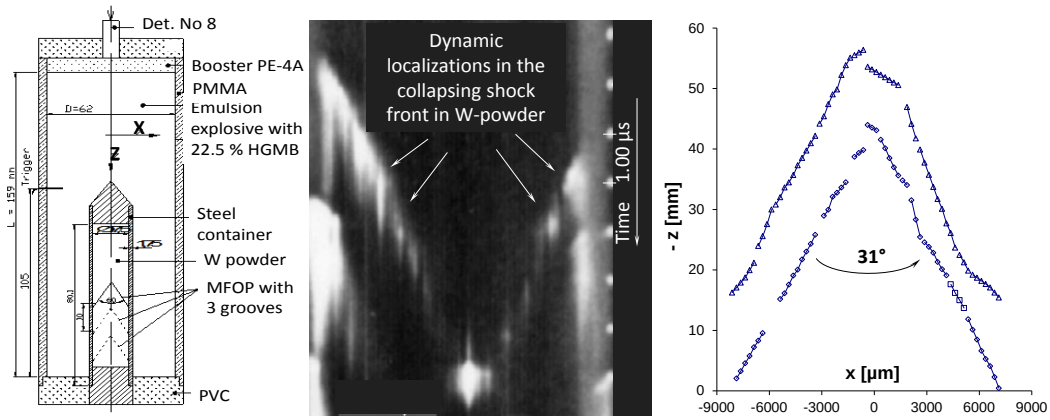

Fig. 5. Revealing the fluctuations in collapsing shock field in the Dynamic Performance Test of Tungsten Powder Compaction [2].

1. M. Mendonça, I. Plaksin, J. Campos, and J. Góis, Aqueous Explosives with TNT, *Chem. Phys. Repts*., 1998, vol. 17, nos. 1–2, p.p. 137–150.
2. Plaksin, et.al., Novelties in Physics of Explosive Welding and Powder Compaction, J. Phys. IV (Paris), 2003, vol. 110, pp. 797–802 (2003).

ADVANCED HIGH-TEMPERATURE CERAMICS BASED ON ZIRCONIUM DIBORIDE AND SILICIDE: COMBUSTION SYNTHESIS AND APPLICATION

A. Yu. Potanin[1], Yu. S. Pogozhev[1], I. V. Yatsuk[1], E. A. Levashov[1], D. Yu. Kovalev[2], and N. A. Kochetov[2]

[1]National University of Science and Technology MISiS, Leninsky pr. 4, Moscow, 119049 Russia
[2]Institute of Structural Macrokinetics and Materials Science, Russian Academy of Sciences, Chernogolovka, Moscow, 142432 Russia

e-mail: a.potanin@inbox.ru

Ceramic composites based on zirconium diboride ZrB_2 belong to the class of high-temperature materials widely used at temperatures over 1800°C and in aggressive media [1]. This is due to the fact that ZrB_2 exhibits a unique combination of physical and mechanical properties: high melting point (>3000°C), high thermal conductivity, high hardness, and good resistance to abrasion and aggressive environments [2]. The addition of Si and Al to boride matrix composites can improve some of the above mentioned properties like thermal stability and oxidation resistance.

Thermal barrier and high-temperature oxidation resistance of the coatings deposited with ZrB_2-based cathodes have a great potential for protection of leading edge parts on hypersonic space vehicles [3]. The use of multicomponent composite cathodes made of zirconium diborides, silicides, and Al dopants for magnetron sputtering of such coatings can be expected to markedly simplify a deposition process, to improve homogeneity of coatings and process reproducibility, and to shorten a deposition time. Required multicomponent compositions can be readily produced by combustion synthesis using the technique of forced SHS compaction [4, 5].

This study is focused on experimental investigations of combustion in Zr–Si–B(Al) mixtures yielding zirconium diboride and silicide doped with Al (10 wt %). We explored the kinetic and mechanism of the combustion process, with special emphasis on the effect of dilution (X = 20–40 %) of green mixtures with final products on burning velocity U_c and combustion temperature T_c. The effect of initial temperature (T_0) on kinetics of the SHS process was also studied (Fig. 1). The increase in T_0 leads to a proportional growth of U_c and T_c. A calculated value of the effective activation energy (225 kJ/mol) allows us to assume that combustion reaction of Zr with B proceeds with involvement of a liquid phase formed upon melting of the Zr–Si eutectic (T_m = 1643 K).

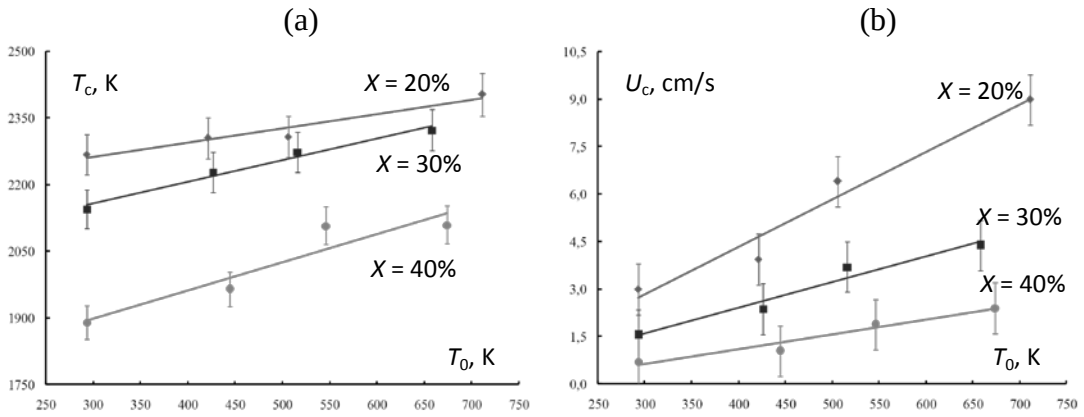

Fig. 1. (a) Combustion temperature T_c and (b) burning velocity U_c as a function of initial temperature T_0 and extent of dilution X.

The dynamics of structural and phase transformations in combustion wave were studied by the method of front quenching in a copper wedge followed by SEM|EDS characterization of different sample areas and also time-resolved XRD.

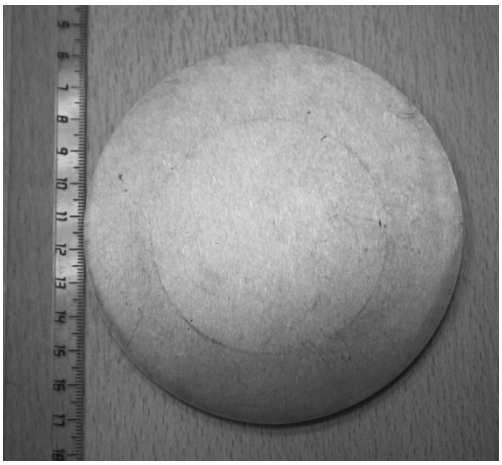

Fig. 2. PVD target of ZrB_2–$ZrSi_2$ composite obtained by forced SHS compaction.

Dense samples of multicomponent cathodes for magnetron sputtering were produced by using the technique of forced SHS compaction (Fig. 2). Their phase composition and structure were studied. It should be noted that the phase composition of the synthesized ceramics slightly differed from the nominal ones.

This work was financially supported by the Russian Ministry for Education and Science in the framework of the Program on Increasing the Competitiveness of MISiS (program no. K2-2014-012).

1. A.L. Chamberlain, W.G. Fahrenholtz, G.E. Hilmas, D.T. Ellerby, High-strength zirconium diboride-based ceramics, *J. Am. Ceram. Soc.*, 2004, vol. 87, no. 6, pp. 1170–1172.
2. S. Meng, F. Qi, H. Chen, Z. Wang, G. Bai, The repeated thermal shock behaviors of a ZrB_2–SiC composite heated by electric resistance method, *Int. J. Refract. Met. H*, 2011, vol. 29, no. 1, pp. 44–48.
3. P. Wang, W. Hann, X. Zhang, N. Li, G. Zhao, S. Zhou, (ZrB_2–SiC)/SiC oxidation protective coatings for graphite materials, *Ceram. Int.*, 2015, Vol. 41, no. 5, pp. 6941–6949.
4. E.A. Levashov, Yu.S. Pogozhev, A.Yu. Potanin, N.A. Kochetov, D.Yu. Kovalev, N.V. Shvyndina, T.A. Sviridova, Self-propagating high-temperature synthesis of advanced ceramics in the Mo–Si–B system: Kinetics and mechanism of combustion and structure formation, *Ceram. Int.*, 2014, vol. 40, no. 5, pp. 6541–6552.
5. Yu.S. Pogozhev, A.Yu. Potanin, E.A. Levashov, D.Yu. Kovalev, The features of combustion and structure formation of ceramic materials in the Cr–Al–Si–B system, *Ceram. Int.*, 2014, vol. 40, no. 10, pp. 16299–16308.

COMPARATIVE TENSILE STRENGTH AND SHEAR STRENGTH OF EXPLOSION CLAD MATERIALS

C. Prothe[1], C. Hurley[1], J. Banker[1], and S. Liu[2]

[1]DMC NobelClad, Mount Braddock, PA, 15465 USA
[2]Colorado School of Mines, Center for Welding, Joining, and Coatings Research, Golden, CO, 80401 USA

e-mail: cprothe@nobelclad.com

The tensile strength of an explosion clad interface can be an important consideration when structural components are to be welded to the clad surface of equipment and for tube sheets in certain shell and tube heat exchanger designs. A considerable amount of data has been published on the bond shear strength features of explosion clad plates. In contrast, minimal data has been presented on the tensile strength of explosion welded interfaces (tested in the through-thickness direction). In general it is relatively easy to perform shear strength tests on clad plates; however, since cladding layers are typically thin, it is relatively difficult to perform through-thickness tensile tests. Because of the lack of clad tensile data, the designer has minimal basis for designing welds for non-pressure retaining components which are attached to the clad surface. Some engineering companies allow welding of lightly loaded, non-pressure bearing internal vessel components direct to the explosion welded clad surfaces, while others require clad removal and attachment to the base steel only. Performing strip back of the cladding metal and welding components to the base steel results in additional manufacturing time and cost; and also increases risk associated with the dissimilar metal weld and CRA weld overlay.

A testing program has been undertaken to establish data on the interface tensile strength properties of explosion clad plates and to compare the results with the interface shear strengths and the bulk mechanical properties of the cladding and base metal components. These tests were conducted in the form of short transverse tensile tests with the clad interface in the central section of the test specimens. A range of cladding and base metals were tested in the "as-clad" condition and with simulated postweld heat treatment (SPWHT).

The 304 stainless steel and Inconel 625 alloy clad shear strength ranged from ~350–550 MPa (51–80 ksi) and was significantly higher than the Cu and Ti alloy clad shear strength of ~200–325 MPa (29–47 ksi). For all of the clad metal combinations tested, the clad tensile strength exceeded the clad shear strength. All of the titanium clad samples broke at the titanium-base metal interface. However, test specimen fracture location was

mixed for the Cu alloy clad materials. Some of the specimen broke in the Cu cladding alloy, some at the weld interface, and some in the base metal. For the 304 stainless steel and Inconel 625 alloy clad materials tested, the strength of the explosion weld always exceeded the strength of the base metal.

The clad tensile strength test data reported, and its relationship with standard clad shear testing, supports the design and analysis of explosion clad equipment. For stainless steel and nickel alloy clad materials the test data may lead to extending the range of applications where direct attachment to EXW clad is permitted.

GRANULAR MATERIALS UNDER SHOCK, BALLISTIC, AND BLAST LOADING

W. G. Proud

Institute of Shock Physics, Blackett Laboratory, Imperial College London,
London, SW&2AZ United Kingdom

e-mail: w.proud@imperial.ac.uk

Abstract—Granular materials are widespread in nature and in manufacturing. Their particulate nature gives them compressive strength of a similar order of magnitude as many continuous solids, a vanishing small tensile strength and a variable shear strength that is highly dependent on the precise loading conditions. Previous studies have shown the effect of composition, morphology and particle size; however, compared to metals and polymers, granular materials are not so well understood. This paper will present some recent results for granular materials, placing these within the wider context. Two areas will be dealt with (*i*) the effect of the skeletal strength of the material and (*ii*) the displacements associated with ballistic impact. One clear observation is the basic similarity of behaviour of quartz-based sands in compression across a range of particle sizes. However, the precise pathway of compression is strongly dependent on the initial conditions and connectivity within the granular bed, which requires the development of a suitable parameter to describe the material. In addition, the propagation of blast waves through dry and dampened granular material has been investigated; the addition of significant amounts of liquid in granular beds causes the mechanism of transmission of blast from one of percolation through the bed pores to one of stress transmission through the granules of the bed. It has been shown, however, that limited amounts liquid can retard propagation within blast-loaded beds by approximately an order of magnitude. This talk will conclude with data on percolation through dampened granular beds using a shock tube as the pressure driver. The effect of particle shape and size is investigated using angular grains of quartz sand as well as smooth glass microspheres.

Shock Studies. The results of variation in stress level are shown in Fig. 1 which is typical for all the quartz sphere studies. The traces are offset for clarity. Here it can be seen that the pre-cursor evolves significantly with stress level. At stresses below 1.4 GPa the pre-cursor is clearly visible, while at higher levels it is not resolved and a single rising shock wave is seen. Studies conducted by Neal *et al.* indicated that the wave speed, within experimental error, is either approximately fixed or decreases slightly with stress, while that of the following wave increases rapidly. The stress value associated with this wave increases with decreasing particle size, 0.3 GPa for 180–212 μm and 0.15 GPa for 425–

500 μm, this can be explained by the fracture strength of particles being higher the smaller the particle. The following wave is associated with a marked change in density of the material.

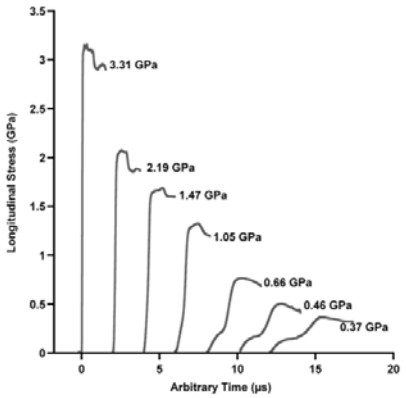

Fig. 1. Granular precursor wave evolution with shock wave level: a typical response of granular bed with increasing shock stress.

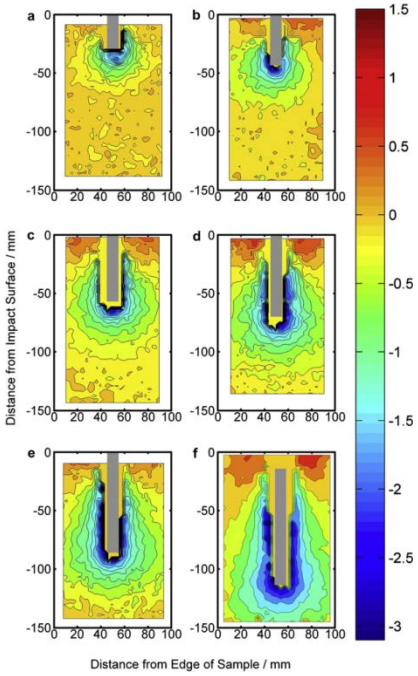

Fig. 2. Displacement around a penetrator striking a sand target at 200 m s^{-1}. The letters a–f correspond to the times after impact, 100 μs between each image.

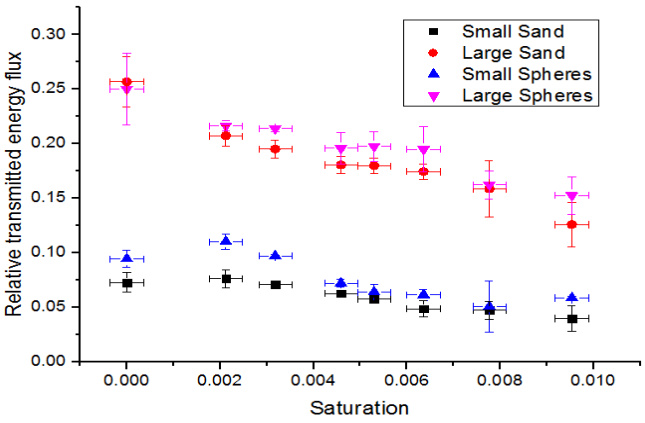

Fig. 3. The fraction of the energy flux through a 10 cm granular beds, struck by a 2 bar blast wave, showing the variation in attenuation with small additions of liquid.

Ballistic Studies. Granular materials are often used to mitigate ballistic impact. In this case the ability of granules within the bed to fracture or rotate and for pore collapse to occur gives a number of mechanisms to absorb energy from an impacting body. Ballistic impact is generally a complex 3D scenario; in the experiments outlined here the penetration was always normal to the interface allowing the system to be considered as 2D axisymmetric. The main experimental technique used here is flash radiography, the results of which are analyzed using image correlation techniques to produce maps of internal displacement within a granular bed. Results will contrast the outcome of dynamic impact as shown in Fig. 2. Here vertical displacements are recorded. It can be seen that in this case the displacements are localized around the impactor. The presentation will contrast these results with those obtained for low strain-rate loading.

Blast Mitigation. A shock tube was used in these blast-loading studies, consisting of 3 tubes along with a section for introducing different length of granular beds. The driver and the driven tubes are 1.22 m long with an internal diameter of 60 mm. The driver tube is separated from the driven sections by a double diaphragm breech. The driven tube is initially at ambient pressure and the shock propagates along this section. Figure 3 shows the transmitted energy calculated from the integrated pressure-time traces. On this graph a level of 1.00 corresponds to no granular bed being present. The presence of the 10 cm thick large particle size beds drops the transmitted energy to 0.25; the small particle beds drop this energy transmission to less than 0.1. As can be seen the addition of the small amount of water causes this energy to drop even further, roughly halving the transmitted energy by a further 50% resulting in only 14% energy transmission for the large particle bed and 6% for the small particle bed.

1. Jaeger, H.M., Nagel, S.R., Behringer, R.P, Rev. Mod. Phys., 1996, vol. 68, no. 4, pp 1259–1273.
2. Proud, W.G., Chapman, D.J., Williamson, D.M., Tsembelis, K., Addiss, J., Bragov, A., Lomunov, A., Cullis, I.G., Church, P.D., Gould, P., Porter, D., Cogar, J.R., and Borg, J., in *Shock Compression of Condensed Matter-2007*, AIP Conference Proc. 955, pp. 1403–1408.
3. Bragov, A.M., Lomunov, A.K., Sergeichev, I.V., Tsembelis, K., Proud, W.G., *Int. J. Impact Eng*., 2008, vol. 35, pp. 967–976.
4 Tsembelis K., Proud W.G., Vaughan B.A.M., Field J.E., The behaviour of sand under shock wave loading: Experiments and simulations, in *Behaviour of Materials at High Strain Rates: Numerical Modelling*, Benitez F.G. (ed.), DYMAT, Saint-Louis (France), 2002, pp. 193–203.

5. Neal, W.D., The role of particle size in the shock compaction of brittle granular materials, PhD Thesis, Imperial College London, 2012.
6. Neal, W.D., Chapman, D.J., Proud, W.G., Shock-precursor waves in brittle granular materials, in *Shock Compression of Condensed Matter-2011*, AIP Conf. Proc. 1426, pp. 1503–1506.
7. Addiss, J.W., Collins, A.L., Walley, S.M., Proud, W.G., The use of digital speckle radiography to investigate the internal flow fields during the ballistic penetration of sand, in *Rapid Penetration into Granular Media: Visualizing the Fundamental Physics of Rapid Earth Penetration*, Iskander M., Bless S., Omidvar M. (eds.), Elsevier, New York, 2015.
8. Addiss, J.W., Collins, A.L., Proud, W.G., Investigation of the rate dependence of long-rod penetration of granular media using an improved DSR algorithm, in *Shock Compression of Condensed Matter-2009*, AIP Conference Proc. 1195, pp. 1357–1360.
9. Addiss, J.W., Collins, A.L., Proud, W.G., Optimisation and use of a digital speckle radiography algorithm for investigation of long rod penetration of granular media, in *Shock Compression of Condensed Matter-2009*, AIP Conference Proc. 1195, pp. 1313–1316.
10. Walley, S.M., Collins, A.L., Addiss, J.W., Promratana, K,. Bobaru, F., Proud, W.G., Williamson, D.M., *Int. J. Impact Eng*., 2011, vol. 38, no. 12, pp. 951–963.
11 Proud, W.G., *J. Phys.: Conf. Ser.*, 2014, vol. 500, 112052; DOI: 10.1088/1742-6596/500/11/112052

CONSTRUCTIVE APPLICATIONS OF SHOCK WAVES: IMPORTANCE OF DETONATION VELOCITY

R. Prümmer

KIT Karlsruhe, Germany

e-mail: rolfap@gmx.de

EXPLOSIVE FORMING was established in the early 60s of last Century. The knowledge was taken from underwater explosions (Cole, Schauer, Snay, et al.) as usual in military research with high explosives. Is this logical? Deeper investigations by the author do not verify this assumption and reveal that low explosives but with a higher charge instead are better for the product.

EXPLOSIVE WELDING was discovered during explosive Forming operations done at too high velocity. A formed metal sheet got stuck with the forming die. Investigations revealed a wavy local connection of the sheet metals with the die. Today the parameters for explosive welding are well known. The conditions leading to a wavy or flat interphase can be forecast from the mechanical properties of the sheet metal. In the development of for this reason a necessary explosive weldability window were involved several investigators (Deribas, Wittman, Cowan, Holtzmann, et al.). The main parameter, collision velocity, should not exceed 120% of the sound speed value of the materials involved. As in a parallel set-up of explosive welding, the collision velocity is equal to the detonation velocity of the explosive; problems can arise when metals like lead or depleted uranium are to be welded. Solutions can be found in arrangements like inclined set-up or hot explosive welding. Usually detonation velocities of 2000 m/s are common in explosive welding.

EXPLOSIVE CUTTING is a procedure principally similar to explosive welding. A metal jet is generated in both cases. However, in explosive cutting the jet is the goal. In order the jet be large in size and of high velocity, the setup mush have large inclination, usually about 90 degrees. Such a jet is capable of penetrating the plates and cutting them. It is needless to say that hollow cones instead of inclined plates create such jets which are capable of penetrating thick metal plates and used in military operations. The procedure of explosive cutting is well developed and possibly the procedure is applicable to dismantling atomic power plants. The necessary charges can be fixed at thick walled pressure vessels in radioactive environment within short times and the cut

segments be transported. In this way, strained ships were cut into transportable segments.

EXPLOSIVE HARDENING makes use of the possibility to increase the dislocation density in metals without massive deformation. But there exists a maximum detonation velocity of the explosive in direct contact with the metal part. In case of too high detonation velocity and high pressure, the metal is heated and subsequent partial annealing can occur. Explosive hardening was applied to railway frogs of the Transsiberian Railway by Deribas. Manganese steel is the most suitable kind of steel for explosive hardening.

EXPLOSIVE COMPACTION at a first glance should be performed using high explosives: the higher the pressure, the higher the achieved density of the compact. Wrong! In comparison with conventional static compression, there exist release waves! This feature is complex and will be explained thoroughly for the case of cylindrical samples.

MEDICAL APPLICATION OF SHOCK WAVES is a most recent development and at the same time the most exciting one. Today kidney stones in human body are no more taken out by intrusive medical operations. Underwater created shock waves enter the human body and are focused onto the kidney stone and destroy it by shock ablation. The fragments go off the natural way. In early investigations, the patient was in a bath tub together with the shock device. Today a shock wave device is attached to the patients back and the shock wave created by electric discharge. The latest developments will be reported at presentation.

OPTICAL DETONATION MEASUREMENTS AND DESIGN OF EXPLOSION CHAMBER FOR SMALL SAMPLES OF EXPLOSIVES

J. Quaresma[1], J. Pimenta[1], R. Mendes[1], J. Gois[1], J. Campos[1], L. Deimling[2], and T. Keicher[2]

[1]ADAI–Association for the Development of Mechanical Engineering, LEDAP–Laboratory of Energetics and Detonics, Department of Mechanical Engineering, University of Coimbra, Rua Luis Reis Santos, Coimbra, 3030-788 Portugal
[2]Fraunhofer Institut für Chemische Technologie (ICT), Pfinztal, 76327 Germany

e-mail: andrade.campos@dem.uc.pt

The experimental detonation measurements use more and more optical techniques (using optical fibers) based on detonation thermal radiation measurements. Initially, it was observed and recorded with a multichannel optical analyzer using multi-fiber optical probes. However, a fast streak camera (with delicate triggering mechanisms and sweep time evaluations) is always a condition to record the results. These conclusions lead us to develop a more simplified method, based in single optical fibers and fast optical/electric sensors connected to a digital signal analyzer. Two kinds of optical multimode fibers can be used in these measurements: PMMA and silica fibers. In a similar way, two kinds of optoelectronic receivers were used, as a function of optical range (maximum sensibility at 650 nm and 850 nm). Rise time is less than 50 ns. The position and length of a single optical fiber, inside explosive sample, is presented and discussed. It can be inserted in vertical, horizontal, or with a fixed angle related to the detonation plan. Two fibers allow more precise evolution and measurements. Silica fibers of 60 μm in diameter provide more precise experimental measurements, due to reduced diameter and lower ignitability with detonation products.

In order to perform these experiments, with small explosive samples, a new explosion chamber was designed and fabricated. The reference explosives were PETN and industrial emulsion explosive. Prediction of detonation properties of emulsion explosive was done using thermochemical computer code, named THOR. Expansion of detonation products, after initial vacuum conditions, is predicted using the JWL parameters. It was confirmed by 3D Autodyn simulations in underwater conditions. THOR code allows the calculation of initial isentrope and expansion adiabat. Designed explosion chamber was based on AD-Merkblätter Standards for P355 steel. Wall thickness was discussed and final dimensions were optimized. Final values show optimized wall thickness close to 3 mm, from a commercial beer barrel of 50 L volume. Design and validating simulations and experiments prove the possibility of having a

small stainless steel explosion chamber for explosive charges up to 60 g. In order to design and build a final laboratory-scale explosion chamber, the commercial beer barrel is inserted inside a P355 steel cylindrical chamber, with 30-mm wall thickness, with full opening and closing operations electronically controlled. Ignition and optical measurements are integrated with this system. Safety norms and procedures were applied during charging operations. Evacuation of the chamber before explosion afforded the collection and analysis of reaction products after detonation.

FRACTAL ANALYSIS OF CLUSTERS FORMED AT THE INTERFACES IN EXPLOCXLAD MULTILAYER STRUCTURES

A. E. Rosen[1], V. D. Krevchik[2], M. B. Semenov[2], A. V. Pryshchak[2], and A. A. Rosen[1]

[1] ROMET Ltd., ul. Druzhba 6, Penza, 440067 Russia
[2] Penza State University, ul. Krasnaya 40, Penza, 440026 Russia

e-mail: aerozen@bk.ru, aarozen@bk.ru

As is known, the mechanical properties of exploclad multicomponent composite materials strongly depend on conditions for development of contact surfaces at the interface [1].

We suggest a theoretical approach to the problem based on the method of fractal dimensionality [2] of interlayer boundaries and the physics of fast processes responsible for formation of the above boundaries. The governing equations involve the equations of thermal conductivity and diffusion in conditions of of shock loading.

The fractal analysis was applied to a group of exploclad multilayer composite materials comprising of 3–10 light-gage layers of chromonickel steel, carbon steel, and aluminum.

Our results may turn useful in designing new multilayer light-gage corrosion resistant materials for the needs of metallurgy and nuclear power engineering [3]. Relevant details will be discussed at presentation.

We are grateful to Prof. Hiroyuki Sasaki, National Institute of Livestock and Grassland Science, Japan, for making accessible his program package for fractal analysis.

1. V.I. Lysak, S.V. Kuz'min, *Explosive Welding*, Moscow: Mashinostroenie-1, 2005 (in Russian).
2. A.M. Sinev, The stochastic Baker–Hausdorff formula and its applications to quantum relaxation processes, *Mathem. Notes*, 2008, vol. 84, no. 3, pp. 395–408.
3. I.S. Los', Yu. P. Perelygin, A.E. Rozen, S.Yu. Kireev, *Multilayer Light-Gage Corrosion Resistant Materials*, Penza: Izd. Penz. Gos. Univ., 2015 (in Russian).

MECHANISM OF PATTERNING AT THE INTERFACE OF EXPLOSIVELY WELDED Cu/Cu PLATES

V. V. Rybin[1,2], E. A. Ushanova[3], and N. Yu. Zolotorevsky[1,2]

[1]Peter the Great Polytechnic University, ul. Politekhnicheskaya 29, St. Petersburg, 195251 Russia
[2]Research Institute of Mechanical Engineering, Russian Academy of Sciences, ul. Belinskogo 85, Nizhnii Novgorod, 603024 Russia
[3]Central Research Institute of Structural Materials PROMETEY, ul. Shpalernaya 49, St. Petersburg, 191015 Russia

e-mail: elinaus@mail.ru

The main requirement for explosive welding technology is to provide high adhesion strength of welded metal in the bond zone. The quality of the bond is determined by the features of plastic deformation of metal in a very narrow bond zone (NBZ), which characteristic transverse dimension is estimated at about 10 μm. Plastic deformation of the metal is characterized by the extreme conditions: shear and compressive stresses are distributed non-uniformly over the range around 10 MPa, the plastic deformation rate is close to 10^6 s^{-1}, the values of accumulated plastic deformation are greater than unity, i.e., typical of severe plastic deformation.

Until recently, the physics and mechanics of crystalline solids did not say much about the features of plastic deformation taking place in such unusual conditions as well as about its elementary mechanisms. The answers to these and similar questions can only be obtained on the basis of direct experimental observation of structures formation and subsequent evolution within the NBZ by using high-resolution methods of transmission and scanning electron microscopy. For a long time, such studies have not been conducted due to specific methodical difficulties. In recent years they have been overcome and the multi-level complex picture of NBZ formation during explosive welding has been suggested [1–5]. In this communication, we give a brief overview of our recent results obtained for explosive welding of copper to copper.

A systematic study of deformation structures on a macro, meso, and micro level was carried out using optical metallography, TEM, and EBSD. On a micro level, i.e. inside the smallest uniformly oriented crystallites (fragments), the plastic deformation is realized by a classical mechanism of nucleation and subsequent propagation of individual dislocations. Therewith, when the macroscopic deformation is relatively small and there is no fragmentation of initial grains to highly disoriented volumes, the dislocations can form slightly disoriented cell structures inside the grains. With

increasing degree of deformation a grain fragmentation occurs, and a deformation-induced fragmented meso structure begins to develop. A characteristic feature of its evolution is the formation of meso bands, which represent chains and bands consisting of great number of fragments (Fig. 1).

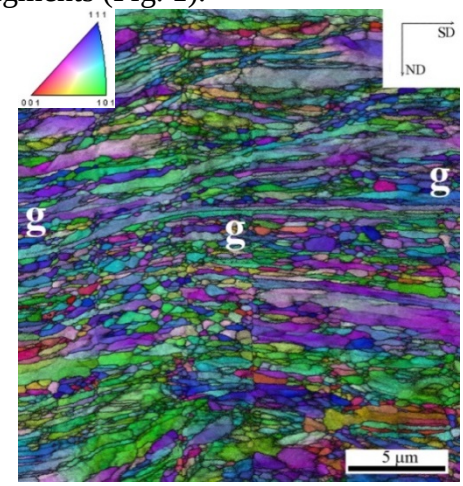

Fig. 1. IPF map of deformation meso structure in the NBZ: g-g-g is the boundary between the upper and lower plates; SD is the direction parallel to the local portion of the bonding interface, and ND is the direction normal to the SD.

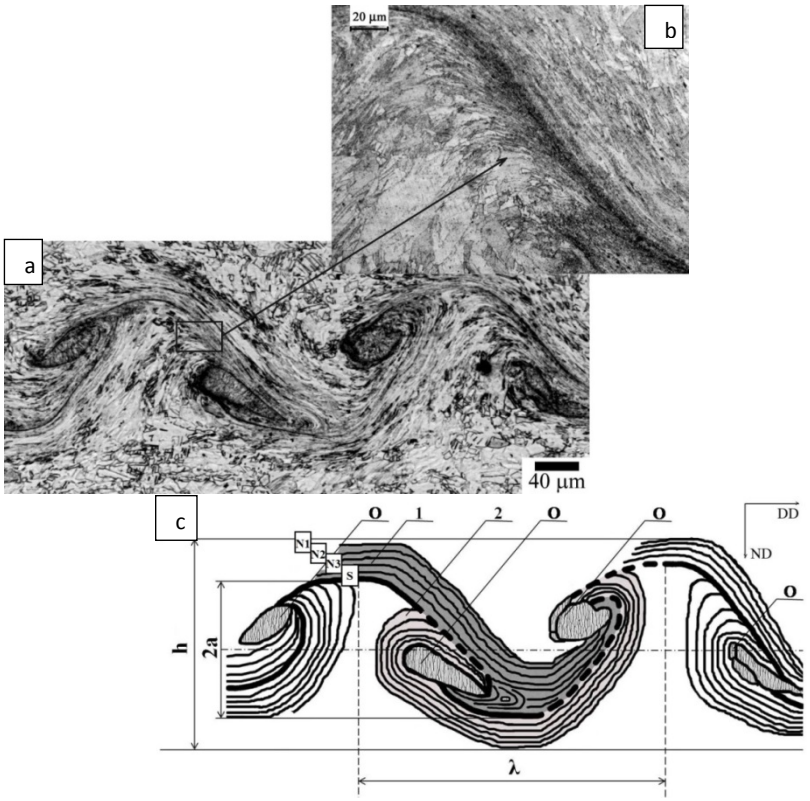

Fig 2. Structure of the NBZ of the Cu/Cu explosive joint: (a) optical micrograph; (b) magnified image of the NBZ region highlighted in the figure with a rectangle; (c) schematic image of the structure: thick line corresponds to the bond surface of the copper plates; N1, N2, N3, S are the regions investigated using the EBSD analysis; 1, 2 are the plastic streams; O is the fusion region; DD is the detonation direction; ND is the direction perpendicular to the detonation direction.

The typical element of the macrostructure was called a plastic stream. It consists of several meso bands parallel to each other (generally curved) and is located immediately adjacent to the bonding interface. On a macro level, the plastic stream represents an elementary vortex. The length of the plastic stream is equal to the wavelength of the wavy bonding interface between the welded plates. (Fig. 2).

Analysis of disorientation distributions within the fragmented structure detected in the NBZ allowed us to identify and classify the mechanisms of structure formation operating in the NBZ of the Cu/Cu weld joint. These are: (1) fragmentation of grain volumes, (2) dynamic deformation twinning, (3) fragmentation of random and twin boundaries, and (4) recrystallization. Using computer modeling of disorientation distributions, the contributions of above mechanisms to the structure formation in the NBZ of the welded joint were determined.

This work was supported by the Russian Science Foundation (project no. 15-13-20030).

1. V.V. Rybin, E.A. Ushanova, S.V. Kuzmin, V.I. Lysak, The nature of plastic flow in bond zone of explosively welded metals, *Tech. Phys. Lett*., 2011, vol. 37, no. 12, pp. 1100–1103.
2. V.V. Rybin, E.A. Ushanova, N.Yu. Zolotorevskii, Features of disoriented structures in a copper–copper bilayer plate obtained by explosive welding, *Tech. Phys*., 2013, vol. 58, no. 9, pp. 1304–1312.
3. V. V. Rybin, N. Yu. Zolotorevskii, E. A. Ushanova, Fragmentation of crystals upon deformation twinning and dynamic recrystallization, *Phys. Met. Metallogr*., 2015, vol. 116, no. 7, pp. 730–744.
4. H. Paul, M. Faryna, M. Prazmowski, R. Banski, Changes in the bonding zone of explosively welded sheets, *Arch. Metall. Mater*., 2011, vol. 56, no, 2, pp. 463–474.
5. H. Paul, L. Litynska-Dobrzynska, M. Prazmowski, Microstructure and phase constitution near the interface of explosively welded aluminum/copper plates, *Metall. Mater. Trans. A*, 2013, vol. 44, pp. 3836–3851.

STRUCTURE OF BIMETALS AS STIDIED BY SYNCHROTRON RADIATION

K. Saksl[1,2], J. Ďurišin[3], O. Milkovič[4], Z. Szulc[5], L. Ciupiński[6], and A. Arnbjörnsson[7]

[1] Institute of Materials Research, Slovak Academy of Sciences, Košice, Slovak Republic
[2] Institute of Physics, P.J. Šafárik University, Park Angelinum, Kosice, 04154 Slovak Republic
[3] Faculty of Electrical Engineering and Informatics, Technical University of Košice, Letná 9, Košice, 04200 Slovak Republic
[4] Faculty of Metallurgy, Technical University of Košice, Košice, Slovak Republic
[5] Explomet–Opole (High-Energy Techniques Works), Opole, Poland
[6] Faculty of Materials Science and Engineering, Warsaw University of Technology, 141 Wołoska Street, Warsaw, 02-507 Poland
[7] Materials, Biotechnology, and Energy Innovation Center Iceland, Árleyni 8, Reykjavík, 112 Iceland

e-mail: ksaksl@saske.sk

Explosive welding is used for joining of wide variety of similar or fundamentally dissimilar materials that cannot be joined by any other welding or bonding technique. In the present work, the composite bimetal plates of 254 SMO high-alloy austenitic stainless steel and P355NH pressure vessel steel produced by explosion welding were studied.

Chemical composition of P355NH ferritic steel (in wt. %): 0.18% C; 0.35% Si; 1.19% Mn; 0.015%P; 0.002% S; 0.005% N; 0.041% Al; 0.20% Cu; 0.02% Cr, 0.22% Ni; 0.004% Mo; 0.003% V; 0.003% Ti was clad by the austenitic 254 SMO steel (in wt %): 0.014% C; 0.39% Si; 0.38% Mn; 0.021% P; 0.001% S; 19.99% Cr; 17.96% Ni; 6.05% Mo; 0.012% Nb; 0.69% Cu; 0.41% Co; 0.213% N. Thickness of the P355NH base material was 10 mm and of the 254 SMO clad 3 mm. Sizes of the welded sheets were 800 × 520 mm. The welding procedures were carried out by the EXPLOMET-Opole company.

To determine phase composition and microstructure parameters of the interface and surrounding regions, a hard X-ray micro-diffraction experiment was performed at beamline P07 at PETRA III (electron storage ring operating at energy 6 GeV with beam current 100 mA) in DESY Hamburg, Germany. During the experiment, monochromatic synchrotron radiation of energy 78 keV (λ = 0.01589 nm) was used. The beam of photons was focused by compound refractive lenses down to a spot with the size of 3 × 20 μm. The sample was positioned perpendicularly to the direct beam by adjusting the

tilt of supporting cradle with precision ±0.25 deg adjusted by the steepest transition (measured by absorption) between the clad and base materials. The materials interface was scanned shot-by-shot along a straight path (red full line marked in Fig. 1c) of length 0.4 mm with step width of 1 μm. The scan was continued further down to the ferritic steel by coarser 0.1 mm step up to the total distance 1.5 mm (dashed red line marked in Fig. 1). During each step, the sample was illuminated by high-intensity hard X-rays for 0.5 seconds. The resulting 2D XRD patterns were recorded using a Perkin Elmer 1621 detector. The intensity was then integrated to 2θ by using the Fit2D software.

Fig. 1a shows the prepared bimetallic system. The sample subjected to our synchrotron study was 5 × 5 × 13 mm dimension (Fig. 1b) and cut out by electric discharge process.

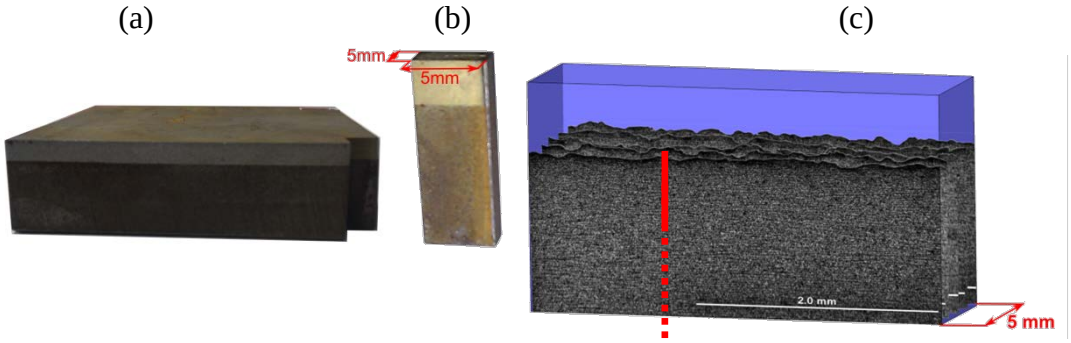

Fig. 1. (a) Bimetal consisting of base ferritic steel P355NH at the bottom and 254 SMO clad on top as prepared by explosion welding, (b) sample for synchrotron study, (c) Three-dimensional view (5 cross sections) of the ferritic/austenitic bimetal investigated by micro diffraction. Ferritic steel (gray areas at the bottom) was obtained from crystallographic cuts. For reasons of clarity the austenite parts were removed from pictures. Wavy interface between the two materials is obvious. The red full line represents a shot-by-shot scan along a straight path of length 0.4 mm with a step of width 1 μm. The scan was continued further down to steel side with a coarser step of 0.1 mm (dashed part of the line).

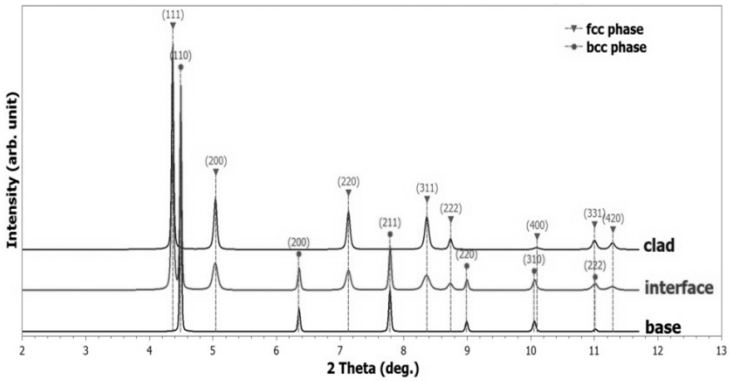

Fig. 2. XRD patterns of the investigated bimetal.

Fig. 2 shows the XRD patterns from different parts of the bimetal: ferritic side measured 190 μm far from the center of the joint (black curve at the bottom), austenitic 210 μm from the center, but in the opposite direction (blue curve on the top of the picture) and center of the joint itself (represented by red curve in between). Material measured in center of the joint consists of two phases: *fcc*-Fe (austenite), *bcc*-Fe (ferrite) in equal proportion and small fraction of orthorhombic Fe_3C (cementite). No other intermetallics have been found.

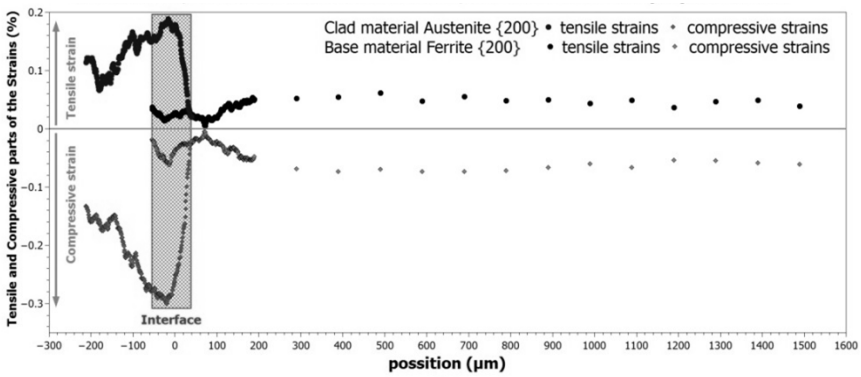

Fig. 3. Distributions of tensile and compressive internal strains in bimetal after explosive welding.

Further we analyzed internal strains induced in bimetal by explosion. Our approach is based on calculation of distances between (200) crystallographic planes measured azimuthally along the (200) Debye–Scherrer rings. Fig. 3 shows the distribution of internal strains in the sample. The most critical place with highest strain anisotropy was found in austenite: ~30 μm from the center of the joint.

SELF-PROPAGATING HIGH-TEMPERATURE SYNTHESIS OF CAST HIGH-ENTROPY ALLOYS BASED ON 3*d* AND 4*d* ELEMENTS

V. N. Sanin, D. M. Ikornikov, D. E. Andreev, N. V. Sachkova, and V. I. Yukhvid

Institute of Structural Macrokinetics and Materials Science, Russian Academy of Sciences, Chernogolovka, Moscow, 142432 Russia

e-mail: svn@ism.ac.ru

High entropy alloys (HEAs), or multi-component alloys, are a new point of interest in materials science and engineering. HEA is an alloy that contains at least five major metallic elements ($n \geq 5$), each in concentration between 5 and 35 at. % [1]. The configuration entropy of HEAs is given by the expression $S_{conf} = R\ln(n)$, where R is the universal gas constant, assuming the alloys in a fully (close to fully) random state (random solid solution) [2], and that S_{conf} is much higher than that of conventional alloys with one or two principal elements. Depending on the alloy composition, HEAs can possess many interesting mechanical and physical properties [3, 4], and great potential for use as high-temperature [5] and coating materials [6] with high hardness and wear resistance.

Nevertheless preparation of multicomponent materials is not an easy task. One has to ensure highly homogeneous distribution of the elements over the entire alloy. Moreover, the presence of reactive components (Ti, Al, Zr, Hf, etc.) will require expensive mold materials and complicated equipment.

In this work, we investigated a cost-effective SHS process for fabricating cast high-entropy alloys based on 3*d* ($NiCrCoFeMnAl_x$) and 4*d* elements ($NbTiMoZrCrAl_{0.5}Si_x$, $NbMoZrWHfTaCr_x$) through the following aluminothermic reaction:

$$(MeO)_1 + (MeO)_2 + (MeO)_3 + (MeO)_i + \alpha Al + (FA) \rightarrow HEA + Al_2O_3 + Q$$

where (MeO) = NiO, Cr_2O_3, Co_3O_4, MoO_3, Nb_2O_5, WO_3, etc.; Al is metal reducer; FA is an additive facilitating phase segregation; and Q the reaction heat. The flowsheet of the process is presented in Fig. 1.

After initiation with an igniting coil, SHS reaction frontally propagates downward. Because the attained temperatures (up to 3000°C) are well above the m.p. of reaction products, the melt represents a mixture of multicomponent mutually insoluble metals (HEAs) and oxide (Al_2O_3) phases. Due to strongly different specific weights, these phases undergo gravity-assisted phase separation. As the result, the cast multicomponent HEA is formed. Combustion was performed at centrifugal acceleration a = 10–400 g. In

this way we expected to (a) improve the yield of target product, (b) remove gaseous byproducts, (c) diminish the grain size in the product, and (d) make product composition more uniform.

Table 1 shows the nominal composition of the alloys used in experiments.

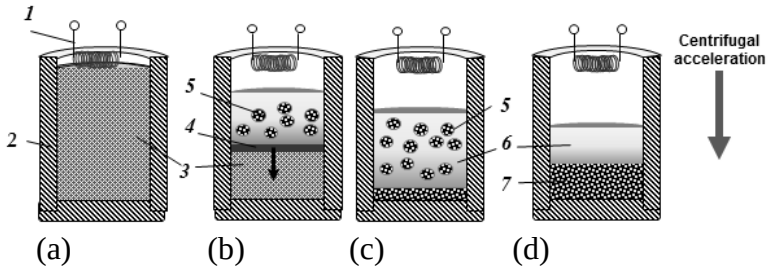

Fig. 1. Flowsheet of the process for fabrication of cast HEAs: (a) charge preparation, (b) combustion, (c) phase separation, (d) patterning: *1*, igniting coil; *2*, refractory mold; *3*, green mixture; *4*, combustion front; 5, alloy globules; 6, oxide melt; and *7*, cast HEA.

Table 1. Composition of alloys based on 3*d* elements.

Alloy	Atomic ratio	Elemental composition, wt %						
		Ni	Cr	Co	Fe	Mn	Al	Cu
HEA-I	NiCrCoFeAlCu	18.5	16.8	18.6	17.6		8.5	20
HEA-II	$NiCrCoFeMnAl_{0.6}$	19.9	17.6	19.9	18.9	18.6	5.1	–
	$NiCrCoFeMnAl_{1.2}$	18.7	16.5	18.8	17.8	17.5	10.7	–
	$NiCrCoFeMnAl_{1.6}$	17.8	15.8	18.0	16.9	16.7	14.8	–
	$NiCrCoFeMnAl_{2.0}$	16.9	14.9	17.0	16.1	15.8	19.3	–

Table 2. Composition of alloys based on 4*d* elements.

Alloy	Atomic ratio	Elemental composition, wt %						
		Nb	Ti	Mo	Zr	Cr	Al	Si
HEA-III	$NbTiMoZrCrAl_{0.5}Si_{0.1}$	23.5	12.1	24.2	23	13.1	3.4	0.7
	$NbTiMoZrCrAl_{0.5}Si_{0.4}$	23.0	11.8	23.7	22.6	12.8	3.3	2.8
	$NbTiMoZrCrAl_{0.5}Si_{1.0}$	22.0	11.6	22.7	21.6	12.3	3.2	6.6
	$NbTiMoZrCrAl_{0.5}Si_{1.3}$	21.6	11.1	22.3	21.2	12.1	3.2	8.5
	$NbTiMoZrCrAl_{0.5}Si_{1.6}$	21.2	10.9	21.9	20.8	11.9	3.1	10.2
	$NbTiMoZrCrAl_{0.5}Si_{2.0}$	20.7	10.7	21.3	20.3	11.5	3.0	12.5
		Elemental composition, wt %						
		Nb	Mo	Zr	Cr	W	Hf	Ta
HEA-IV	NbMoZrWHfTa	11.3	11.6	11.1	0	22.3	21.7	22
	$NbMoZrWHfTaCr_{0.5}$	10.9	11.4	10.7	3.1	21.6	21	21.3
	$NbMoZrWHfTaCr_{1.0}$	10.6	11	10.4	5.9	21	20.4	20.7

An increase in the Al (Si, Cr) content of HEAs was found to markedly change the microstructure and phase composition of HEAs. Synthesized HEAs-II type alloys $NiCrCoFeMnAl_x$ with high Al contents (up to 19 wt %) had unique nano-sized structure (Fig. 2) consisting of NiAl as a body phase and nano-sized (rounded) precipitates of polymetallic solid solution (*fcc*/*bcc*).

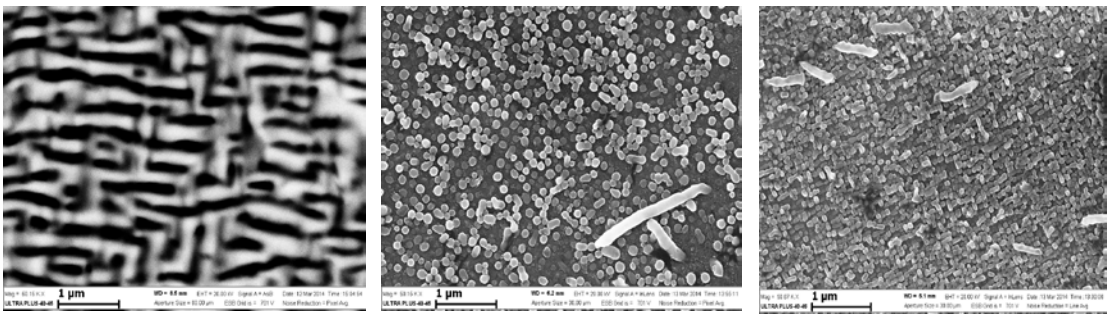

(a) (b) (c)

Fig. 2. SEM images of cast HEAs (after etching): (a) HEA-II-0.6, (b) HEA-II-1.6, and (c) HEA-II-2.0.

Synthesis conditions for the above cast HAEs as well as XRD and SEM results will be discussed at presentation. This work can be regarded as the first positive experience

on SHS-preparation of cast HEAs based on 3*d* and 4*d* elements. The present results can be expected to make engineering background for industrial-scale cost-effective manufacturing of new HEAs with valued properties.

This work was financially supported by the Russian Foundation for Basic Research (project no. 16-08-00398).

1. J.W. Yeh, S.K. Chen, S.J. Lin, J.Y. Gan, T.S. Chin, T.T. Shun, C.H. Tsai, S.Y. Chang, Nanostructured high-entropy alloys with multiple principal elements: Novel alloy design concepts and outcomes, *Adv. Eng. Mater.*, 2004, vol. 6, pp. 299–303.
2. F. Otto, Y. Yang, H. Bei, E.P. George, Relative effects of enthalpy and entropy on the phase stability of equiatomic high-entropy alloys. *Acta Mater*., 2013, vol. 61, pp. 2628–2638.
3. M.H. Tsai, Physical properties of high entropy alloys, *Entropy*, 2013, vol. 15, pp. 5338–5345.
4. D.B. Miracle, J.D. Miller, O.N. Senkov, C. Woodward, M.D. Uchic, J. Tiley, Exploration and development of high entropy alloys for structural applications, *Entropy*, 2014, vol. 16, no. 1, pp. 494–525.
5. Y. Lu, Y. Dong, S. Guo, L. Jiang, H. Kang, T. Wang, B. Wen, Z. Wang, J. Jie, Z. Cao, *et al*., A promising new class of high-temperature alloys: Eutectic high-entropy alloys, *Scientific Reports 4*; http://www.nature.com/srep/2014/140827/srep06200/full/srep06200.html
6. W.J. Shen, M.H. Tsai, J.W. Yeh, Machining performance of sputter-deposited $Al_{0.34}Cr_{0.22}Nb_{0.11}Si_{0.11}Ti_{0.22})_{50}N_{50}$ high-entropy nitride coatings. *Coatings*, 2015, vol. 5, no. 3, pp. 312–325.

EFFECT OF REMELTING TEMPERATURE ON STRUCTURAL HEREDITY OF CAST Co AND Ni BASED SHS-PRODUCED ALLOYS

V. V. Sanin[1], Yu. A. Anikin[1], V. I. Yukhvid[2], and M. R. Filonov[1]

[1]National University of Science and Technology MISiS, Leninskii pr. 4, Moscow, 119049 Russia
[2]Institute of Structural Macrokinetics and Materials Science, Russian Academy of Sciences, Chernogolovka, Moscow, 142432 Russia

e-mail: sanin@misis.ru

Heat-resistant high alloys of Ni, Co, and Fe find their application in components for turbines, rockets, and heat exchangers operating in the range 700–1100°C. Efforts on the design of new alloys and elaboration of new processes for their production are ever in progress. Nevertheless, metallurgical approach (molding) to industrial-scale fabrication of machine parts from such alloys still remains prevalent. Modern production of components from the superalloys by casting generally includes the step of producing cold-charged materials (CCMs) with regulated chemical composition and microstructure and casting the products directly to a predetermined shape. The quality and technology of smelting CCMs can have a significant impact on the parameters of casting technology and properties of the final products.

Marked advance in service parameters of final components can be achieved by using the following approach to manufacturing cast materials: (1) synthesis of cast CCMs by centrifugal SHS [1–3] and (2) their remelting under reduced pressure or in an inert atmosphere followed by casting into a mold with desired geometry.

SHS process was performed at centrifugal accelerations a = 10–400 g. In this way, we expected to (a) improve the yield of target product, (b) remove gaseous byproducts, (c) diminish the grain size in the product, and (d) make product structure more uniform. Thus synthesized CCMs exhibited a uniform distribution of the elements over the entire ingot. Experiments were performed the following two composites: (*i*) Co alloyed with Nb, Cr, Mo, W, Al, and C (alloy **I***)* and (*ii*) Ni alloyed with Al, Cr, Mo, Mn, Hf, and B (alloy **II**).

The influence of CCMs remelting temperature on the phase composition and microstructure of resultant materials was determined by using a VIK-VMR apparatus as described elsewhere [4].

The remelting of CCM was carried out at 1500, 1600, and 1700°C. Typical microstructures are exemplified in Fig. 1. An increase in remelting temperature is seen

to markedly change the microstructure of the alloys under study. Similarly, studies have been made for the system Ni-base (alloy **II**).

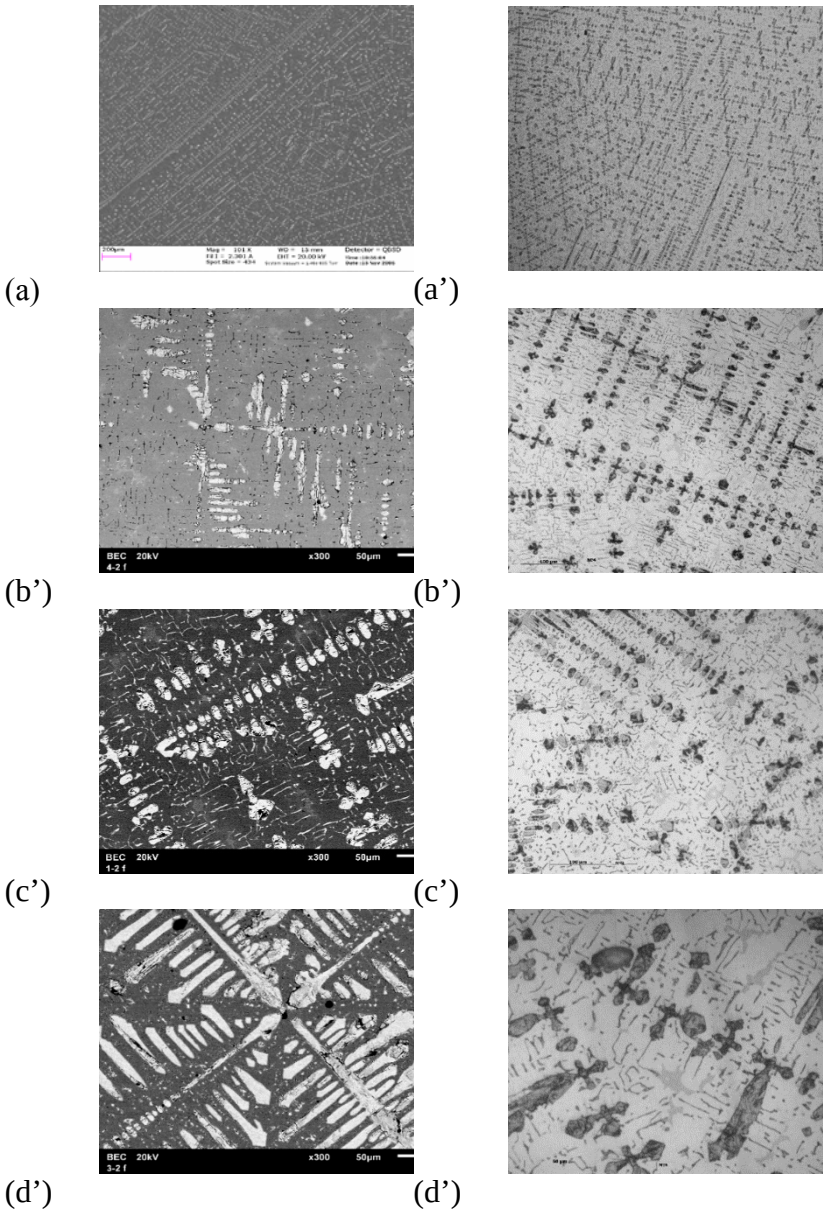

Fig. 1. SEM images of alloy **I:** SHS-produced (a, a') and after remelting at 1500 (b, b'), 1600 (c, c') and 1700°C (d, d').

A Co-based high alloy doped with Nb, Cr, Mo, W, Al, and C was produced by centrifugal SHS. And also NiAl-based high alloy doped with Mo, Cr, and B was produced by centrifugal SHS in atmospheric air. We explored the influence of remelting at temperatures above its melting point on its structural heredity. Induction remelting in vacuum at temperatures exceeding the melting point by more than 100°C was found to markedly enlarge the size structural constituents and lead to liquation. Our results can be expected to provide a technological background for a new cost-effective two-stage process: (a) SHS fabrication of refractory alloys with a desired composition and (b) their metallurgical reprocessing into ingots of appropriate configuration.

1. V.I. Yukhvid, V.N. Sanin, A.G. Merzhanov, The influence of high artificial gravity on SHS processes, in *Processing by Centrifugation*, L.L. Regel and W.R. Wilcox, Eds., Amsterdam: Kluwer Academic, 2001. pp. 185–200.
2. V.I. Yukhvid, D.E. Andreev, V.N. Sanin, Zh.A. Sentyurina, Yu.S. Pogozhev, E.A. Levashov, Centrifugal SHS of cast Ti–Al–Nb–Cr Alloys, *Int. J. Self-Propag. High-Temp. Synth.*, 2015, vol. 24, no. 4, pp. 177–181.
3. V. Sanin, D. Andreev, D. Ikornikov, V. Yukhvid, Cast Intermetallic alloys and composites based on them by combined centrifugal casting–SHS process, *Open J. Met.*, 2013, vol. 3, no. 2B, pp. 12–24. doi 10.4236/ojmetal.2013.32A2003
4. M.R. Filonov, Yu.A. Anikin, , Yu.B. Levin. *Theoretical Basis for Production of Amorphous and Nanocrystalline Alloys by Rapid Quenching*, Moscow: Izd. MISiS, 2006 (in Russian).

PROSPECTS FOR USING STONELEY WAVES IN MONITORING THE QUALITY OF CLAD METALS

V. A. Sel'skii[1] and A. A. Sel'skii[2]

[1]ZAO IMPUL'SNYE TECKHNOLOGII, Krasnoyarsk, Russia
[2]RTS Research and Education Center, Krasnoyarsk, Russia

e-mail: limom1@yandex.ru

Nowadays, the quality of rolled metal sheets is checked by using direct piezoelectric transducers (PETs) all over the entire sheet surface. In this context, it seems reasonable to detect the location of defects with the normal waves such as Rayleigh waves, Lamb waves, Stoneley waves, etc.

In this work, we attempted to excite such waves in Cu (5mm)–Ti (1 mm)–Al (35 mm) sheets and to accommodate them for rapid detection of defects in clad plates.

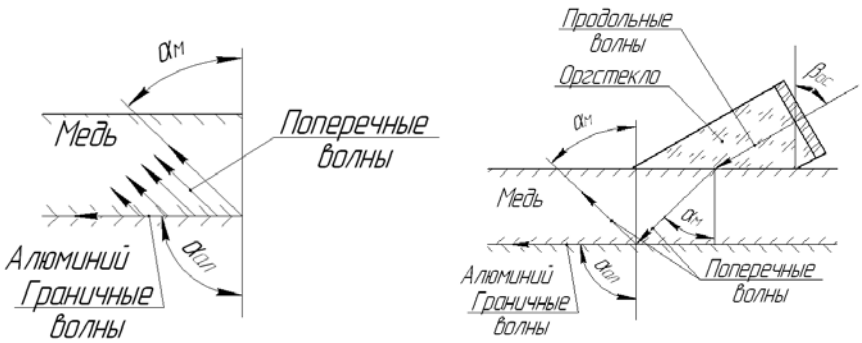

(a) (b)

Fig. 1. (a) Refraction and transformation of acoustic waves and (b) the transversal waves generating interfacial Stoneley waves.

Using the Snellius law the scheme of incident and propagating waves presented in Fig. 1a, we have:

$$\frac{\sin \alpha_{\text{м}}}{c_t^{\text{м}}} = \frac{\sin \alpha_{\text{ал}}}{c_t^{\text{ал}}}, \qquad (1)$$

whence

$$\alpha_{\text{м}} = \arcsin\left(\frac{C_t^{\text{м}} \times \sin\alpha_{\text{ал}}}{C_t^{\text{ал}}}\right), \qquad (2)$$

where $C_t^{\text{ал}}$ = 3130 m/s is the velocity of transversal waves in Al and $\sin\alpha_{\text{ал}} = \sin 90° = 1$, so that $\alpha_{\text{м}} = \arcsin(2440/3130) = 51.2°$.

In terms of the Snellius law, such a wave must generate transverse waves in copper propagating at angle $\alpha_{\text{м}}$ (cf. Fig. 1b). The generation of Stoneley waves as well as their echoes can be detected with a single PET installed at the surface of Cu plate.

Experimental verification of the idea was carried out the geometry depicted in Fig. 2.

Two PETs were placed onto the copper surface and gradually slid apart up to a separation of 0.5 m. A strong signal was observed throughout, with no response to a finger touch. Prism receivers (30, 40, and 50°) showed the absence of transversal waves in the Al bulk. The echo from the plate butt end could be distinguished from noise only at separations of up to 150 mm.

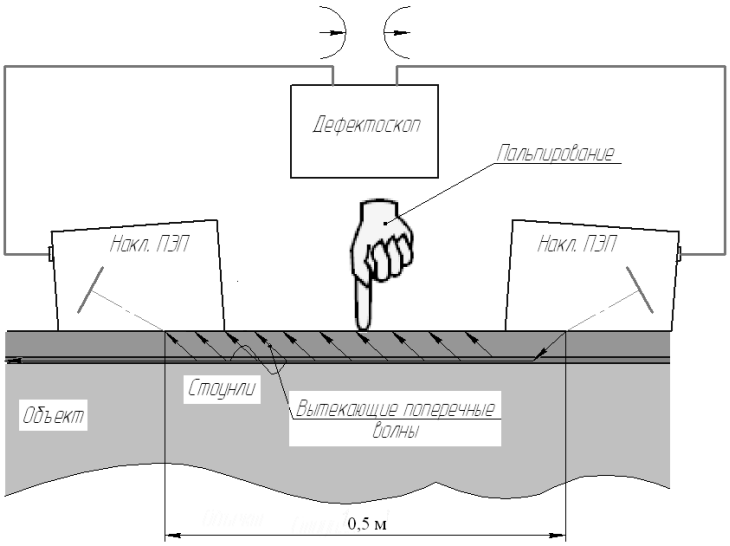

Fig. 2. Schematic of the experimental setup.

Our results suggest that better results and better prospects for practical implementation can expectedly be obtained in case of lower ultrasound frequencies (<1.25 MHz).

INFLAMMATION OF PYROPHORIC POWDERS: THEORETICAL ANALYSIS

B. S. Seplyarskii, T. P. Ivleva, and M. I. Alymov

Institute of Structural Macrokinetics and Materials Science, Russian Academy of Sciences, Chernogolovka, Moscow, 142432 Russia

e-mail: sepl@ism.ac.ru

Although the inflammation of pyrophoric metal powders in air represents a serious safety problem [1], no theoretical model of the phenomenon has been suggested so far. In this work, we fill this gap and suggest a model based on our preliminary results [2].

A bulk-density layer of powder mixture of nanosized reactant is in contact with ambient atmosphere at initial temperature T_0. The reaction with oxidizer is infiltration-controlled and yields porous condensed products. The temperatures of gas and porous matter are assumed to be the same and heat sink into environment id neglected. Upon reaching some certain extent of conversion η_{1c}, a diffusion barrier is formed on the surface of reactant particles.

In terms of classical combustion theory, the governing equations can be written in the form:

$$\frac{\partial\theta}{\partial\tau}=\frac{\partial^2\theta}{\partial\xi^2}+f(\tau,\xi),\qquad \frac{\partial\eta}{\partial\tau}=\mathrm{Le}\frac{\partial^2\eta}{\partial\xi^2}+\gamma\, f(\tau,\xi),$$

$$\frac{\partial\eta_1}{\partial\tau}=\nu\gamma f(\tau,\xi),\qquad f(\tau,\xi)=\begin{cases}(1-\eta)\exp\dfrac{\theta}{1+\beta\theta} & \text{for}\quad \eta<1\quad\text{or}\quad \eta_1<\eta_{1k}\\ 0 & \text{for}\quad \eta=1\quad\text{or}\quad \eta_1=\eta_{1k}\end{cases},$$

Initial and boundary conditions:

$$\tau=0:\quad \theta=0,\quad \eta=\eta_n,\quad \eta_1=0$$

$$\tau>0:\quad \xi=0:\quad \frac{\partial\theta}{\partial\xi}=0,\quad \eta=0,$$

$$\xi=L_\xi:\quad \frac{\partial\theta}{\partial\xi}=\frac{\partial\eta}{\partial\xi}=0.$$

$$a_c = \frac{\lambda_c}{c_c\,\rho_c}, \quad t_* = \frac{c_c RT_0^2}{EQ}\frac{\rho_c}{\rho_g a_0^n k_0}\exp\left(\frac{E}{RT_0}\right), \theta = \frac{E}{RT_0^2}(T - T_0), \quad \tau = \frac{t}{t_*}, \xi = \frac{x}{x_*}, \beta = \frac{RT_0}{E}, \quad x_* = \sqrt{\frac{\lambda\, t_*}{c_c\,\rho_c}}$$

$$\gamma = \frac{c_c RT_0^2}{EQ}\frac{\rho_c}{\rho_g a_0}, \eta = \frac{a_0 - a}{a_0}, \quad \eta_1 = \frac{\rho_{c0} - \rho_c}{\rho_{c0}}, Bi = \frac{\alpha\, x_*}{\lambda}, \quad , \mathrm{Le} = \frac{D_{\mathrm{ef}}}{a_c},$$

Here the nomenclature is typical and can be found elsewhere [3].

Our aim was to check the validity of conclusion [2] that the induction time for ignition τ_{ign} is defined by the γ/Le ratio, i.e. is inversely proportional to penetration depth $L_{ch} \approx \sqrt{\mathrm{Le}/\gamma}$. As is seen in Fig. 1a, τ_{ign} is defined by the γ/Le ratio rather than by by each individual parameter. The smaller L_{ch}, the longer τ_{ign}. At γ/Le = const, θ_{max} decreases with an increase in Le (see Fig. 1b), despite better conditions for infiltration of gas reactant.

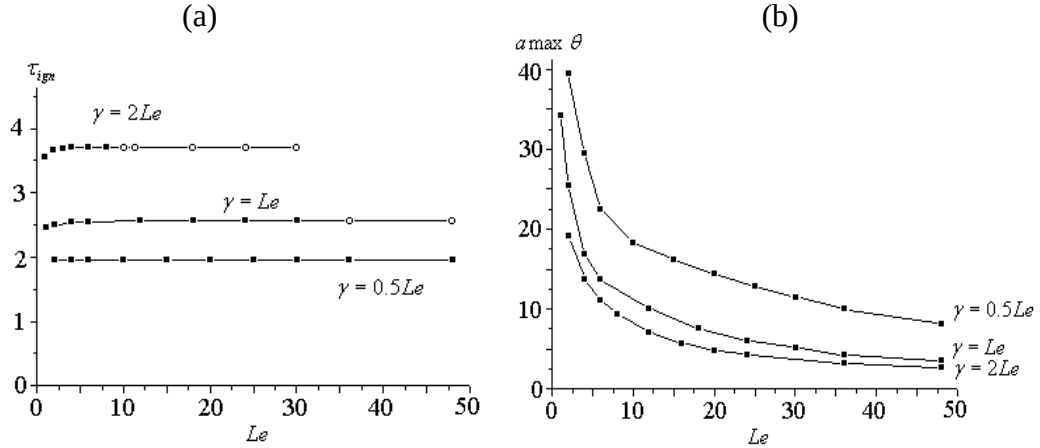

Fig. 1. Induction period τ_{ign} (a) and temperature θ_{max} (b) as a function of Lewis number Le for different γ/Le ratios.

Numerical calculations have shown that τ_{ign} is independent on η_{1c}, while θ_{max} was found to decrease with decreasing η_{1c}. Therefore, we recommend that the passivation conditions for nanopowders would provide a decrease in η_{1c} and in dimensionless thermal effect of reaction $1/\gamma$.

This work was financially supported by the Russian Science Foundation (project no. 16-13-00013).

1. Zllobinskii B.M., Ioffe V.G., Zlobinski V.B., *Inflammability of Metals and Alloys*, Moscow: Metallurgiya, 1972 (in Russian).
2. Alymov M.I., Seplyarskii B.S., Gordopolova I.S., Ignition of pyrophoric powders: An entry-level model, *J. Phys. Conf. Series (JPCS)*: XXX Int. Conf. on Equations of State for Matter, March 1–6, 2015, Elbrus, Russia.
3. Aldushin A.P., Ivleva, T.P., *Int. J. Self-Proppag. High-Temp. Synth*., 2015, no. 4, pp. 182–186.

SHS JOINING OF Mo WITH NiAl AND TiAl

A. S. Shchukin[1], D. Vrel[2], and A. E. Sytschev[1]

[1]Institute of Structural Macrokinetics and Materials Science, Russian Academy of Sciences, Chernogolovka, Moscow, 142432 Russia
[2]Laboratoire des Sciences des Procédés et des Matériaux–LSPM-CNRS UPR3407 Bâtiment L1, 99 Av. J.B. Clément, Villetaneuse, 93430 France

e-mail: shchukin@ism.ac.ru

The feasibility of SHS joining between Mo substrate and Ni_3Al intermetallic was demonstrated by us previously [1]. In order to improve the strength of joint, in this work we suggest to use preliminary cold working of Mo surface by mechanical alloying (MA) in the presence of Ni + Al or Ti + Al powder mixtures, which could be expected to result in deposition of reactive (activated) layer onto the Mo surface [2].

Typical results are presented in Figs. 1 and 2. It follows that the length of thus deposited layers reaches a value of up to 200 μm. In case of Ni + Al mixtures, Mo partially penetrated into the activated layer in the form of prolonged particulates (see Fig. 2a); but in case of Ti + Al powders, no Mo penetration was detected.

Fig. 1. Mo cylinder before and after MA with Ti + Al mixture.

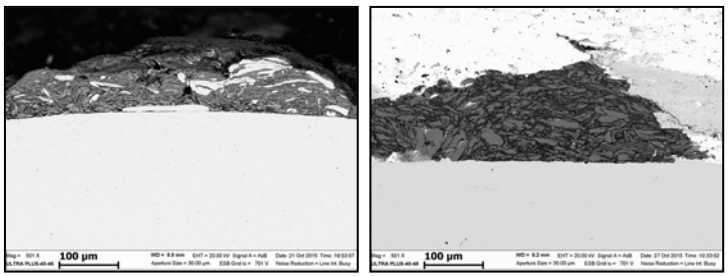

(a) (b)

Fig. 2. Cross section of coatings deposited by MA in the presence of (a) Ni + Al and (b) Ti + Al powder mixtures.

Cold-worked Mo cylinders were then housed and pressed in respective powder mixtures in the form of pellets 20 mm in diameter and 10 mm thick (cf. Fig. 3) and ignited via a Ni–Al booster. Figure 3 demonstrates the occurrence of good joining (SHS welding) between Mo and surrounding intermetallic material.

In the Mo–[Ni + Al] sample (Fig. 3a), the adjacent intermetallic layer consists of NiAl and Ni_3Al grains with oxide interlayers in between, which is typical of MA in air.

Mo globules in the coating have a size of 100–200 nm similar to what had been found for W [3]. Delamination of the Mo surface during MA also favors the formation of strong weld seam.

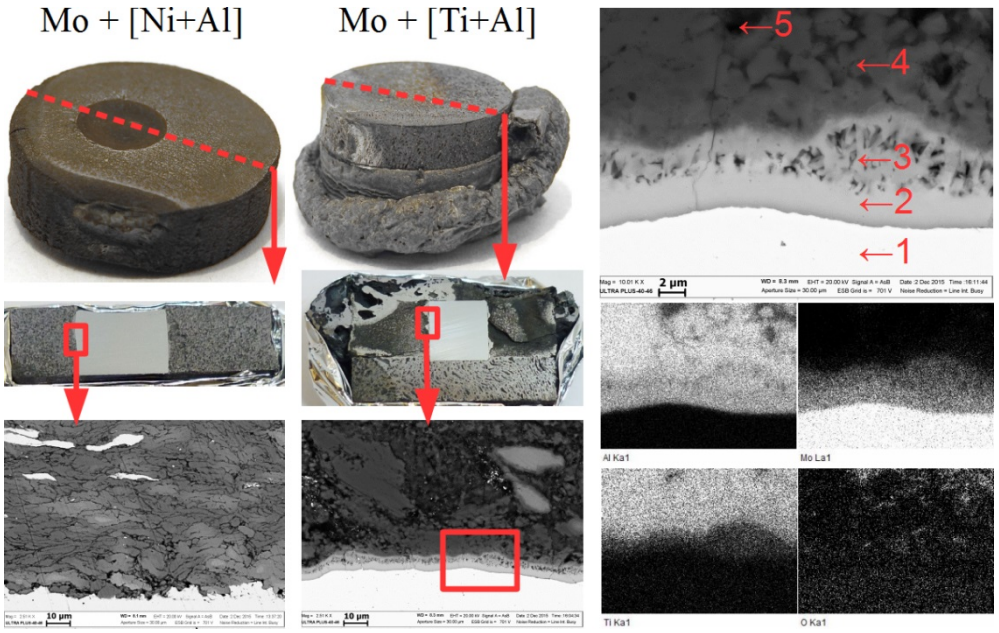

(a) (b) (c)

Zone	O	Al	Ti	Mo
1	-	0.9	-	99.1
2	-	39.8	-	60.2
3	1.4	45.2	9.5	43.9
4	2.5	59.3	35.4	2.9
5	16.8	46.4	32.9	4.0

Fig. 3. (a) Mo–[Ni + Al] and (b) Mo–[Ti+Al] samples after combustion in an SHS mode; EDX results (in wt %); and (c): elemental maps.

In Mo–[Ti + Al] samples (Fig. 3b), a 200-μm coating comprises $TiAl_3$ intermetallic with inclusions of unreacted Ti and TiAl intermetallic at a separation of above 200 μm from the coating. The EDS data suggest that composition of the transition layer (2–10 μm thick) is close to Al_8Mo_3 compound with a narrow homogeneity range. The transition layer between Mo and $TiAl_3$ coating can be expected to act as a strengthening agent and diffusion barrier.

1. A.E. Sytschev, S.G. Vadchenko, O.K. Kamynina, N.V. Sachkova, Simultaneous synthesis and joining of a Ni–Al-Based Layer to Mo foil by SHS, *Int. J. Self-Propag. High-Temp. Synth.*, 2009, vol. 18, no. 3, pp. 213–216.

2. S. Romankov, W. Sha, S.D. Kaloshkin, K. Kaevitser. Fabrication of Ti–Al coatings by mechanical alloying method, *Surf. Coat. Technol*., 2006, vol. 201, no. 6, pp. 3235–3245.
3. A.E. Sytschev, D. Vrel, Yu.R. Kolobov, D.Yu. Kovalev, E.V. Golosov, A.S. Shchukin, S.G. Vadchenko, Combustion synthesis in the Ni–Al–W system: Some structural features, *Int. J. Self-Propag. High-Temp. Synth*., 2013, vol. 22, no. 2, pp. 110–113.

WEAR/CORROSION RESISTANT INTERMETALLIC Fe–Al COATINGS: PREPARATION AND CHARACTERIZATION

S. V. Skiba, Ch. G. Pak, A. V. Pryshchak

Penza State University, ul. Krasnaya 40, 440026 Penza, Russia

e-mail: skibaserg89@mail.ru

An effective way to protection of metallurgical aggregates is the deposition of intermetallic Fe–Al coatings that are known for their heat and corrosion resistance. Such alloys can be fabricated by the methods of conventional [1] and powder metallurgy [2, 3], mechanoactivated SHS [4], and gas-dynamic sputtering (GDS). The powders are either subjected to compaction or used in deposition of coatings [5, 6].

In this communication, we report on fabrication of Fe–Al coatings by combined use of GDS and SHS methods and characterization of their phase composition, structure, and mechanical properties.

At the first stage, the powder particles accelerated by a supersonic gas jet with a temperature of 350–500°C (i.e. below their melting point) were deposited onto a substrate As a result, there was no gas evolution (no pores) and no oxidation, and the particles got immobilized on the surface. Deposition was performed in two way: (a) in a layer-by-layer mode by alternating the supply of Al an Fe particles and (b) by using the Al–Fe mixtures activated in a ball mill for 2, 4, and 6 h.

At the second stage, the deposited Al–Fe layers were ignited and allowed to burn in a mode of frontal SHS reaction. According to XRD data, thus prepared intermetallic coatings comprise largely of Fe_3Al and FeAl.

1. M. Jablonska, A. Jasik, and A. Hanc, Structures and phase transitions of the alloys on the basis of Fe–Al intermetallics, *Arch. Mater. Sci. Eng*., 2008, vol. 29, no. 1, pp. 16–19.
2. X. Amils et al., Structural, mechanical, and magnetic properties of nanostructured FeAl alloys during disordering and thermal recovery, *Nanostruct. Mater*., 1999, vol. 11, no. 6, pp. 689–695.
3. X. Amils et al., Hardening and softening of FeAl during milling and annealing, *Intermetallics*, 2000, no. 8, pp. 805–813.
4. T.L. Talako et al., Mechanoactivated SHS of FeAl-based nanocomposite powders, *Int. J. Self-Propag. High-Temp. Synth*., 2009, vol. 18, no. 2, pp. 125–132.

5. T.C. Totemeier, R.N. Wright, W.D. Swank, Residual stresses in high-velocity oxy-fuel metallic coatings, *Metall. Mater. Trans. A*, 2004, vol. 35, pp. 1807–1814.
6. F.G. Lovshenko, G.F. Lovshenko, A.S. Fedosenko, Patterning, structure, and mechanical properties of mechanically alloyed Fe–Al powders and coatings made thereof, *Vestn. Belarus.-Russ. Univ*., 2012, no. 1 (34), pp. 36–50.

MICROSTRUCTURE, CORROSION RESISTANCE, AND MECHANICAL ENDURANCE OF CLAD MATERIALS USED IN GEOTHERMAL PLANTS

H. Słomińska[1], M. Gloc[1], J. Kamiński[1], Ł. Ciupiński[1], G. Kwiatkowski[2]

[1] Warsaw University of Technology, University Research Centre Functional Materials, Warsaw, Poland
[2] ZTW EXPLOMET Co. A. Gałka, Z. Szulc, Opole, Poland

e-mail: ha.slominska@gmail.com

Plate materials are innovative and find wide application such as in geothermal power engineering. Investigated materials had the same base, P355NH carbon steel. The clads were Inconel C-276, austenitic-ferritic stainless steel SAF 2507, and high-alloy austenitic stainless steel 254 SMO.

The aim of this work was microstructural observation of bonded materials and estimation of highest bonding parameters. Samples were cut, grinded, and polished. The microstructures were relevant by etching of the base and plate material. The ion etching was applied to reveal the joint microstructures. The studies were conducted by using optical (KEYENCE) and scanning electron microscopy (Hitachi SU-70). It was demonstrated that microstructures adjacent to the joint were deformed and refined. Melted zones and the post heat treatment decarbonized areas were exposed. The microstructures after chemical etching and ion etching are given in Figs. 1 and 2.

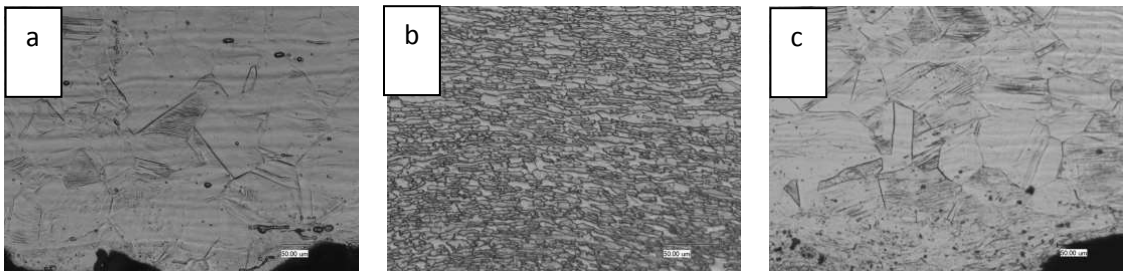

Fig. 1. Microstructures after chemical etching: (a) C-276, (b) SAF2507, and (c) 254SMO.

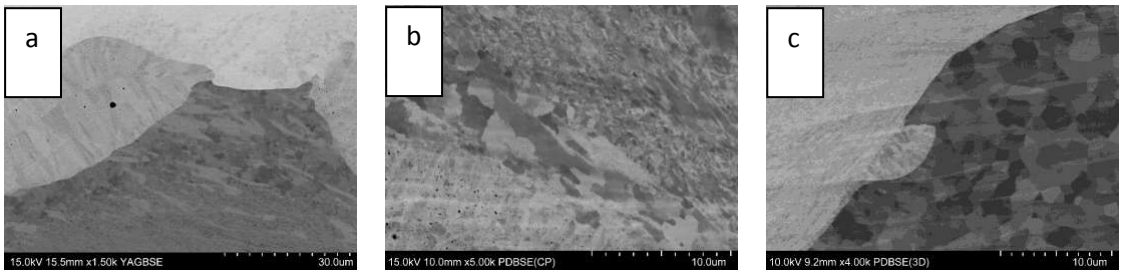

Fig.2. Microstructures of joints after ion etching: (a) C-276, (b) SAF2507, and (c) 254SMO.

Further investigations were oriented toward corrosion resistance. Samples were installed in a specific cell where the clad material was exposed to 0.5 M NaCl solution for 1 h. Corrosion effects were monitored with an AUTOLAB device. The impedance and polarization currents were measured. Results were presented as the potential–current density plots. To find out which plate demonstrated better corrosion resistance, the Tafel lines values of current density and corrosion potential were determined. The smaller values obtained, the better corrosion resistance to environment.

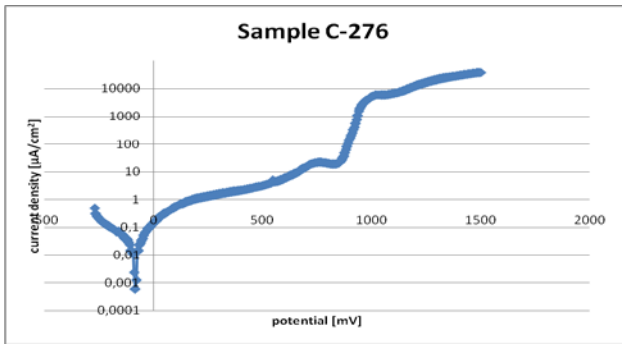

I_{cor} = 0,0125 µA
E_{cor} = –94 mV

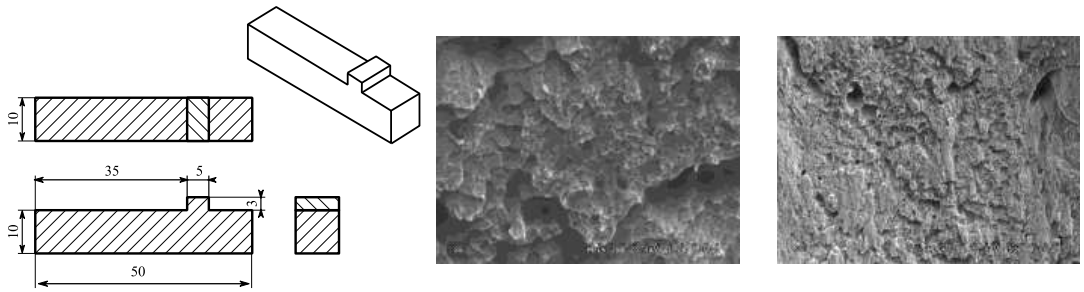

The mechanical properties of joints were also measured. Samples were cut in a special way and placed in a home-made shear test machine. Shear stresses were evaluated and tabulated. Ruptured surfaces were explored by SEM.

1. M. Gloc, M. Wachowski, W. Zielinski, T. Plocinski, K.J. Kurzydlowski, Microstructural and microanalysis investigations of bond titanium grade1/low alloy steel St52-3N obtained by explosive welding, *J. Alloys Comp*., 2016, vol. 671.
2. A.T. Krawczynska, M. Gloc, K. Lublinska, Intergranular corrosion resistance of nanostructured austenitic stainless steel, *J. Mater. Sci*., 2013, vol. 48, no. 13, pp. 4517–4523.
3. H. Modin, S. Modin, *Metallurgical Microscopy*, London: Butterworths, 1973.
4. J. Baszkiewicz, M. Kamiński, *Korozja*, Warszawa: Oficyna Wydawnicza Politechniki Warszawskiej, 2006.

COMBUSTION SYNTHESIS OF Eu-DOPED Ca-α-SiAlON PHOSPHORS

K. L. Smirnov

Institute of Structural Macrokinetics and Materials Science, Russian Academy of Sciences, Chernogolovka, Moscow region, 142432, Russia

e-mail: kosm@ism.ac.ru

α-SiAlONs are solid solutions based on silicon nitride that appear due to incorporation of metal ions $Me^{\nu+}$ accompanied by partial replacement of Si–N by Al–O (*n*) and Al–N (*m*) links for charge compensation in the elementary cell. Accordingly, their composition is described by the elemental formula $Me_{m/\nu}Si_{12-(m+n)}Al_{m+n}O_nN_{16-n}$, where ν is the valence of embedded metal ion. Originally α-SiAlONs have been designed as structural materials operating in severe conditions. Recently, much attention was given to Eu-doped α-SiAlONs because of their encouraging luminescent properties (excitability by blue light, high conversion efficiency, low thermal quenching, high chemical stability), and high potential for color correction of white LEDs [1]. To date, Eu-doped α-SiAlON phosphors are produced by solid-state reaction at high temperature and high pressure [2], carbothermal reduction and nitridation [3], and gas reduction and nitridation [4]. These methods, however, suffer various drawbacks such as critical synthesis conditions, impurity contamination, and poor crystallization. Consequently, developing new efficient methods for synthesis α-SiAlON phosphors is a hot subject of research.

In this work, $Ca_xEu_ySi_{12-(m+n)}Al_{m+n}O_nN_{16-n}$, where $x + y = m/2$, were selected for investigation. Combustion synthesis (CS) was realized through the exothermic chemical reaction of powdered mixtures that contain Si, Al, CaO, and Eu_2O_3 with high pressure N_2 gas. Experimentally established were green compositions ensuring maximal extent of conversion, influence of elemental composition on phase composition, crystal structure, and microstructure of synthesized Ca-α-SiAlONs. The excitation and emission spectra of synthesized α-$(Ca,Eu)_{m/2}(Si,Al)_{12}(O,N)_{16}$ compounds are presented in Figs. 1 and 2. The excitation spectra exhibit broad maxima peaked around 300 and 400 nm. The emission spectra are broad and position of their peak depends on both *m*/2 and *y*. An increase in *m*/2 decreases the rigidity of SiAlON lattice, while an increase in Eu^{2+} content *y* decreases a separation between the Eu^{2+} cations. Both factors promote non-radiative deactivation due to intensification of electron-vibrational transitions and energy transfer between the Eu^{2+} ions. This must lead to the Stokes shift and a decrease in the intensity of emission bands. Positions of the band maximum as a function of *m*/2 and *y* are presented in Figs. 3a, 4a).

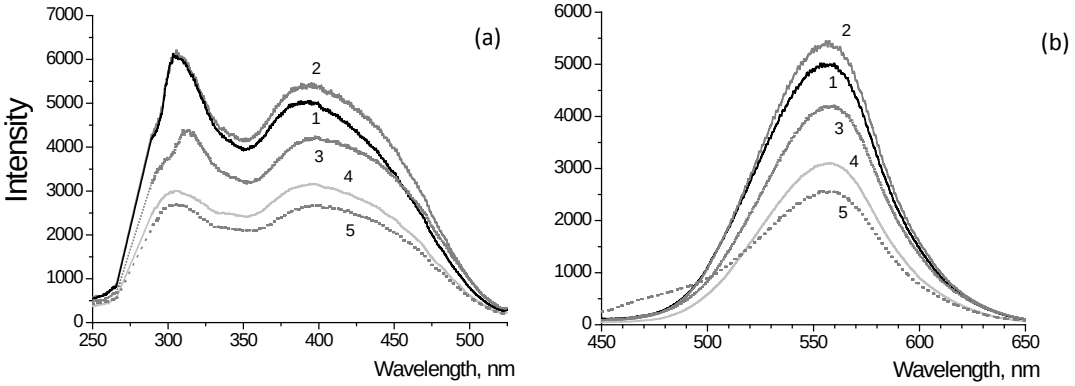

Fig. 1. Excitation (a) and emission (b) spectra of α-$(Ca,Eu)_{m/2}(Si,Al)_{12}(O,N)_{16}$ with $m/2$ = 0.4 (1), 0.6 (*2*), 0.8 (*3*), 1.0 (*4*), and 1.2 (*5*); Ca/Eu ≈ 9 : 1.

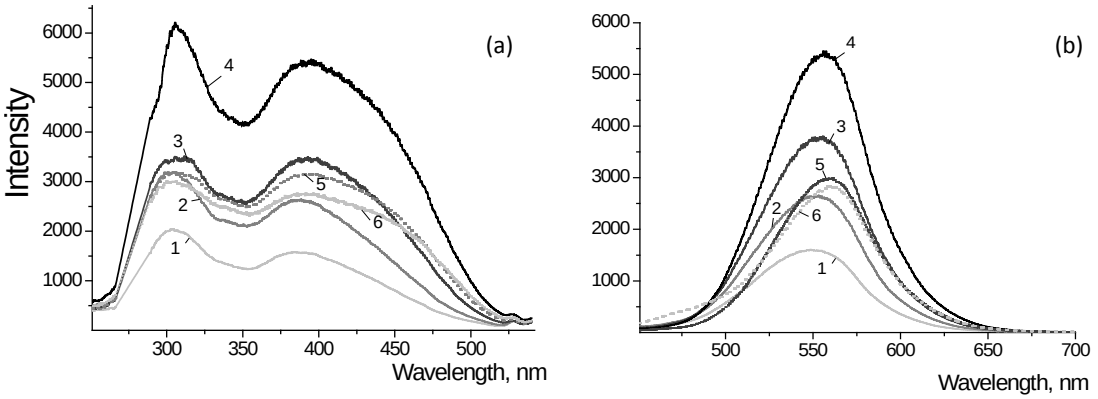

Fig. 2. Excitation (a) and emission (b) spectra α-$Ca_xEu_y(Si,Al)_{12}(O,N)_{16}$ with y = 0.006 (*1*), 0.012 (*2*), 0.03 (*3*), 0.06 (*4*), 0.12 (*5*), and 0.18 (*6*); $x + y = 0.6$.

For Ca-α-SiAlON:Eu with constant x/y ratio the fluorescence intensity grows due to an increase in the amount of luminescing Ca-α-SiAlON:Eu within the range of partially stabilized α-SiAlON ($0 < m/2 < 0.55$) and then gradually comes down within the range of fully stabilized α-SiAlON ($0.55 < m/2 < 1.2$) (Fig. 3b). For Ca-α-SiAlON:Eu within the range of fully stabilized α-SiAlON with $m/2 = 0.6$, the emission intensity increases proportionally to y within the range $0 < y < 0.06$ (Fig. 3b). At higher concentrations of Eu^{2+} ($y > 0.06$), the effect of concentration quenching becomes more pronounced (Fig. 4b).

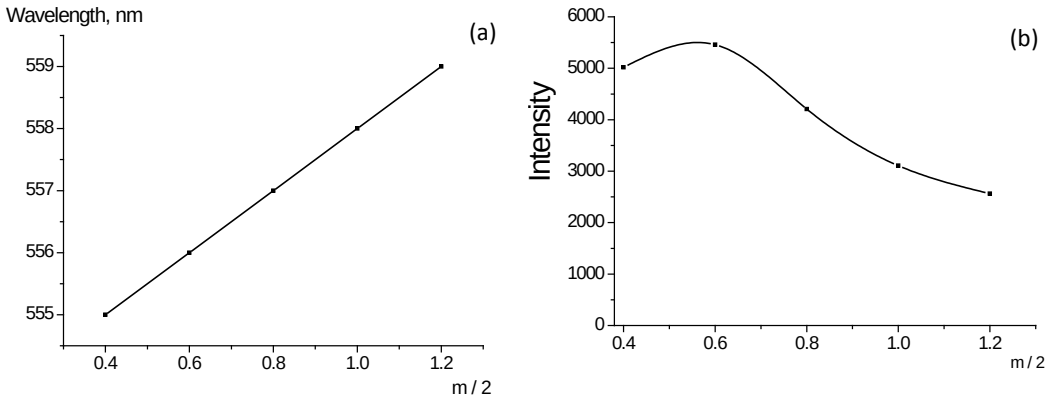

Fig. 3. Position of band maximum (a) and band intensity (b) in the fluorescence spectra of α-$(Ca,Eu)_{m/2}(Si,Al)_{12}(O,N)_{16}$ as a function of $m/2$; Ca/Eu ≈ 9 : 1.

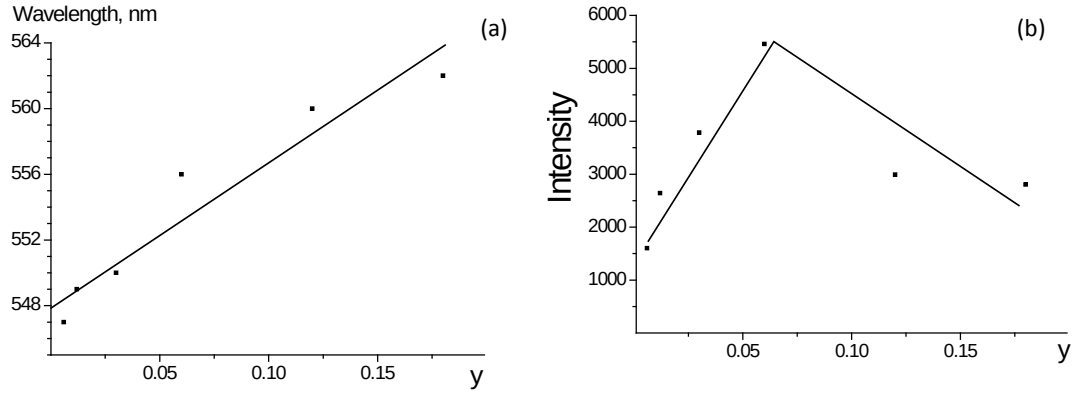

Fig. 4. Position of band maximum (a) and band intensity (b) in the fluorescence spectra of α-$Ca_xEu_y(Si,Al)_{12}(O,N)_{16}$ as a function of y ($x + y = 0.6$).

1. Xie, R.-J., Hirosaki, N., Silicon-based oxynitride and nitride phosphors for white LEDs: A review, *Sci. Technol. Adv. Mater.*, 2007, vol. 8, nos. 7–8, pp. 588–600.
2. Xie, R.-J., Hirosaki, N., Sakuma, K., Yamamoto, Y., Mitomo, M., Eu^{2+}-doped Ca-α-SiAlON: A yellow phosphor for white light-emitting diodes, *Appl. Phys. Lett.*, 2004, vol. 84, pp. 5404–5406.
3. Zhang, H.C., Horikawa, T., Hanzawa, H., Hamaguchi, A., Machida, K., Photoluminescence properties of α-SiAlON:Eu^{2+} prepared by carbothermal reduction and nitridation method, *J. Electrochem. Soc.*, 2007, vol. 154, no. 2, pp. J59–J61.
4. Suehiro, T., Hirosaki, N., Xie, R.-J., Mitomo, M., Powder synthesis of Ca-α-SiAlON as a host material for phosphors, *Chem. Mater.*, 2005, vol. 17, no. 2, pp. 308–314.

COMBUSTION SYNTHESIS AND PROPERTIES OF SiAlON–BN COMPOSITES

K. L. Smirnov

Institute of Structural Macrokinetics and Materials Science, Russian Academy of Sciences, Chernogolovka, Moscow, 142432 Russia

e-mail: kosm@ism.ac.ru

Solid solutions of β-Si_3N_4 of general formula $Si_{6-z}Al_zO_zN_{8-z}$ (z = 0.0–4.2) are known for their excellent hardness, strength, and wear/corrosion resistance, which explains their wide use in various engineering applications [1]. Hexagonal BN exhibits good dielectric properties combined with high thermal conductivity and corrosion resistance at exceeding law wettability with melts [2]. Addition of BN to ceramic composites greatly improves their thermal shock resistance, machinability, and decreases friction [3–6]. SiAlON–BN composites are highly promising for metallurgical applications: nozzles and pipes for metal pouring, annular breakers, crucibles, thermocouple casing, etc. In this context, it seemed interesting to apply combustion synthesis to its fabrication in a cost-effective one-stage process.

The synthesis of β-$Si_{6-z}Al_zO_zN_{8-z}$–BN composites was based on infiltration combustion (FC) of Si–Al–B powder compacts in nitrogen gas. Green mixtures also contained some amount of diluents, β-$Si_{6-z}Al_zO_zN_{8-z}$ and BN, in order to suppress the dissociation of product and coagulation of Si and Al into inactive agglomerates. Compacts with relative density d_{rel} = 0.62–0.64 were prepared by CIP at 50 MPa. Combustion was performed at $P(N_2)$ up to 150 MPa. Because of high green density, the samples could only be ignited for $P(N_2)$ > 30 MPa (see Fig. 1). With increasing $P(N_2)$, burning velocity U and combustion temperature T are seen to gradually attain the values of 0.9–1.6 mm/s and 2400–2600 K, respectively.

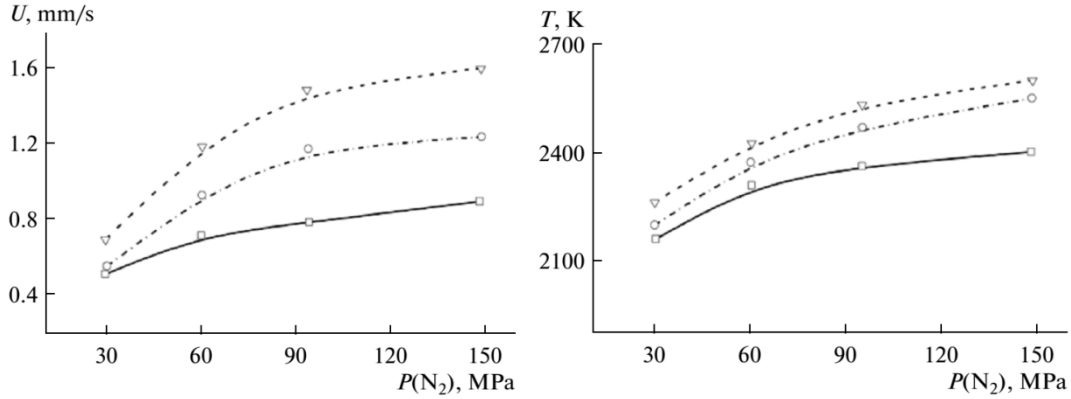

Fig. 1. Burning velocity U and combustion temperature T as a function of $P(N_2)$ in synthesis of β-$Si_{6-z}Al_zO_zN_{8-z}$: z = 0.5 (∇), 1.7 (○), and 3.3 (□).

An increase in $P(N_2)$ is accompanied by change in a mode of FC. At $P(N_2)$ = 30 MPa, key governing factors are low amount of N_2 in pores and insufficient gas permeability. In these conditions FC proceeds in a mode of unsteady or surface combustion and yields strongly non-uniform and cracked products. For $P(N_2)$ around 100 MPa, FC becomes frontal and hence most suitable for synthesis of uniform target material.

Structure of β-$Si_{6-z}Al_zO_zN_{8-z}$-BN ceramics is strongly affected by presence of oxide and metal melts within the combustion wave. For BN contents < 5 wt % synthesized composites had non-uniform structure that cannot be eliminated upon variation in green composition. For BN > 15 wt %, volume changes were minimal. Better results are attained for BN = 5–15 wt %, this opens up a way to fabrication of zero defected ceramics with elevated density due to the effect of volume shrinkage. Volume shrinkage was found to grow proportionally to [Al, Si, B] and SiO_2 content of green mixture. Volume shrinkage also depends on sample diameter D. Its value diminished at some critical values: $D_{min} \approx 30$ mm and $D_{max} \approx 70$ mm. Both can be associated with heat losses. The existence of D_{max} can be explained by difficulties in ensuring heat insulation of large samples from cold walls of SHS reactor. The existence of D_{min} is conditioned by an increase in the fraction of heat release dissipated into environment.

The flexural strength of synthesized composites was found to obey the well-known expression $\sigma = \sigma_0 \exp(-bP)$ where P is porosity, $b = 4$, and $\sigma_0 = 240$ MPa. Figure 2 gives σ_f as a function of temperature drop ΔT in thermal shock tests of composites containing different amounts of BN. For BN < 15 wt %, parameters ΔT are close to those typical of sintered sialons and reaction-bonded Si_3N_4 and slightly below that of hot-pressed Si_3N_4. For BN ≥ 20 wt %, accurate ΔT measurements could not be performed exactly.

Nevertheless, its residual strength even at $\Delta T > 800°C$ was higher than that of ceramics with lower BN content by a factor of 1.5.

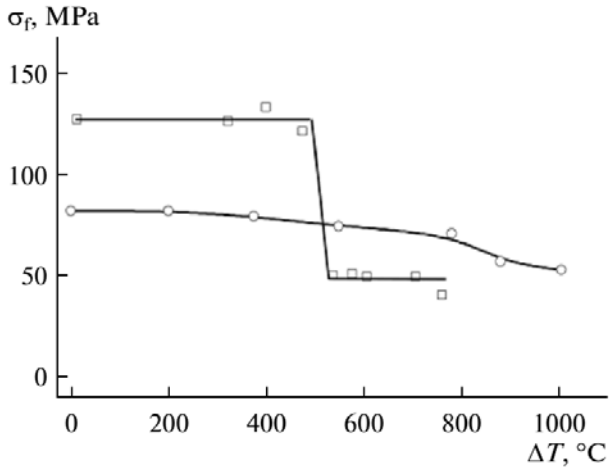

Fig. 2. Flexural strength as a function of temperature drop ΔT in thermal shock tests of β-$Si_{4.3}Al_{1.7}O_{1.7}N_{6.3}$–BN ceramics containing (□) 10 wt % and (○) 23 wt % BN.

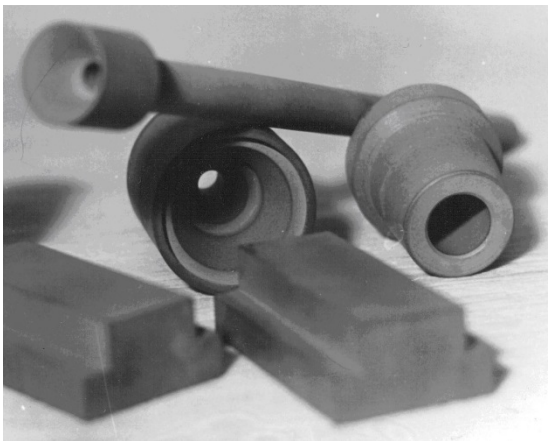

Fig. 3. Items made of β-$Si_{4.3}Al_{1.7}O_{1.7}N_{6.3}$–BN composites: nozzles for casting metal and lining plates.

Optimal combination of tribological parameters was exhibited by the composites containing 10 wt % BN. The friction coefficient of synthesized composites was found to vary within the range 0.3–0.7, the lowest values corresponding to composites with BN ≥ 20 wt %. But high BN contents negatively affect the wear resistance. Synthesized composites are also readily machinable with WC-based cutting instruments; some of thus produced items are shown in Fig. 3.

This work was financially supported by the Russian Foundation for Basic Research (project no. 15-03-01051_a).

1. Ekström, T. and Nygren, M., SiAlON ceramics, *J. Am. Ceram. Soc.*, 1992, vol. 75, no. 2, pp. 259–276.
2. Haubner, R., Wilhelm, M., Weissenbacher, R., and Lux, B., Boron nitrides: Properties, synthesis and applications, *Struct. Bonding*, 2002, vol. 102, no. 1, pp. 1–45.
3. Shuba, R., and Chen, I.-W. Machinable α-SiAlON/BN composites, *J. Am. Ceram. Soc.*, 2006, vol. 89, no. 7, pp. 2147–2153.
4. Wei, D., Meng, Q., and Jia, D., Mechanical and tribological properties of hot-pressed h-BN/Si_3N_4 ceramic composites, *Ceram. Int.*, 2006, vol. 32, no. 5, pp. 549–554.
5. Gao, L., Jin, X., Li, J., Li, Y., and Sun, J., BN/Si_3N_4 nanocomposite with high strength and good machinability, *Mater. Sci. Eng. A*, 2006, vol. 415, nos. 1–2, pp. 145–148.
6. Sinclair, W. and Simmons, H., Microstructure and thermal shock behavior of BN composites, *J. Mater. Sci. Lett.*, 1987, vol. 6, no. 6, pp. 627–629.

ADDITIONAL GAS FORMATION DURING ROCK BREAKAGE BY BLASTING

V. V. Sobolev and N. V. Bilan

National Mining University, K. Marx Av. 19, Dnipropetrovsk, 49005 Ukraine

e-mail: valeriysobolev@rambler.ru

Composition of explosion products under blasting borehole or blast-hole charges in rock is always different from the composition of the products formed during explosion in air. It was established experimentally by Rossi [1] that under blasting of various explosives in rock a total amount of harmful gases reaches 220% as compared with their amount in the case of explosion in air; as well as under blasting of one type explosives in different rocks it is up to 1000%.

Total amount of noxious gases in crushed rock is almost similar to the figure in case of explosion in air, but at the same blasting charges in loosened coal the amount of noxious gases is doubled. The CO/CO_2 ratio is increased at about the same factor with a growth in hardness coefficient of rocks from $f = 10$ to $f = 18$. According to Cook [2], the NO_2 concentration in the blasted rock mass increases with depth, thus CO_2 concentration rapidly decreases with increasing depth.

Expected conclusion follows from the analysis of experimental results [1–3] that the composition of explosion products is varied both with the chemical composition of explosives, blasting conditions, and the physicochemical properties of rocks, which profound effect is stronger than the effect of the explosives composition on the total amount of toxic gases and new gas molecules in the detonation products.

Practice shows that not only an additional amount of harmful gases generally, but also new gases specifically are formed in the explosion products. According to [1–3], the formation of additional harmful gases in the detonation products of blast-hole or other explosive charges used for rock breakage is a result of secondary chemical reactions. Reactions behavior requires certain physical conditions that would provide the breakage of primary stable molecules in the explosion products. Such conditions can meet the appropriate thermodynamic parameters and/or developing of quantum-mechanical effects.

Our evaluation shows that additional harmful gases are generated in the volume of the charging chamber in the explosion products through which passes the shock wave reflected from the walls of the chamber. Besides the formation of additional amount of harmful gases takes place in the air-borne explosion products. But in both cases, several times increase in the amount of harmful gases remains out of question. Consequently, one of the most likely reasons for increasing the amount of harmful gases can be

considered catalytic reactions of the explosion products with the components of atomically rough surfaces on newly formed cracks.

The purpose of the work is a discussion of most probable mechanisms for formation of additional harmful gases in the detonation products under rock breakage by blasting.

We have considered a system consisting of two atoms (chemical bond) and a single ion. the system under investigation is a statistical model and the part of molecules enters into the field of charge influence during the approach of a molecule and a point charge, or with the surface having electric charges. At room temperature, the electric field intensity at a distance of 10^{-9} m from a monovalent ion is around $1.5 \cdot 10^{7}$ V/cm. If the energy of the molecule is high enough for its approach to some critical distance to the ion, it can happen bond breaking.

Thus, in studies of chemical bond stability between the particles of rock surface and the molecules of explosion products the main reason for initiating the first elementary act such as bond breaking is a point charge, or local group of point charges (e.g., ions). The behavior of the chemical bond in the dynamics was evaluated using the Coulomb center in the physico-mathematical model. Figure 1 shows the change in the bond energy of N_2 molecule as a function of distance from the ion and its charge magnitude.

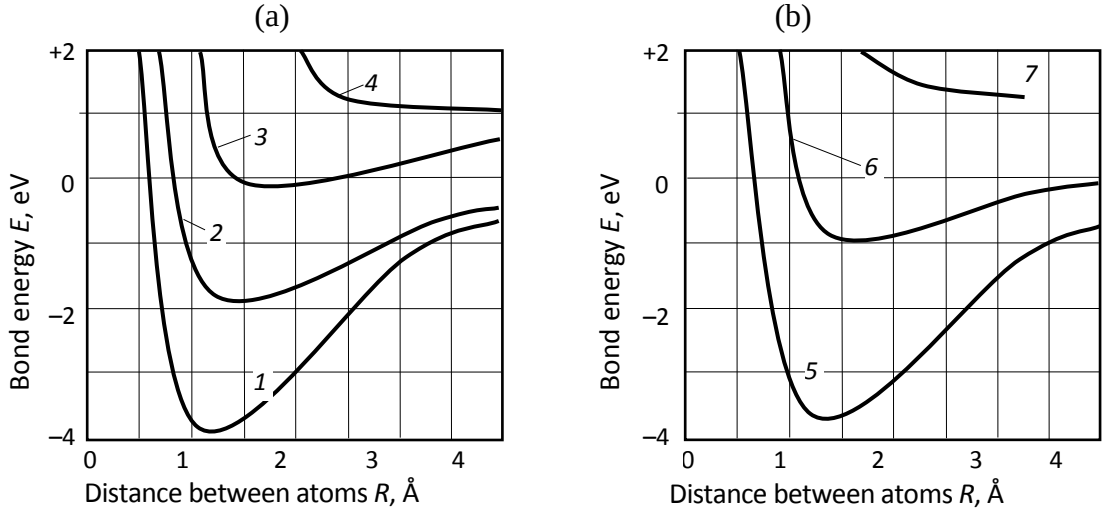

Fig. 1 Changes in the potential energy $E(R)$ of N_2 molecule in the field of negative charge Z: (a) with magnitude Z (distance H from the charge to the chemical bond $2.5 \cdot 10^{-10}$ m); (b) with distance H at $Z = (–4)$; *1*, non-excited molecule; *2*, *3*, *4*, molecule in the field of charge Z (–2), (–4) and (–8), respectively; *5*, *6*, *7*, molecule is from the charge at the distance $H = 10^{-9}$, $5\ 10^{-10}$, and $1.5 \cdot 10^{-10}$ m, respectively.

The problem of bond stability was solved for the system 'ion–N_2 molecule'. The distance from the ion for which bond N_2 is broken, increases with growth in the ion

charge, and according to numerical simulation, with increasing density of the charge distribution on the surface or with the temperature growth under otherwise equal conditions. Comparing the conditions of bond breaking, this regularity holds true for compounds with a lower binding energy. For example, bond breaking of CO_2 molecule occurs at bigger distances from the charge than that of N_2. Figure 1 shows that the distance from the ion at which the N_2 bond breaking increases with increasing the ion charge, which is confirmed by changes in the energy curve $E(Z^{\pm}, R)$ in the presence of an ion. In the field of a charge the function $E(Z^{-}, R)$ is flattened, its minimum is reduced compared with the function $E(R)$.

In our opinion, the mechanism of the formation of additional harmful gases during blasting in coal must take into account the effect of the transition of the organic mass of coal into gas and radicals, especially during the blasting breakage. During coal breakage crack propagation velocity is 360–900 m/s, velocity of the explosion products in the cracks is 300–400 m/s at the gas pressure $(25–50)\cdot10^5$ Pa, which may initiate chemical processes. The components of the penetrating gas stream at these parameters interact actively with electrical charges on solid surfaces, whereby chemical compounds are formed. Besides the amount of gases generated from the organic mass of coal allow us to increase by several times the concentration of coal gases and other mobile components involved in the reactions with explosion products.

The numerical simulation revealed that the fundamental reason for the formation of additional gases is catalytic reactions at the newly formed surfaces. A necessary and sufficient condition for breaking of chemical bonds is the influence of the field of a point charge on the state of chemical bond stability. In general, the activity of chemical reactions on the surfaces of newly formed cracks increases with the temperature growth of the system.

1. B.D. Rossi, *Control of Noxious Gases in Blasting Work and New Methods for Testing Industrial Explosives*, Jerusalem: Israel Program for Scientific Translations, 1971.
2. M.A. Cook, *The Science of Industrial Explosives*, Salt Lake City, Utah: IRECO Chemicals, 1974.
3. L.V. Dubnov, N.S. Bakharevich, A.I. Romanov, *Industrial Explosives*, Moscow, Nauka, 1988 (in Russian).

COMBUSTION SYNTHESIS IN (Ti–Al)/(Ni–Al) BILAYERS

A. E. Sytschev[1], D. Vrel[2], O. D. Boyarchenko[1], N. V. Sachkova[1], and S. G. Vadchenko[1]

[1]Institute of Structural Macrokinetics and Material Science, Russian Academy of Sciences, Chernogolovka, Moscow, 142432 Russia
[2]Laboratoire des Sciences des Procédés et des Matériaux – LSPM-CNRS UPR3407 Bâtiment L1, 99 avenue J.B. Clément, Villetaneuse, 93430 France

e-mail: sytschev@ism.ac.ru

We investigated the peculiarities of wave propagating and combustion synthesis in bilayers of (Ti–Al)/(Ni–Al) powder compacts. The burning velocities were measured for specimens with equimolar compositions of (Ti–Al)/(Ni–Al) which were compacted at the pressure of 2000 Bar up to a relative density of 0.6–0.65. Since the combustion wave could not propagate through the Ti–Al layer, the heat released from the exothermic reaction in the Ni–Al layer was used to preheat and ignite a neighboring Ti–Al layer.

Commercial powders of Ti, Ni, and Al were used as raw materials. Stoichiometric compositions (50 wt % Ti + 50 wt % Al) and (50 wt % Ni+ 50 wt % Al) were mixed in a Turbula 3D mixer and pressed into cylindrical pellets 20 mm in diameter and 5–6 mm thick. Ignition was carried out with a graphite paper as shown in Fig. 1.

Thermal data were recorded by an infrared imaging camera (AVIO TVS 2000ST). This apparatus is equipped with a lens exhibiting a field of view, at the chosen working distance, of 9.5 × 6.25 cm and each pixel of one infrared picture corresponds to an area of 0.79 × 0.79 mm. The infrared thermography gives a two dimensional representation of the thermal evolution and can be coupled to the structural evolutions. The images are artificially color enhanced, ranging from white for the hottest regions on each image, through red, yellow, green and blue, to black for the coolest regions. Nine points (1–9) were selected to analyze the characteristics and velocity of the combustion wave in the bilayer specimens as shown in Fig. 1. The location of the combustion wave front along the direction of propagation at different times was measured and calculated to determine the front velocity.

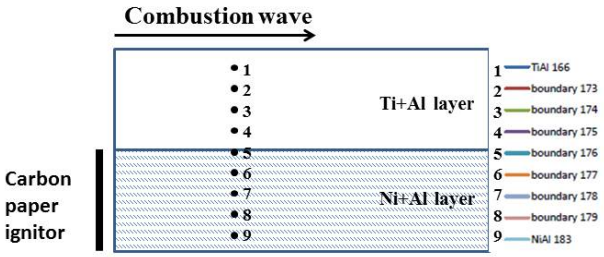

Fig.1. Geometry of combustion.

Figure 2 shows the still frames of combustion. The burning velocity in the Ni–Al layer was about 10 cm/s., which is markedly higher than that in the Ti–Al layer (1 cm/s).

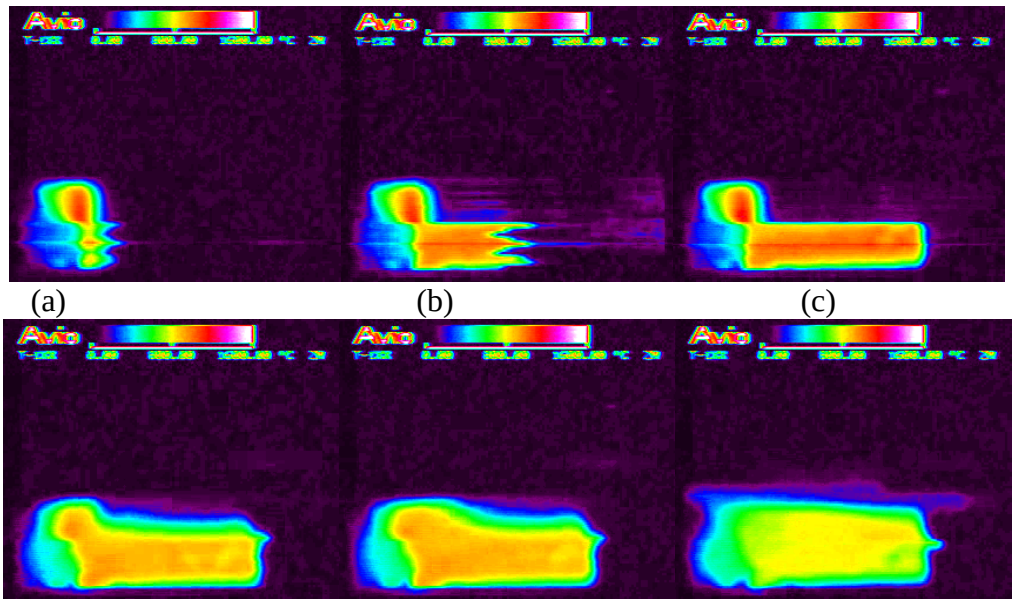

Fig. 2. Still frames of combustion in (Ti–Ni)/(Ni–Al) bilayers.

Preheating accelerated the wave propagation in in the Ti–Al layer, while the ignition created a combustion wave propagating a the direction normal to the layer plane. In other words, there were two combustion waves, overlapping, stepwise pushing forward, and appearing in the form of arc.

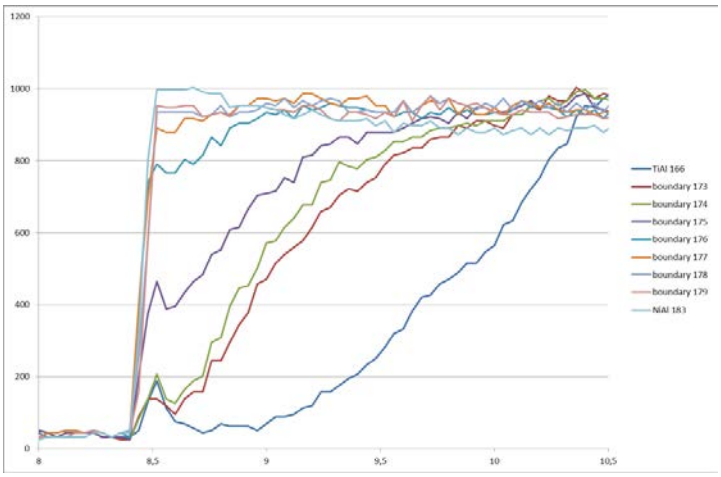

Fig. 3. Temporal profiles of optical emission from combustion front (time in s).

The data of SEM analysis demonstrated the occurrence of SHS joining betwee the layers, with formation of a transition layer about 200 μm thick and a sharp diffusion barrier for Ti in the Ni–Al layer.

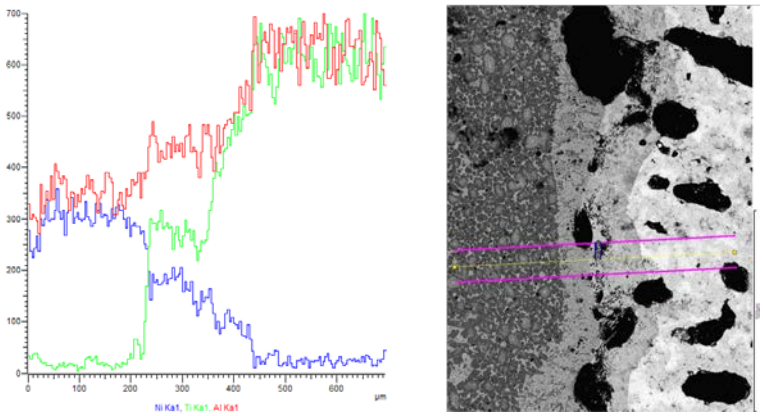

Fig. 4. (a) SEM image of transition layer and (b) concentration profiles of the elements in the vicinity of interface in the (Ti–Ni)/(Ni–Al) sandwich.

Combustion in the Ni–Al layer initially yields $NiAl_3$ in strongly exothermic reaction also resulting in formation of a large amount of Ni melt. This is followed by formation of Ni_2Al_3 and then NiAl intermediates. Melted Ti from the second layer deeply penetrates into the Ni–Al layer, thus giving rise to formation, in the transition layer, of the matrix comprised of a compound close to $TiNi_{0.5}Al_{0.4}$ (33.6 wt % Ni, 12.2 wt % Al) and doped with dendrite grains of Ti_3Al.

DETONATION PARAMETERS OF LOW-DENSITY PETN AND RDX BASED HIGH EXPLOSIVES

K. A. Ten[1], E. R. Pruuel[1], A. O. Kashkarov[1], I. A. Spirin[2], A. L. Mikhailov[2], L. I. Shekhtman[3], V. V. Zhulanov[3], and A. A. Deribas[4]

[1]Lavrent'ev Institute of Hydrodynamics, Siberian Branch, Russian Academy of Sciences, pr. Lavrent'eva 15, Novosibirsk, 63009 Russia
[2] Institute for Explosion Physics, ul. Mira 37, Sarov, 607190 Russia
[3]Budker Institute of Nuclear Physics, Siberian Branch, Russian Academy of Sciences, pr. Lavrent'eva 11, Novosibirsk, 630090 Russia
[4]Institute of Structural Macrokinetics and Materials Science, Russian Academy of Sciences, Chernogolovka, Moscow, 142432 Russia

e-mail ten@hydro.nsc.ru

When used as an X-ray source, synchrotron radiation (SR) has a number of unique features. Major ones are high flux intensity, which allows using very short exposure time ($\tau \leq 1$ ns), high frequency (Δt = 5–250 ns), and small angular divergence. Due to these advantages as compared with a conventional X-ray pulse apparatus, it is possible to register radiation passing through a matter, producing a well-resolved multi-frame pattern of density distribution in shock waves and detonating high explosive.

For comparison, similar experiments were conducted with mixtures of TEN + soda and hexogen + soda, in which the HEs were used in the form of standard fine fraction (not recrystallized). The detonation parameters (the detonation velocity and density distribution) of the mixtures stayed the same, but the critical size of the mixtures increased up to 20 mm.

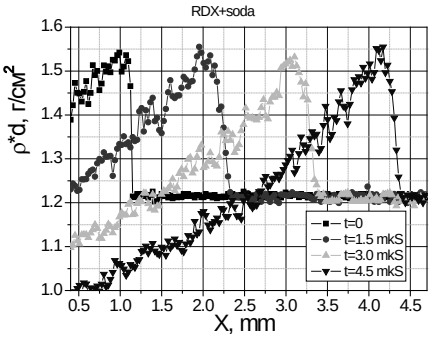

Fig.1. Mass distribution (g/cm^2) in detonation of RDX + soda mixture. The detonation velocity is 2.1 km/s.

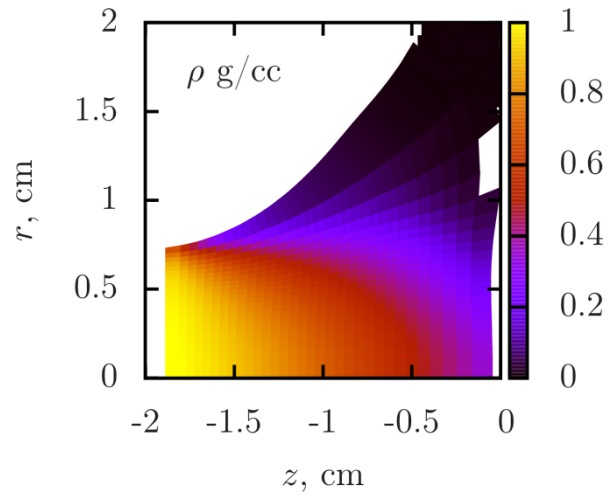

Fig.2. Density distribution in detonation of RDX +soda mixture.

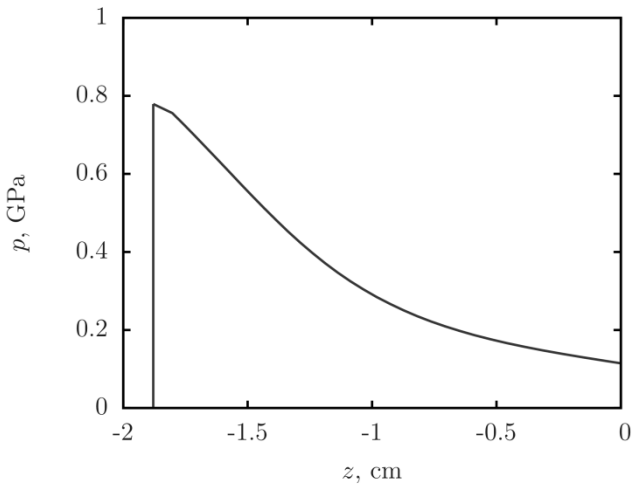

Fig. 3. Pressure profile.

At the experimental station of BINP SB RAS accelerator VEPP-3, experiments with SR application were conducted to study detonating samples of bulk density charges of PETN + soda and RDX + soda mixtures (20 mm in diameter). The mixed high explosives (HE) had a very low initial density (~0.5 g/cm^3) and low detonation velocity (~2 km/s). With a small critical diameter (~3 mm), this composition is very promising if applied to explosive welding [1]. All samples of mixed high explosives were prepared at Sarov and delivered to Novosibirsk. The experiments were carried out in two arrangements: longitudinal measurement of X-ray absorption and transverse measurement of X-ray absorption (with the detector arranged across the direction of

detonation). SR was registered with the home-designed detector DIMEX [2]. The measurement procedure is described elsewhere [3, 4]. The outcomes of the first experiments included density distribution in the front during detonation of the compound. Density values at the Neumann peak (1.1 g/cm^3) at a detonation velocity of 2.1 km/s were also obtained (Fig. 1). The chemical peak width was 2.5–3.0 mm. The transverse measurement of absorption produced volume distributions of pressure and density (Figs. 2, 3), as well as fields of the velocity of projection of the detonation products.

1. L.A. Andreevskikh, Yu. P. Dedenkov, O.B. Drennov, A.L. Mikhailov, N.N. Titova, A.A. Deribas, Explosive mixture for explosive welding of thin foils, *Propell. Explos. Pyrotech*., 2011, vol. 36, no. 1. pp. 48–50.
2. Aulchenko V.M., Bondar A.E., Kudryavtsev V.N., Nikolenko D.M., Papushev P.A., Pruuel E.R., Rachek I.A., Ten K.A., Titov V.M., Tolochko B.P., Zhilich V.N., Zhulanov V.V., Shekhtman L.I., GEM-based detectors for SR imaging and particle tracking**,** *J. Instrum*., 2012, vol. 7, no. 3, pp. 1–18.
3. E.R. Pruuel, K.A. Ten, B.P. Tolochko, L.A. Merzhievskii, L.A. Luk'yanchikov, V.M. Aul'chenko, V.V. Zhulanov, L.I. Shekhtman, V.M. Titov, Implementation of the capability of synchrotron radiation in a study of detonation processes, *Dokl. Phys*., 2013, vo. 58, no. 1, pp. 24–28.
4. V.M. Titov, E.R. Pruuel, K.A. Ten, L.A. Luk'yanchikov, L.A. Merzhievskii, B.P. Tolochko, V.V. Zhulanov, L.I. Shekhtman, Experience of using synchrotron radiation for studying detonation processes, *Combust. Explos. Shock Waves*, 2011, vol. 47, no. 6, pp. 3–15.

SENSITIVITY OF LIQUID ENERGETIC MATERIALS BY SIMPLE TESTING

A. V. Tyutyaev and V. P. Trebunskikh

Samara State Technical University, ul. Molodogvardeiskay 244, 443100 Russia

e-mail: tyutyaev@mail.ru

As is known, none of the methods for determining the sensitivity of liquid high-energy materials (LHE) to impact cannot provide absolute evaluation of their safety. In case of liquid explosives, there are some problems associated with the aggregate state. The probability of explosion by impact is known to depend on both chemical nature of LHE and various external factors. The sensitivity of liquid explosive in the presence of gas bubbles multiply increases as compared to that in the absence of gas bubbles. In this case, a local hot spot is formed as a result of compression and heating of the gas inside the bubbles. The impact sensitivity of liquid explosives is determined by standard methods that use a metal cap filled with LHE. The accuracy and interpretation of the results depend on the fact that a most part of the impact energy is spent on the deformation of the cap. It is also important mechanism of initiation. If there are gas bubbles in the liquid, the initiation occurs at a strike of lower energy. Spots of heating and ignition in this case are the result of the compression and heating of the gas in the bubbles.

A mathematical model of thermal and hydrodynamic processes that occur during compression of gas bubbles in LHE was suggested in [1]. The results of LHE sensitivity determination were obtained by using a standard impact machine. Instead of the metal cap (in the standard method) polyurethane foam was used as cylindrical container with LHE. The choice of foam was made because it has a highly developed porosity, inert, insoluble in most LHE, and easily deformed by mechanical action. Important point is the choice of impact machine and roller device (see Fig. 1).

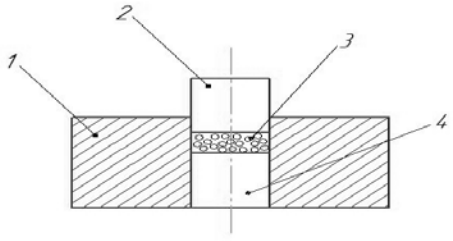

Fig. 1. Roller device: *1* coupling; *2*, *4* upper and lower rollers; *3* polyurethane foam with LHE.

Tests were made with elastic impact (1), polyurethane foam (1-p) and 1-c (with cap) to estimate the total energy loss. Beat with a load of 10kg was performed with heights ranging 100–600 mm. Quantification was performed according to the following:

$$E_{ad} = E_{im} - E_{re},$$

where E_{ad} the loss or deformation of the foam cap and impact machine, E_{im} the impact energy, and E_{re} the rebound energy. E is calculated from the formula

$$E = mgh,$$

where m the load weight and h the height of a reset or rebound. The results are collected in Table 1 and Fig. 2.

A large number of tests with different liquid explosives were made. It was found that the test LHE to impact in appliance 1 with polyurethane foam (device 1-p) to a large extent reflect the real mechanical sensitivity due to the small loss of impact energy on the deformation of the metal cap, as well as the best differentiation LHE sensitivity due to the higher resolution of this method.

For example, the impact energy corresponding to the lower limit for the particular explosions for nitroglycerine has decreased by a factor of 6. Absolute values are decreased by about 2–3 J. This can be attributed to loss of impact energy to deformation of the cap. The method of determining the sensitivity of LHE in device 1-p has a significantly higher resolution than standard. For example, explosion parameters for nitroglycerine when tested with a cap differ from the results of tests in 1-p by a factor of 6.3. Thus, we can conclude that the test LHE to strike in 1-p to a larger extent reflects the real sensitivity to mechanical stress due to the exclusion of loss of impact energy on the deformation of the metal cap, as well as the best differentiation LHE sensitivity due to the higher resolution of the method. In device 1-p, the foam cylinder was used with a diameter of 10 mm and a height of 5 mm.

Table 1. Total energy loss in the impact machine and in roller devices 1, 1-p, 1-c.

Drop height h, mm	Impact energy E_{im}, J	Energy loss		
		1	1-p	1-c
100	9.81	2.45	3.43	8.83
200	19.62	4.42	5.40	12.26
400	39.24	9.81	10.79	19.52
600	58.86	18.64	20.60	27.96

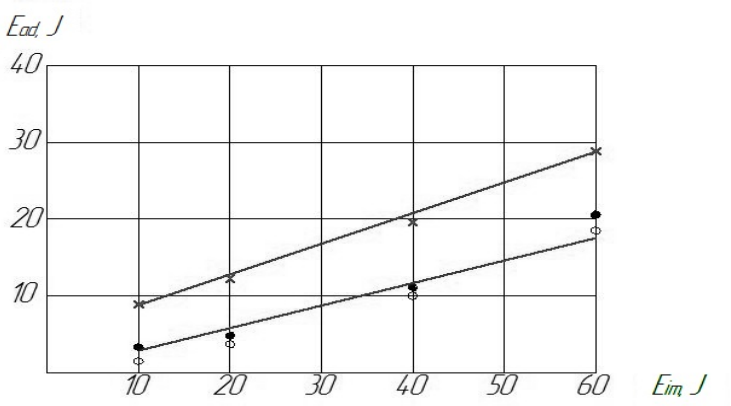

Fig. 2. Absorbed energy E_{ad} vs. impact energy R_{im}: (○) device 1, (●) device 1-p, and (×) device 1-c.

The data in Table 1 and Fig. 2 indicate that at low drop height (100 mm), the energy loss in devices 1 and 1-p are 25 and 35%, respectively, while in device 1-c, 90% of the impact energy. At high drop height, energy loss in device 1-p is almost equal to the elastic impact energy (difference 2.5–3.3%). The deformation of the cap made a value of 25–40% of the impact energy. Thus, we can conclude that the foam contributes 4–8 times less distortion during impact as compared with the cap.

Experimental studies on the absorption capacity of the foam were performed with cylinders with a diameter of 10 mm and a height of 2, 4, 5, 8, and 10 mm. The 2-mm foam cylinder was capable of absorbing about 250 mg of LHE.

Determination of explosion frequency was made by using of 10 kg and 2 kg of LHE. Various liquids with different viscosity were tested. With device 1-p, we get the opportunity to build up complete curves of explosion frequency and to determine the lower explosion limits for most LHE.

1. A. Tyutyaev, A. Dolzhikov, I. Zvereva, Phenomenological models of explosive systems initiation at mechanical influences, *Proc. 17th Seminar on New Trends in Research of Energetic Materials*, Pardubice, Czech Republic, April 9–11, 2014.

IGNITION OF TUNGSTEN–TEFLON MIXTURES

S. G. Vadchenko and M. I. Alymov

Institute of Structural Macrokinetics and Materials Science, Russian Academy of Sciences, Chernogolovka, Moscow, 142432 Russia

e-mail: vadchenko@ism.ac.ru

Green mixtures containing 70% W, 25% Teflon, and 5%Al (by weight) were prepared with an intention that the combustion products would contain WC as the main product. Aluminum was added as an initiator. Combustion was carried out under 1 atm of Ar.

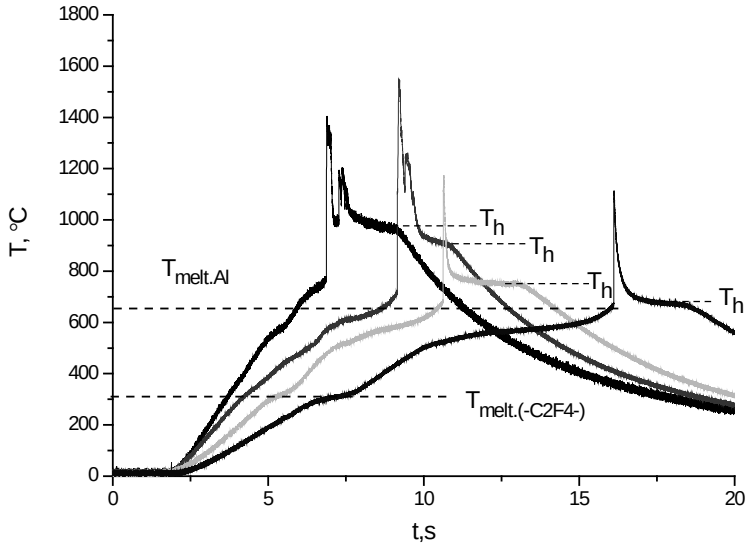

Fig. 1. Thermograms of combustion at different heating temperatures T_h.

Temperature profiles of the processes at different heating temperatures T_h are presented in Fig. 1. The isothermal plateau around 320°C corresponds to Teflon melting while that around 600°C, to its spumescence as a result of decomposition at temperatures above 415°C. In the presence of Al, ignition gets started below the melting point of Al and thus initiates the combustion reaction of tungsten with Teflon. In the absence of Al, the combustion of tungsten does not occur until 1100°C. Combustion of W–Teflon–Al mixtures proceeds in a pulsation mode and yields largely WC.

This work was financially supported by the Russian Foundation for Basic Research (project no. 16-03-00777-a).

EXPLOSIVE WELDING OF EXTRA-LARGE CLAD PLATES: DYNAMIC FEATURES

V. S. Vakin[1] and A. Z. Krasilnikov[2]

[1] ZAO ENERGOMETALL, St. Petersburg, 195220 Russia
[2] Baltic State Technical University VOENMECH, St. Petersburg, Russia

e-mail: v.vakin@emet.ru

This work is a logical follow-up of the study on basic aspects as well as physical and technical specificity of production of extra-large bimetallic plates. The previous results of this study have been presented at EPNM meetings since 2008 [1–6]. This study is an important priority for enhancement of technological capabilities of ZAO ENERGOMETALL.

A welding package consisting of the base and cladding plates is considered as an oscillating system launched at the moment of charge initiation. While bonding, the waves of elastic deformation are spreading through both base and cladding layers, thus causing significant influence on the line of contact between the welded surfaces and the bond quality. Furthermore, when using the enlarged multilayer cladding layer with non-uniform welds, the wave of elastic and plastic deformations travels through the weld line in a specific way.

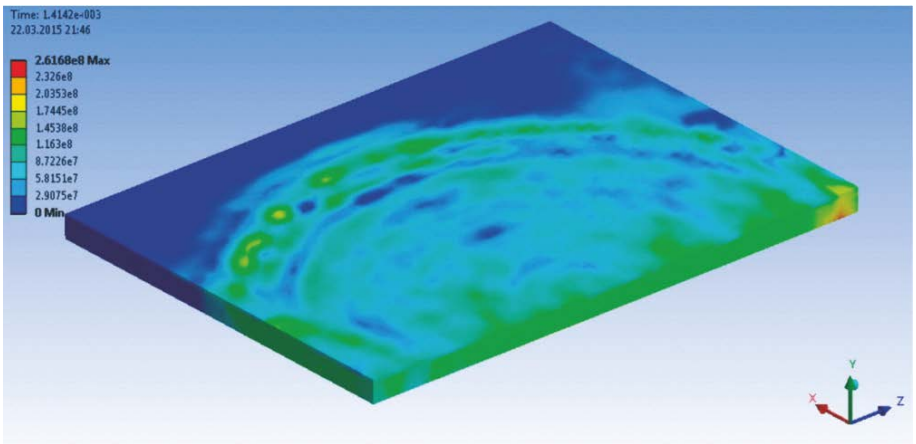

Controlling the dynamic properties of the welding package enables to expand the range of materials welded and dimensions of bimetallic products providing bond quality specified by the technical applications.

1. V.S. Vakin, Optimization of blast characteristics for production of large-size bimetal plates, *Proc. EPNM-2008*, Lisse, Netherlands.
2. V.S. Vakin, Optimization of blast characteristics for explosive production of large-size clad plates, in *Explosive Production of New Materials: Science, Technology, Business, and Innovations*, Moscow: Torus Press, 2008.
3. V.S. Vakin, Production of clad plates of extreme dimensions, *Proc. EPNM-2014*, Krakow, Poland.
4. V.S. Vakin, A.Z. Krasilnikov, Y.L. Marushin, Calculation and cladding of profiled surface of the superconducting coil PF1 ITER contacts, *Proc. EPNM-2014*, Krakow, Poland.
5. V.S. Vakin, Explosion welding of steels with Al–Mg and Ti alloys: Comparative analysis, *Proc. EPNM-2012*, Strasbourg, France.
6. V.S. Vakin, Features of weld bonding of aluminum-magnesium alloy AlMg6 with carbon and stainless steel, *Proc. EPNM-2012*, Strasbourg, France.

INFLUENCE OF CYCLIC THERMAL LOADING ON THE QUALITY OF WELD SEAM

V. S. Vakin[1] and O. G. Zotov[2]

[1]ZAO ENERGOMETALL, St. Petersburg, 195220 Russia
[2]Peter the Great Polytechnic University, St. Petersburg, Russia

e-mail: info@emet.ru

Investigated were the influence of dross inclusions into the weld seam and the effect of subsequent annealing, PWHT, and cyclic thermal loading on the quality of weld seam. Discussed is the development of defect map caused by diffusional oxidation of steel base followed by delaminating.

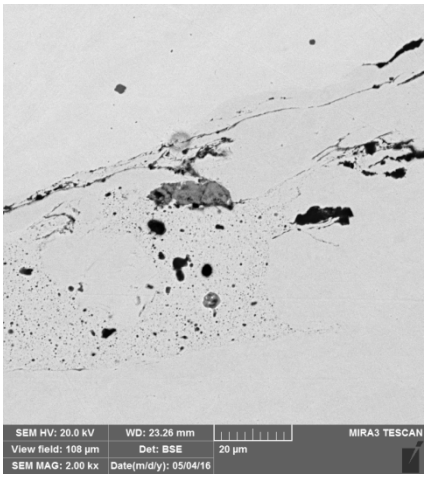

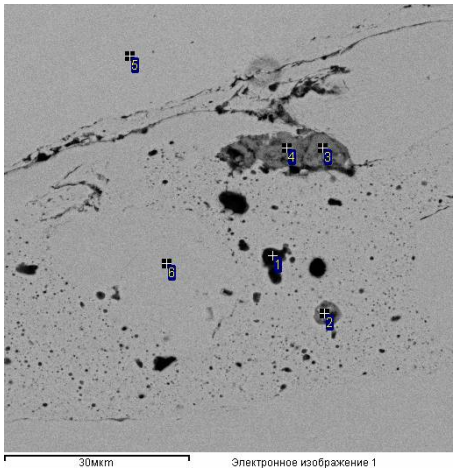

All results in wt %.

Spot	O	Na	Al	Si	S	K	Ti	Cr	Mn	Fe	Ni	Mo
1	23.36	0.89	2.99	12.61		1.99		5.07	1.81	50.55	0.72	
2	15.11		0.45	4.60		0.27		3.54	1.18	73.97	0.87	
3	24.42			0.81				2.43	0.46	70.99	0.89	
4	8.11			0.53	0.27			3.00	0.54	86.37	1.18	
5				0.75			0.33	17.37	1.21	70.89	9.46	
6				0.53				1.41	0.58	96.95		0.54
Max	24.42	0.89	2.99	12.61	0.27	1.99	0.33	17.37	1.81	96.95	9.46	0.54
Min	8.11	0.89	0.45	0.53	0.27	0.27	0.33	1.41	0.46	50.55	0.72	0.54

EFFECT OF POST HEAT TREATMENT ON MECHANICAL PROPERTIES OF LAYERED Al–Ti AND Fe–Ti LAMINATES OBTAINED BY EXPLOSIVE WELDING

M. Wachowski[1], L. Sniezek[1], I. Szachogluchowicz[1], and T. Plocinski[2]

[1]Military University of Technology, Faculty of Mechanical Engineering, Gen. S. Kaliskiego 2, Warsaw, 00-908 Poland
[2]Warsaw University of Technology, Faculty of Materials Science and Engineering, Woloska 141, Warsaw, 02-507 Poland

e-mail: marcin.wachowski@wat.edu.pl

The subject of this paper is explosive welding used to produce devices for military applications and chemical industry. Surface protection and production of light-weight materials with excellent mechanical properties are one of the most important issues in production of modern engineering structures due to increasing demands in the area of efficiency, strength, reliability and fatigue life of required applications. These requirements are fulfilled by coatings, but due to different chemical composition and structure of the connected materials, sometimes joining process is impossible to obtain by conventional welding or bonding methods [1, 2]. This problem can be solved by using an explosive welding method, which is one of the most effective technical engineering processes among joining methods. It is used to join a wide variety of similar or different metals such as aluminum and titanium or steel and titanium [3, 4].
An important criterion for application of explosively welded plates in military, chemical devices, nuclear reactors (i.e. heat exchangers), aviation and aerospace industry is softening of the joint typically provided by applying of the post heat treatment. Necessity of heat treatment of explosively welded plates is dictated by many factors, especially by the level of stress in the bonded materials. Stress in the bond zone generates plastic deformation and consequently strengthening of bimetal. Post welding heat treatment also provides expected properties of bimetallic material, especially the mechanical properties of base material, corrosion resistance of the cladded material and ballistic properties of whole laminate [5,6]. Due to a wide range of applications of explosively welded materials and the necessity for heat treatment, the problem of useful lifetime of the products obtained by this method becomes important and should be well understood by focusing on metallographic and mechanical aspect of the materials after welding.
The study was carried out using welded sheets of aluminum AA2519 alloy plates with titanium grade 5 plates (Fig. 1a) and carbon steel S355J2+N plates with titanium grade 1

(Fig. 1b). Examined plates were provided by EXPLOMET company (Poland). The applied post welding heat treatment in case of first mentioned laminate was annealing at 530–550°C for 2 h, quenching in water at room temperature and then aging at 165°C for 10 h to strengthen it. Heat treatment of second laminate was performed at a temperature of 600°C for 1.5 h with cooling in furnace to 300°C and in air to room temperature according to ASME UCS-56 Sector VIII [7]. The mechanical properties of titanium–steel laminate before and after heat treatment were examined applying three-points bending tests with cyclic loads and hardness measurements. The mechanical properties of aluminum-titanium laminate before and after heat treatment were examined applying low cycle axial tensile. Research of both laminates include fracture surfaces investigated using optical (OM) and scanning electron microscope (SEM).

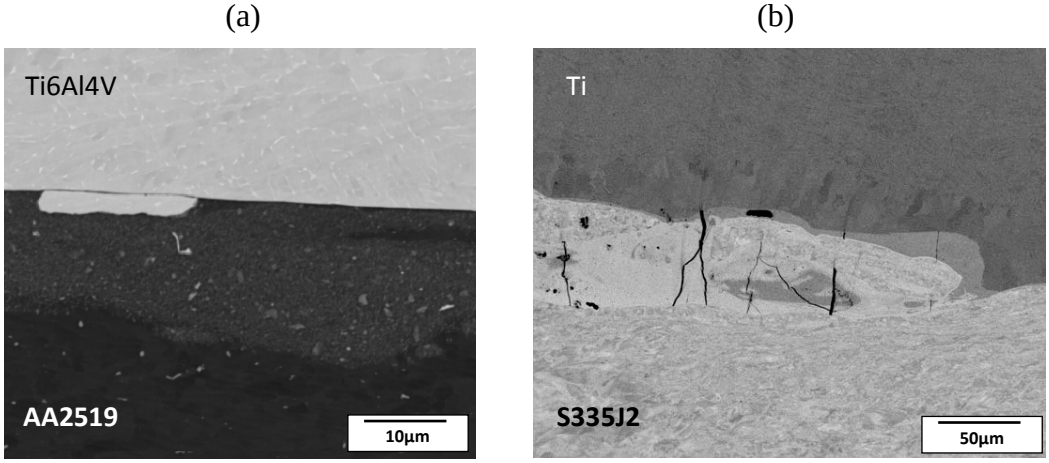

Fig. 1. Microstructure of laminates : AA2519/Ti6Al4V (a) S355J2+N/Ti grade 1 (b)

The results reveal significant influence of heat treatment on microstructure and mechanical properties of the welded plates. Post welding heat treatment in titanium-steel plates contributes to decrease of the fatigue strength due to formation of brittle intermetallic phases during the heat treatment. Post welding heat treatment in Al–Ti plates contributes to reduce residual stress and improvement in strength properties.

1. A. Karolczuk, K. Kluger, M. Kowalski, F. Zok, G. Robak, Residual stresses in steel–titanium composite manufactured by explosive welding, *Mater. Sci. Forum*, 2012, vol. 726, pp. 125–132.
2. L. Cizek, D. Ostroushko, E. Mazancova, Z. Szulc, R. Molak, M. Wachowski, M. Prazmowski, Structure and properties of sandwich material steel Cr13Ni10 + Ti after explosive cladding, *Metall. J.*, 2009, vol. 62, no. 6, pp.110–112.

3. D. Cutter, What you can do with explosion welding, *Welding J.*, 2006, vol. 6, p. 40.
4. F. Findik, Recent developments in explosive welding, *Mater. Design*, 2011, vol. 32.
5. S. Krol, Heat treatment of explosively welded bimetallic clad materials, *Welding International*, 1991, vol. 5, no. 12.
6. E.A. Prikhodko, I.A. Bataev, V.S. Lozhkin, V.I. Mali, M.A. Esikov, The effect of heat treatment on the microstructure and mechanical properties of multilayered composites welded by explosion, *Adv. Mater. Res.*, 2012, vols. 535–537.
7. ASME Section VIII Div. 1 Part UCS-56: Requirements for pressure vessels constructed of carbon and low alloy steels.

PROTECTIVE MULTILAYER Al–Ti MATERIAL WITH ENHANCED BALLISTIC RESISTANCE

Z. Wilk[1], P. Koślik[1], and A. Gałka[2]

[1] Instytut Przemysłu Organicznego, ul. Annopol 6, Warszawa, 03-236 Poland
Oddział zamiejscowy, ul. Zawadzkiego 1, 42-693 Krupski Młyn, Poland
[2] EXPLOMET, ul. Oświęcimska 100 H, Opole, 45-461 Poland

Presented are the results of ballistic tests on protective capacity of a layered Ti–Al material (7 layers with a total thickness of 28 mm) against the action of explosive charge detonation. The tested multilayer system was made by explosive welding in a single technological cycle appropriately with alternating layers of Ti 10 mm + Al 3 mm + Ti 3 mm + Al 3 mm + Ti 3 mm + Al3 mm + Ti 3 mm. In the experiments, small caliber liner shaped charges with a diameter of 32 mm/60º and 18 g of explosive materials based on RDX (type H-Pp-32/60) were used. The depth of the perforation and the volume of crater in the stack control plates of thickness 10 mm with steel S235 type were determined. Based on these results, the absorption capacity of kinetic energy by the multilayer stream of Ti/Al was estimated. For adopted test system (see Fig. 1), a computer model of the system using Autodyn 2D software has been designed and tested. Furthermore, the piercing jet cumulative multilayer protective system was also analyzed.

Fig. 1. Test setup for protective capacity ofmultilayer Ti–Al system.

Research was conducted in the framework of Applied Research Program NCBR in Poland (project no. PBS2/A5/35/2013: New advanced Al–Ti layered materials with enhanced ballistic resistance for aerospace applications for 2013–2016).

SHOCK WAVE SYNTHESIS OF MULTILAYER GRAPHENE FROM DRY ICE

H. Yin[1], Q. Du[2], and P. Chen[2]

[1] Institute of Systems Engineering, China Academy of Engineering Physics, Mianyang, Sichuan Province, 612900 China
[2] State Key Laboratory of Explosion Science and Technology, Beijing Institute of Technology, Beijing, 100081 China

Multilayer graphene sheets were synthesized by reduction of dry ice (CO_2) with calcium hydride (CaH_2) in conditions of shock loading. In addition, by adding urea to the reaction system, nitrogen-doped graphene material was formed in a one-step shock wave treatment.

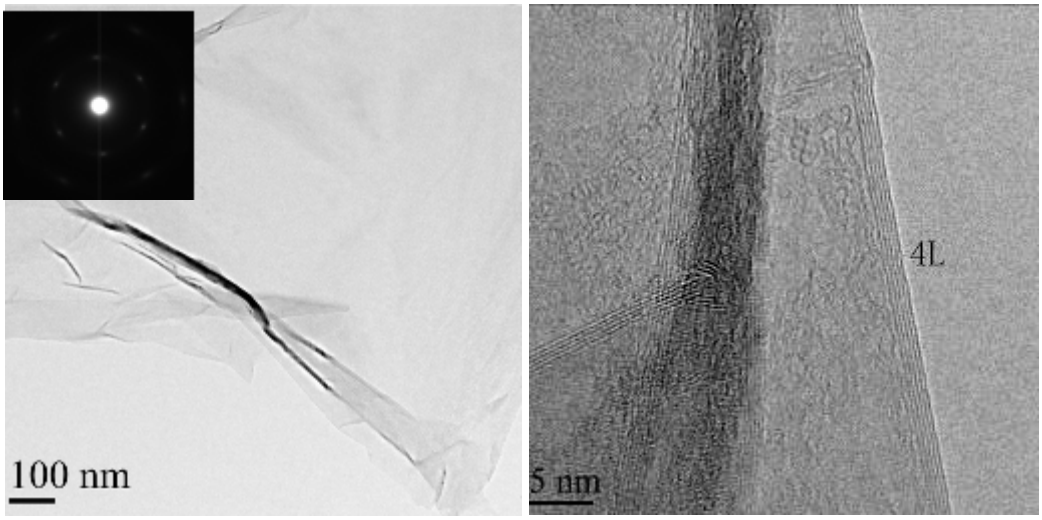

Fig.1 TEM images of multilayer graphene: (a) typical films, the insert shows SEAD pattern and (b) HRTEM image of four layers.

The recovered samples were characterized by transmission electron microscopy, scanning electron microscopy, Raman spectroscopy, and X-ray photoelectron spectroscopy. The pressure and temperature are two important factors in the synthesis of multilayer graphene. Shock synthesis of graphene materials requires a balance between the growth rate of graphene materials and the formation rate of carbon atoms. Typical TEM images and diffraction pattern of shock synthesized graphene are shown in Fig. 1.

METALLOTHERMIC SHS REACTIONS INVOLVING NIOBIUM OXIDE

V. I. Yukhvid[1], D. E. Andreev [1], V. N. Sanin[1], N. V. Skachhkova[1], and M. I. Alymov[1]

Institute of Structural Macrokinetics and Materials Science, Russian Academy of Sciences, Chernogolovka, Moscow, 142432 Russia

e-mail: yukh@ism.ac.ru

As is known, SHS reactions [1, 2] can also be carried out in a mode of metallothermic reactions in the field of centrifugal forces [3, 4] to obtain cast ingots of target products.
In this communication, we report on fabrication of Nb–Si alloys containing some alloying agents (Hf, Ti и Al) by using Nb_2O_5/Al/Si/Hf/Ti green mixtures (100 g, a = 10–500 g). Combustion products were characterized by SEM (Zeiss Ultra plus) and XRD (DRON-3M). The overall reaction scheme can be represented in the form:

$$n_1Nb_2O_5 + n_2Al + n_3Hf + n_4Ti = m_1Nb + m_2Al_2O_3 + m_3HfO_2 + m_4TiO_2 \quad (1)$$

$$m_1Nb + m_2Al + m_3Hf + m_4Ti + n_5Si = m_1Nb/m_2Al/m_3Hf/m_4Ti/n_5Si \quad (2)$$

$$m_2Al_2O_3 + m_3HfO_2 + m_4TiO_2 = m_2Al_2O_3/m_3HfO_2/m_4TiO_2 \quad (3)$$

The metallic ingot was found to contain (*i*) solid solution in Nb, (*ii*) Nb_5Si_3, and (iii) inclusions of Nb_3Al and oxides of Nb and Hf. The replacement of Hf and Si by $HfSi_2$ in reaction (1) was found to increase its content in resultant ingot, which can be used as a tool for regulating the service parameters of synthesized composites.

This work was financially supported by the Russian Foundation for Basic Research (project no. 15-08-01142).

1. A.G. Merzhanov, I.P. Borovinskaya, Combustion synthesis of refractory compounds, *Dokl. Akad Nauk SSSR*, 1972, vol. 204, no. 2, pp. 366–369.
2. A.G. Merzhanov, A.S. Mukasyan, *Tverdoplamennoe gorenie* (Solid-Flame Combustion), Moscow: Torus Press, 2007.
3. V.I. Yukhvid, Modifications of SHS processes, *Pure Appl. Chem.*, 1992, vol. 64, no. 7, pp. 977–988.
4. V.I. Yukhvid, Liquid-Phase SHS reactions: New lines of research and task objectives, *Tsvet. Metall.*, 2006, no. 5, pp. 62–78.

SHS-PRODUCED TiAl CAST ALLOYS FOR ADDITIVE MANUFACTURING TECHNOLOGIES

V. I. Yukhvid[1], D. E. Andreev[1], V. N. Sanin[1], D. M. Ikornikov[1], E. A. Levashov[2], Zh. A. Sentyurina[2], A. A. Zaitsev[2], Yu. S. Pogozhev[2]

[1]Institute of Structural Macrokinetics and Materials Science, Russian Academy of Sciences, Chernogolovka, Moscow, 142432 Russia
[2]National University of Science and Technology MISiS, Leninskii pr. 4, Moscow, 119049 Russia

e-mail: yukh@ism.ac.ru

Aiming at fabrication of granulated heat-resistant materials (HRMs) of new generation [1], we elaborated the process involving (1) synthesis of semi-product cast ingots by centrifugal SHS, (2) vacuum induction remelting of semi-product into massive electrodes for sputtering, and (3) preparation of spherical granules by centrifugal sputtering [2, 3].

Centrifugal SHS. Either Ti/Al/Nb_2O_5/Cr_2O_3 and TiO_2/Al/Nb_2O_5/Cr_2O_3 powder mixtures or their combinations were used as green compositions. In order to raise combustion temperature, in some cases CaO_2/Al mixtures were added as an energizer. Metallothermic reaction in a centrifugal machine yielded the ingots of HRM shown in Fig. 1a. The influence of process parameters on the quality of synthesized ingots has been studied in detail and optimized. In Fig. 1b, the bright and dark (oxide) inclusions are seen too be uniformly distributed over the grey Ti–Al matrix. The matrix and bright inclusions were found to contain TiAl as a main phase and Ti_3Al as an admixture.

(a) (b) (c)

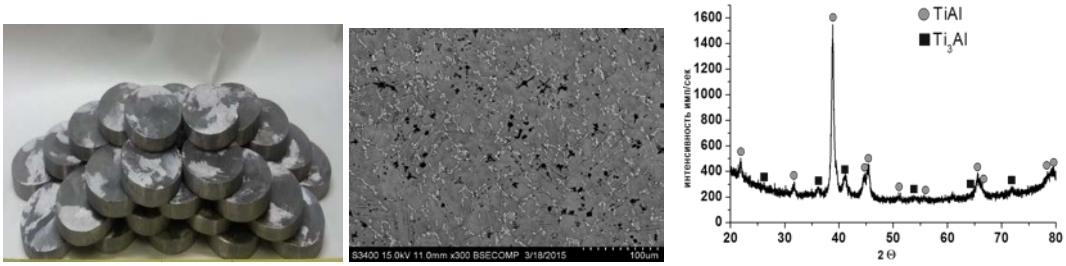

Fig. 1. (a) Overall view of cast ingots (450–500 g each), (b) their microstructure, and (c) phase composition.

Vacuum induction remelting into electrodes. The remelting of SHS-produced TiAl ingots at 1600–1650°C was performed in a VIPKhT oven. The melt was cast into a steel mold heated to 500–700°C to obtain a 15-kg cylinder shown in Fig. 2a.

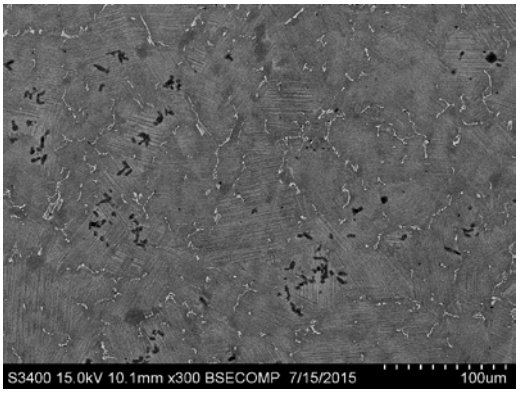

Fig. 2. (a) Overall view and (b) microstructure of HRM after remelting.

As follows from Fig. 2b, the remelting markedly improved the material structure. Table 1 presents the chemical composition of as-prepared and remelted HRMs: the remelting changed the material composition only slightly.

Table 1. Chemical composition of HRMs (wt %).

Green composition	As-prepared				After remelting			
	Ti	Al	Nb	Cr	Ti	Al	Nb	Cr
$Ti/Al/Nb_2O_5/Cr_2O_3$	65.0	27.3	4.3	3.4	61.3	30.6	4.9	3.2
$TiO_2/Al/Ca/Nb_2O_5/Cr_2O_3$	58.9	29.3	5.3	3.5	-	-	-	-

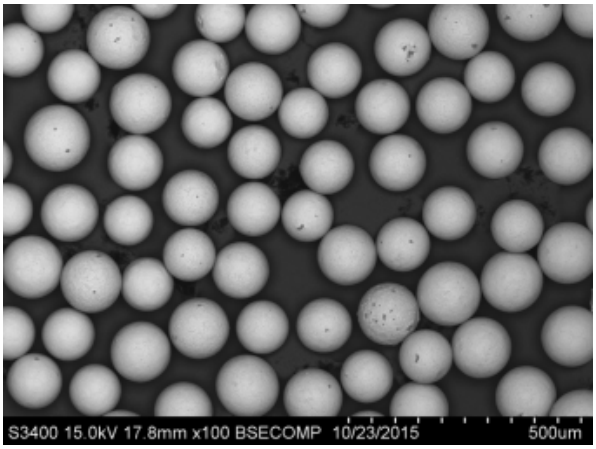

Fig. 3. Spherical granules of HRM with a particle size of 100–125 μm.

Preparation of spherical granules. Prior to centrifugal sputtering, the electrodes were heated with a plasmatron. The overall view of thus prepared granules is given in Fig. 3. The porosity of the granules is low and decreases with their size. The chemical/phase composition of the granules was close to those in Table 1.

This work was financially supported by the Russian Ministry for Education and Science in the framework of Program on Priority Directions of R & D in the years 2014–2020 (agreement no. 14.578.21.0040, project code RFMEFI57814X0040).

1. I. Gibson, D.W. Rosen, B. Stucker, *Additive Manufacturing Technologies: Rapid Prototyping to Direct Digital Manufacturing*, Springer Science & Business Media, 2009.
2. V.I. Yukhvid, D.E. Andreev, V.N. Sanin, Zh.A. Sentyurina, Yu.S. Pogozhev, E.A. Levashov, Centrifugal SHS of cast Ti–Al–Nb–Cr alloys, *Int. J. Self-Propag. High-Temp. Synth*., 2015, vol. 24, no. 4, pp. 176–180.
3. A.A. Zaitsev, Zh.A. Sentyurina, Yu.S. Pogozhev, E.A. Levashov, V.N. Sanin, V.I. Yukhvid, D.E. Andreev, M.A. Mikhailov, Yu.Yu. Kaplanskii, Cast alloyed NiAl electrodes for fabricating spherical granules by centrifugal sputtering, *Izv. Vyssh. Uchebn. Zaved, Tsvet. Metall*., 2015, no. 4, pp. 15–24.

FABRICATION OF TUNGSTEN/COPPER BIMETAL BY HOT-EXPLOSIVE WELDING

Q. Zhou[1], P.W. Chen[1], and J.R. Feng[1]

[1]State Key Laboratory of Explosion Science and Technology, Beijing Institute of Technology, Beijing, 100081 China

e-mail: pwchen@bit.edu.cn

Explosive welding is suitable for the joining of metals with big difference in properties, such as the copper/tungsten bimetal that is difficult to weld by conventional method due to the large thermal expansion mismatch. But the crack problem due to the brittleness of W restricts the application of explosive welding [1, 2]. In order to eliminate cracking, the heating a W plate is necessary and this proved to be an effective way to shock consolidation of pure W powders [3]. In this work, the copper/tungsten bimetal was fabricated by hot explosive welding.

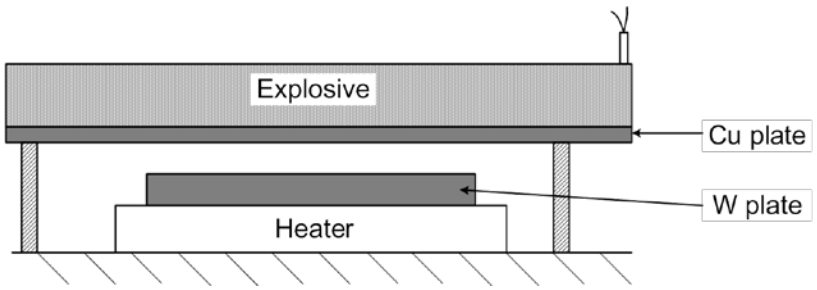

Fig. 1. Schematic of hot explosive welding.

In present experiments, the copper plate with a thickness of 2mm was joined with a tungsten plate with varied thicknesses (0, 1, and 2 mm) using the technique of hot explosive welding. The powder explosive based on ammonium nitrate with a detonation velocity of 2300 m/s was used in these experiments. The thickness of explosive layer was fixed to 15 mm, and the parameters were adjusted by changing the stand-off distance between 1.5 and 3 mm. The collision angle β and velocity V_p were calculated by using the Deribas equation [4]. The configuration of hot explosive welding is presented in Fig. 1, where an electrical heating plate was used to preheat the tungsten plate to a temperature as high as 500°C. By contrast, the explosive welding of 2-mm tungsten without preheating was also carried out. The experimental results showed unsuccessful welding with plenty of cracks in tungsten plate, as shown in Fig. 2a. A crack-free

copper/tungsten bimetal was successfully obtained by hot explosive welding with the W plate 1 mm thick, as shown in Fig. 2b.

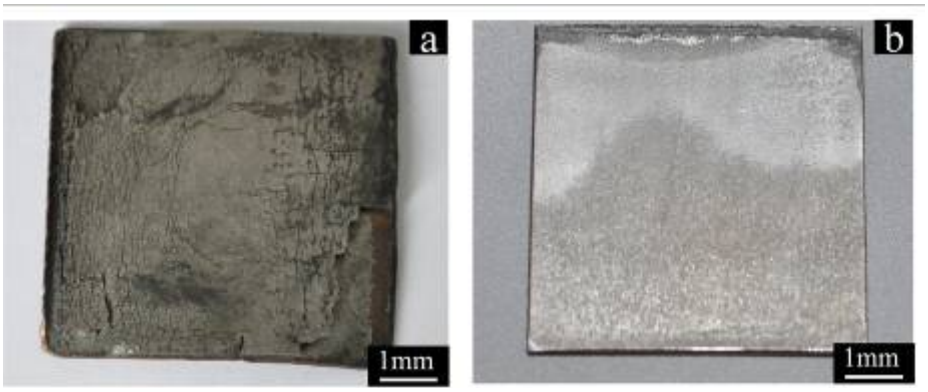

Fig. 2. Explosive welding of Cu/W pair without (a) and with (b) preheating.

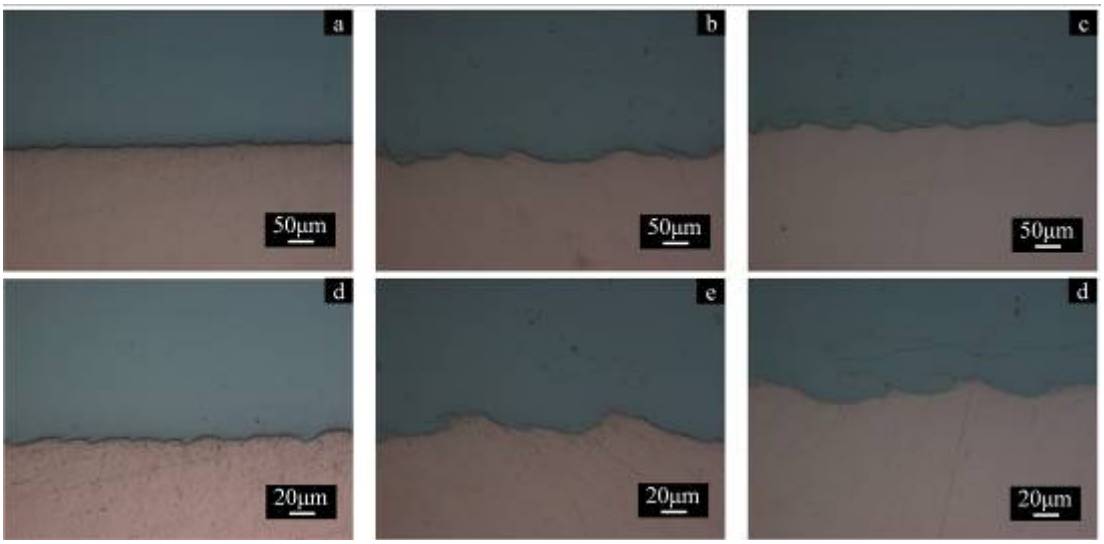

Fig. 3. Cu/W interfaces formed in different conditions of explosive welding: (a, d) β = 14.1°, V_p = 566 m/s; (b, e) β = 15.6°, V_p = 623 m/s; and (c, f) β = 17.4°, V_p = 693 m/s.

All the samples were obtained at a fixed preheating temperature of 500°C, and the smooth interface turned into wavy structure as the parameter increased, as shown in Fig. 3. The wavy interface can be obtained under the conditions (β = 15.6°, V_p = 623m/s), which is lower than the case without preheating (β = 19.5°, V_p = 780 m/s). It implies that the heating reduces the hardness and strength and increases the ductility of tungsten plate, which is the key factor for eliminating the cracks in a W plate. As the thickness of

W plate increased to 2 mm, the cracks occurred again because the brittle-to-ductile transition temperature of W increases as the thickness increases.

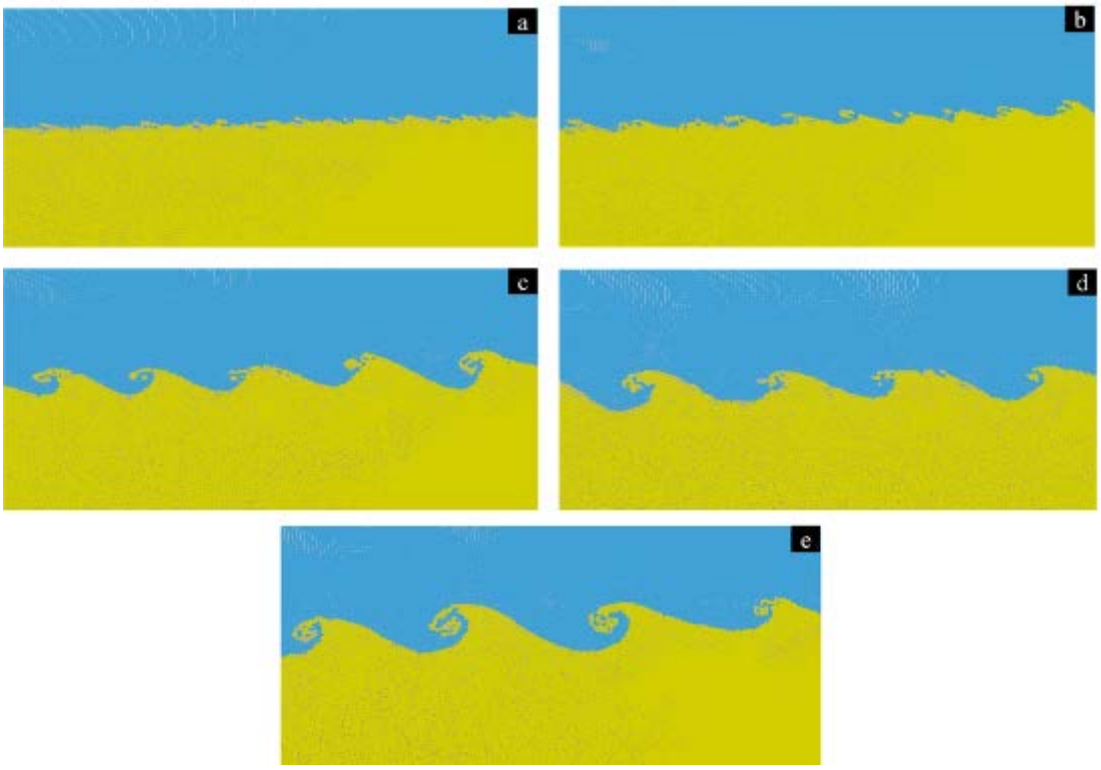

Fig.4. Simulated results for the W/Cu interfaces formed under different conditions.

A 2D model of inclined impact was developed to simulate the formation of the wavy interface in the W–Cu bimetal by using the SPH method. Figure 4 shows the simulated results for the tungsten/copper interfaces formed under various conditions. The effects of parameter and preheating temperature on the wavy interface were also analyzed; and the formation mechanism of wavy interface was also analyzed based on the simulation and the microstructure observation. The results of numerical simulation will be demonstrated at presentation.

1. C. Sun, S. Wang, W. Guo, W. Shen, C. Ge, Bonding interface of W–CuCrZr explosively welded composite plates for plasma facing components, *J. Mater. Sci. Technol.*, 2014, vol. 30, no. 12, pp. 1230–1234.
2. P. Manikandan, J.O. Lee, K. Mizumachi, A. Mori, K. Raghukandan, K. Hokamoto, Underwater explosive welding of thin tungsten foils and copper, *J. Nucl. Mater.*, 2011, vol. 418, nos. 1–3, pp. 281–285.

3. Q. Zhou, P. Chen, Fabrication and characterization of pure tungsten using the hot-shock consolidation, *Int. J. Refr. Met. Hard Mater*., 2014, vol. 42, pp. 215–220.
4. A. Deribas, Science of explosive welding: State of art, in *Impact Engineering and Applications*, A. Chiba, S. Tanimura, and K. Hokamoto, Eds., Elsevier (UK), 2001.

BONDING AND WAVE FORMATION AT THE EXPLOSIVE WELDING OF LOW-PLASTIC MATERIALS

B. S. Zlobin[1], A. A. Shtertser[1], V. V. Kiselev[1], A.V. Plastinin[2]

[1]Design and Technology Branch, Lavrent'ev Institute of Hydrodynamics, Siberian Branch, Russian Academy of Sciences, ul. Tereshkovoi 29, Novosibirsk, 630090 Russia
[2]Lavrent'ev Institute of Hydrodynamics, Siberian Branch, Russian Academy of Sciences, pr. Lavrent'eva 15, Novosibirsk, 630090 Russia

e-mail: asterzer@mail.ru

A number of works, such as [1], show that the formation of bonding at the high-speed oblique collision of metal plates goes along with a flow of particles occurring in the welding gap (the cumulative flow). The cumulative flow results from the high-degree localization of deformation near the collision region [1]. At the explosive welding of materials of different strength, the less strong material makes the major contribution into the bonding formation conditioning. As is shown experimentally, the particle flow generated by a thin (0.8 mm) copper layer promotes the welding of two quenched steel plates (hardness 42 and 32 HRC) in the collision mode corresponding to the copper strength [1]. The copper layer is set in the starting section of the welding area and is preliminary welded to one steel plate with the aid of an emulsion explosive [2, 3].

The explosive welding is often accompanied by the wave formation, though it is not necessary for the strong bonding. The detailed review of the works on wave formation investigation and theoretical modeling is presented in [4, 5]. Note that there is still no consensus on this topic. Experience shows that, aside for the geometrical parameters of welding (plate thickness, collision angle), the wave size also depends on the physical (density ρ, acoustic stiffness ρc) and strength (hardness) characteristics of the welded materials, and in the first place of the stronger one. When welding low-plastic metals and alloys, wave formation results in cracking; as a rule, cracks start in the joint region where the maximal deformations occur, and their (deformations) value depends on the wave amplitude (Fig. 1) [6]. Cracking impedes producing multi-layer materials involving, for example, molybdenum or titanium alloys, as well as high-strength quenched steels. It is possible to prevent cracking on the joint boundary via reducing somehow the wave dimensions.

Experiments similar to the ones described in [2] were carried out to study the influence of the strength on the wave dimensions. Three steel samples of different hardness (145HB, 33HRC, and 45HRC), and one aluminum sample (40HB) were clad simultaneously with a copper plate of 1 mm (70HB) in accordance with the model

shown in Fig. 2. The measured detonation velocity of explosive at the welding is D = 2.8 km/s, the computed collision angle $\gamma = 12°$. After the welding, micro sections were made from the produced bimetallic samples, and wave dimensions were measured in three sections, one within 20 mm from the sample beginning, second in the middle, and the third within 10 mm from the end of each sample.

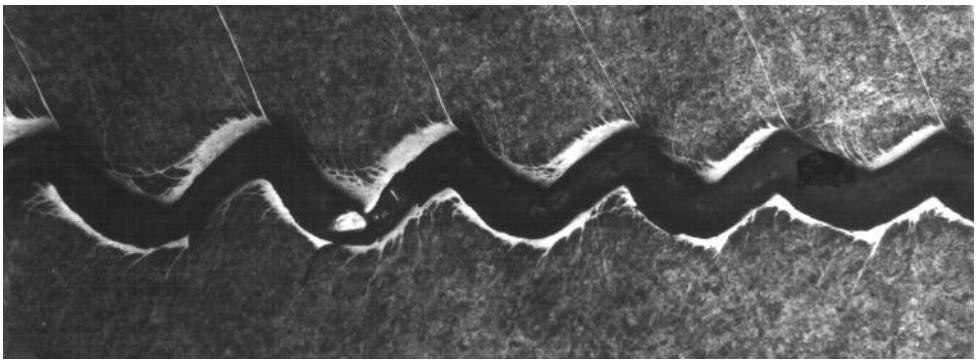

Fig.1. Shear cracks caused by the wave formation.

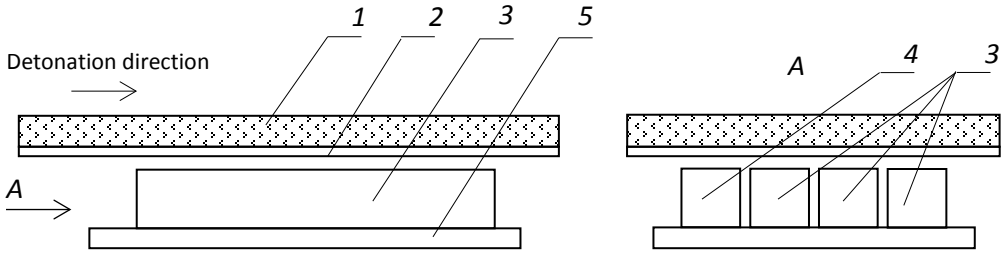

Fig. 2. Welding of a copper plate with samples of different hardness: *1* explosive charge, *2* copper plate; *3* steel samples, *4* aluminum sample, and *5* base.

The measurement results are presented in the Table 1 below.

Table 1. The length (λ, mm) and amplitude (*a*, mm) of waves in the junction region.

Hardness	Section *1*		Section *2*		Section *3*		Average value	
	λ	*a*	λ	*a*	λ	*a*	λ	*a*
45HRC	0.302	0.071	0.283	0.071	0.267	0.071	0.280	0.070
33HRC	0.380	0.114	0.401	0.114	0.362	0.114	0.380	0.110
145HB	0.457	0.157	0.485	0.157	0.442	0.157	0.460	0.160

As the hardness of steel samples rises, the wave dimensions decrease, and the hardness variation imposes the strongest effect on the wave amplitude. The Table 1 shows that, as the hardness rose by approximately three times, the wave length λ changed by 1.6 times, whereas the amplitude *a* changed by 2.2 times. As the hardness of the strongest of welded materials rises more, the junction shape trends to the waveless, as is demonstrated in [2] for the couple stainless steel (150HB)–cemented carbide (89HRA).

The density ratio of the welded materials also influences considerably on the deformation processes character and on wave dimensions in the bonding zone. Thus, the bonding zone on the copper-steel interface has the well-defined wavy structure, whereas the copper-aluminum interface features the lack of waves.

In practice, a technological sub-layer of more ductile material is commonly used for the successful explosive welding of two metals of high strength and low plasticity. Our experiments show that wave dimensions depend not only on geometrical, physical and strength parameters of welded materials, but on the succession of layers welding. Namely, if the accelerated steel plate is previously clad by the thin copper layer, then wave amplitude is less than in case when the base steel plate is previously clad by the same copper layer.

The developed approaches enable bonding of low-plasticity metals and alloys.

1. A.A. Shtertser, B.S. Zlobin, Flows, strains, and the formation of joints in oblique collision of metal plates, *J. Appl. Mech. Tech. Phys.*, 2015, vol. 56, no. 5, pp. 927–935.
2. B. Zlobin, V. Sil'vestrov, A. Shtertser, A. Plastinin, V. Kiselev, Enhancement of explosive welding possibilities by the use of emulsion explosive, *Arch. Metall. Mater.*, 2014, vol. 59, no. 4, pp. 1587–1592.
3. B.S. Zlobin, V.V. Silvestrov, A.A. Shtertser, A.V. Plastinin, Explosive welding of dissimilar metals: New horizons opened up by emulsion, in *Explosive Production of New Materials: Science, Technology, Business and Innovations* (Proc. EPNM-2014 Symp.), A.A. Deribas, Yu.B. Scheck, Eds., Cracow: Nokturn, 2014, pp. 270–273.
4. I.V. Yakovlev, G.E. Kuz'min, V.V. Pai, *Wave Formation under Oblique Collisions: Collected Articles*, Novosibirsk: Izd. Inst. Discrete Mathematics and Informatics, 2000 (in Russian).
5. I.V. Yakovlev, V.V. Pai, *Explosive Welding of Metals*, Novosibirsk: Izd. SO RAS, 2013 (in Russian).
6. I.D. Zakharenko, B.S. Zlobin, Effect of the hardness of welded materials on the position of lower limit of explosive welding, *Comb. Explos. Shock Waves*, 1983, vol. 19, no. 5, pp. 689–692.

MICROWAVE RADIATION FOR SYNTHESIS OF CARBIDES AND CATALYTIC DECOMPOSITION OF HYDRAZINE

A. R. Zurnachyan and R. A. Mnatsakanyan

Nalbandyan Institute of Chemical Physics, National Academy of Sciences, Yerevan, 0014 Armenia

e-mail: alina.zurnachyan@gmail.com

In past decades, microwave (MW) radiation is increasingly being used for activating chemical reactions. The use of microwave energy is increasing worldwide and its application in the chemical industry is one of current task objectives. The use of microwave heating for direct synthesis, as well as in catalytic reactions, is promising not only from the standpoint of energy savings but also for selectivity of chemical reactions. Another advantage of microwave oven is uniform and high speed heating throughout the volume of the sample compared with conventional heating.

The catalytic decomposition of hydrazine has been of interest for many years since this process successfully used in a monopropellant in satellite propulsion. Transition metal carbides such as molybdenum and tungsten carbides (e.g. Mo_2C, WC) catalysts are active in hydrazine decomposition reaction [1–4]. Currently, there are many methods for the synthesis of molybdenum and tungsten carbides due to the wide spectrum of use of these compounds in various areas. The existing methods [5] allow synthesizing the carbides with pre-planned properties, including specific surface area, one of desired parameters for the high activity of heterogeneous catalysts. Tungsten and molybdenum carbides show sufficiently high activity in the various catalytic reactions in which they have successfully replace catalysts containing noble metals [6]. Due to high efficiency of time and energy, the application of microwave (MW) heating is interest for the synthesis of chemical compounds, including also the synthesis of molybdenum and tungsten carbides.

This work is devoted to the use of microwave radiation for the synthesis of molybdenum and tungsten carbides and testing these systems as catalysts for hydrazine monohydrate decomposition in the liquid phase under MW radiation. The synthesis was carried out in a quartz flow reactor placed vertically in a household microwave oven (2.45 GHz, 900 W). Ammonium paramolybdate, molybdenum, tungsten powder, and their oxides were used as initial compounds. The carbon source was Vulcan XC-72R.

The optimal conditions were defined - the composition of initial mixture, the purging time, time and mode of MW heating, which provides 100% yield of end-products. The measurement of specific surface area and pore size distribution of the samples have

shown that, in contrast to traditional methods of carbide synthesis, MW heating method provides specific surface areas from $10m^2/g$ to $70m^2/g$ and a narrow pore distribution in the range of 20-30 A^o. SEM & TEM analyses results have shown that the carbide particles are sufficiently uniform with narrow particle size distribution in the range of 20-30 nm (Fig. 1).

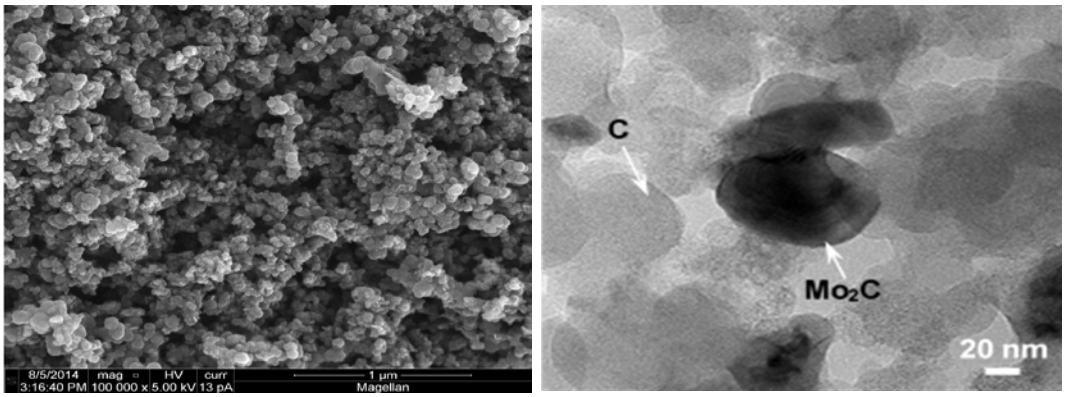

Fig. 1. SEM & TEM analyses of 70% Mo2C/C system

The effect of MW radiation on the catalytic decomposition of hydrazine in the liquid phase was studied for the first time. The catalytic activity of carbides in the decomposition of hydrazine hydrate was investigated in a Teflon autoclave. Experiments have shown that in the presence of tungsten and molybdenum carbides in the conditions of MW radiation as well as at conventional heating the reaction proceeds only in the direction of ammonia and nitrogen.

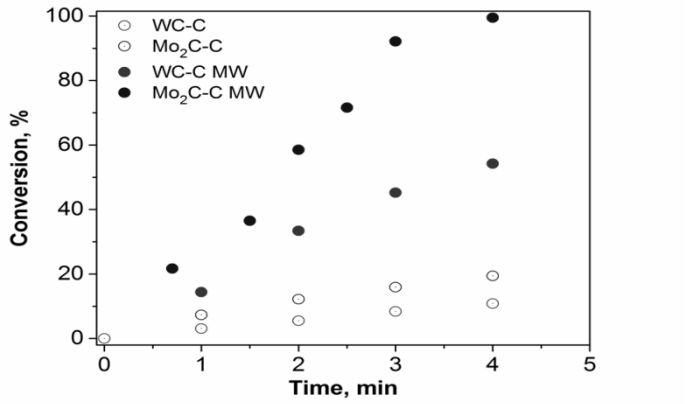

Fig. 2. Conversion of hydrous hydrazine.

In the Fig. 2 compared conversion of hydrazine in the presence of molybdenum and tungsten carbides with and without MW irradiation at 180W power. It can be seen that the highest conversion occurs in the presence of molybdenum carbide under MW radiation. The temperature of reaction is about 70^{o}C. In the presence of the Vulcan XC-72R, and also without a catalyst, in both cases the conversion of hydrazine hydrate was 0%.

1. X. Chen, T. Zhang, M. Zheng, Z. Wu, W. Wu, C. Li, The reaction route and active site of catalytic decomposition of hydrazine over molybdenum nitride catalyst, *J. Catal.*, 2004, vol. 224, no. 2, pp. 473–478.
2. X. Chen, T. Zhang, M. Zheng, L. Xia, T. Li, W. Wu, X. Wang, C. Li, Catalytic decomposition of hydrazine over R–Mo_2C/γ-Al_2O_3 catalysts, *Ind. Eng. Chem. Res.*, 2004, vol. 43, pp. 6040-6047.
3. C. Liang, L. Ding, A. Wang, M. Zhiqiang, J. Qiu, T. Zhang, Microwave-Assisted Preparation and Hydrazine Decomposition Properties of Nanostructured Tungsten Carbides on Carbon Nanotubes, *Ind. Eng. Chem. Res.*, 2009, vol. 48, no. 6, pp. 3244-3248.
4. X. Chen, T. Zhang, P. Ying, M. Zheng, W. Wu, L. Xia, T. Li, X. Wang, C. Li, A novel catalyst for hydrazine decomposition: molybdenum carbide support on gamma-Al_2O_3, *Chem. Commun.*, 2002, no. 3, pp. 288–289.
5. O.H. Pierson, *Handbook of Refractory Carbides and Nitrides: Properties, Characteristics, Processing and Applications*, Noyes Publications, 1996.
6. S.T. Oyama, *Catalysis Today*, 1992, vol. 15, no. 2, pp. 179–200.

EXPERIMENTAL METROLOGY AND TECHNIQUES FOR SUB-MILLIMETER OPTICAL OBSERVATION OF DETONATION REACTION PHENOMENA AND PERFORMANCE EVALUATION OF CRYSTALLINE EXPLOSIVES

I. Plaksin†, L. Rodrigues, R. Mendes, J. Ribeiro, J. Campos, J. Góis, S. Plaksin

ADAI–Association for the Development of Mechanical Engineering, LEDAP–Laboratory of Energetics and Detonics, Department of Mechanical Engineering, University of Coimbra, Rua Luis Reis Santos, Coimbra, 3030-788 Portugal

e-mail: luis.j.rodrigues@gmail.com

The use of optical fibers and electronic streak cameras allow for sub-millimeter resolution of detonation dynamics and phenomena. A variety of pioneering experimental techniques permit the use of very small sample masses (in the order of tens of grams) for the characterization of performance – velocity of detonation, peak pressure, shock front curvature and smoothness – as well as sensitivity related parameters – critical diameter, shock to detonation run length and run time. Other innovative techniques allow for more fundamental research of detonation dynamics, including the observation of the reaction of single crystals and the resolution of shock velocity and peak pressure fields in inert shocked media. These techniques have particular interest in the study of crystalline explosives: due to the characteristic small-scale heterogeneity and anisotropy of polymer bonded explosives (PBXs), the reaction dynamics exhibit inhomogeneities and local detonation intensity perturbations; these perturbations can negatively impact the smoothness of the acceleration of metallic liners. This is of particular interest in the of performance enhancement of small shaped charges but might virtually be also of interest in other application fields, such as explosive welding/cladding and shock compaction/sintering. Some experimental setups will be presented, as well as representative examples of results.

MODIFICATION OF NANODIAMOND BY ADDITION OF AMINO GROUPS WITH BIOLOGICAL APPLICATION AIM

S. Y. Stavrev

Nano Tery, Sofia, Bulgaria

e-mail: prof.stavrev@gmail.com

The possibilities for using of detonation nanodiamond with a targeting effect are analyzed with the aim of medical, dermatological and cosmetic application. Tree variants of technologies for modification of nanodiamond surface with amino groups are examined. The proposed technologies are proved with examples.

HOT EXPLOSIVE CONSOLIDATION OF NANOSTRUCTURED Ta–Cu AND Ta–Ag COMPOSITES: FABRICATION AND PROPERTIES

A. Peikrishvili[1,3], G. Maniashvili[2], B. Godibadze[1], T. Gegechkori[2], E. Chagelishvili[1], M. Tsiklauri[1], and A. Dgebuadze[1]

[1] Tsulukidze Mining Institute, Tbilisi, 0186 Georgia
[2] Andronikashvili Institute of Physics, Tbilisi, 0186 Georgia
[3] Tavadze Institute of Metallurgy and Materials Science, Tbilisi, 0186 Georgia

e-mail: apeikrishvili@yahoo.com

Mixtures of Ta–Cu and Ta–Ag nanopowders (precursors) were compacted to a nearly theoretical density by using the technique of Hot Explosive Consolidation (HEC). The percentage of constituent phases in was varied between 10 and 90%. In order to obtain nanostructured billets the tantalum precursors had a particle of around 80 nm. As a matrix phase, we used conventional copper and silver powders with a mean particle size of 5μm. During processing, the temperature could be made as high as 1000°C while pressure, up to 10 GPa. Figure 1 presents the SEM images of precursor blends while Fig. 2, those of Ta–20% Cu and Ta–10% Ag composites obtained by HEC at T = 9400°C and P = 10 GPa.

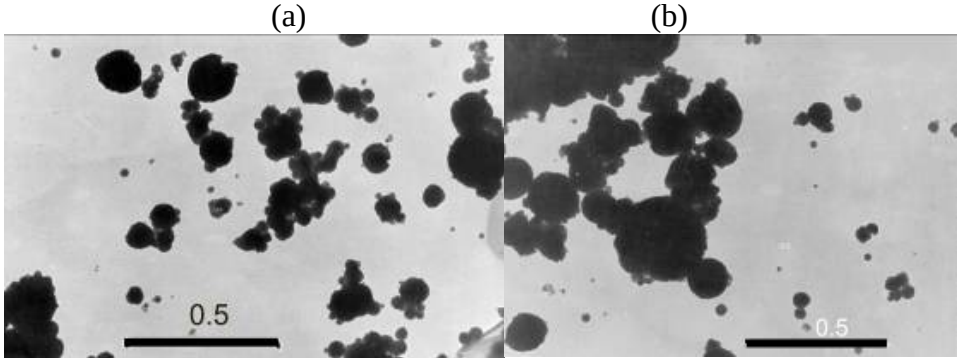

Fig. 1. SEM images of precursor blends: (a) Ta–20%Ag and (b) Ta–20%Cu.

The use of nanosized Ta–Cu (Ag) blends and their HEC allows the fabricating of cylindrical billets with a density close to theoretical, without cracks and on retention the nanosized of Ta grains. The consolidated samples showed good integrity and electrical properties. The structure and characteristics of obtained materials depend on their phase composition, distribution of the phases, and consolidation conditions. The electrical properties (resistance and susceptibility) of the consolidated Ta–Cu and Ta–Ag composites were found to depend on their phase composition and density.

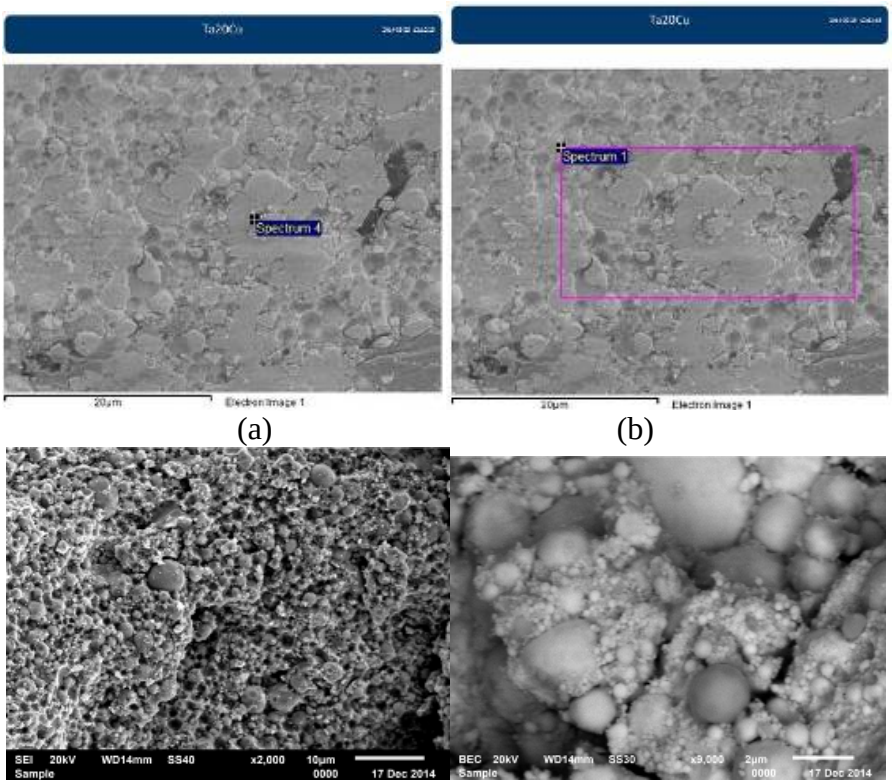

Fig. 2. SEM images of Ta–20% Cu and Ta–10% Ag composites after HEC at 9400°C and 10 GPa.

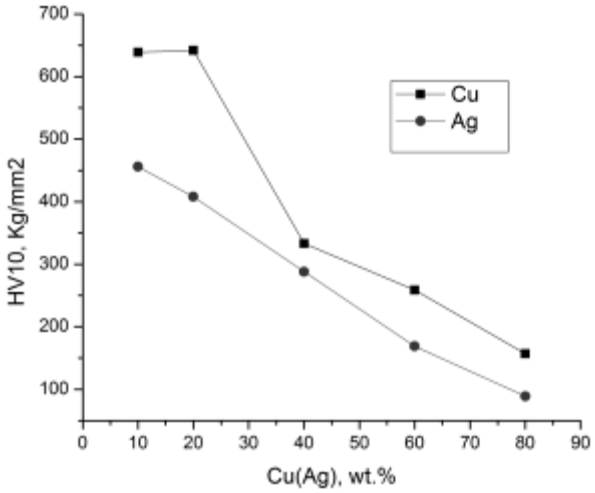

Fig. 3. Hardness H_V vs. the Cu(Ag) content of composites fabricated by HEC at 940°C and 5GPa.

As follows from Fig. 3, the hardness of Ta–Cu (Ag) composites decreases with increasing the Cu(Ag) content. The high hardness for nanostructured Ta–Cu (Ag) composites at low contents of the matrix phase may be explained by plastic deformation and fragmentation of individual tantalum grains.
The above mentioned and other details of preparing Ta–Cu and Ta–Ag precursors that would ensure high density of cylindrical billets with a perfect structure and uniform distribution of constituents will be discussed at presentation.

TECHNICAL PROGRAM

XIII International Symposium on Explosive Production of New Materials: Science, Technology, Business, and Innovations (EPNM-2016)

June 20–24, 2016
Coimbra, Portugal

Organized by

Institute of Structural Macrokinetics and Materials Science, Russia

Association for Development of Industrial Aerodynamics (ADAI) at the University of Coimbra, Portugal

International Advisory Committee

Fortov V.E. Honorary member	(Russia)	Peikrishvili A.	(Georgia)
		Pervukhin L.B.	(Russia)
Alfimov M.V.	(Russia)	Plaksin I.	(Portugal)
Alymov M.I.	(Russia)	Prothe C.	(USA)
Banker J.G.	(USA)	Prümmer R.	(Germany)
Campos J.	(Portugal)	Remond Y.	(France)
Carton E.	(Netherlands)	Ribeiro J.	(Portugal)
Chen P.	(China)	Rozen A.E.	(Russia)
Deribas A.A.	(Russia)	Shtertser A.A.	(Russia)
Galka A.	(Poland)	Stavrev S.Ya.	(Bulgaria)
Hokamoto K.	(Japan)	Szulc Z.	(Poland)
Ivanov V.V.	(Russia)	Tavadze G.F.	(Georgia)
Kecskes L.J.	(USA)	Thadhani N.N.	(USA)
Levashov E.A.	(Russia)	Veehmayer M.	(Germany)
Lis J.	(Poland)	Yücel O.	(Turkey)
Mendes R.	(Portugal)	Yukhvid V.I.	(Russia)
Moon J.G.	(Korea)	Vakin V.S.	(Russia)
Nesvadba P.	(Czechia)	Zięba P.	(Poland)
Paul H.	(Poland)		

Organizing Committee

Alymov M.I., co-chairman	(Russia)	Louro C.S.	(Portugal)
Mendes R., co-chairman	(Portugal)	Sytschev A.E.	(Russia)
Likhanova O.O., coordinator	(Russia)	Amelina O.V.	(Russia)
Ramos A., exe. secretary	(Portugal)	Loureiro A.	(Portugal)
Sanin V.N.	(Russia)	Pires A.	(Portugal)
Pervukhin L.B.	(Russia)		
Ribeiro J.	(Portugal)		

Program/Publication Committee

Mendes R.	(Portugal)
Alymov M.I.	(Russia)
Deribas A.A.	(Russia)
Ribeiro J.	(Portugal)
Pervukhin L.B.	(Russia)
Scheck Yu.B.	(Russia)

Monday, June 20

9:00–10:00 Registration

10:00–11:00 **Opening ceremony**

Prof. Vladimir E. Fortov (Russia)
Prof. João Gabriel (Portugal)
Prof. Xavier Viegas (Portugal)
Prof. Ricardo Mendes (Portugal)
Prof. Mikhail I. Alymov (Russia)
Prof. Andrey A. Deribas (Russia)

11:00 – 11:20 | Coffee break

11:20
V. E. Fortov (Russia)
LIGHT AND ELECTRIC DETONATION

12:00
C. Prothe, C. Hurley, J. Banker, and S. Liu (USA)
COMPARATIVE TENSILE STRENGHT AND SHEAR STRENGHT OF EXPLOSION CLAD MATERIALS

12:20
V. S. Vakin and A. Z. Krasilnikov (Russia)
EXPLOSIVE WELDING OF EXTRA-LARGE CLAD PLATES:
DYNAMIC FEATURES

12:40
M. Najwer and G. Kwiatkowski (Poland)
STRENGTH PROPERTIES OF Al2519/Ti6Al4V BIMETALL FABRICATED BY EXPLOSIVE WELDING

13:00–14:00 | Lunch

14:00
A. E. Rosen, V. D. Krevchik, M. B. Semenov, A. V. Pryshchak, and A. A. Rosen (Russia)
FRACTAL ANALYSIS OF CLUSTERS FORMED AT THE INTERFACES IN EXPLOCXLAD MULTILAYER STRUCTURES

14:20
G. Carvalho, R. M. Leal, I. Galvão, R. Mendes, J. B. Ribeiro, and A. Loureiro (Portugal)
EFFECT OF ALUMINIUM TEMPERING ON THE QUALITY OF EXPLOSIVE WELDING

14:40
M. I. Alymov (Russia)
RECENT ADVANCEMENTS OF ISMAN IN SHS AND IN EXPLOSION/COMBUSTION-ASSISTED MATERIALS PROCESSING

15:00
T. Babul, M. Baranowski, and A. Olbrycht (Poland)
COMPOSITE Cu–C COATINGS

15:20
S. N. Pakhomov (Ukraine)
INDUSTRIAL EXPERIENCE ON EXPLOSIVE WELDING OF STEEL–Al ALLOY TRANSITION ELEMENTS FOR AEROSPACE APPLCATIONS

15:40
B. S. Zlobin, A. A. Shtertser, V. V. Kiselev, and A.V. Plastinin (Russia)
BONDING AND WAVE FORMATION AT THE EXPLOSIVE WELDING OF LOW-PLASTIC MATERIALS

16:00–16:20 | Coffee break

16:20
I. A. Bataev, S. Tanaka, I. D. Kuchumova, O.E. Matts, D.V. Lazurenko, K. Hokamoto, and A.A. Bataev (Russia/Japan)
METASTABLE STRUCTURES FORMED AT THE INTERFACE IN EXPLOSIVELY WELDED MATERIALS

16:40
Q. Zhou, P.W. Chen, and J.R. Feng (China)
FABRICATION OF TUNGSTEN/COPPER BIMETAL BY HOT EXPLOSIVE WELDING

17:00
S. Yu. Ananev, T. I. Borodina, G. E. Valiano, A. A. Deribas, and B. D. Yankovsky (Russia)
CHARACTERISTICS OF STEEL AND TITANIUM CYLINDERS AFTER EXPLOSIVE JOINING

17:20
V. V. Rybin, E. A. Ushanova, and N. Yu. Zolotorevsky (Russia)
MECHANISM OF PATTERNING AT THE INTERFACE OF EXPLOSIVELY WELDED Cu/Cu PLATES

17:40
L. B. Pervukhin, O. L. Pervukhina, I. V. Denisov, and T. A. Shishkin (Russia)
EXPERIMENTAL EVIDENCE FOR FORMATION OF SHOCK PLASMA DURING EXPLOSIVE WELDING

18:00
In Memorium – Prof. Igor Plaksin

18:30 | Welcome drink - Loggia

Tuesday, June 21

9:00
W. G. Proud (Great Britain)
GRANULAR MATERIALS UNDER SHOCK, BALLISTIC,
AND BLAST LOADING

9:40
V. P. Efremov, A. I. Frolov, and V. E. Fortov (Russia)
ULTRUFAST PROPAGATION OF DESTRUCTION WAVE IN SILICA FIBERS

10:00
G. Carvalho, R. M. Leal, I. Galvão, R. Mendes, J. B. Ribeiro, and A. Loureiro (Portugal)
EXPLOSIVE WELDING OF ALUMINUM AND COPPER: EFFECT OF BASE PLATE MATERIAL

10:20
M. Gloc, Ł.Ciupiński, and G. Kwiatkowski (Poland)
INFLUENCE OF HYDROGEN ON EXPLOSION-WELDED CORROSION RESISTANT CLAD MATERIALS FOR GEOTHERMAL PLANTS

10:40
A. V. Khorin, A. V. Pryshchak, D. L. Chernyshev, and A. P. Pen'shin (Russia)
FORMATION OF INTERMETALLIC INTERLAYERS IN EXPLOCLAD Al–Cu COMPOSITES: CALCULATED KINETIC PARAMETERS

11:00 – 11:20 | Coffee break

11:20
V. A. Grachev, A. E. Rosen, G. V. Kozlov, S. G. Usatyi, A. A. Rosen, and D. A. Verevkin (Russia)
EXPLOCLAD MULTILAYER MATERIALS WITH ENHANCED SERVICE LIFE FOR REPOSITORY OF LIQUID RADIOACTIVE WASTES

11:40
D. M. Fronczek, R. Chulist, L. Litynska-Dobrzynska, Z. Szulc, N. Schell, P. Zieba, and J. Wojewoda-Budka (Poland)
EXPLOSIVE WELDING FOLLOWED BY ANNEALING: MICROSTRUCTURE OF Al/Ti/Al AND Al/Mg/Al CLADS

12:00
O. A. Burtseva, A. O. Drennov, and O. B. Drennov (Russia)
EXPLOSIVE WELDING OF PIPES

12:20
E. Mazancová, K. Saksl, D. Ostroushko, M. Ďurišin, D. Balga, J. Szabo, and P. Kučera (Czechia/Slovakia)
PROPERTIES OF Ti–Cr18Ni10 CLAD METALL UNDER DYNAMIC LOADING

12:40
A.V. Tyutyaev and V.P. Trebunskikh (Russia)
SENSITIVITY OF LIQUID ENERGETIC MATERIALS BY SIMPLE TESTING

13:00 – 14:00 | Lunch

14:00
O. L. Pervukhina, I. A. Schastlivaya, A. M. Fedorov, L. B. Pervukhin, and P.A. Nikolaenko (Russia)
TENSILE STRENGTH OF WELD SEAM IN EXPLOCLAD STEEL/Ti SHEETS

14:20
D. V. Lazurenko, V. I. Mali, I. A. Bataev, Yu. N. Malyutina, B. N. Kyzylova, M. A. Esikov, and R. I. Kuz'min (Russia)
EXPLOSIVE WELDING OF MULTILAYER TITANIUM/LOW-ALLOY STEEL COMPOSITES USING TANTALUM–COPPER AND NIOBIUM–COPPER INSERTS

14:40
D. Ostroushko, E. Mazancová, K. Saksl, M. Ďurišin, D. Balga, and J. Szabo (Czechia/Slovakia)
MICROSTRUCTURE, PHASE COMPOSITION, AND MECHANICAL PROPERTIES OF Ti–Cr18Ni10 CLAD METAL

15:00
D. L. Chernyshev and N.A. Baidarova (Russia)
HIGHLY DURABLE HIGH-MODULUS Al–Cu COMPOSITES BY EXPLOSIVE WELDING AND SUBSEQUENT HEAT TREATMENT

15:20
I. S. Los, A. E. Rozen, M. S. Gus'kov, A. A. Rozen, and D. A. Verevkin (Russia)
MECHANICAL TESTING OF EXPLOCLAD CORROSION-RESISRANT LIGHT-GAGE MULTILAYER SHEETS

15:40
V.S. Vakin and O.G. Zotov (Russia)
INFLUENCE OF CYCLIC THERMAL LOADING ON THE QUALITY OF WELD SEAM

16:00 | Visit to Paço das Escolas

20:00 | Dinner at CCDD

Wednesday, June 22

9:00
R. Prümmer (Germany)
CONSTRUCTIVE APPLICATIONS OF SHOCK WAVES: IMPORTANCE OF DETONATION VELOCITY

9:40
D. B. Kryukov, M. S. Gus'kov, and D. S. Gus'kov (Russia)
EXPLOCLAD Ti–Al–Ti COMPOSITE WITH IMPROVED STRENGTH PARAMETERS

10:00
M. Wachowski, L. Sniezek, I. Szachogluchowicz, and T. Plocinski (Poland)
EFFECT OF POST HEAT TREATMENT ON MECHANICAL PROPERTIES OF LAYERED LAMINATES Al–Ti AND Fe–Ti OBTAINED BY EXPLOSIVE WELDING METHOD

10:20 | Poster session

11:00 – 11:20 | Coffee break

11:20
V. B. Bozhevolnov, Yu. V. Bozhevolnov, A. M. Yafyasov, and M. C. Archipov (Russia)
DETONATION SYNTHESIS OF NANOPARTICLES: A FLOW-REACTOR MODEL

11:40
A. Peikrishvili, L. Kecskes, B. Godibadze, E. Chagelishvili, and G. Tavadze (Georgia/USA)
SHOCK-ASSISTED SHS AND CONSOLIDATION OF Ta–Al AND Nb–Al COMPOSITES

12:00
H. Yin, Q. Du, and P. Chen (China)
SHOCK WAVE SYNTHESIS OF MULTILAYER GRAPHENE FROM DRY ICE

12:20
S. V. Aydinyan, H. V. Kirakosyan, S. L. Kharatyan, A. Peikrishvili, G. Mamniashvili, B. Godibadze, E. Sh. Chagelishvili, D. R. Lesuer, and M. Gutierrez (Armenia/Georgia/USA/Spain)
SYNTHESIS AND FABRICATION OF CU–W COMPOSITES COMBINING SHS AND HEC TECHNOLOGIES

12:40
K. A. Ten, E. R. Pruuel, A. O. Kashkarov, I. A. Spirin, A. L. Mikhailov, L. I. Shekhtman, V. V. Zhulanov, and A. A. Deribas (Russia)
DETONATION PARAMETERS OF LOW-DENSITY PETN AND RDX BASED HIGH EXPLOSIVES

13:00 – 14:00 | Lunch

14:00 | Visit to Figueira da Foz, Montemor-o-Velho

Thursday, June 23

9:00
A. A. Deribas
CUBIC SILICON NITRIDE: SYNTHESIS AND APPLICATIONS

9:40
V. M. Batrashov, Ch. G. Pak, and D. O. Gus'kov (Russia)
FABRICATION OF HEAT-RESISTANT CERAMIC CRUCIBLES FOR MELTING ALLOYED STEELS AND NON-FERROUS METALS BY ALUMINOTHERMIC SHS

10:00
A. Peikrishvili, G. Maniashvili, B. Godibadze, T. Gegechkori, E. Chagelishvili, M. Tsiklauri, and A. Dgebuadze (Georgia)
HOT EXPLOSIVE CONSOLIDATION OF NANOSTRUCTURED Ta–Cu AND Ta–Ag COMPOSITES: FABRICATION AND PROPERTIES

10:20
A. R. Luchenok, L. V. Sudnik, G. V. Smirnov, N. V. Kirshina, and V. S. Tkachuk (Belarus)
EXPLOSIVE COMPACTION OF POWDERS

10:40
A. R. Zurnachyan and R. A. Mnatsakanyan (Armenia)
MICROWAVE RADIATION FOR SYNTHESIS OF CARBIDES AND CATALYTIC DECOMPOSITION OF HYDRAZINE

11:00
S. V. Skiba, Ch. G. Pak, and A. V. Pryshchak (Russia)
WEAR/CORROSION RESISTANT INTERMETALLIC Fe–Al COATINGS: PREPARATION AND CHARACTERIZATION

11:00 – 11:40 | Coffee break

11:40
I. Plaksin, L. Rodrigues, R. Mendes, J. Ribeiro, J. Campos, J. Góis, S. Plaksin
EXPERIMENTAL METROLOGY AND TECHNIQUES FOR SUB-MILLIMETER OPTICAL OBSERVATION OF DETONATION REACTION PHENOMENA AND PERFORMANCE EVALUATION OF CRYSTALLINE EXPLOSIVES

12:00
P. Nesvadba, J. Kucera, M. Kunzel, and J. Pachman (Czechia)
IMPACT VELOCITY OF CLADDING METAL AS MEASURED BY PHOTONIC DOPPLER VELOCIMETRY (PDV)

12:20
K. Hokamoto (Japan)
A NEW METHOD TO MAKE UNIDIRECTIONAL POROUS STRUCTURE BY EXPLOSIVE WELDING TECHNIQUE

12:40
V.P. Efremov, E.I. Zakatilova, I.V. Maklashova, A.A. Deribas, and N.V. Shevchenko (Russia)
THERMAL ANALYSIS OF DETONATION NANODIAMONDS

13:00 – 14:00 | Lunch

14:00
Z. Wilk, P. Koślik, and A. Gałka (Poland)
PROTECTIVE MULTILAYER Al–Ti MATERIAL WITH ENHANCED BALLISTIC RESISTANCE

14:20
K. Saksl, J. Ďurišin, O. Milkovič, Z. Szulc, L. Ciupiński, and A. Arnbjörnsson (Slovakia/Poland)
STRUCTURE OF BIMETALS AS INVESTIGATED BY SYNCHROTRON RADIATION

14:40
A. Mori, S. Tanaka, and K. Hokamoto (Japan)
OBSERVATION OF METAL JET GENERATED BY INCLINED COLLISION USING A POWDER GUN

15:00
A. Yu. Dolgoborodov, V. G. Kirilenko, A. A. Shevchenko, and M. A. Brazhnikov (Russia)
MECHANOACTIVATION AND DETONATION OF AMMONIUM PERCHLORATE/NANO-Al MIXTURES

15:20
S. Nandagopal, A. Kotbagi, S. Singh, A. Kumar, and M. Gupta (India)
A RAPID, LOW-TEMPERATURE, SAFE PROCESS FOR DRYING WATER-WET NITRAMINES WITH REUSABLE SOLVENTS

15:40
V. A. Sel'skii and A. A. Sel'skii (Russia)
PROSPECTS FOR USING STONELEY WAVES IN MONITORING THE QUALITY OF CLAD METALS

16:00 – 16:20 | Coffee break

16:20
J. Campos, R. Mendes, J. Quaresma and J. Pimenta (Portugal)
METAL-OXIDE NANOPARTICLE FORMATION FROM CONDENSED PRODUCTS OF DETONATION – MODELLING AND EXPERIMENTAL DEVELOPMENTS

16:40
V. A. Pervuninskikh and A. V. Pryshchak (Russia)
SECURITY COMPLEX FOR FAST DEPLOYMENT OF EXPLOSIVE WORKS

17:00
J. Quaresma, J. Pimenta, R. Mendes, J. Gois, J. Campos, L. Deimling, and T. Keicher (Portugal/Germany)
OPTICAL DETONATION MEASUREMENTS AND DESIGN OF EXPLOSION CHAMBER FOR SMALL SAMPLES OF EXPLOSIVES

17:20
S. Y. Stavrev (Bulgaria)
MODIFICATION OF NANODIAMOND BY ADDITION OF AMINO GROUPS WITH BIOLOGICAL APPLICATION AIM

17:40
V. V. Sobolev and N. V. Bilan (Ukraine)
ADDITIONAL GAS FORMATION DURING ROCK BREAKAGE BY BLASTING

20:00 | Dinner at Palácio de S. Marcos

Friday, June 24

9:00
J.T. Li, Z.C. Yang, and G.G. Liu (China)
COMBUSTION SYNTHESIS OF HIGH-ENTROPY ALLOYS AND THERMOELECTRIC MATERIALS

9:20
V. I. Yukhvid, D. E. Andreev, V. N. Sanin, D. M. Ikornikov, E. A. Levashov, Zh. A. Sentyurina, A. A. Zaitsev, and Yu. S. Pogozhev (Russia)
SHS-PRODUCED TiAl CAST ALLOYS FOR ADDITIVE MANUFACTURING TECHNOLOGIES

9:40
Z. G. Aslamazashvili, G. V. Zakharov, G. Sh. Oniashvili, G. F. Tavadze, and M. N. Chikhradze (Georgia)
SHS OF FINE-GRAINED CERAMICS CONTAINING CARBIDES, NITRIDES, AND BORIDES

10:00
V.N. Sanin, D.M. Ikornikov, D.E. Andreev, N.V. Sachkova, and V.I. Yukhvid (Russia)
SELF-PROPAGATING HIGH-TEMPERATURE SYNTHESIS OF CAST NANO-STRUCTURED 'HIGH-ENTROPY' ALLOYS BASED ON 2*d* AND 3*d* ELEMENTS

10:20
A. Yu. Potanin, Yu. S. Pogozhev, I. V. Yatsuk, E. A. Levashov, D. Yu. Kovalev, and N. A. Kochetov (Russia)
ADVANCED HIGH-TEMPERATURE CERAMICS BASED ON ZIRCONIUM DIBORIDE AND SILICIDE: COMBUSTION SYNTHESIS AND APPLICATION

10:40
Ch. G. Pak, V. M. Batrashov, and G. A. Koshkin (Russia)
CERMET COATINGS BY ALUMINOTHERMIC SHS

11:00 – 11:20 | Coffee break

11:20
V.I. Yukhvid, D.E. Andreev , V.N. Sanin, N.V. Skachhkova, and M.I. Alymov (Russia)
METALLOTHERMIC SHS REACTIONS INVOLVING NIOBIUM OXIDE

11:40
O.K. Kamynina, S.G. Vadchenko, A.S. Shchukin, and I.D. Kovalev (Russia)
DEPOSITION OF MULTILAYER CERAMIC COATINGS ONTO Ti SUBSTRATE BY SHS METHOD

12:00 | Closing ceremony

Poster Presentations
10:20–11:00
Wednesday, June 22, 2016

M.I. Alymov, I.S. Gordopolova, and A.A. Deribas (Russia)
ONCE MORE ON THE ROLE OF SHOCKED GAS IN EXPLOSIVE WELDING

M.I. Alymov, N.M. Rubtsov, B.S. Seplyarskii, V.A. Zelenskii, and A.B. Ankudinov (Russia)
SELF-INFLAMMATION OF Fe NANOPOWDERS IN AIR: INFLUENCE OF PASSIVATION

M.I. Alymov, S.G. Vadchenko, I.V. Saikov, and I.D. Kovalev (Russia)
SHOCK COMPACTION OF TUNGSTEN/TEFLON POWDER MIXTURES

D.E. Andreev, D.M. Ikornikov, V.I. Yukhvid, and V.N. Sanin (Russia)
SYNTHESIS OF Ti–Al-BASED INTERMETALLICS FROM OXIDE RAW MATERIALS BY CENTRIFUGAL SHS

A.F. Belikova, S.N. Buravova, and E.V. Petrov (Russia)
ABNORMAL MASS TRANSFER IN CONDITIONS OF SHOCK LOADING

O.D. Boyarchenko, A.E. Sytschev, L.M. Umarov, A.S. Shchukin, I.D. Kovalev, and M.A. Sichinava (Russia)
$NiAl/Cr_2O_3$ COMPOSITE BY THERMAL EXPLOSION

S.N. Buravova and N.I. Mukhina (Russia)
LE CHATELIER PRINCIPLE AND SPALL DAMAGEABILITY

S.N. Buravova, E.V. Petrov, and A.S. Shchukin (Russia)
SPHEROIDIZATION OF PERLITE IN THE BANDS OF LOCALIZED DEFORMATION

I.V. Denisov, O.L. Pervukhina, and I.V. Saikov (Russia)
STRUCTURAL INHOMOGENEITY OF WELD SEAM IN BRASS/STEEL CLAD METAL FABRICATED BY EXPLOSIVE WELDING

N.L. Fedotova, I.B. Chudakov, I.A. Korms, S.Yu. Makushev, L.B. Pervukhin, I.V. Saikov, and A.Yu. Malakhov (Russia)
HIGH-SRENGTH AND HIGH-DAMPING CLAD METAL
BY EXPLOSIVE WELDING

S.V. Fortova, V.V. Shepelev, A.P. Pronina, and P.S. Utkin (Russia)
MATHEMATICAL MODELING OF RAYLEIGH–TAYLOR INSTABILITY AT THE INTERFACE OF TWO COLLIDING METAL PLATES

R.D. Kapustin (Russia)
COMBUSTION SYNTHESIS OF REFRACTORY AND HEAT-INSULATING ALUMINOSILICATE COMPOSITES

A. Karolczuk, Z. Szulc, K. Kluger, M. Najwer, and G. Kwiatkowski (Poland)
RESIDUAL STRESS DISTRIBUTION IN THREE LAYER PLATE OBTAINED BY EXPLOSIVE WELDING

D.S. Khrenov, A.V. Sobol'kov, A.I. Elkin, A.V. Aborkin, and A.E. Sytschev (Russia)
PROTECTIVE Al–2Mg–*n*C COATINGS BY COLD GAS-DYNAMIC SPUTTERING: DEPOSITION AND CHARACTERIZATION

A.A. Kondakov, I.A. Studenikin, A.V. Linde, N.A. Kondakova, and V.V. Grachev (Russia)
MAX PHASE TI_2AlN BY SINTERING IN VACUUM

D.Yu. Kovalev, A.Yu. Potanin, E.A. Levashov, and N.F. Shkodich (Russia)
COMBUSTION SYNTHESIS OF MAGNESIUM DIBORIDE:
A TIME-RESOLVED XRD STUDY

D.Yu. Kovalev and M.A. Luginina (Russia)
TEMPERATURE DEPENDENCE OF Ti_2AlN THERMAL EXPANSION AS DETERMINED FROM HIGH-TEMPERATURE XRD DATA

D.Yu. Kovalev, M.A. Luginina, and S.G. Vadchenko (Russia)
SHS IN Zr–Al–C SYSTEM: A TIME-RESOLVED XRD STUDY

G. Kwiatkowski, Z. Szulc, M. Najwer, and M. Gloc (Poland)
PROSPECTS FOR USING EXPLOCLAD MATERIALS IN GEOTHERMAL APPLICATIONS

M.A. Luginina and D.Yu. Kovalev (Russia)
THERMAL STABILITY OF MAX PHASE TI_2AlN IN VACUUM

M.A. Luginina, D.Yu. Kovalev, S.G. Vadchenko, S.V. Konovalikhin, and A.E. Sytschev (Russia)
NOVEL MAX PHASE IN Zr–Ti–Al–C SYSTEM: SYNTHESIS AND STRUCTURE

A.Yu. Malakhov, I.V. Saikov, L.B. Pervukhin, and P.A. Nikolaenko (Russia)
EXPLOSIVE WELDING OF LONG-LENGTH PIPES AND RODS

A.Yu. Malakhov, I.V. Saikov, L.B. Pervukhin, and P.A. Nikolaenko (Russia)
Ti–Cu CONDUCTIVE CYLINDERS BY EXPLOSIVE WELDING

AUTHOR'S INDEX

L

M

N

O

P

Q

R

S

T

U

V

Y

W

Z